Prediction of Lateral Restraint Forces in Sloped Z-section Supported Roof Systems using the Component Stiffness Method

By

Michael W. Seek

Dissertation submitted to the Faculty of

Virginia Polytechnic Institute and State University

in partial fulfillment for the requirements of the degree of

Doctor of Philosophy

in

Civil Engineering

Thomas M. Murray, Chair

Finley A. Charney

W. Samuel Easterling

Mehdi Setareh

Elisa Sotelino

January 29, 2007

Blacksburg, VA

Keywords: purlin, Z-section, lateral bracing, cold-formed, through-fastened, standing seam, diaphragm, metal building, finite element method, component stiffness method.

Prediction of Lateral Restraint Forces in Sloped Z-section Supported Roof Systems using the Component Stiffness Method

Michael W. Seek

(ABSTRACT)

Z-sections are widely used as secondary members in metal building roof systems. Lateral restraints are required to maintain the stability of a Z-section roof system and provide resistance to the lateral forces generated by the slope of the roof and the effects due to the rotation of the principal axes of the Z-section relative to the plane of the roof sheathing. The behavior of Z-sections in roof systems is complex as they act in conjunction with the roof sheathing as a system and as a light gage cold formed member, is subject to local cross section deformations.

The goal of this research program was to provide a means of predicting lateral restraint forces in Z-section supported roof systems. The research program began with laboratory tests to measure lateral restraint forces in single and multiple span sloped roof systems. A description of the test apparatus and procedure as well as the results of the 40 tests performed is provided in Appendix II.

To better understand the need for lateral restraints and to provide a means of testing different variables of the roof system, two types of finite element models were developed and are discussed in detail in appended Paper I. The first finite element model is simplified model that uses frame stiffness elements to represent the purlin and sheathing. This model has been used extensively by previous researchers and modifications were made to improve correlation with test results. The second model is more rigorous and uses shell finite elements to represent the Z-section and sheathing.

The shell finite element model was used to develop a calculation procedure referred to as the Component Stiffness Method for predicting the lateral restraint forces in Z-section roof systems. The method uses flexural and torsional mechanics to describe the behavior of the Z-section subject to uniform gravity loads. The forces generated by the system of Z-sections are resisted by the "components" of the system: the lateral restraints, the sheathing and Z-section-to-rafter connection. The mechanics of purlin behavior providing the basis for this method are discussed in appended Paper II. The development of the method and the application of the method to supports restraints and interior restraints are provided in appended papers III, IV and V.

ACKNOWLEDGEMENTS

I would like to thank Dr Thomas Murray for his support and guidance. I am awed by his ability to teach and inspire students and consider it an honor to have him as an advisor. I would also like to extend thanks to Dr Samuel Easterling for his support and for suggesting that I pursue doctoral studies. I am thankful to Dr Finley Charney for serving on my committee, providing me access to SAP 2000, and challenging me in the classroom as Computer Analysis of Structures was one of the most beneficial classes I took. I would also like to thank Dr Elisa Sotelino and Dr Mehdi Setareh for their help in my research. I would like to thank Brett Farmer and Dennis Huffman for all of their help at the Structures Laboratory, teaching me so much that can't be taught in a classroom, and fostering an appreciation for country music. Clark Brown deserves many thanks for all of his help with my many battles with my nemesis – instrumentation. I extend thanks to Ann Crate for making my presentations and papers look so nice and helping me submit the proper paperwork to stay out of trouble with the bureaucrats. I would like to thank all of those that helped me at the structures laboratory, in particular Michael Shoemaker, Jason Marshall, and my "big brother" Onur Avci.

I would like to thank the Metal Building Manufacturer's Association and the American Iron and Steel Institute for their financial support of this research. I have developed friendships with many of the people from both organizations and am thankful to each of them for improving my knowledge and research through their questions and comments.

Many people have inspired and supported me through this endeavor. I would like to thank my parents, Walter and Dottie, for instilling in me values of hard work and humility and for fostering an inquisitive mind, my sisters, Julie and Amy, for being great friends and setting such a high standard for me to live up to, my sweetie, Lee Bryant, for her love, patience, companionship, and support, all of my friends in Blacksburg, particularly Dave and Stephanie, for providing diversions from the stress of research, my neighbor and adopted grandmother, Lois, for her love and home cooking, my puppy, KD, for always making me feel loved, to my doctors and nurses after my accident, for nursing me back to health, and to Gary, for inspiration and perspective.

TABLE OF CONTENTS

Title Page....i
Abstract....ii
Acknowledgements....iii
Table of Contents....iv
List of Figures....vi
1. Introduction....1
   1.1 Overview....1
   1.2 Z-section Supported Roof Systems....2
   1.3 Review of Existing Research....3
      1.3.1 Analytical Methods for Predicting Lateral Restraint Forces....3
      1.3.2 Experimental Testing to Determine Lateral Restraint Forces....9
      1.3.3 Current Design Practice....10
   1.4 Objectives and Methods....10
2. Component Stiffness Method....13
   2.1 Flexural Behavior of Single Span End Restrained Z-section....13
      2.1.1 Behavior Neglecting Sheathing Rotational Restraint....13
      2.1.2 Behavior Including Sheathing Rotational Restraint....16
   2.2 Flexural Behavior of Single Span Z-sections with Interior Restraints....19
   2.3 General Procedure....21
      2.3.1 Single Purlin with Flexible Restraints....22
      2.3.2 Multiple Purlin System....23
      2.3.3 Stiffness of Components....23
      2.3.4 Calculation of Restraint Forces....28
      2.3.5 System performance....29
3. Finite Element Model Analyses....30
   3.1 Development of Finite Element Models for Predicting Lateral Restraint Forces....30
   3.2 Finite Element Model to Develop Prediction Equations....31
4. Discussion, Conclusions and Future Work....34
5. References....35
6. Nomenclature....37
Vita....38

Appendix I – Papers……………………………………………………………………...…39

Paper I……………………………………………………………………………………42

"Computer Modeling of Sloped Z-Purlin Supported Roof Systems to Predict Lateral Restraint Force Requirements." - Published in the Conference Proceedings of the 17th International Specialty Conference on Cold-Formed Steel Structures (2004)

Paper II…………………………………………………………………………….....56

"Mechanics of Lateral Brace Forces in Z-Purlin Roof Systems" - Published in the Conference Proceedings of the Structural Stability Council Annual Stability Conference (2005)

Paper III………………………………………………………………………………77

"Component Stiffness Method to Predict Lateral Restraint Forces in End Restrained Single Span Z-Section Supported Roof Systems with One Flange Attached to Sheathing." - Published in the Conference Proceedings of 19th International Specialty Conference on Cold-Formed Steel Structures (2006).

Paper IV………………………………………………………………………………92

"Lateral Brace Forces in Single Span Z-Section Roof Systems with Interior Restraints Using the Component Stiffness Method." - Published in the Conference Proceedings of the Structural Stability Council Annual Stability Conference (2007)

Paper V……………………………………………………………………………….108

"Prediction of Lateral Restraint Forces in Single Span Z-section Roof Systems with One Flange attached to Sheathing using the Component Stiffness Method" - Submitted to The Journal of Constructional Steel Research for publication (July 2007)

Appendix II - Results of Laboratory Tests of Lateral Restraint Forces……………………….142

Appendix III – Summary of Equations to Predict Lateral Restraint Forces and Example Problems……………………………………………………...231

LIST OF FIGURES

Figure 1.1 Free Body Diagram Neubert and Murray Equation.. 7

Figure 2.1 External Forces Acting on Z-section 14

Figure 2.2 Unrestrained and Restoring Displacement.. 15

Figure 2.3 Rotation of Z-section at Midspan.. 17

Figure 2.4 Free Body Diagram including Rotational Resistance of the Sheathing 19

Figure 2.5 Displaced Shape of Z-section Restrained at Mid-Span 20

Figure 2.6 Rotation of Z-section with Interior Restraints 21

Figure 2.7 Free Body Diagram of Z-section 22

Figure 2.8 End Restraints.. 24

Figure 2.9 Deformation of Z-section at Support Restraint... 24

Figure 2.10 Rafter Connections.. 27

Figure 3.1 Representation of Elements in Shell Finite Element Model...................................... 31

Prediction of lateral restraint forces in sloped Z-section supported roof systems using the component stiffness method

1. Introduction

1.1 Overview

The Component Stiffness Method was developed to predict lateral restraint forces in Z-section supported roof systems. The research program began with full scale roof system tests that measured lateral restraint forces on roofs with varying slopes. These tests are briefly discussed in appended Paper I *Computer Modeling of Sloped Z-Purlin Supported Roof Systems to Predict Lateral Restraint Force Requirements* and more thoroughly reported in Appendix II *Results of Laboratory Tests of Lateral Restraint Forces*. To better understand and build upon the test data, two types finite element models were developed based upon the laboratory tests. These models are outlined in appended Paper I. The flexural behavior of Z-sections and their interaction with roof sheathing that provides the basis for the Component Stiffness Method is presented in appended Paper II *Mechanics of Lateral Brace Forces in Z-Purlin Roof Systems.* The development of the Component Stiffness Method for roof systems with supports restraints and interior third points restraints is presented respectively in appended Paper III *Component Stiffness Method to Predict Lateral Restraint Forces in End Restrained Single Span Z-Section Supported Roof Systems with One Flange Attached to Sheathing* and appended Paper IV *Lateral Brace Forces in Single Span Z-Section Roof Systems with Interior Restraints Using the Component Stiffness Method*. In appended Paper V, *Prediction of Lateral Restraint Forces in Single Span Z-section Roof Systems with One Flange attached to Sheathing using the Component Stiffness Method,* a concise summary with some practical applications of the method are provided.

The main body of this dissertation is intended to guide the reader through the development of the Component Stiffness Method. A review of the research related to the lateral brace forces in Z-section supported roof systems that contributed to the development of the component stiffness method is provided. The main body follows the progression of the research from laboratory testing, to finite element modeling, to the development and application of the prediction method. A general discussion is provided in the main body and the reader is referred to the appended papers for more detailed discussions.

1.2 Z-section Supported Roof Systems

Over the past five decades, metal building systems have become increasingly popular. Most of their use has been in the manufacturing sector because the use of extremely efficient tapered girders coupled with lightweight Z-sections and sheathing allows for large floor spaces to be inexpensively placed under roof. Recent advances in weatherproofing of standing seam systems in addition to increased variety in durable architectural finishes has seen metal building systems used in applications previously only considered for conventional building systems like churches, schools, and low rise commercial spaces.

The Z-section is a major contributor to success of metal buildings. As a roof framing member, it can efficiently span 20 to 35 feet. The shape of the Z-section allows it to be nested for efficient handling and transportation. Z-sections are typically cold-rolled from coil stock and due to recent advances in automation, they can be produced very rapidly. Furthermore, the majority of steel used for the production of the Z-sections is recycled, which is important given the building industry's recent emphasis on green engineering.

Despite their many advantages, Z-sections present significant challenges to designers. One aspect that has challenged designers is the need to provide lateral restraint for Z-section systems. Due to the rotated principal axes of a Z-section, when loaded in the plane of its web, it has the tendency to deflect laterally in addition to its vertical deflection. Load eccentricity on the top flange of the Z-section, attachment of the top flange to sheathing and second order effects cause the Z-section to twist. To accommodate thermal expansion, a certain amount of flexibility is often designed into the connection between the Z-section and sheathing. Because Z-sections are typically placed on top of the rafters, forces applied to the sheathing must be transferred through the Z-section to the rafters. The transferred forces include effects due to the slope of the roof and effects of load applied eccentrically to the top flange of the Z-section. To maintain stability, it is often necessary to provide external lateral restraint to a Z-section. Given all of the factors involved, however, quantifying the amount of restraint required is a difficult undertaking.

1.3 Review of Existing Research

1.3.1 Analytical Methods for Predicting Lateral Restraint Forces

In their paper, "Unsymmetrical Bending of Beams with and without Lateral Bracing," Zetlin and Winter (1955) provided a simplified means for calculating stresses and brace forces in beams loaded on axes rotated from their principal axes by introducing the concept of modified moments of inertia and a fictitious horizontal load. A beam loaded on axes rotated from its principal axes will deflect laterally in addition to the deflection in the plane of the applied load. Using the modified moments of inertia and fictitious horizontal load, conventional constrained bending formulas can be used to determine the lateral deflection of a Z-section, which has principal axes rotated from the orthogonal planes of the web and flange. Lateral brace forces are calculated by equating the deflection due to the real horizontal force with the deflection caused by the fictitious horizontal force. In a case where the Z-section is restrained at each point at which load is applied, the lateral restraint force perpendicular to the web of the Z-section reduces to:

$$R = U\left(\frac{I_{XY}}{I_X}\right) \tag{1.1}$$

where U is a transverse load applied in the plane of the web, I_X is the moment of inertia of the full unreduced section about the centroidal axis perpendicular to the web, and I_{XY} is the product of inertia of the full unreduced section about the centroidal axes parallel and perpendicular to the web. For this restraint force to hold true, the Z-section must be rotationally restrained at each brace point and at each end of the Z-section. The formulation does not account for the effects of an eccentrically applied load or the attachment of one flange of the Z-section to sheathing. However, Zetlin and Winter's formulation provides an excellent basis for the understanding of the behavior of brace forces for Z-section roof systems.

Because the majority of Z-section applications involve attachment of the top flange to sheathing, Needham (1981) set out to determine the forces in the sheathing in the absence of external restraints. He developed a mathematical model that assumed simply supported Z-sections, rigid panel diaphragm stiffness, no external lateral braces and allowed no translation between the Z-section and the panel. The uniform load on the sheathing was thought to be transferred to the purlin at an eccentricity of b/6, where b is the flange width. Using the restraint force developed by Zetlin and Winter ($R=U(I_{XY}/I_X)$) and equilibrating the externally applied torques due to the eccentrically applied load and the eccentric application of the sheathing at a distance of d/2 from the shear center, Needham arrived at the following equation for total lateral brace force:

$$P_L = W\left[\left(\frac{I_{XY}}{I_X}\right)(\cos\theta - 1) - \sin\theta + \frac{b}{3d}\right] \tag{1.2}$$

where W is the total load applied in the plane of the web for a system of Z-sections, d is the depth of the Z-section, b is the width of the top flange of the Z-section, and θ is the roof slope - angle between the vertical and the web of the Z-section. It should be noted that for small slopes, $\cos\theta \approx 1$ and Equation (1.2) reduces to;

$$P_L = W\left[\frac{b}{3d} - \sin\theta\right] \tag{1.3}$$

Needham found that Equation (1.2) correlated well with test results, although correlation was dependent upon the chosen eccentricity and the eccentricity did not always correspond to b/6.

Ghazanfari and Murray (1983) attempted to predict restraint forces using an iterative mathematical model. The model was based on a single purlin with the top flange attached to sheathing over a simple span subjected to three bracing configurations: end torsional restraints, end torsional restraints with three interior restraints applied at quarter points, and interior restraints at quarter points without end torsional restraints. In their formulation, translation between the purlin and sheathing was prevented. The mathematical model assumed no panel rotational stiffness, a vertical load eccentricity of b/3, rigid braces, and the horizontal restraint provided by the sheathing, W_h to be uniformly distributed along the top flange of the purlin. Ghazanfari and Murray quantified the amount of lateral force by imposing displacement compatibility between the top flange of the purlin and the sheathing, that is

$$u_v + u_{vt} + u_{2ndOrder} = u_h + u_{ht} + u_p \tag{1.4}$$

where

u_v = the lateral displacement due to the uniformly applied vertical load
u_{vt} = lateral displacement due to the torque of the gravity load acting on the purlin top flange
$u_{2ndOrder}$ = lateral displacement due to second order effects,
u_h = lateral displacement due to the lateral restraining forces
u_{ht} = lateral displacement due to torque of eccentric lateral restraint
u_p = lateral displacement of the diaphragm

Due to the inclusion of second order effects, the force in the sheathing is dependent upon the deflection of the sheathing but the deflection of the sheathing cannot be determined without knowing the force in the sheathing. The process is therefore iterative and a computer program was developed to arrive at a solution. Through their analysis, Ghazanfari and Murray determined the most critical parameters for determining lateral brace forces to be purlin span, sheathing diaphragm stiffness, the eccentricity of the load applied to the top flange, and the location of the purlin principal axes. They also determined that for systems with three intermediate braces, 2nd order effects were negligible.

Using the frame analysis program, STRUDL, Elhouar and Murray (1985a; (1985b) were able to apply the principles developed by Ghazanfari and Murray (1983) and expand them to system models with multiple purlin lines over multiple spans. Their models consisted of line elements with rotated principal axes representing the purlins placed in the model at the centroid of the purlin. To give the model depth, at intervals of L/12, line elements of length d/2 connected the purlin to the sheathing. At each rafter location, an element of length d/2 connected the purlin line element to a fixed external restraint. The sheathing was modeled as a truss with chevron style diagonals. The sheathing had no rotational stiffness and was modeled to have a diaphragm stiffness, G', of 2500 lb/in. The diaphragm stiffness was chosen as an upper bound above which increases in diaphragm stiffness had little effect on restraint forces based on the work of Ghazanfari and Murray (1983). Included in the model was an assumed load eccentricity of b/3, applied as a torque in the model along the centroidal axis of the purlin. The model was calibrated to the full scale laboratory test results of Curtis and Murray (1983) and quarter scale experimental test results of Seshappa and Murray (1985).

Elhouar and Murray modeled three restraint configurations: end restraints, mid-span restraints and third point restraints. Restraint was applied as a rigid restraint at the top of the purlin (in the plane of the sheathing). A parametric study using the results of the models was performed and equations for end restraints, mid-span restraints and third-point restraints were developed for flat slope roofs. The equations were corrected based on the results of Seshappa and Murray to include roof slope. The single span equations developed are a function of the top flange width, b, the purlin depth, d, the purlin thickness, t, and the number of purlins restrained, n_p. Multiple span systems were subject to the same parameters, but had the additional parameter of span length, L, included in the equation formulation. A significant improvement over previous prediction methods was introduced in the n_p parameter. This parameter attempted to account for a system effect observed in laboratory tests whereby as the number of purlin lines increased, the restraint force per purlin decreased.

The model developed by Elhouar and Murray was revisited by Danza and Murray (1998) to evaluate two additional restraint configurations: quarter points and third points + supports. Like the Elhouar and Murray study, the models investigated only represented a flat slope roof and a panel diaphragm stiffness of 2500 lb/in. From the results of the models a parametric study was performed and equations similar to those developed by Elhouar and Murray were derived.

Neubert and Murray (1998; (2000)) also used the Elhour and Murray frame element model to develop a series of prediction equations. The research was focused upon developing equations based upon mechanics rather than heavy reliance upon parametric studies and included diaphragm stiffness in the formulation. The finite element models used by Neubert and Murray assigned different properties to the elements connecting the purlin to the external supports, accounted for roof slope by varying the vertically and horizontally applied loads, and varied the diaphragm stiffness by adjusting the properties of the members representing the purlin sheathing. The analysis investigated the affects of the eccentricity of the gravity load acting through the top flange of the purlin by evaluating both a zero eccentricity load case and a load case with an applied eccentricity of b/3.

The equation developed by Neubert and Murray was based on the theoretical work developed by Zetlin and Winter. Using a free body diagram of a purlin with the horizontal brace force introduced by Zetlin and Winter acting at the centroid of the purlin. The vertical component of the gravity load (parallel to the web of the purlin) is assumed to act at some eccentricity along the top flange of the purlin, δb, and the downslope component of the gravity load acts horizontally in the plane of the sheathing. The free body diagram is shown in Figure (1.1).

With the extermal restraint, P_0, applied at the top flange, by summing moments about the base of the purlin and solving for P_0, Neubert and Murray arrived at the basic equation for restraint force for a single purlin:

$$P_0 = W\left[\left(\frac{I_{xy}}{2I_x} + \frac{\delta b}{d}\right)\cos\theta - \sin\theta\right] \tag{1.5}$$

To account for the effects of bracing configuration, diaphragm stiffness, and system effects, the

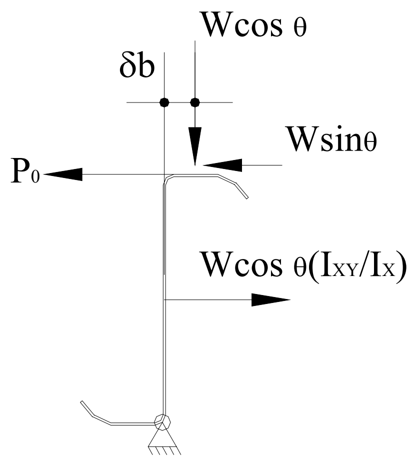

Figure 1.1 Free Body Diagram Neubert and Murray Equation

restraint force for a single purlin is multiplied by several constants and multipliers developed from the analysis of the finite element models. Recommendations were made for supports, midpoint, third point, quarter point and third point + supports restraint configurations over both single and multiple spans.

Hancock et al. (2002) used a finite element model that implemented the modifications introduced by Neubert and Murray to the Elhouar and Murray model. They further modified the model by including the warping torsional restraint of the purlin and looked at the effects of using a bridging system which provides rotational restraint in addition to lateral restraint to the purlin. Tests were performed to validate the models and it was concluded that the mode used by Neubert and Murray with modifications could be used to predict bracing forces in systems where bridging provides rotational restraint.

Lucas et al. (1997a) developed a finite element model using the elasto-plastic finite element developed by Chin et al. (1994) to represent the purlin and through-fastened sheathing. Their model of a single purlin with two half spans of sheathing effectively represented the cross-sectional distortion of the purlin section and the rotational and diaphragm restraint of the sheathing. The model divided the purlin web into four elements, flanges into two elements, and flange lips into single elements. Rib elements were included in the representation of the sheathing. Gravity load was applied directly to the sheathing and attachment between the purlin and the sheathing was made at the node at the center of the top flange of the purlin, effectively creating an eccentricity of $\delta = 1/2$ to the gravity load. The model was compared to several tests and was able to predict within 5% the failure load of purlins subjected to uplift loading over single, double and triple spans. The failure mode in the tests and predicted by the models was by local buckling of the free flange.

To reduce the computational time of their finite element models, Lucas et al. (1997b) provided means to represent the sheathing as a series of rotational and translational springs applied at the middle nodes of the purlin top flange rather than as finite elements. To determine the appropriate diaphragm stiffness of the springs, several “Double Beam Shear Tests” were performed on common sheathing profiles available in Australia. It was determined that the finite element model was not sensitive to diaphragm stiffness values in the range of typical profiles so a “standard” diaphragm stiffness value of 1000 kN/rad (224 kips/rad) was adopted. Rotational stiffness of the sheathing was determined from “Torsional Restraint Tests” performed on typical sheathing profiles. Although the model was sensitive to the rotational restraint of the sheathing in the range of tested values, it was found that rotational stiffness was primarily a function of purlin thickness and depth and independent of the panel type. Comparing this simplified model to laboratory test results, the researchers found that they could accurately predict within 10% the local buckling failure load of Z- and C- sections subjected to uplift loadings.

Using Generalized Beam Theory (GBT), Heinz (1994) developed differential equations to describe the flexural and torsional behavior of a Z-section considering the lateral and torsional resistance provided by the sheathing at the top flange of the Z-section. His analysis considered the lateral restraint provided by the sheathing to be rigid but incorporated the finite stiffness of the torsional restraint provided by the sheathing. He recognized that the flexibility of the Z-section-to-sheathing connection was a function of the bending of the sheathing, local deformation of the sheathing screw, deformation of the insulation between the sheathing and Z-section, and the local deformation of the top flange of the Z-section at the screw hole. Heinz outlined a test procedure to quantify the torsional stiffness of the connection between the purlin and sheathing. Using the finite difference method, Heinz solved the differential equations from GBT for uniformly loaded single and twin-span systems and provided solution curves of the maximum rotation and warping moment. Based on the first order deformation of the Z-section, solution curves for second order magnifiers are provided.

1.3.2 Experimental Testing to Determine Lateral Restraint Forces

Needham (1981), in support of his analytical developments, performed tests on a flat slope, single span system with two purlins spaced at 5 ft 0 in. and connected by sheathing panels. The purlins were restrained laterally at the supports and the restraint forces were measured to be approximately 10% of the applied gravity load.

Tests performed by Ghazanfari and Murray (1982) showed negligible differences in restraint forces for diaphragm stiffness values greater than 1500 lb/in and that second order effects were negligible in cases where intermediate braces were applied. They performed nine tests using a two purlin line setup over a single span. Several bracing configurations and panel diaphragm stiffness values were investigated.

Curtis and Muray (1983) investigated the difference in restraint forces with respect to the number of purlin lines by testing systems with two, six and seven purlin lines. The tests were performed on flat slope, single spans with restraints applied at the ends (support restraints). The results of the tests showed the existence of system effects, the phenomenon by which as the number of restrained purlins is increased, the restraint force per purlin decreases.

Seshappa and Murray (1985) developed quarter scale models to evaluate mid-points, third points and supports restraint configurations over single and multiple spans with multiple purlins. A total of 28 tests were performed, with one series of tests investigating slopes between 0:12 and 1.5:12. Their tests showed that the difference in restraint force for sloped roofs could be accounted for by subtracting the downslope component of the gravity force from restraint force on a flat slope roof.

Rivard and Murray (1986) tested supports, mid-points and third points restraints configurations using standing seam sheathing on systems of purlins over single and multiple spans. The tests showed that the equations developed by Elhouar and Murray (1985b), though initially based upon through-fastened systems, could be applied to systems with standing seam sheathing.

Lee and Murray (2001) performed full scale tests on two and four purlin line systems over single and multiple spans. They investigated supports, midpoint, third point, quarter point and third point + support restraint configurations using both through-fastened and standing seam sheathing. The specimens were tested on pitches ranging between 0:12 and 4:12. The tests showed that the restraint force is linear with respect to the applied load. When the test results were compared to the prediction equations developed by Elhouar and Murray (1985b) and those of Danza and Murray (1998), the correlation was inconsistent. Better correlation existed between the test results and the equations proposed by Neubert and Murray (1998). The best correlation was realized for single span tests with through-fastened sheathing for supports, third points and midpoints restraints, although the correlation was dependent upon the chosen eccentricity of the load applied to the purlin top flange. There were greater inconsistencies between the various prediction methods and the tests for standing seam systems and multi-span systems.

1.3.3 Current Design Practice

Section D3.2.1 of the *North American Specification for the Design of Cold-Formed Steel Structural Members with Commentary* (2001) provides recommendations for the bracing forces of C- and Z-sections with one flange attached to sheathing. Provisions are provided for single and multiple-span roof systems with lateral restraints applied at the supports, third points or midspan of the purlin. The prediction method is based on the work by Elhouar and Murray (1985b) in which a parametric study using finite element models was performed. The restraint force for Z-sections is a function of the total gravity load between supports, W, purlin top flange width, b, depth of the section, d, thickness of the purlin, t, number or restrained purlins, n_p, and for multi-span systems, the span length, L. For example, the lateral restraint force, P_L of a single span purlin system with restraints at supports is

$$P_L = 0.5\left[\frac{0.220b^{1.22}}{n_p^{0.72}d^{0.90}t^{0.33}}\cos\theta - \sin\theta\right]W \tag{1.6}$$

The equations were originally developed from tests and finite element models of flat slope roof systems. Roof slope, θ, is accounted for by multiplying flat slope restraint force by cosθ and subtracting out the downslope component of the gravity load, Wsinθ. A positive result from Equation 1.6 indicates needed resistance to upslope translation (at low roof slopes) while a negative result indicates needed resistance to downslope translation (higher roof slopes).

1.4 Objectives and Methods

The metal building industry is very competitive and the systems utilized are extremely efficient. The current methods for predicting lateral restraint forces often predicted forces that seemed unreasonable to the designer or equations were improperly applied. The goal of this research was to develop an improved means of predicting lateral restraint forces in Z-section supported roof systems. A greater understanding of Z-section behavior was sought so that the prediction method would have a greater foundation in mechanics. The many manufacturers have different philosophies about the most efficient roofing system configurations and are resistant to standardization. Each manufacturer has different sheathing and means of connecting the sheathing, Z-section-to-rafter attachments, and lateral bracing mechanisms. Substantial research and development has been invested in determining the most efficient configuration from both a structural and installation approach. Each manufacturer has confidence and experience with its own roof system, so there is reluctance to change. Consequently, the ultimate objective was to develop a method to accurately predict the lateral restraint forces in Z-section roof systems that is flexible enough to accommodate the wide variety of roof systems in use in industry today. The result is the Component Stiffness Method which provides the needed flexibility to a good degree of accuracy, but at the expense of simplicity of calculations.

The research program began with full scale tests of sloped Z-section roof systems to supplement the limited number of tests of sloped systems, as the majority of tests had been performed on flat slope systems and only the tests by Lee and Murray (2001) had considered roof slope. Tests were performed on single 20 ft span systems with two, four and six Z-section lines and continuous span systems with six purlin lines. Both through-fastened sheathing and standing seam sheathing with an articulating clip were investigated. The test program investigated five bracing configurations for each system: supports, third points, midpoints, quarter points and third points plus supports. In each test, measurements of the restraint force were taken at incremental roof pitches from 0:12 to 4:12 at a load level of approximately 20 psf. The specimens were tested in the elastic range and none were taken to failure load. In all, 40 tests were performed. A more detailed description of the tests and a full summary of the results are provided in Seek and Murray (2004)and in Appendix II.

In the next phase of research, two finite element models were developed and compared to the laboratory test results as well as the tests performed by Lee and Murray (2001). The first model was based on the Elhouar and Murray (1985) model including the modifications by Nuebert and Murray (1999). Further modifications were made to the model to improve correlation with the laboratory test results. Recommendations are made for use of this model for predicting lateral restraint forces in appended Paper I. A fairly simple model to construct, this frame finite element model provides a good means of predicting lateral restraint forces on simple roof systems for typical design practice.

The second finite element model was developed using the structural analysis software SAP 2000 Version 8.3 by Computers and Structures, Inc. The first order linear elastic model utilizes shell elements to represent the purlin and sheathing with loads applied uniformly to the sheathing. The model is a good representation of a Z-section roof system in the elastic range and provides an excellent means of predicting lateral restraint forces particularly for complex configurations and loadings. Recommendations are made for the practical use of this model in design in appended Paper I, although due to its size and complexity, is more suited for research and development than typical design.

The final phase of the research involved the development of a calculation method for predicting lateral restraint forces. To develop prediction equations, a database of models was developed to investigate the effects of different Z-section cross sectional properties, sheathing diaphragm stiffness, sheathing to Z-section connection rotational stiffness, span, and restraint height. In addition to the restraint force, moments in the sheathing and rafter support as well as the lateral displacement of the system were extracted from each model. Each of the extracted forces or moments and the corresponding displacement from each model was then used to develop equations for the stiffness of each of the components of the system. The forces generated by the system are then distributed according to the relative stiffness of each of the components of the system, hence the Component Stiffness Method.

2. Component Stiffness Method

The Component Stiffness Method uses a mechanics based approach to determine the lateral restraint forces in Z-section roof systems. Solution of the problem begins with determining the flexural behavior of the Z-section with fully rigid lateral restraints. The deformed shape of the Z-section is quantified accounting for the influence of the rotated principal axes of the Z-section and the effects of the diaphragm and rotational stiffness of the sheathing. The restraint force determined considering rigid restraints provides an upper bound solution to the problem. However, all restraint configurations have some flexibility, allowing the lateral movement of the top flange of the Z-section at the restraint location. A small amount of movement is permissible and in permitting movement, some of the force generated is distributed to the system due to the inherent resistance of the system. The stiffness of the resisting components of the system must therefore be computed and compared to the stiffness of the restraint to determine the net restraint force.

2.1 Flexural Behavior of Single Span End Restrained Z-section

The flexural behavior of a Z-section in a roof system is complicated due to the interaction between the sheathing and Z-section and the fact that the principal axes of the section are rotated relative to the plane of the roof sheathing. However, the interaction between the two can be reconciled by enforcing compatibility of the unrestrained lateral displacements of the section at midspan with the restoring displacements of the resisting sheathing. The behavior of a Z-section with end restraints provides the basis for the Component Stiffness Method. A detailed discussion of the basic flexural behavior is included in appended Paper II.

2.1.1 Behavior Neglecting Sheathing Rotational Restraint

In the analyses, loads are applied to a Z-section as shown in Figure 2.1. To account for roof slope, θ, the uniformly applied gravity load, w, is divided into a vertical component, $wL\cos\theta$, acting parallel to the plane of the Z-section web and a downslope component, $wL\sin\theta$, that acts in the plane of the sheathing. The vertical component of the gravity load is assumed to act at some eccentricity, δb, on the top flange of the Z-section as proposed by Ghazanfari and Murray (1983). Considering the vertical component acting eccentrically on the top flange, the lateral displacement at the top flange of the Z-section (the sheathing elevation) is determined initially by ignoring the resistance provided by the sheathing. This "unrestrained" displacement is a combination of the horizontal deflection and rotation of the Z-section at mid-span. The Z-section deflects horizontally (perpendicular to the plane of the web) because the principal axes are rotated relative to the plane of the web. Using the conventional constrained bending deflection formula for mid-span deflection, the modified moment of inertia and the fictitious horizontal force introduced by Zetlin and Winter (1955), the lateral deflection of the Z-section resulting from a uniformly applied load is calculated. Using the torsional formulas of Carter and Seaburg (1997), the rotation of the section at mid-span due to the uniformly applied torque because of the top flange load eccentricity is determined. Using a small angle approximation, the lateral displacement of the top flange of the Z-section relative to the shear center is the rotation of the section at mid span multiplied by one-half the depth of the section. The net unrestrained displacement of the top flange is the sum of the horizontal displacement, $\Delta_{x,cen}$, and the displacement due to rotation of the section, $\Delta_{x,torsion}$, as shown in Figure 2.2.

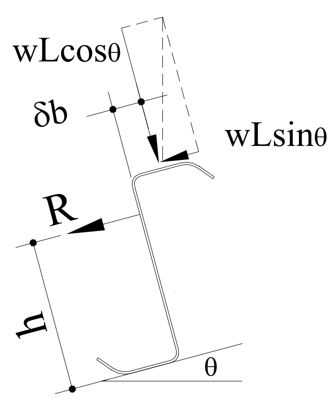

Figure 2.1 External Forces Acting on Z-section

In roof systems, uniform resistance to the lateral movement is provided by the sheathing. The diaphragm, perpendicular to the web of the purlin, will develop a uniform force, w_{rest}, resisting this lateral movement. Again, using the modified moments of inertia of Zetlin and Winter (1955), the lateral restoring displacement of the Z-section due to this uniform restraint force, $\Delta_{x,restoring,center}$, in the sheathing can be quantified. Because the sheathing applies the uniform restraining force at the top flange of the Z-section, it causes torsion of the Z-section.

The rotation of the Z-section and corresponding lateral deflection relative to the shear center at mid-span, $\Delta_{x,restoring,torsion}$, are quantified in the same manner as the unrestrained displacement.

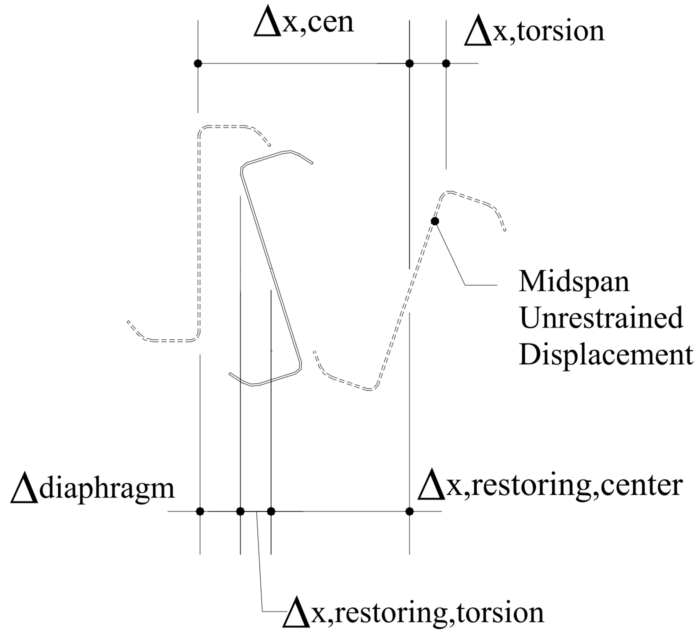

Figure 2.2 Unrestrained and Restoring Displacement

The uniform restraint force generated by the sheathing also causes deformation of the sheathing. It is assumed that all of the deformation of the diaphragm is due to shear deformation and bending deformations are considered negligible. For a sloped roof, the downslope component of the gravity load acting in the plane of the sheathing causes additional deformation of the diaphragm. The net displacement of the diaphragm, $\Delta_{diaphragm}$, is the sum of these two deflections.

Referring to Figure 2.2, by equating the unrestrained displacements with the restoring displacement due to sheathing resistance, the magnitude of the uniform restraint force in the sheathing is

$$w_{rest} = w \cdot \sigma \tag{2.1}$$

where

$$\sigma = \frac{\dfrac{5\left(\dfrac{I_{XY}}{I_X}\cos\theta\right)L^4}{384EI_{mY}} + \dfrac{(\delta b\cos\theta)d}{2}\dfrac{a^2\beta}{GJ} + \dfrac{L^2\sin\theta}{8G'\mathrm{Width}}}{\dfrac{5L^4}{384EI_{mY}} + \dfrac{d^2}{4}\dfrac{a^2\beta}{GJ} + \dfrac{L^2}{8G'\mathrm{Width}}} \tag{2.2}$$

In the above equation, L is the span of the Z-section, E is the modulus of elasticity of the Z-section, I_{mY} is the modified moment of inertia developed by Zetlin and Winter (1955), G is the shear modulus (11,200 ksi), J is the polar moment of inertial of the Z-section, G' is the shear stiffness of the diaphragm and Width is the tributary width of the diaphragm perpendicular to the span of the Z-section. Equations for the torsional terms, a, which accounts for the torsional warping stiffness of the Z-section, and β, which is a constant based on the torsional and span properties of the Z-section, are provided in the summary of nomenclature provided in Section 6 of this document. The above equation, therefore gives the uniform force transferred from a uniformly loaded Z-section to the sheathing attached to its top flange taking into account roof slope, eccentric location of gravity force on top flange, and diaphragm stiffness. The equation assumes that the end restraint is perfectly rigid, preventing movement of the top flange at the ends of the Z-section, and the equation ignores the rotational resistance provided by the sheathing. For ease of calculations, it is convenient to define σ as the proportion of the uniformly applied vertical load transferred into uniform force in the sheathing. The uniform restraint force, w_{rest}, is resolved entirely within the sheathing and the restraint force that must be resisted externally may be found by summing moments due to the externally applied loads about the base of the Z-section, or

$$R = \frac{wL}{h}(\delta b \cos\theta - d \sin\theta) \tag{2.3}$$

where, w is the gravity load applied uniformly along the length of the Z-section, L is the span of the Z-section and h is the height along depth of the Z-section measured from the base at which the horizontal restraint is applied.

2.1.2 Behavior Including Sheathing Rotational Restraint

The above formulation neglects an important part of the purlin-sheathing system, the rotational resistance to Z-section torsion provided by the sheathing. The rotational stiffness of the sheathing has a significant effect on the behavior of the Z-section, reducing the rotation of the Z-section through the development of moments along the length of the Z-section. The moments developed in the sheathing, however, affect the amount of force that must be restrained by the external restraints. The effect of the rotational stiffness of the sheathing is presented in detail in Paper III in the Appendix.

For a Z-section with end restraints, the rotation of a Z-section is restricted at its ends and increases to maximum at mid-span, Φ, as shown in Figure 2.3 (a). The variation of the rotation is approximated as parabolic along the length of the Z-section. The connection between the sheathing and the Z-section resists this rotation through the development of a moment along the length of the Z-section, $M_{torsion}$, as shown in Figure 2.3 (b). The moment in the sheathing is proportional to the rotation of the Z-section and the stiffness of the sheathing's resistance to the rotation of the Z-section, K_{mclip}, is defined as the moment developed in the connection per unit rotation of the Z-section per unit length along the span. The moment caused by the resistance of the sheathing results in an additional rotation of the Z-section, $\Phi_{Mtorsion}$, as shown in Figure 2.3 (b). The net rotation of the purlin, Φ_{net}, is the sum of the rotation caused by the eccentrically applied gravity load, the rotation caused by the uniform lateral resistance of the sheathing at the top flange, and the rotation due to the sheathing moment, or

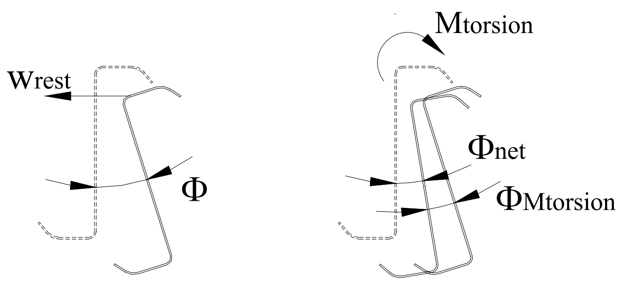

(a) Rotation without Rotational Resistance *(b) Net Rotation with Rotational Resitance*

Figure 2.3 Rotation of Z-section at Midspan

$$\phi_{net} = \left(w(\delta b \cos\theta) - w_{rest} \frac{d}{2} \right) \frac{a^2\beta}{GJ} - \phi_{net} \cdot K_{mclip} \left(\frac{\kappa}{GJ} \right) \tag{2.4}$$

Equation (2.4) is simplified to yield

$$\phi_{net} = \left(w(\delta b \cos\theta) - w_{rest} \frac{d}{2} \right) \tau \tag{2.5}$$

Where

$$\tau = \frac{\dfrac{a^2\beta}{GJ}}{1 + K_{mclip} \dfrac{\kappa}{GJ}} \tag{2.6}$$

An equation is provided in the nomenclature of Section 6 for the torsional term, κ, which is a constant based on the torsional and span properties of the Z-section.

The uniform restraint force equation (Equation (2.2)) is modified to account for this change in rotation by substituting in the torsional term τ in place of $a^2\beta/GJ$. Therefore, including the effects of the rotational stiffness of the sheathing, the proportion of the uniformly applied gravity load transferred to the uniform restraint force in the sheathing is

$$\sigma = \frac{\dfrac{5\left(\dfrac{I_{XY}}{I_X}\cos\theta\right)L^4}{384EI_{mY}} + \dfrac{(\delta b\cos\theta)d}{2}\tau + \dfrac{L^2\sin\theta}{8G'\mathrm{Width}}}{\dfrac{5L^4}{384EI_{mY}} + \dfrac{d^2}{4}\tau + \dfrac{L^2}{8G'\mathrm{Width}}} \tag{2.7}$$

Upon solving for the uniform restraint force provided by the sheathing, the moment generated in the sheathing due to the torsional rotation of the Z-section is determined. This moment is determined by integrating the moments along the length of the Z-section assuming a parabolic distribution along the span of the Z-section. The resulting moment, referred to as $M_{parabolic}$ in appended Paper III and $M_{torsion}$ in appended Paper IV is equal to

$$M_{Torsion} = \tfrac{2}{3}K_{MClip}\cdot wL\left(\sigma\frac{d}{2} - (\delta b\cos\theta)\right)\tau \tag{2.8}$$

A second moment is generated in the connection between the Z-section and sheathing due to local deformation of the top flange of the purlin. This moment was accounted for by a multiplier in appended Paper III and later modified in appended Paper IV to equal

$$M_{local} = -wL\cdot\delta b\cos\theta\cdot k_{local} \tag{2.9}$$

where

$$k_{local} = \frac{K_{MClip}}{K_{MClip} + \dfrac{Et^3}{3d}} \tag{2.10}$$

In the above equation, E is the modulus of elasticity of the Z-section, t is the thickness of the Z-section and d is the depth of the Z-section.

To include the moments generated in the sheathing, $M_{torsion}$ and M_{local}, the free body diagram of the Z-section changes as shown in Figure 2.4. The total external restraint force is determined by summing moments about the base of the Z-section due to the externally applied forces and the internally generated Z-section-sheathing moments.

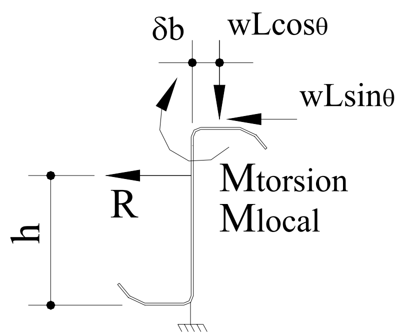

Figure 2.4 Free Body Diagram including Rotational Resistance of the Sheathing

$$R = wL \cdot \frac{\delta b \cos\theta - d \sin\theta}{h} + \frac{M_{torsion}}{h} + \frac{M_{local}}{h} \tag{2.11}$$

Equation (2.11) provides the total upper bound restraint force for a single purlin with rigid restraints at each end. Much of the restraint force is dependent upon the eccentricity of the gravity load on the top flange of the purlin. As discussed in appended Paper IV, the eccentricity at which the gravity load acts appears to be a function of the torsional stiffness of the purlin – the greater the torsional stiffness of the Z-section the less the effective eccentricity – and the local deformation of the Z-section top flange. Most analysis has been performed with an assumed eccentricity of δ= 1/3 which typically results in a good approximation of the restraint force. For low slope roofs, it is conservative to assume a higher eccentricity while at higher slopes, a lower value of eccentricity results in a conservative estimate of restraint force. A more detailed analysis of the interaction between the sheathing and Z-section is required to better understand this behavior.

2.2 Flexural Behavior of Single Span Z-sections with Interior Restraints

Conceptually, an end restrained Z-section poses less problems than one with internal restraints. For an end-restrained Z-section, all boundary restraints (vertical, lateral and rotational) are applied at the end of the Z-section and it is free to deflect at midspan (although partially restrained by the sheathing). In appended Paper II, some of the nuances of the behavior of a Z-section with interior restraints were introduced. For example, a Z-section not attached to sheathing, supported vertically and horizontally at the bottom flange at each end, restrained laterally at mid-span at the top flange, and loaded uniformly in the plane of the web as shown in Figure 2.5, has the tendency to deflect laterally but movement of the top flange is prevented by the mid-span restraint. To maintain equilibrium, the restraint force at the interior restraint must be zero. To maintain compatibility, the Z-section deforms at the ends and mid-span as shown in Figure 2.5.

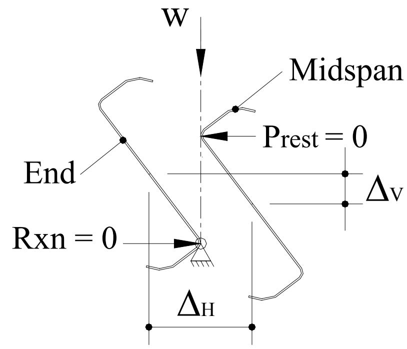

Figure 2.5 Displaced Shape of Z-section Restrained at Mid-Span

The behavior of a Z-section with an interior restraint at first glance, appears to have behavior quite different from that of one with end restraints. However with some modifications as discussed in appended Paper IV, the calculation of restraint forces for an interior restrained Z-section is similar to that of a Z-section with end restraints. Like the end restraint case, a uniform restraint force is generated in the diaphragm as it resists the lateral movement in the Z-section. In calculating this restraint force, there is a slight difference between an interior restraint case and supports restraint case. First, for a supports case, displacement compatibility is determined at the mid-span of the member. For an interior case, compatibility of the lateral displacements is taken at the restraint location, and the lateral movement of the top flange due to torsion of the section rotation is taken at mid-span for calculation simplicity. Accounting for these differences, Equation (2.7) is modified for a third point restraint configuration to yield

$$\sigma = \frac{\dfrac{11\left(\dfrac{I_{XY}}{I_X}\cos\theta\right)L^4}{972EI_{mY}} + \dfrac{(\delta b\cos\theta)d}{2}\tau - \dfrac{L^2\sin\theta}{18G'\text{Width}}}{\dfrac{11L^4}{972EI_{mY}} + \dfrac{d^2}{4}\tau + \dfrac{L^2}{9G'\text{Width}}} \tag{2.12}$$

To determine the magnitude of the restraint force generated, the rotation of the Z-section must be quantified. Like the supports restraint case, the uniform restraint force at the top flange of the Z-section in addition to the vertical component of the gravity load applied eccentrically to the top flange of the Z-section cause torsional rotation. This rotation, $\Phi_{Torsion}$ in Figure 2.6, represents the rotation of the mid-span relative to the end of the Z-section and is the same as for a supports restraint configuration. Because restraint is applied at the interior of the Z-section and there is flexibility in the diaphragm, there is an additional rotation of the end of the Z-section, Φ_{End} in Figure 2.6. Using a small angle approximation, this rotation is the deflection of the diaphragm, Δ_{diaph} in Figure 2.6, at the end of the Z-section divided by the depth of the Z-section and is constant along the length of the Z-section. The rotational stiffness of the sheathing resists the rotation of the Z-section and generates the moment

$$M_{torsion} = wL\left[\tfrac{2}{3}k_{mclip}\tau\left(\sigma\frac{d}{2} - \delta b\cos\theta\right) + \frac{L^2 k_{mclip}}{6G'\cdot Width\cdot d}\left(\frac{\sigma}{3} + \frac{\sin\theta}{6} - \frac{\delta b\cos\theta}{2d}\right)\left(1 - \tfrac{2}{3}k_{mclip}\tau\right)\right] \quad (2.13)$$

The first term in the brackets represents the moment due to the rotation of the midspan of the Z-section relative to the end of the Z-section, $\Phi_{Torsion}$, and is identical to the moment generated for a supports restraint configuration. The second term represents the moment generated due to the end rotation, Φ_{End}, of the Z-section for a third points restraint configuration. The overturning moment is the sum of the moments about the base of the Z-section due to the externally applied loads and the moment generated in the sheathing due to torsional effects and local deformation effects given by Equation (2.11).

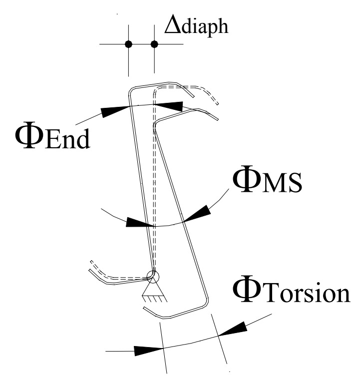

Figure 2.6 Rotation of Z-section with Interior Restraints

2.3 General Procedure

The restraint force from Equation (2.11) represents the force generated in an end restrained or interior restrained Z-section provided that the restraint rigidly restricts movement of the top flange of the Z-section at the restraint location. It represents the effects of load eccentricity on the top flange of the purlin, the effect of the downslope component of the gravity load in the plane of the sheathing, and the effects of the rotational deformation of the Z-section and the resistance of the sheathing to this deformation. This force is an upper bound restraint force assuming a rigid restraint. Real lateral restraints, however, have some flexibility. As the restraint permits lateral deflection of the top flange at the restraint location, resistance is developed by the connection between the sheathing and the purlin and the rafter connection. This inherent resistance of the Z-section is referred to as a system effect which, through this inherent resistance of the Z-section, reduces the external restraint force.

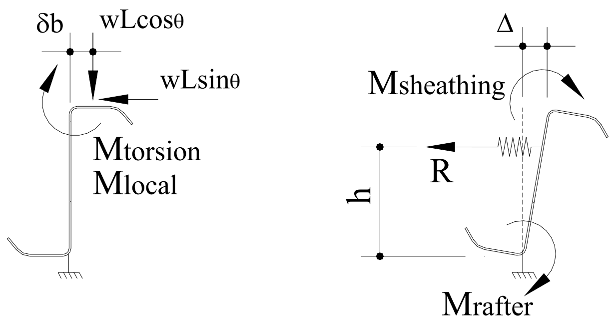

(a) Generated Forces and Moments (b) Resisting Forces and Moments

Figure 2.7 Free Body Diagram of Z-section

2.3.1 Single Purlin with Flexible Restraints

The restraint force given by Equation (2.11) is the upper bound restraint force considering the restraint to be rigid. As flexibility is introduced at the restraint, the top flange of the Z-section moves laterally at the restraint location. The Z-section is approximated to rotate about the support location and using a small angle approximation, the rotation of the Z-section is the lateral displacement of the top flange at the restraint divided by the depth of the Z-section. As the Z-section rotates, moments are developed in the connection between the Z-section and the sheathing and at the rafter location as shown in Figure 2.7. Equilibrium of the Z-section is determined including these additional moments

$$R = wL \cdot \frac{\delta b \cos\theta - d \sin\theta}{h} + \frac{M_{Torsion}}{h} + \frac{M_{Local}}{h} + \frac{M_{Sheathing}}{h} + \frac{M_{Rafter}}{h} \qquad (2.13)$$

The force at the restraint is related to the moments in the sheathing and rafter through the stiffness of each of these "components". The stiffness of the restraint, K_{rest}, is defined as the force at the top flange of the Z-section per unit lateral displacement of the top flange of the Z-section. The sheathing moment stiffness, K_{shtg}, is defined as the total moment developed along the length of the Z-section per unit lateral displacement of the top flange of the Z-section. The rafter moment stiffness, K_{rafter}, is defined as the moment developed in the connection between the rafter and Z-section per unit lateral displacement of the top flange of the Z-section at the support location. By relating the sheathing and rafter moments to the restraint force through the relative stiffness of each of the components, the restraint force is

$$R = \left(wL \cdot \frac{\delta b \cos\theta - d \sin\theta}{h} + \frac{M_{Torsion}}{h} + \frac{M_{Local}}{h} \right) \cdot \frac{K_{rest}}{K_{rest} + K_{shtg} + K_{rafter}} \tag{2.14}$$

2.3.2 Multiple Purlin System

In multiple purlin line systems, restraint is typically applied to only a few of the purlin lines in the system. In development of the equations, it is assumed that there is some mechanism that transfers the restraint force from the system Z-sections, those Z-sections not directly restrained, to the external restraints. In through-fastened sheathing systems, the sheathing transfers this force. In standing seam systems where lateral movement between the sheathing and Z-section is permitted by flexible clips, some external mechanism such as strapping must be provided to help transfer the restraint force.

To relate each purlin line, the system of purlins is approximated as a single degree of freedom system. The mechanism that transfers the restraint force from the system purlins to the restraint is assumed to be rigid. The displacement of the top flange of each purlin at the restraint location is therefore the same. The force in each component of the system is related to the lateral deflection of the system at the restraint location through the stiffness of each component. The total stiffness of the system then is the sum of the restraint stiffness, rafter stiffness, and sheathing stiffness for each purlin.

2.3.3 Stiffness of Components

A detailed discussion of the development of stiffness values for the restraints, the rafter connection and the sheathing is provided in appended Paper III. The stiffness values reported in appended Paper III are defined according to the force or moment in each component relative to the deflection at the *restraint height*, e.g. the distance from the base of the purlin to the elevation at which the restraint is applied. With further developments in the Component Stiffness Method, it became apparent that it is more efficient to consider the stiffness as the force in each component relative to the deflection at the top flange of the purlin. Changes made to the equations are provided herein.

Restraint Stiffness. Restraints at the frame line are provided by either antiroll anchorage devices which resist the movement of the purlin with a stiffened plate as shown in Figure 2.8(a) or by a discrete brace which provides lateral resistance at a discrete location along the depth of the purlin and is typically used in conjunction with flange bolts as shown in Figure 2.8(b).

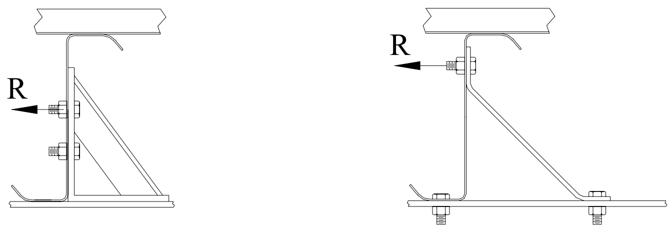

(a) Anti-roll Anchorage *(b) Discrete Brace*

Figure 2.8 End Restraints

The stiffness of each restraint is defined as the force developed at the top flange of the Z-section at the restraint per unit displacement of the top flange at the restraint location. As shown in Figure 2.9, the deformation at the restraint is the combination of the deformation of the restraint device, Δ_{device}, and the deformation of the web of the purlin relative to the restraint, Δ_{config}.

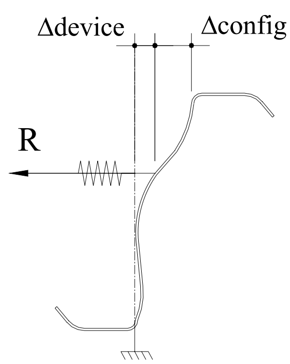

Figure 2.9 Deformation of Z-section at Support Restraint

The total stiffness at the restraint, provided in Equation (2.15) is the combination of the stiffness of the device at the height at which the restraint is applied, and the stiffness of the web of the purlin as the force is transferred transverse to the web of the purlin from the top flange to the height of the restraint. The development of stiffness values for each case is discussed in more detail in appended Paper III.

$$K_{rest} = \frac{\left(\frac{h}{d}\right)^2 K_{device} \cdot K_{config}}{\frac{h}{d} K_{device} + K_{config}} \tag{2.15}$$

Equation 2.15 deviates from the equivalent equation in appended Paper III as it is multiplied by h/d. It was found in subsequent analyses that it is more convenient to define the restraint stiffness at the top flange of the Z-section then at the height of the restraint. Therefore, Equation 2.15 provided here defines the restraint stiffness as the force at the top flange per unit displacement of the top flange whereas Equation (4) in appended Paper III defines the restraint stiffness as the force at the restraint height per unit displacement of the top flange of the purlin.

Appended Paper III provides a means of approximating the configuration stiffness, K_{config}, for two restraint configurations, an antiroll clip and a discrete brace. The relationship for approximating the configuration stiffness for a discrete brace is based upon mechanics and modified based on the results of finite element analysis. The equation will typically overestimate the stiffness of the restraint configuration, which will lead to a conservative approximation of restraint force but may underestimate the amount of deflection in the system. Conversely, for an antiroll anchorage device, the relationship for approximating the configuration stiffness is based solely upon mechanics as no finite element analysis or tests were performed. Antiroll anchorage devices typically posses greater strength than is required in most roof systems but, depending on the height of the antiroll anchorage device, may not have the necessary stiffness to laterally restrain the top flange of the Z-section. Consequently, the prediction equation for the configuration stiffness of an antiroll anchorage device will typically underestimate the stiffness which will lead to a conservative approximation of lateral displacement but may underestimate the amount of force resisted by the antiroll anchorage device. The original equation for the configuration stiffness of an antiroll anchorage device presented in Paper appended III (Equation 6) for simplicity has been reduced to

$$K_{config} = \frac{3Eb_{ar}t^3}{(d-h)^3}\left(\frac{d}{h}\right) \tag{2.16}$$

Equation (2.16) may therefore be substituted for Equation (6) in appended Paper III.

The restraint stiffness at the frame line may also be determined by a fairly simple test procedure outlined in detail in appended Paper V. In this test procedure, load is applied laterally at the top flange of a short segment of Z-section representative of the restraint device at the rafter. As load is applied, the lateral deflection of the top flange is measured. The net restraint stiffness, that is, the combined configuration and device stiffness, for the particular device and purlin is determined as the load applied at the top flange per unit displacement at the top flange.

Restraint stiffness for an interior restraint configuration consists of only the device stiffness and the configuration stiffness is assumed to be rigid, i.e. there is no deformation of the Z-section top flange relative to the restraint. The restraint is assumed to be applied at or as near as possible to the top flange of the Z-section (within 2 times the inside bend radius from the top flange). In doing so, deformation of the web at the restraint relative to the top flange is eliminated and the assumption of the configuration stiffness as rigid is valid. The restraint stiffness is therefore only a function of the device stiffness. Providing lateral restraint at mid-bay requires transferring the restraint force from the interior of the bay to the frame lines, such as a horizontal truss. The stiffness of the entire load path in transferring the load to the frame lines must be considered. Balancing of restraint forces of opposing Z-sections across the ridge of a structure was not considered as an interior restraint as a part of this research.

Rafter connection stiffness. The connection between the Z-section and rafter can posses considerable stiffness and provide resistance to the lateral forces developed in Z-section roof systems. In appended Paper III, for a supports restraint configuration, the rafter stiffness is categorized according to whether the Z-section is directly restrained or is a system Z-section. The restrained Z-section rafter stiffness is further subcategorized as either a discrete brace or antiroll anchorage. The rafter connection for system Z-sections is subdivided according to whether the rafter connection is flange bolted or a web plate connection.

Subsequent analysis has shown that solution of the problem may be simplified by eliminating the calculation of the rafter stiffness at the restrained purlin. For systems with discrete braces, the rafter stiffness is negligible and therefore the increased simplification warrants the elimination. For an antiroll anchorage configuration, the rafter stiffness is included in the modified configuration stiffness specified by Equation (2.16).

For an interior restraint configuration the connection at the rafter is approximated to be pinned. For a flange bolted connection configuration, this approximation is suitable and typically provides a conservative estimation of restraint force. If a web plate connection is used along the frame lines as shown in Figure 2.10(b), the web plate can provide considerable stiffness and invalidates the assumption of a pinned end for which the equations were developed. The prediction equations for an interior restraint configuration will not adequately predict restraint force or deflection in this case. The configuration should instead be considered a third points plus supports configuration.

Sheathing Stiffness. The connection between the Z-section and the sheathing can provide considerable stiffness to the resistance of lateral restraint forces. As the top flange of the Z-section at the restraint moves laterally due to the flexibility of the restraint, each Z-section is approximated to rotate as a rigid body about its base at the frame line. Through this rotation, a moment is developed in the connection between the Z-section and sheathing. The moment due to the rigid body rotation is uniform along the length of the Z-section. However, as was shown in Section 2.1.2, as the Z-section is subjected to a uniform torsional moment, the mid-span of the Z-section rotates relative to the ends, causing an additional moment with a parabolic distribution.

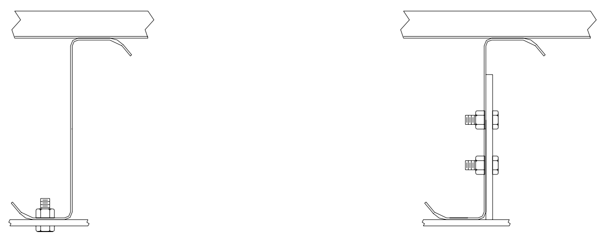

(a) Flange Bolted *(b) Web Plate*

Figure 2.10 Rafter Connections

Due to local deformation of the purlin, the moment is further modified from the results of finite element analysis.. The stiffness of the sheathing, K_{shtg} is defined as the total moment developed along the length of the purlin per unit lateral displacement of the purlin at the restraint location.

$$K_{shtg} = \frac{K_{mclip} L}{d}\left(\frac{\frac{1}{4}Et^3}{0.38K_{mclip} d + 0.71\frac{1}{4}Et^3}\right)\left(1 - \tfrac{2}{3}K_{mclip}\tau\right) \tag{2.17}$$

Because this moment varies with respect to the lateral deflection of the sheathing at the restraint, it is treated separately from the torsional moment developed in the sheathing. A more detailed description of the differences between the torsional moment and the sheathing stiffness moment is provided in appended Paper III.

In appended Paper III, a second equation for the sheathing stiffness is provided for a Z-section that is directly restrained. This equation takes into account the additional moment generated due to local deformation of the web at the restraint location. This increased moment effectively increases the sheathing stiffness. This additional effect is small and in the interest of simplicity of equations, Equation (2.17) can be used in lieu of Equation (23) provided in appended Paper III

2.3.4 *Calculation of Restraint Forces*

The total lateral stiffness of the system of Z-sections is the sum at each purlin of the restraint stiffness, the sheathing stiffness, and, for a supports restraint configuration only, the rafter stiffness, or

$$K_{total} = \sum K_{rest} + \frac{\sum K_{shtg} + \sum K_{rafter}}{d} \tag{2.18}$$

Note that this is a slight departure from Equation (2) in appended Paper III as the system sheathing and rafter moments are divided by depth, d, instead of restraint height, h, to normalize the stiffness at the sheathing level. Also, for simplicity, the restrained purlin sheathing and rafter stiffness is eliminated. For an interior restraint configuration, the connection between the rafter and the sheathing is assumed to be pinned so the rafter stiffness is eliminated and Equation (2.18) is reduced to Equation (9) as shown in appended Paper IV.

The total lateral force generated by the system of Z-sections is the sum of the upper bound forces calculated from Equation (2.11) for each individual Z-section. For a uniform system of purlins, that is the same purlin size with the magnitude of uniform load on each purlin the same, Equation (2.11) need only be calculated for a single purlin and multiplied by the number of purlins in the system. If the magnitude of the uniform load or the purlin size varies within a bay, Equation (2.11) must be calculated for each different purlin and the summed for all of the purlins in the bay.

To determine the total restraint force, the total lateral force in the system is multiplied by the ratio of the stiffness of the restraints to the total stiffness of the system, or

$$R = \sum \left(wL \cdot \frac{\delta b \cos\theta - d \sin\theta}{h} + \frac{M_{torsion}}{h} + \frac{M_{local}}{h} \right) \frac{\sum K_{rest}}{K_{total}} \tag{2.19}$$

The difference between the total upper bound lateral force and the total restraint force is the amount of load distributed to the system due to the system effects of the rafter and sheathing stiffness. To determine the distribution of forces between multiple restraints, the force in each individual restraint determined by multiplying the total restraint force by the ratio of the stiffness of the individual restraint to the total restraint stiffness.

2.3.5 System performance

There are two other aspects that must be considered when determining the effectiveness of the restraint. First, lateral deformation of the system must be considered. Lateral deflection should be checked at the restraint location as excessive deformation could lead to failure. In the event that adequate stiffness is not provided to limit deflection, the stiffness of the restraints can be increased by adding restraints or increasing the stiffness of the existing restraints. Lateral deflection also needs to be checked at the extremes of the system to ensure that the diaphragm has sufficient stiffness to transfer the forces along the length of the purlin to the restraints. Calculation of the lateral deflection of the mid-span of the system is provided in appended Paper III for a supports restraint configuration and the lateral deflection of the purlin ends for an interior restraint configuration is provided in appended Paper IV.

The second aspect critical to the performance of the restraints that must be considered is the force transferred from the sheathing to the purlin at the restraint location. From the results of finite element models, the force in the sheathing is transferred out over a small distance along the length of the purlin and can be significant, even exceeding the restraint force for a supports restraint configuration. This force must be determined to ensure that the fasteners between the sheathing and purlin have adequate capacity to transfer the restraint force.

3. Finite Element Model Analyses

3.1 Development of Finite Element Models for Predicting Lateral Restraint Forces

An existing finite element model was improved and a new model developed for predicting the lateral restraint forces in Z-section roof systems. The finite element models, calibrated to test results, allowed for the limited number of laboratory tests to be expanded to investigate the different variables in the development of the equations. The finite element models also provide a means of rational analysis to predict lateral restraint forces for more complex roof systems.

Improvements were made to the frame finite element model developed by Elhouar and Murray (1985) and modified by Neubert and Murray (1998). These improvements are discussed in detail in appended Paper I. The model uses frame elements to represent the Z-section and a truss system to represent the diaphragm. Modifications were made to the properties of Z-section elements and the diaphragm was redefined to make the properties more uniform. These modifications improved the correlation of the finite element models with the test results. The advantage of this model is the simplicity in which it can be set up. An engineering office with a basic frame analysis program can develop and analyze a roof system with this model. An entire roof can easily be modeled and run in a timely manner. The simplicity of the model has some disadvantages in that it approximates the behavior of the Z-section, particularly the end conditions. It does not capture the local deformations at the restraint locations and at the support locations.

A shell finite element model to predict lateral restraint forces that takes advantage of accessible finite element analysis programs available today was also developed. The first order linear elastic model uses shell finite elements to represent the purlin and sheathing. External restraints are modeled using frame finite elements and the connection between the purlin and sheathing is made by a spring element. Gravity loads are directly applied to the sheathing as area loads. A more detailed discussion of the development of the model is provided in appended Paper I. The model provides a fairly accurate and detailed approximation of a purlin system to predict restraint forces. Plots showing the correlation of the finite element model with the results of laboratory tests is presented in Appendix II "Results of Laboratory Tests of Lateral Restraint Forces" The model accurately represents the flexibility introduced to the system at the restraint location and the system has the flexibility to model different restraint methods and configurations (such as interior rotational restraints). The complexity of the model limits its usefulness for day to day design use, however. The shell finite element model is also limited in practicality based on the sheer size of the model. A three span model with 10 purlin lines can have upwards of 100,000 elements and run times can be significant.

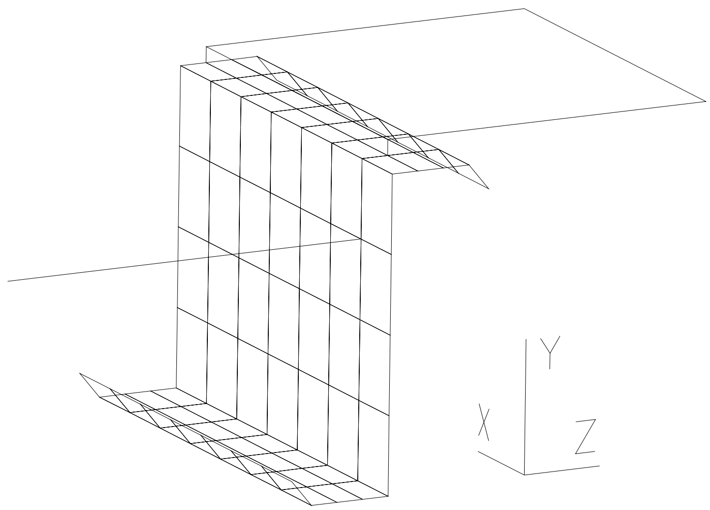

Figure 3.1 Representation of Elements in Shell Finite Element Model

3.2 Finite Element Model to Develop Prediction Equations

To develop prediction equations, a database of finite element models was evaluated. Four database series of finite element models were investigated. Upon completing each series, equations were developed and refined. As knowledge was gained in previous rounds, refinements to both the finite element model and the analysis procedure were made.

For the initial database of tests, a 10Z2.6 purlin (10 in. deep with a 2.6 in. wide flange) spanning 20 ft – 0 in. and spaced at 54 in. provided the basic purlin layout. Most tests were performed with eight purlin lines, however some tests were performed with four purlin lines. For each purlin/sheathing combination, five restraint configurations were investigated – supports, midpoints, third points, quarter points and third points + supports. The main variables influencing the restraint force are purlin thickness, rotational stiffness of the connection between the purlin and sheathing, and height of the external restraint relative to the web of the purlin. The purlin thicknesses were chosen to envelop the typical range of thicknesses used in the industry: 0.060 in., 0.097 in., and 0.135 in. Four link (connection between purlin and sheathing) rotational stiffness values were investigated: 500 lb-in/rad, 1000 lb-in/rad, 5000 lb-in/rad, and

10,000 lb-in/rad. Restraint was applied at three locations along the web of the purlin: at mid-depth, at ¾ depth from the base of the purlin and at the top of the purlin. Thus for each of the single span and multiple span systems, when looking at the five different restraint configurations the total number of models evaluated for both single span and three span through-fastened systems is 180 (five restraints times three purlin thicknesses times four link stiffness values times three restraint height locations = 180).

For the initial series of tests, the diaphragm shear stiffness of the through-fastened models was maintained at 27,500 lb/in. for consistency with the modeling performed by Neubert and Murray (2000) For most systems, a diaphragm stiffness above 10,000 lb/in is essentially rigid and it was found in preliminary tests of the finite element model that very little variation existed in restraint forces for diaphragms ranging in stiffness from 10,000 lb/in to 27,500 lb/in. The bending thickness of the sheathing was maintained at 0.33 in. corresponding to a moment of inertia of 0.036 in^4/ft width – typical for 26 ga. through-fastened panel with 1 1/4 in. ribs.

The second database series of tests investigated the effects of purlin depth and span on restraint forces. Two depths of purlins, 8 in. and 12 in, with a 2.6 in flange spanning 20ft – 0 in. and a 10 in. purlin with a 2.6 in flange spanning 30 ft – 0 in. were investigated. The same sheathing properties, range of purlin thicknesses and purlin-sheathing connection stiffness values as the first database series were used for the second series. The tests were only performed for a supports restraint configuration.

The third database series investigated the effects of the stiffness of the diaphragm on the restraint forces. All of the models utilized a 10Z2.6 purlin as was used for the first series of models. The same range of purlin thickness and sheathing – purlin connection rotational stiffness values as the first series were used. Diaphragm stiffness (G’) values of 250 lb/in, 1000 lb/in, 2500 lb/in and 7500 lb/in were investigated.

From each model, results were extracted and used to develop the Component Stiffness Method. The lateral restraint force at each location, the moment in the connection between the purlin and the sheathing at one ft intervals along the span of each purlin, and the moment at the purlin to rafter connection were recorded. In addition to these forces and moments, the lateral displacement of the top flange of the Z-section at the rafters, quarter points and third points was recorded. By relating the forces and moments to lateral displacement of the top flange of the Z-section at the restraint location, stiffness values for each of the components: restraints, rafter connection and sheathing, were derived. From each model, the restraint stiffness, the rafter connection stiffness of each purlin, and the sheathing stiffness of each purlin was assembled into a database. Using *SigmaPlot* Ver 8.0, stiffness equations for each of the components derived from mechanics were modified to improve correlation with the database values. The resulting equations are presented in appended Paper III.

4. Discussion, Conclusions and Future Work

The Component Stiffness Method is a valuable tool for both predicting lateral restraint forces in Z-section roof systems and predicting the performance of the roof system. The method has advanced the engineering community's understanding of the flexural behavior of Z-sections and the interaction between the Z-section and the sheathing. Because the method is based upon mechanics principles, it can be adapted to other bracing configurations not explicitly studied here.

Two types of finite element models have been presented for predicting lateral restraint forces. The first model, a frame finite element model, has been improved from the work of previous researchers. The improvements made have been based upon the results of laboratory tests. The simplicity of the model lends itself to day-to-day use in predicting lateral restraint forces for common bracing configurations. The second model uses shell elements to model the purlin and sheathing in a roof system. This model shows good correlation with test results and provides the most accurate representation of the roof system. The model is a valuable tool for research and development of alternative bracing systems and complex purlin and bracing configurations, but the size of the model and the number of elements limits its usefulness for routine analysis of lateral restraint forces in Z-section roof systems.

Thus far, only equations for single span systems have been derived using the Component Stiffness Method. The principles of the Component Stiffness Method apply to multiple span systems, however there are details of multiple span systems that must be worked out – particularly the effect of interaction of adjacent bays on the distribution of restraint forces. There are also several other common restraint configurations that the derived equations could account for, namely supports plus interior lateral restraints and supports plus interior rotational restraints.

There are several aspects of the finite element models that require further investigation. The interaction between the sheathing and the purlin in the generation of the effective load eccentricity requires further study. Systems of purlins with standing seam sheathing that incorporates lateral movement in the clip should be modeled perhaps with a nonlinear spring to better capture the behavior of purlins incorporating this type of system. Second order effects are considered negligible, but a more sophisticated finite element model would help to understand the second order behavior and help to discover cases where second order effects may pose problems.

5. References

Carter, C. J., and P. A. Seaburg. (1997). *Steel Design Guide #9, Torsional Analysis of Structural Steel Members*, American Institute of Steel Construction, Inc., Chicago, IL.

Chin, C. K., G. A. Al-Bermani, and S. Kitipornchai. (1994). "Non-Linear Analysis of Thin-Walled Structures Using Plate Elements." *International Journal For Numerical Methods in Engineering*, 37, 1697-1711.

Curtis, L. E., and T. M. Murray. (1983). "Simple Span Z-purlin Tests to Determine Restraint Force Accumulation." *Fears Structural Engineering Laboratory Report No. FSEL/MBMA 83-02*, University of Oklahoma, Norman, Oklahoma.

Danza, M. A., and T. M. Murray. (1998). "Lateral Restraint Forces in Quarter-Point and Third-point Plus Support Braced Z-Purlin Supported Roof Systems." *Research Report CE/VPI-ST-99/07*, Department of Civil and Environmental Engineering, Virginia Polytechnic Institute and State University, Blacksburg, VA.

Elhouar, S., and T. M. Murray. (1985a). "Stability Requirements of Z-Purlin Supported Conventional Metal Building Roof Systems." Annual Technical Session Proceedings, Structural Stability Research Council, Bethlehem, PA 343-353.

Elhouar, S., and T. M. Murray. (1985b). "Prediction of Lateral Restraint Forces for Z-purlin Supported Roof Systems." *Fears Structural Engineering Laboratory Report No. FSEL/AISI 85-01*, University of Oklahoma, Norman, Oklahoma.

Ghazanfari, A., and T. M. Murray. (1982). "Simple Span Z-purlin tests with Various Restraint Systems." *Fears Structural Engineering Laboratory Report No. FSEL/MBMA 82-01A*, University of Oklahoma, Norman, Oklahoma.

Ghazanfari, A., and T. M. Murray. (1983). "Prediction of the Lateral Restraint Forces of Single Span Z-purlins with Experimental Verification." *Fears Structural Engineering Laboratory Laboratory Report No. FSEL/MBMA 83-04*, University of Oklahoma, Norman, Oklahoma.

Hancock, G. J., J. Kiang, M. Bambach, L. Teh, and P. K. Ong. (2002). "Forces in Bridging and Bracing Systems for Roof Purlins with Concealed Fixed Sheathing." Department of Civil Engineering, University of Sydney, 8.

Heinz, D. A. (1994). "Application of Generalized Beam Theory to the Design of Thin-Walled Purlins." *Thin Walled Structures*, 19, 311-335.

Lee, S., and T. M. Murray. (2001). "Experimental Determination of Required Lateral Restraint Forces For Z-Purlin Supported, Sloped Metal Roof Systems." *CE/VPI-ST 01/09*, Virginia Polytechnic Institute and State University, Blacksburg, VA.

Lucas, F. G., G. A. Al-Bermani, and S. Kitipornchai. (1997a). "Modelling of Cold-Formed Purlin-Sheeting Systems - Part 1: Full Model." *Thin Walled Structures*, 27(3), 223-243.

Lucas, F. G., G. A. Al-Bermani, and S. Kitipornchai. (1997b). "Modelling of Cold-Formed Purlin-Sheetin Systems - Part 2. Simplified Model." *Thin Walled Structures*, 27(4), 263-286.

Needham, J. R. (1981). "Review of the Bending Mechanics of Cold-Formed Z-purlins," Department of Civil Engineering, University of Kansas, Manhattan, Kansas.

Neubert, M. C., and T. M. Murray. (1998). "Estimation of Required Restraint Forces in Z-Purlin Supported, Sloped Roofs Under Gravity Loads." *Research Report CE/VPI-ST-99/12*, Department of Civil and Environmental Engineering, Virginia Polytechnic Institute and State University, Blacksburg, VA.

Neubert, M. C., and T. M. Murray. (2000). "Estimation of Required Restraint Forces: Z-purlin Supported, Sloped Roofs Under Gravity Loads." *Proceedings of Structures Congress 2000 - Advanced Technology in Structural Engineering*.

North American Specification for the Design of Cold-Formed Steel Structural Members with Commentary. (2001). American Iron and Steel Institute, Washington, D.C.

Rivard, P., and T. M. Murray. (1986). "Anchorage Forces in Two Purlin Line Standing Seam Z-purlin Supported Roof Systems." *Fears Structural Engineering Laboratory Report No. FSEL/MBNA 86-01*, University of Oklahoma, Norman, Oklahoma.

Seek, M. W., and T. M. Murray. (2004). "Testing of the Lateral Restraint Force Requirments of Sloped Z-Purlin Supported Standing Seam and Through Fastened Roof Systems with Two, Four and Six Purlin Lines." *CE/VPI-ST 04/01*, Virginia Polytechnic and State University, Blacksburg, VA.

Seshappa, V., and T. M. Murray. (1985). "Experimental Studies of Z-purlin Supported Roof Systems Using Quarter Scale Models." *Fears Structural Engineering Laboratory Report No FSEL/MBMA 85-02*, University of Oklahoma, Norman, Oklahoma.

Zetlin, L., and G. Winter. (1955). "Unsymmetrical Bending of Beams with and without Lateral Bracing." *Proceedings of the American Society of Civil Engineers*, 81, 774-1 to 774-20.

6. Nomenclature

$$I_{mY} = \frac{I_X I_Y - I_{XY}^2}{I_X} \qquad a = \sqrt{\frac{EC_W}{GJ}} \qquad \lambda = \frac{1}{a}\sqrt{\frac{GJ}{EC_W}}$$

$$\tau = \frac{\dfrac{a^2\beta}{GJ}}{1 + \dfrac{K_{mclip}}{GJ}\kappa} \qquad \beta = \frac{L^2}{8a^2} + \frac{1}{\cosh\left(\dfrac{L}{2a}\right)} - 1 \qquad \kappa = \frac{8a^4}{L^2}\left(\frac{\cosh\left(\dfrac{L}{2a}\right) - 1}{\cosh\left(\dfrac{L}{2a}\right)}\right) + \frac{5L^2}{48} - a^2$$

b	=	width of Z-section top flange (in) (mm)
Bay	=	total width of diaphragm perpendicular to span (ft) (m)
d	=	depth of Z-section (in) (mm)
E	=	modulus of elasticity (29,500,000 psi) (203,400 MPa)
G	=	shear modulus (11,200,00 psi) (77,200 MPa)
h	=	height of applied restraint measured from base of Z-section parallel to web (in) (mm)
I_X	=	moment of inertia of full unreduced section about axis perpendicular to the plane of the web (in^4) (mm^4)
I_{XY}	=	product of inertia of full unreduced section about major and minor centroidal axes (in^4) (mm^4)
K_{mclip}	=	combined rotational stiffness of sheathing and connection between the Z-section and sheathing (lb-in/ft) (N-m/m)
L	=	span of Z-section (ft) (m)
n_P	=	number of restrained purlins per anchorage device
P_L	=	total overturning force generated per purlin (lb) (N)
R	=	lateral restraint force (per restraint) of a system of purlins (lb) (N)
t	=	thickness of Z-section (in)
U	=	applied loading (lb)
w	=	uniform loading on Z-section (lb/ft) (N/m)
W	=	total load between supports applied uniformly to a system of Z-Sections (lb) (N)
Width	=	tributary width of diaphragm (perpendicular to Z-Section Span) per Z-section.(in) (mm)
δ	=	load eccentricity on Z-section top flange (1/3)
θ	=	angle between the vertical and the plane of the Z-section web (degrees)

VITA

Michael Seek was born on February 7, 1975 in Roanoke, Virginia to Walter and Dorothy Seek. His family moved to Johnson City, Tennessee in December 1976 where he grew up with his older sister Julie and younger sister Amy. He graduated from University High School in May 1993 and attended Virginia Tech in the fall of the same year. Michael worked as a co-op student with Rust Environment and Infrastructure and Walter Seek Engineering and received his Bachelor of Science degree in Civil Engineering from Virginia Tech in May 1998. After graduating, he worked for Alliance Engineering in Richmond, Virginia and in May 2000 was transferred to Baltimore, Maryland where he worked until June 2001. He was accepted to the Graduate School at Virginia Tech in the Department of Civil and Environmental Engineering and began his studies in August 2001. He began performing research on metal building roof systems under the auspices of Dr. Thomas Murray in January 2002. Michael became a registered professional engineer in the Commonwealth of Virginia in January 2004. He received his Master of Science degree from Virginia Tech in May 2005 and became a doctoral student in the same program in August 2005 continuing to work under the guidance of Dr. Thomas Murray. He began working for his father at Walter Seek Engineering in December 2006.

APPENDIX I

APPENDED PAPERS

APPENDIX I

APPENDED PAPERS

Paper I

Title Computer Modeling of Sloped Z-Purlin Supported Roof Systems to Predict Lateral Restraint Force Requirements

Authors Michael W. Seek, PE; Thomas M. Murray, Ph.D., PE

Publication *Conference Proceedings, 17th International Specialty Conference on Cold-Formed Steel Structures.* 2004. Department of Civil Engineering, University of Missouri-Rolla, Rolla, Missouri.

Paper II

Title Mechanics of Lateral Brace Forces in Z-Purlin Roof Systems

Authors Michael W. Seek, PE; Thomas M. Murray, Ph.D., PE

Publication *Conference Proceedings, Structural Stability Research Council Annual Stability Conference. 2005.* Structural Stability Research Council, University of Missouri-Rolla, Rolla, Missouri.

Paper III

Title Component Stiffness Method to Predict Lateral Restraint Forces in End Restrained Single Span Z-Section Supported Roof Systems with One Flange Attached to Sheathing.

Authors Michael W. Seek, PE; Thomas M. Murray, Ph.D., PE

Publication *Conference Proceedings, 18th International Specialty Conference on Cold-Formed Steel Structures.* 2006. Department of Civil Engineering, University of Missouri-Rolla, Rolla, Missouri.

Paper IV

Title	Lateral Brace Forces in Single Span Z-Section Roof Systems with Interior Restraints Using the Component Stiffness Method.
Authors	Michael W. Seek, PE; Thomas M. Murray, Ph.D., PE
Publication	*Conference Proceedings, Structural Stability Research Council Annual Stability Conference. 2007.* Structural Stability Research Council, University of Missouri-Rolla, Rolla, Missouri.

Paper V

Title	Prediction of Lateral Restraint Forces in Single Span Z-section Roof Systems with One Flange attached to Sheathing using the Component Stiffness Method
Authors	Michael W. Seek, PE; Thomas M. Murray, Ph.D., PE
Publication	Submitted to the Journal of Constructional Steel Research for publication July 2007.

Seek, M. W., and Murray, T.M. (2004). "Computer Modeling of Sloped Z-Purlin Supported Roof Systems to Predict Lateral Restraint Force Requirements." *Conference Proceedings, 17th International Specialty Conference on Cold-Formed Steel Structures.* Department of Civil Engineering, University of Missouri, Rolla. Rolla, Missouri.

Computer Modeling of Sloped Z-Purlin Supported Roof Systems to Predict Lateral Restraint Force Requirements

Michael W Seek, PE[1] and Thomas M Murray, Ph.D., PE[2]

Abstract

Lateral restraint or anchorage forces in Z-purlin supported through-fastened and standing seam (concealed clip) roof systems have been studied using the finite element method. Results from frame element models as well as full plate models are presented and compared to experimental results. Single and three span continuous systems with five restraint configurations were examined at roof slopes varying from zero to eighteen degrees from the horizontal. Recommendations for modification of existing anchorage force prediction equations are made.

Introduction

Z-Purlin supported roof systems have long been used by the metal building industry as a cost effective means of covering large roof systems. The development of standing seam systems has solved the thermal expansion and sealing problem of through-fastened systems. Their suitability in these applications has resulted in increased use as roof systems for conventional structures.

---

[1]Graduate Research Assistant, Virginia Tech, Blacksburg, VA, USA.
[2]Montague Betts Professor of Structural Steel Design, Virginia Tech, Blacksburg, VA, USA.

As a flexural member, the Z-purlin presents significant challenges from an analysis perspective. When an unrestrained Z-purlin is loaded in the plane of its web, it deflects laterally as well as vertically. Torsion is induced as a result of second order effects of the lateral displacement. Its stability is contingent upon its attachment to the rafters, attachment to the roof sheathing and the application of external lateral restraint. Lateral restraint is typically applied in discrete locations along the length of a purlin.

Due to the many variables involved, the behavior of Z-purlin supported roof systems is difficult to accurately predict. A means of predicting lateral restraint forces is currently specified in the North American Specifications in Section D3.2.1 (AISI, 2003). It has been found from tests performed by Lee and Murray (2001) and the authors that the AISI equations can be overly conservative for low slope roofs and unconservative for roofs with large slopes.

In an effort to provide a reliable means of predicting lateral restraint, two computer models have been investigated. The first model with frame type finite elements had been developed previously by Elhouar and Murray (1985) and modified by Neubert and Murray (1999). It has been found that with further modifications to this model, good correlation to test results is realized. A second finite element model utilizing shell elements to represent the purlin and sheathing was also developed. It too has been shown to have good correlation with test results. The models will provide a means of modifying the lateral restraint force prediction equations proposed by Neubert and Murray (1999; Hancock, Murray, and Ellifritt, 2001) to allow for the direct calculation of lateral restraint forces.

Frame Finite Element Model

The frame element stiffness model used in the current analysis was first developed by Elhouar and Murray (1985). This model was correlated to full scale and quarter scale test results. Through regression analyses of the model results, a series of parametric prediction equations was proposed and adopted by AISI. The equations, functions of purlin depth, thickness, flange width, and the number of purlins restrained, provide the basis for the current lateral restraint provisions specified in Section D3.2.1 of the North American Specifications (AISI 2003).

One important factor that the Elhouar and Murray (1985) study did not take into account is diaphragm stiffness. The frame element model was revisited by Neubert and Murray (1999) and modified to include variation of diaphragm panel stiffness. As a result of this work, a new methodology for the prediction of lateral restraint forces was proposed incorporating purlin cross sectional properties, diaphragm stiffness, and system effects. This prediction method is referred to as the Neubert and Murray Method.

The representation of the purlin used in these studies is shown in Figure 1. It is discretized into 12 segments along its length so that the third points, quarter points and midpoints all coincide with a node location. The purlin is comprised of Type A, B, C and F elements.

The Type A elements are the main components representing the purlin. The local X axis of the Type A element is oriented along the global X axis, but the member is rotated such that the local z and y axes correspond to the principal Y2 and X2 axes respectively as defined in the AISI Cold-Formed Steel Design Manual (1996). The section properties of the element correspond to the gross section properties of the purlin, i.e. Area = Area of the Purlin, $I_{zz} = I_{y2}$, $I_{yy} = I_{x2}$. To account for warping torsional stiffness and eliminate large torsional displacements, the torsional constant, J is set at an arbitrarily high value of 10 in^4 (416 x 10^4 mm^4).

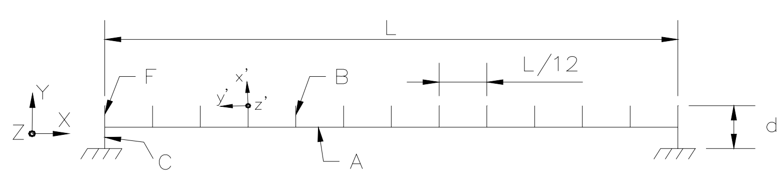

Figure 1. Model of Purlin in Frame Finite Element Model

Table 1. Frame Model Properties

Element Type	Model Area	Model Iyy	Model Izz	Model J
A	Area of Purlin	Ix2	Iy2	10 (416 x 10^4 mm^4)
B	$\frac{Lt}{12}$	$\frac{Lt^3}{144}$	J	Ix2
C	$\frac{Lt}{2}$	$\frac{Lt^3}{24}$	J	Ix2
F	$\frac{Lt}{12}$	$\frac{Lt^3}{288}$	J	Ix2

Type B and F elements connect the Type A element with the roof sheathing and have properties corresponding to L/12 and L/24 of the purlin respectively. The local axes of these elements are denoted in Figure 1 by x′, y′ and z′. The most important property of these elements is the moment of inertia about the local y′ axis, I_{yy}. This property, in the case of the type B element, is the moment of inertia of a rectangular element with width equal to the tributary width of the element, L/12, and a height equal to the purlin thickness, t. The remaining properties of the Type B and F elements are denoted in Table 1.

Type C elements provide connection between the Type A element and the rafter supports and have the same local axes as the type B and F elements. A major departure from previous models is the treatment of the moment of inertia about the y-axis, I_{yy}. To eliminate excessive deformation of the type C element, Elhouar and Murray (1985) increased its moment of inertia twelve fold from that equivalent to a tributary width of L/2 to a value of:

$$I_{yy} = \frac{Lt^3}{2} \tag{1}$$

Neubert and Murray (1999) felt this value still resulted in excessive deflections and consequently underestimated restraint force results, so the value of I_{yy} was increased arbitrarily to 1 in^4 (416 x 10^3 mm^4) to eliminate all bending deformation about the y axis in the Type C element. In the current study, it was found that results closer to test results are realized if this value is reduced back to a value equal to the tributary width of the Type C element of L/2. The resulting value for the moment of inertia about the y-axis is then

$$I_{yy} = \frac{Lt^3}{24} \tag{2}$$

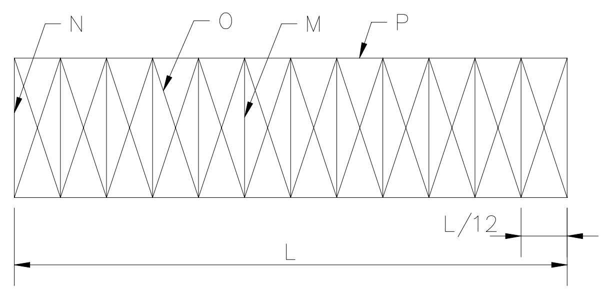

Figure 2 Diaphragm Elements

Figure 2 shows the "truss" diaphragm configuration used in this study. It follows the configuration used by both Elhouar and Murray (1985) and Neubert and Murray (1999) with some modification. The diaphragm is attached to the purlin at the top of the Type B and Type F elements. The diaphragm is comprised of type M, N, O and P elements, which are modeled as truss elements, i.e. bending stiffness about all axes is released and the element has only axial stiffness. The properties of these elements are derived from two stiffness sub-models. The first model, shown in Figure 3(a), is used to determine the cross sectional area of the diagonal type O elements, A_O, based on the desired diaphragm stiffness. Once the area of the Type O element is known, the second stiffness model, shown in figure 3(b), is solved for the area of the type N, M, and P elements, A_N, A_M, and A_P, respectively, to yield the true axial stiffness of the sheathing. Analyses of the models yields:

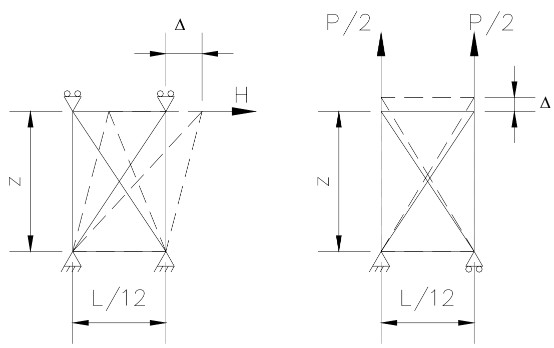

(a) (b)

Figure 3. Cantilever Diaphragm Models

$$A_O = \frac{G' z(\alpha^2 + 1)^{3/2}}{2E\alpha^2} \tag{3}$$

$$A_N = \frac{\sqrt{b^2 + 4ac} - b}{2a} \tag{4}$$

$$A_M = 2A_N \tag{5}$$

$$A_P = \alpha A_N \tag{6}$$

where

$$a = 2E\alpha\left(\alpha^2 + 1\right)^{3/2} \tag{7}$$

$$b = 2A_O E(\alpha^4 + 1) - K_{axial} z^2 \left(\alpha^2 + 1\right)^{3/2} \tag{8}$$

$$c = \frac{K_{axial} A_O z^2}{\alpha} \tag{9}$$

$$\alpha = \frac{z}{\left(L/12\right)} \tag{10}$$

$$K_{axial} = \frac{A_{panel} E}{z} \quad (11)$$

and

z = Purlin Spacing c. to c. (in.) (mm)
L = Purlin Span (in.) (mm)
E = Modulus of Elasticity (ksi) (MPa)
G' = Panel Diaphragm Stiffness (kip/in.) (N/mm)
A_{panel} = Panel Cross Sectional Area (in^2/in panel width) (mm^2/mm width)

Previous applications of the diaphragm model in the Figure 2 model have used rigid supports for the immediate lateral restraints as shown in Figure 4 (a). In laboratory tests and actual field conditions, these restraints have a finite stiffness. Through analysis of the finite element models, Watson and Sears, (2003) discovered that variation of the stiffness of the lateral restraint can have a large effect on the restraint force. To simulate the stiffness of the restraints in laboratory tests, a beam of equal stiffness is modeled between rafter supports. Lateral restraints are attached to the beam along the purlin span as shown in Figure 4 (b). The connection between the diaphragm and beam is made by a type E element – a truss element with cross sectional area equivalent to a ½ in. (12.7 mm) diameter threaded rod as was used in the experimental tests.

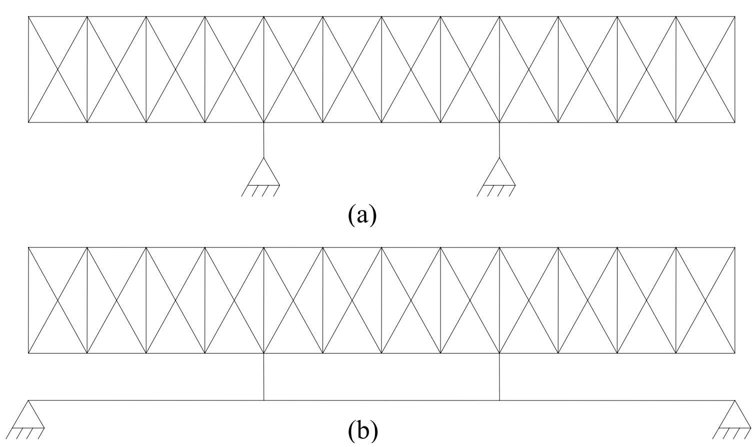

Figure 4. Restraint Anchorage

In many standing seam roof systems, the clip connection between the purlin and standing seam sheathing incorporates a slider tab that allows the sheathing to move relative to the purlin to accommodate thermal expansion of the roof. To simulate this flexibility, the clip connection was modeled with a two node Link element. A Link element allows the user to define translational and rotational spring stiffness values between two nodes. The Link element is given a linear translational spring stiffness of 500 lb/in. (87.6 N/mm) in the direction parallel to the roof seams and perpendicular to the web of the purlin. This value was chosen because it gave the best correlation with test results.

Gravity loads are applied as uniformly distributed force along the Type A elements. The gravity force is divided into vertical and horizontal components according to the roof slope. The vertical force is w cos(θ) and the horizontal force is w sin(θ), where θ is the roof slope angle and w is the tributary linear load on each purlin. Because the vertical component of the gravity load is thought to act at an eccentricity of 1/3 the width of the top flange, an additional torque, T, is applied to the nodes at the top of the Type B and F elements,

$$T = w\cos(\theta) \times {}^{b}\!/_{3} \times {}^{L}\!/_{12}$$

where b is the width of the purlin top flange.

Shell Finite Element Model

A plate element finite element model was developed using SAP 2000 Nonlinear V8, which has nonlinear capabilities. However, the analyses were restricted to linear, first order analyses. The model is comprised of two types of shell elements to represent the purlin and deck. The purlin is discretized into 2 in. (50.8 mm) segments along the length. A representation of the purlin is shown in Figure 5. The web is divided into four equal segments, the flange into three equal segments, and each edge stiffener into a single element. The discretization was chosen so as to maintain a maximum four to one aspect ratio for all elements. Each element has a bending and membrane thickness equal to the purlin thickness.

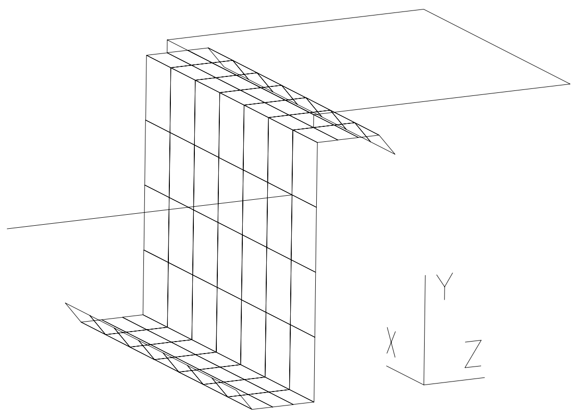

Figure 5. Shell Finite Element Model

The sheathing panel is modeled with 12 in. (305 mm) along the length of the purlin by 10.8 in. (274 mm) between purlin elements. (10.8 in. x 5 panels = 54 in. (1370 mm) purlin spacing). The membrane thickness of these elements is equivalent to the nominal thickness of the sheathing panel. To account for the bending stiffness provided by sheathing ribs, the bending stiffness of the element is equivalent to that of the deck, that is:

$$t_{sheathing} = \sqrt[3]{12\, I_{sheathing}} \tag{13}$$

where $I_{sheathing}$ is the sheathing moment of inertia per unit of width.

To provide for variable panel shear stiffness, an orthotropic material was used, which allowed the shear modulus to be entered explicitly. Using a small model similar to the Cantilever Test for Diaphragms (*Cold-Formed* 1996), the shear modulus was adjusted until the desired panel shear stiffness was reached. Table 2 shows the panel diaphragm stiffness and respective shear modulus values used.

Table 2. Shell Diaphragm Properties

Panel Diaphragm Stiffness (lb/in) (N/mm)	Shear Modulus (psi) (MPa) (Based On Panel Membrane Thickness = 0.0197 in.) (0.5 mm)
500 (876)	25000 (172)
1000 (175)	50000 (345)
2500 (438)	115000 793)
7500 (1313)	297000 (2048)
12500 (2189)	442000 (3047)
20000 (3502)	617000 (4254)
27500 (4816)	775000 (5343)

The attachment between the deck and the purlin is by a 2 node Link element. For the through fastened system models, the link represents the semi-rigid moment connection between the deck and purlin. Thus the link element has reduced stiffness for moment transfer between the purlin and deck about the Global X axis. The link attachment matched the fastener spacing of the laboratory test, that is, 12 in. (305 mm) For the standing seam models, the link element represented the standing seam clip attaching the sheathing to the purlin. The clip does not completely restrain rotation between the panel and purlin and many systems incorporate slider tabs that allow displacement between the sheathing and purlin. Therefore, for standing seam models, the link elements are spaced at 24 in. (610 mm) intervals to match clip spacing and are given translational spring stiffness in the global Y and rotational spring stiffness about the global X axis. The link element attaches the sheathing to the purlin at a distance of 1/3 of the flange width.

Load is applied directly to the sheathing as a uniformly distributed area load in both the global Y direction (gravity) and the global Z direction (downslope). To account for roof slope, the load in the global Y direction is equal to U cos(θ) and in the global Z direction is equal to U sin (θ), where U is the uniformly distributed load and θ is the roof slope.

At each simulated rafter support location, the purlin is restrained against translation in the Global Y and Z directions as well as rotation about the Global X axis. This restraint is applied at a discrete point at the centerline of the rafter support at the base of the purlin web.

The lateral restraint is applied in a similar manner as the frame element models. To match test specimens, the lateral restraints, modeled as a truss elements with the cross sectional area of a ½ in. (12.7 mm) diameter rod, are attached to the web of the purlin 2 ½ in. (63.5 mm) below the top of the purlin. Rather than attaching these restraint rods to a rigid support, a beam representing the test specimen was modeled similar to Figure 4 (b).

Comparison of Finite Element Models with Laboratory Test Results

To test the validity of the anchorage force prediction current equations in Section D3.2.1 of the North American Specification, the method proposed by Neubert and Murray (1999), and the modified finite element models, a series of full scale laboratory tests was performed. The tests were performed using 10ZS2.6x0.097 purlins spaced at 54 in. (1372 mm) center to center. The purlins spanned 20 ft (6096 mm) for the single span tests and three 20 ft (6069 mm) spans for the multiple span tests. For the multiple span cases, the purlins were lapped a total of 6 ft (1829 mm) centered over the rafter. The tests included combinations of two, four, and six purlins on single spans and six purlins lines over multiple spans. Each of these combinations was tested using conventional through fastened sheathing and standing seam sheathing and clips with slider tabs. The test apparatus permitted variation in slope from zero to a 4:12 pitch. For each purlin arrangement and bracing configuration, the test specimen was loaded uniformly to approximately 20 psf. (958 Pa). Six anchorage force measurements at incremental slopes between 0 and 4:12 were taken. Five different anchorage configurations were investigated: Supports, 3rd Points, Midpoints, Quarter Points and 3rd Points + Supports.

For virtually all combinations of purlins and restraint configurations, the North American specification equations give poor correlation with the test results. The results are typically highly conservative for low slope roofs but tend to be unconservative for roof pitches above 2:12.

The prediction method proposed by Neubert and Murray (1999) resulted in better correlation than the North American Specification method. Considering the Supports, 3rd Points and Midpoint restraint configuration on single span systems, the Neubert and Murray method shows good correlation but deviates slightly with increasing number of purlin lines. For Quarter points and 3rd Points + Supports configurations, the Neubert and Murray method does not very well correlate with the test results. A similar trend is observed for the multiple span configurations.

With the modifications made to the frame element models outlined in this article, improved correlation with the test results is realized. The improvement is minor when considering Supports, 3rd points and midpoints restraints because the correlation with the Neubert and Murray method is already fairly good. The improvement is particularly noticeable when considering the 3rd points + Supports and Quarter Points cases. However, for the quarter points restraint using through fastened deck, the results begin to deviate quite dramatically as the number of purlin lines is increased.

The correlation between the test results and the plate finite element models is very good for virtually all test cases. The through fastened cases show the best correlation. The standing seam models show some slight deviation from the test results but still provide a fairly accurate means of predicting restraint forces. The plate finite element model seems to be very stable and less susceptible to slight changes in the model than the frame finite element model. However for large systems of multiple spans with 6 or more purlin lines, run times with the plate finite element model approach 1 hour, while the run time for an equivalent frame finite element model is virtually instantaneous.

Conclusions

Progress has been made towards better predicting the anchorage forces requirements in standing seam roof systems. Modifications have been made to the frame finite element model that was used to develop both the equations in Section D3.2.1 of the North American specifications and the Neubert and Murray Method. Modifications to this model have improved the correlation to test results. Additionally a plate finite element model has been developed that too shows good correlation to test results. It is felt that with improvement to the finite element models, improvements to the Neubert and Murray Method can be made to provide an accurate means of directly calculating the required restraint forces in Z-purlin supported roof systems.

Appendix – References

Cold-Formed Steel Design Manual, (1996). American Iron and Steel Institute, Washington, D.C.

Elhouar , S. and Murray, T.M. (1985). "Prediction of Lateral Restraint Forces for Z-purlin Supported Roof Systems." Fears Structural Engineering Laboratory Report No. FSEL/AISI85-01, University of Oklahoma, Norman Oklahoma, 107 Pages.

Hancock, G. J., Murray, T. M. and Ellifrit, D. S. (2001). *Cold-Formed Steel Structures to the AISI Specification*, Marcel Dekker, New York.

Neubert, M.C. and Murray, T.M. (1999). "Estimation of Required Restraint Forces in Z-purlin Supported, Sloped Roofs Under Gravity Loads." Research Report CE/VPI-ST-99/12. Department of Civil and Environmental Engineering, Virginia Polytechnic Institute and State University, Blacksburg, VA, 112 Pages.

Lee, S.L. and Murray, T.M. (2001). "Experimental Determination of Required Lateral Restraint Forces for Z-Purlin Supported, Sloped Metal Roof Systems." Research Report CE/VPI-ST-01/09. Department of Civil and Environmental Engineering, Virginia Polytechnic Institute and State University, Blacksburg, VA, 104 Pages.

North American Specification for the Design of Cold-Formed Steel Structural Members (2003). American Iron and Steel Institute. Washington, D.C.

Watson, D and Sears, J. (2003). *Progress on Lateral Restraint Forces*. Private Correspondence, September 23.

Appendix – Notation

A_{panel}	= Panel cross sectional area (in^2/in panel width) (mm^2/mm panel width)
A_M	= Area of Type M element (in^2) (mm^2)
A_N	= Area of Type N element (in^2) (mm^2)
A_O	= Area of Type O element (in^2) (mm^2)
A_P	= Area of Type P element (in^2) (mm^2)
E	= Modulus of elasticity (ksi) (MPa)
G’	= Panel diaphragm stiffness (kip/in.) (N/mm)
$I_{Sheathing}$	= Moment of inertia of roof sheathing per unit width (in^4/in.)(mm^4/mm)
I_{X2}	= Minor principal axis moment of inertia (in^4) (mm^4)
I_{YY}	= Moment of inertia about local y axis (in^4) (mm^4)
I_{Y2}	= Major principal axis moment of inertia (in^4) (mm^4)
I_{ZZ}	= Moment of inertia about local z axis (in^4) (mm^4)
L	= Purlin span (in.) (mm)
T	= Torque due to dccentric loading on purlin flange (lb-in) (N/mm)
$t_{sheathing}$	= Equivalent bending thickness of roof sheathing (in.) (mm)
U	= Total uniformly distributed gravity load (psf) (Pa)
w	= Tributary line load on purlin (plf) (lb/in) (N/mm)
z	= Purlin spacing center to center (in.) (mm)
θ	= Roof slope angle (degrees)

Seek, M.W. and Murray, T.M. (2005) "Mechanics of Lateral Brace Forces in Z-Purlin Roof Systems." *Conference Proceedings, Structural Stability Research Council Annual Stability Conference.* Structural Stability Research Council. University of Missouri-Rolla. Rolla, Missouri.

MECHANICS OF LATERAL BRACE FORCES IN Z-PURLIN ROOF SYSTEMS

Michael W Seek, PE[1] and
Thomas M Murray, Ph.D, PE[2]

Z-beams, or Z-purlins, have gained widespread use in both the metal building industry and more recently in conventional building structures because of their structural efficiency, transportability, and their low production costs from recycled materials. Despite their popularity, the industry is still working to understand their behavior. One aspect of that has eluded understanding is the mechanics that generate the need to provide lateral braces in Z-purlin roof systems. This paper investigates the forces in lateral braces applied eccentrically from the shear center of a Z-purlin. Equations have been developed that predict the restraining forces provided by a diaphragm attached to the top flange, taking into account roof slope, diaphragm stiffness and gravity load applied eccentrically to the top flange. The equations are limited to single span roof systems and do not account for torsional restraint supplied by the supports and the bending stiffness of the sheathing. Despite the limitations, the equations developed still provide increased understanding of the behavior of Z-purlin roof systems that generates the need to provide lateral restraints.

EQUATION DEVELOPMENT

In their 1955 paper, Zetlin and Winter provided a simplified means of calculating stresses, deflections, and intermediate brace forces for Z-beams. Derived from moment-curvature relationships, their method

[1]Graduate Research Assistant, Virginia Tech, Blacksburg, VA, USA.
[2]Montague Betts Professor of Structural Steel Design, Virginia Tech, Blacksburg, VA, USA

introduced modified moments of inertia and a fictitious horizontal load. The method allows a designer to use conventional formulas for symmetric (constrained) bending and apply them to the problem of unsymmetric bending. The modified moments of inertia about the orthogonal X and Y axes are:

$$I_{mX} = \frac{I_X I_Y - I_{XY}^2}{I_Y} \qquad (1)$$

$$I_{mY} = \frac{I_X I_Y - I_{XY}^2}{I_X} \qquad (2)$$

and fictitious horizontal load is:

$$U_{FICT} = \frac{I_{XY}}{I_X} U_{REAL} \qquad (3)$$

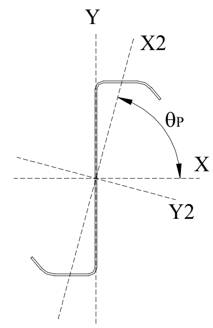

Figure 1. Purlin Axes

To determine the vertical deflection of a Z-beam loaded in the plane of its web, the conventional deflection formula for symmetric bending for a specific load case and the modified X-axis moment of inertia, I_{mX}, can be used. The horizontal deflection can then be determined from the same formula for symmetric bending by using the fictitious horizontal force, U_{fict}, and the modified moment of inertia about the Y-axis, I_{mY}.

For example, the mid-span vertical deflection, Δ_Y, and the corresponding horizontal deflection, Δ_X, for a uniformly loaded, single span, simply supported Z-beam are given by:

$$\Delta_Y = \frac{5wL^4}{384EI_{mX}} \qquad (4)$$

and

$$\Delta_X = \frac{5\left(w\frac{I_{XY}}{I_X}\right)L^4}{384EI_{mY}} \tag{5}$$

The Zetlin and Winter method ignores the second order torsion incurred due to the lateral displacement of the Z-beam, which in some cases can be quite large. Horizontal braces can be used to mitigate horizontal deflection and consequently the second order moments. The modified moments of inertia can again be used to calculate the magnitude of the brace force. Referring to Figure 2(a), in the absence of the horizontal brace, the Z-purlin will deflect laterally according to the fictitious force $U(I_{XY}/I_X)$. The application of the horizontal brace applies a real force, R, which will restore the Z-purlin to its original horizontal position at the point of application of the brace, as shown in Figure 2(b).

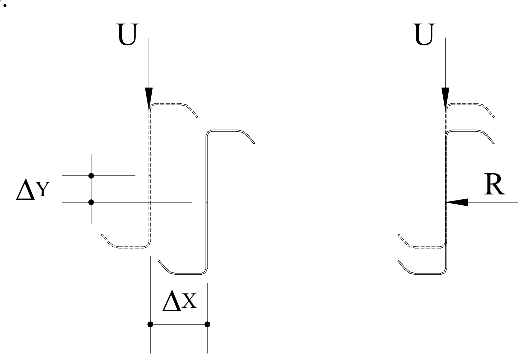

(a) Unrestrained Dislacement (b) Restrained Displacement

Figure 2

Using the previous example, but expanding it to include a horizontal brace force applied at the mid-span of the member, the horizontal deflection needed to restore the Z-purlin to its original horizontal position due to the applied restraint force, R, is

$$\Delta_{X,restraint} = \frac{RL^3}{48EI_{mY}} \tag{6}$$

By setting the horizontal deflection due to the uniformly distributed vertical load equal to the restoring horizontal deflection of the restraint force, the restraint force is:

$$R = \frac{5}{8} w \left(\frac{Ixy}{Ix} \right) L \tag{7}$$

For this to hold true, the applied loads and restraints must act through the shear center of the Z-beam or torsional restraints must be applied. In the event that these conditions are not met, torsional effects must be considered. This is often the case in conventional roof systems utilizing Z-purlins, where at the rafters the Z-purlin is supported by its bottom flange, load is applied to the top flange, and restraint is applied at or near the top flange.

For cases in which torsion cannot be ignored, the method of Zetlin and Winter may be expanded by considering torsional effects as in Carter and Seaburg (1997). When restraint is applied at locations other than the shear center of the purlin, Figure 3 (a), the restraint force is the force that restores the horizontal displacement at that particular location. But to do so, it causes the purlin to twist. The amount of twist can be quantified by resolving the restoring force into two components – a horizontal force applied at the shear center, R, and a couple, M = R*(d/2). Referring to Figure 3(b), the restoring displacements are divided into two components: $\Delta_{x,shearcenter}$, the restoring horizontal displacement due to the component of force applied at the shear center, and $\Delta_{x,torsion}$, the displacement of the top flange relative to the shear center due to the torsion. Using small angle approximation, $\Delta_{x,torsion}$ is equal to Φ*d/2.

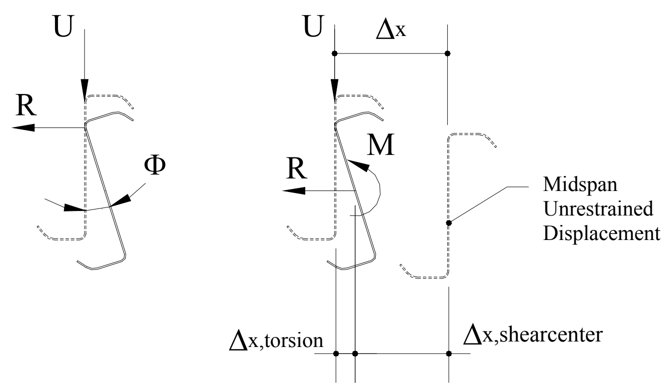

(a) Restraint at Top Flange (b) Forces Resolved at Shear Center

Figure 3. Z-purlin Restrained at Top.

Revisiting the previous example of a uniformly loaded Z-beam, but with horizontal restraint applied at the midspan of the purlin at the top flange, the equation for the unrestrained horizontal deflection due to an applied uniform load in the vertical direction, Δ_X, is the same as before. The restoring horizontal deflection due to the restraint at the shear center, $\Delta_{X,shearcenter}$, is the same as $\Delta_{X,restraint}$ from the previous example. From Carter and Seaburg (1997), the twist angle, Φ, for a beam that is warping free and torsionally restrained at the ends and subjected to a concentrated torque applied at mid-span is:

$$\phi = \frac{ML}{GJ}\alpha \qquad \text{where } \alpha = \frac{1}{\lambda L}\left(\frac{\sinh^2\left(\frac{\lambda L}{2}\right)}{\tanh(\lambda L)} - \frac{\sinh(\lambda L)}{2}\right) + \frac{1}{4}$$

$$\text{and} \qquad \lambda = \sqrt{\frac{GJ}{EC_W}} \tag{8}$$

With M=R*(d/2) and using small angle approximation to obtain $\Delta_{X,torsion} = \Phi*d/2$ yields

$$\Delta_{X,torsion} = \frac{RLd^2}{4GJ}\alpha \tag{9}$$

By equating the horizontal deflection due to the vertically applied load with the restoring horizontal deflection due to the applied brace, that is $\Delta_X = \Delta_{X,shearcenter} + \Delta_{X,torsion}$, and solving for the restraint force yields

$$R = \frac{5\left(w\dfrac{Ixy}{Ix}\right)L^3}{8L^2 + \dfrac{96EI_{mY}}{GJ}\alpha} \tag{10}$$

which is similar to that obtained when torsion is ignored. If the purlin has a large torsional stiffness, the second term in the denominator approaches zero and the restraint force approaches that for a purlin restrained at its shear center, that is, $R=5/8wL(I_{XY}/I_X)$. If the purlin has a small torsional stiffness, the restraint force will approach zero.

It is interesting to note the behavior of the purlin in the absence of torsional restraints at the ends. If the purlin in the above example is supported at each end only by pinned restraints at the bottom flange, and the horizontal brace is applied to the top flange, then the restraint force will counterintuitively be zero. In using the formulation of Zetlin and Winter, the force causing horizontal displacement is fictitious and therefore should not be included in equilibrium equations. Therefore, if moment equilibrium is calculated by summing moments about the pinned supports at the base of the purlin, the restraint force at midspan must be zero. The Z-purlin remains stable in this configuration, but will assume a deflected shape as shown in Figure 4 to satisfy compatibility.

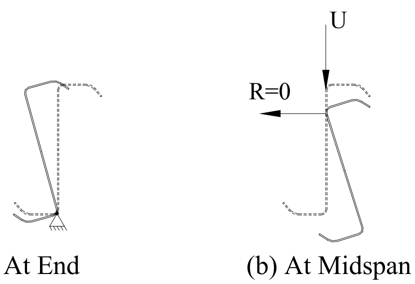

Figure 4. Displaced Shape without End Torsional Restraint

The majority of applications of Z-beams occurs in roof systems in which the top flange is attached to sheathing and the bottom flange is attached to rafter supports. Through its diaphragm stiffness, the sheathing helps restrain the translation of the top flange of the purlin. By using modified moments of inertia and by including the torsional effects described herein, the extent to which the sheathing helps to brace a Z-purlin can be quantified. However, in order to simplify the analysis, the bending stiffness of the sheathing and the rotational stiffness about the purlin longitudinal axis of the connection between the purlin and the rafter are ignored.

Research by Ghazanfari and Murray (1983) has shown that gravity load transferred from sheathing to the top flange of a purlin acts eccentrically along the top flange of the purlin. The closest estimates place this force as acting at an eccentricity of 1/3 times the flange width. In the analytical model, this eccentricity is represented by δb, where b is the flange width and δ is the proportion of the flange width at which the force acts.

To account for roof slope in the analytical model, the gravity load may be transposed onto the purlin orthogonal axes. The vertical component of the gravity load acting along the purlin y-axis is equal to $w*\cos\theta$, where θ is the angle of the roof slope. The component acting along the x-axis, referred to as the downslope component, is equal to $w*\sin\theta$.

The vertical component of the gravity load is transferred through the sheathing to the top flange of the purlin. The downslope component, however, has the tendency to remain in the diaphragm and therefore does not influence the purlin deformation. A summary of the externally applied loads is shown in Figure 5 (a). Resolving the vertical component of the eccentrically applied gravity load about the shear center of the purlin creates a torsional moment as shown in Figure 5 (b).

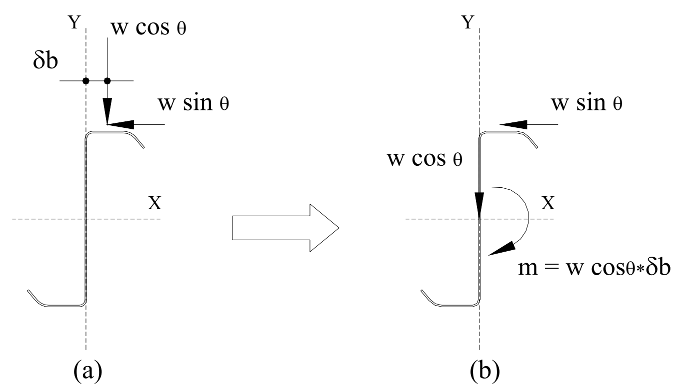

Figure 5 Resolution of Forces to Shear Center

The vertical component of a uniform gravity load causes deflection in the positive x direction by virtue of the fictitious force ($w*\cos\theta(I_{XY}/I_X)$. The horizontal mid-span displacement at the shear center becomes:

$$\Delta_{X,cen} = \frac{5w\left(\frac{I_{XY}}{I_X}\cos\theta\right)L^4}{384EI_{mY}} \tag{11}$$

The moment induced as a result of the eccentric application of the vertical component of gravity load causes the top flange to deflect horizontally relative to the shear center. The displacement of the top flange relative to the shear center can be calculated from the twist angle of a beam subjected to a uniform torsion:

$$\Delta_{X,torsion} = \frac{w(\delta b\cos\theta)d}{2GJ\lambda}\beta \text{ where } \beta = \frac{\lambda^2 L^2}{8} + \frac{1}{\cosh\left(\frac{\lambda L}{2}\right)} - 1 \qquad (12)$$

Combining the translational and rotational deformation, the net horizontal unrestrained displacement of the top flange becomes:

$$\Delta_X = w\left(\frac{5\left(\frac{I_{XY}}{I_X}\cos\theta\right)L^4}{384EI_{mY}} + \frac{(\delta b\cos\theta)d}{2GJ\lambda}\beta\right) \qquad (13)$$

Sheathing attached to the top flange of a Z-purlin provides continuous restraint to the purlin in the form of a uniformly applied force, $w_{restraint}$. Because this force acts at the top flange of the purlin and therefore at an eccentricity of d/2 from the shear center, the restraining force can be resolved into a uniformly applied force and torque applied at the purlin shear center. The horizontal deflection, $\Delta_{X,restraint,cen}$, associated with the restoring force can be calculated from that of a beam subjected to a uniform loading using the modified moment of inertia as shown in Equation 14. The additional deflection at the top flange due to the purlin torsion, $\Delta_{X,restraint,torsion}$, from the Carter and Seaburg (1997) equations is given in Equation 15.

$$\Delta_{X,restraint,cen} = \frac{5w_{restraint}L^4}{384EI_{mY}} \qquad (14)$$

$$\Delta_{X,restraint,torsion} = \frac{w_{restraint} d^2}{4GJ\lambda} \beta$$

$$\text{where } \beta = \frac{\lambda^2 L^2}{8} + \frac{1}{\cosh\left(\frac{\lambda L}{2}\right)} - 1 \qquad (15)$$

The diaphragm is subjected to uniform in-plane loads from both its tendency to restrain the purlin and the downslope component of the gravity loading. Unless the diaphragm is perfectly rigid, it cannot completely restore the top flange to its original horizontal displacement. The deformation due to the restraining force is in the positive X direction, while the downslope gravity load causes a negative X direction displacement. The displacement of the top flange attributed to the stiffness of the diaphragm, $\Delta_{diaphragm}$, can be calculated from the shear deformation of a simply supported beam subjected to a uniform load distribution, where L is the purlin span, width is the dimension of the diaphragm perpendicular to the purlin span, and G' is the panel diaphragm stiffness.

$$\Delta_{diaphragm} = \frac{(w \sin\theta - w_{restraint})L^2}{8G' width} \qquad (16)$$

The sum of the midspan horizontal deflection of the purlin due to the applied gravity loading and the restoring displacement provided by the attachment to the sheathing will equal the net displacement of the diaphragm, that is $\Delta_{diaphragm} = \Delta_x - \Delta_{x,restraint,cen} - \Delta_{x,restraint,torsion}$ as shown in Figure 6.

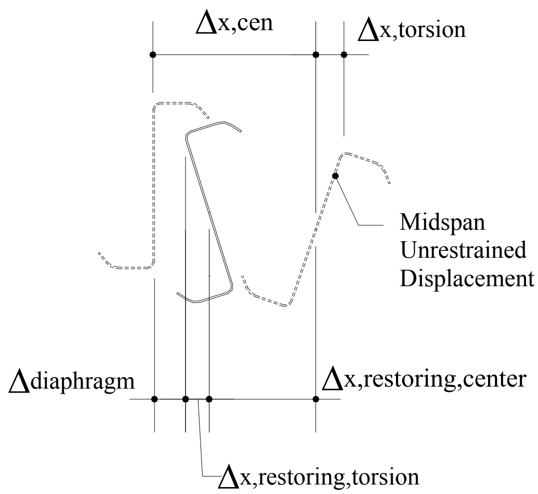

Figure 6 Unrestrained and Restoring Displacements

Solving the displacement equation for the uniform force in the diaphragm, $w_{restraint}$, yields

$$w_{\mathrm{Re}\,stra\,\mathrm{int}} = w \frac{\dfrac{5\left(\dfrac{I_{XY}}{I_X}\cos\theta\right)L^4}{384EI_{mY}} + \dfrac{(\delta b\cos\theta)d}{2GJ\lambda}\beta + \dfrac{L^2\sin\theta}{8G'Width}}{\dfrac{5L^4}{384EI_{mY}} + \dfrac{d^2}{4GJ\lambda}\beta + \dfrac{L^2}{8G'Width}} \tag{17}$$

In summary, the above equation predicts the force transferred to sheathing as a result of the restraint provided by the sheathing for a single span Z-Purlin with its top flange attached to sheathing and subjected to uniform loading. The equation accounts for purlin torsional stiffness, roof slope, eccentric load application at the top flange, and diaphragm stiffness. Two important components of the behavior of Z-purlin roof systems that are not included are the torsional restraint provided by the bending stiffness of the sheathing and the connection between the purlin and rafter. Quantification of these components, from the standpoint of classical mechanics, was found to be difficult and are not included in the formulation.

COMPARISON TO FINITE ELEMENT MODEL

To verify the above formulation, results are compared to finite element models. The finite element model used was a shell finite element model developed in accordance with Seek and Murray (2004). The model consisted of two purlins spaced at 54 in. (1370mm) and spanning 20 ft (6.1m) and connected at the top flange by sheathing. In the connection between the sheathing and purlin, the rotational stiffness about the global X axis was released. The purlins were supported externally by pinned supports at the bottom flange at the junction of the web and flange. Horizontal restraint in the global Z direction was applied to the top flange at each end of the eave purlin. A cross section of the model is shown in Figure 7.

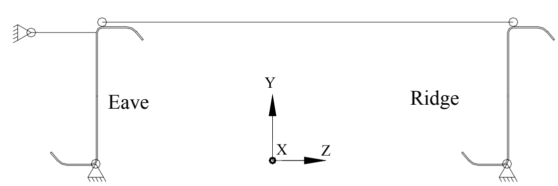

Figure 7 Model Representative Cross Section

The cross sectional properties of the purlins used are given in Appendix B. The vertical component of the gravity load was applied directly to the top flange of the purlin as concentrated forces at 4 in. (100mm) intervals and the downslope component of the gravity load was applied to the sheathing as a uniformly applied area force. The sheathing was given a large membrane thickness of 1 in. (25mm) to eliminate in plane bending of the sheathing. The diaphragm shear stiffness of the model was defined by varying the material shear modulus according to

G=G'/t. So that the purlin and the sheathing do not act as a composite section, the shear stiffness in the global X direction of the connection between the purlin and the sheathing was released.

Case 1

The first model was of a rigid diaphragm on a flat roof slope with the load acting directly over the web of the purlin. Using Equation 17 with $\theta = 0°$, $G' = \infty$, and the purlin properties in Appendix B, $w_{restraint} = 0.1524w$, whereas the finite element model predicts $w_{restraint} = 0.1558w$. Plotting $w_{restraint}$ with respect to position along the length of the purlin from the finite element model for an applied load of 85 lb/ft (1240N/m), Figure 8, shows that the force transfer between the purlin and sheathing is approximately uniform through the middle ¾ span. Interestingly, at the ends, the force reverses quite dramatically. Summing the forces along the length of the purlin, as listed in Table 1, the net force transferred between the purlin and diaphragm is zero. Thus, the restraint force provided by the sheathing to resist unsymmetric bending of the purlin is resolved entirely in the diaphragm and the force in the externally applied brace is zero.

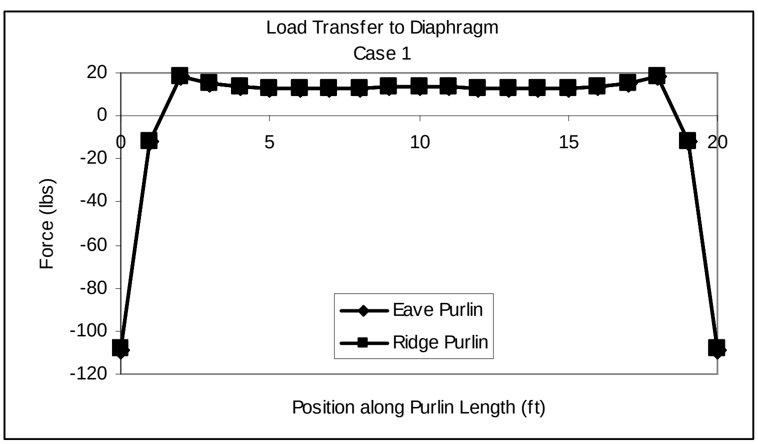

Figure 8 Force Transfer Between Purlin and Sheathing – Case 1

Position Along Purlin (ft)	Force Transfer to Diaphragm (lb)					
	Case 1		Case 2		Case 3	
	Eave	Ridge	Eave	Ridge	Eave	Ridge
0	-108.47	-108.45	-216.04	-77.79	282.24	-93.48
1	-11.92	-11.91	-4.76	12.6	43.34	-3.82
2	18.76	18.76	17.59	7.59	5.54	32.7
3	15.53	15.53	14.75	15.86	20.83	17.8
4	13.71	13.71	16.92	16.71	18.36	18.91
5	13.09	13.09	17.43	17.42	18.1	18.14
6	13.05	13.05	17.74	17.76	17.82	17.77
7	13.14	13.14	17.93	17.94	17.65	17.63
8	13.21	13.21	18.04	18.04	17.57	17.56
9	13.25	13.25	18.09	18.09	17.53	17.53
10	13.27	13.27	18.11	18.11	17.52	17.52
11	13.25	13.25	18.09	18.09	17.53	17.53
12	13.21	13.21	18.04	18.04	17.57	17.56
13	13.14	13.14	17.93	17.94	17.65	17.63
14	13.05	13.05	17.74	17.76	17.82	17.77
15	13.09	13.09	17.43	17.42	18.1	18.14
16	13.71	13.71	16.92	16.71	18.36	18.91
17	15.53	15.53	14.75	15.86	20.83	17.8
18	18.76	18.76	17.59	7.59	5.54	32.7
19	-11.92	-11.92	-4.76	12.6	43.34	-3.82
20	-108.47	-108.45	-216.04	-77.79	282.24	-93.48
Sum	-0.03	0.02	-146.51	146.55	935.48	139.00

Table 1 Force Transfer to Sheathing along Purlin Length

Case 2

To better understand the source of restraint forces in Z-purlin roof systems, the next model investigated is again on a flat slope, but the load is taken to act at an eccentricity of 1/3 the flange width as shown in Figure 10. A diaphragm with a stiffness of 2500 lb/in (440 kN/m) is also considered. Using the properties given in Appendix B, the uniform restraint force in the sheathing from Equation 17 is 0.2070w, while finite element model analysis predicts a uniform restraint force of 0.2084w.

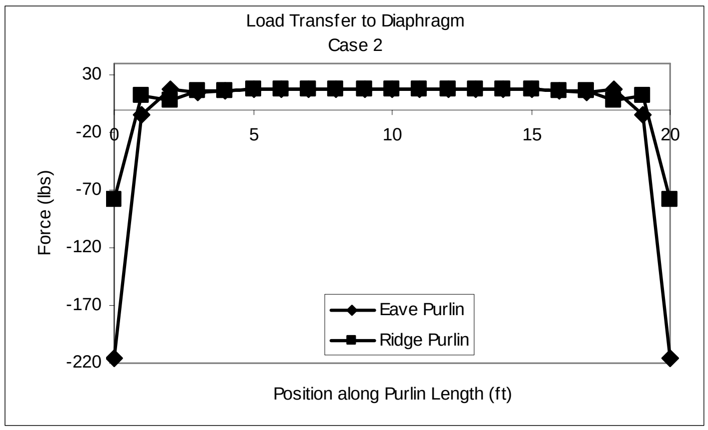

Figure 9 Force Transfer Between Purlin and Sheathing – Case 2

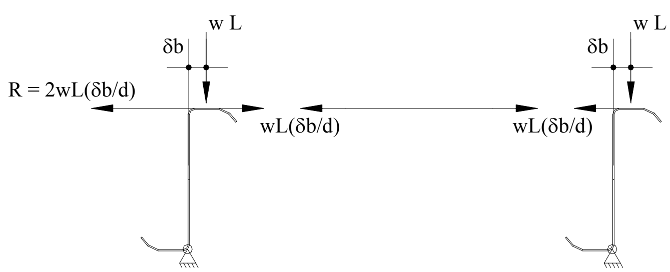

Figure 10 Free Body Diagram - Case 2

By plotting the force transfer from the purlin to the sheathing along the length of the purlin (Figure 9), similarities between Case 1 and Case 2 can be seen. In both purlins, the restraint force is roughly uniform throughout the middle of the purlin then reverses itself at the ends. Unlike the Case 1, however, summation of the forces along the length of the ridge purlin does not equal zero (Table 1). The net force is equal to $wL(\delta b)/d$, the amount of force necessary to equilibrate the torsional moment induced by the gravity load applied eccentrically to the top flange. This net force is transferred through the sheathing to the eave purlin. The net force at the top of the eave purlin is equal and opposite to that of the ridge purlin so that the diaphragm remains in horizontal equilibrium. The net restraint force in the external brace applied at the ends of the eave purlin is 2wL(δb)/d, the summation of the overturning moments induced as a result of the gravity load applied eccentrically to the top flange of both purlins.

Case 3

The final case investigated is one in which the roof slope is taken at a 4:12 pitch (18.43 degrees). A vertical load eccentricity of 1/3 is applied (Figure 11) and a diaphragm stiffness, G'=2500 lb/in (440kN/m), is assigned. From Equation 17, the restraint provided by the sheathing is 0.2062w while the finite element model predicts the restraint force to be 0.2100w. For both the eave and ridge purlin, the force is approximately uniform along middle ¾ of the purlin span as shown in Figure 12. Similar to the previous two cases, the force in the ridge purlin reverses at the ends and the sum of forces transferred from purlin to sheathing is wLcosθ(δb)/d. This force helps to balance some of the downslope component of the gravity load (refer to Figure 11). However, most of the downslope gravity load is transferred out of the sheathing through the eave purlin. The majority of this force is concentrated at the ends of the purlins where the external restraint is applied.

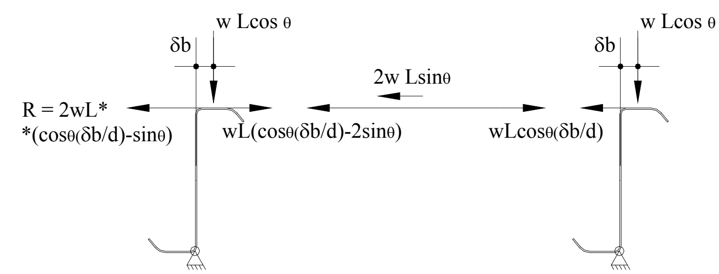

Figure 11 Free Body Diagram - Case 3

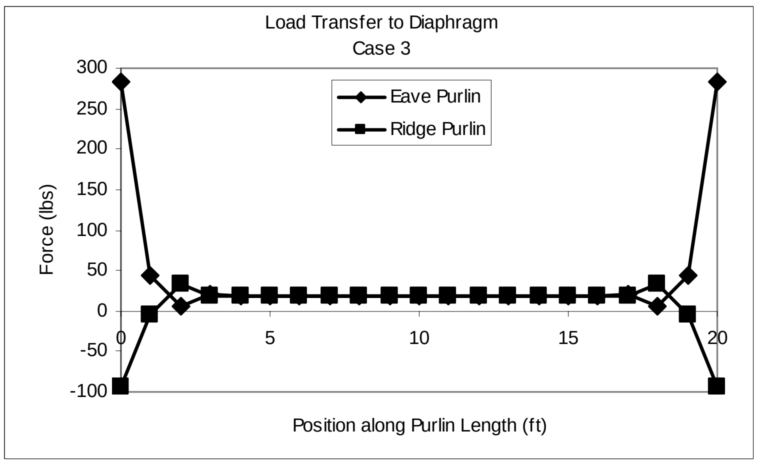

Figure 12 Force Transfer Between Purlin and Sheathing – Case 3

From the free body diagram in Figure 11, it is evident that the external brace lateral brace force is $wL((\cos\theta(\delta b)/d)-\sin\theta)$. The force is independent of the unsymmetric bending properties of the purlin and the diaphragm stiffness. However, the simplified model from which this brace force is derived excludes the restraining moments applied by the rafter supports and the bending stiffness of the sheathing. These moments, as shown in Figure 13, serve to reduce the force in the external lateral restraints. At low slopes, the restraining moments, M_{rafter} and $M_{sheathing}$, are counterclockwise and provide resistance to the clockwise overturning moment caused by the vertical component of the gravity load applied eccentrically to the top flange. With increased roof slope, that is when $\sin\theta > (\delta b/d)\cos(\theta)$, the restraining moments shift to counterclockwise and primarily provide resistance to the downslope component of the gravity load. Because the restraining moments will always serve to reduce the external restraint force, $R = wL((\cos\theta(\delta b)/d)-\sin\theta)$ will serve as an upperbound solution to the problem of restraint forces in Z-Purlin roof systems. The moment restraints provided by the sheathing and rafter supports are dependent upon the purlin thickness, span, torsional properties, sheathing diaphragm and bending stiffness, and the connection between the sheathing and purlin. Consequently these moments are difficult to quantify from the standpoint of classical mechanics and require the implementation of the finite element method to resolve.

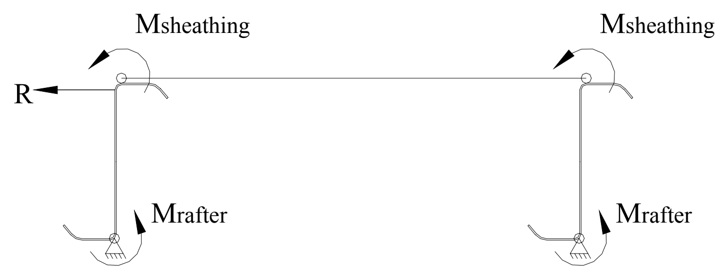

Figure 13 Restraining Moments from Rafter and Sheathing

SUMMARY

A procedure is outlined that provides a means of quantifying the force in a lateral brace applied eccentrically to the shear center of a Z-purlin. The method is extended to determine the restraint force provided by sheathing in a simplified model of a Z-purlin roof system that accounts for loads eccentrically applied to the purlin top flange, sloped roofs and sheathing diaphragm stiffness. The analytical model was verified using a shell finite element model which in turn provided valuable insight into the distribution of forces to externally applied braces. The theoretical model is limited in that it does not account for the stabilizing restraint provided by rafter supports and bending stiffness of the sheathing. Nevertheless, an upper bound solution for the force in an external lateral brace is found and progress is made towards a better understanding of the complex behavior of Z-purlins as used in roof systems.

APPENDIX A - REFERENCES

Carter, Charles J. and Seaburg, Paul A. (1997). *Steel Design Guide #9, Torsional Analysis of Structural Steel Members*. American Institute of Steel Construction, Inc. Chicago, IL.

Ghazanfari, A. and Murray, T.M. (1983). "Prediction of the Lateral Restraint Forces of Single Span Z-Purlins with Experimental Verification." Fears Structural Engineering Laboratory Report No. FSEL/MBMA 83-04, University of Oklahoma, Norman, Oklahoma, 131 pages.

Seek, M. W. and Murray, T. M. (2004). "Computer Modeling of Sloped Z-Purlin Supported Roof Systems to Predict Lateral Restraint Force Requirements." *Conference Proceedings, 17th International Specialty Conference on Cold-Formed SteelStructures.* Department of Civil Engineering, University of Missouri-Rolla. Rolla, Missouri.

Zetlin, L. and Winter, G. (1955). "Unsymmetrical Bending of Beams with and without Lateral Bracing. *Proceedings of the American Society of Civil Engineers.* Vol 81, 774-1 to 774-20.

APPENDIX B – PROPERTIES USED IN ANALYSIS

Purlin Designation: 10ZS2.5X097

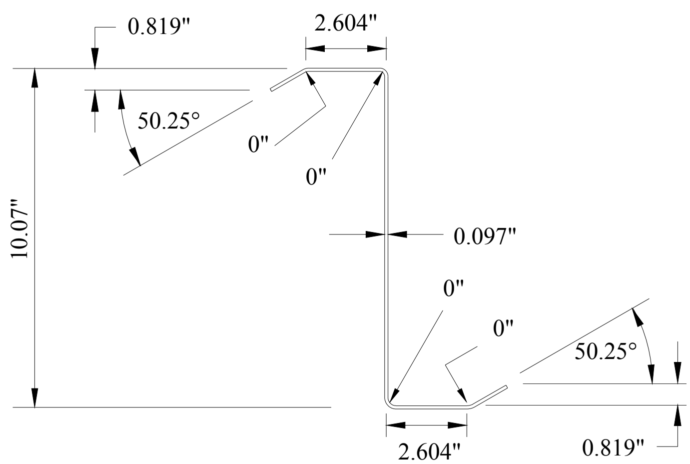

w = 85 lb/ft (1240 N/m)
L = 20 ft (6.1m)
d = 10.07 in. (256 mm)
b = 2.604 in. (66 mm)
t = 0.097 in. (2.5 mm)
E = 29500 ksi (203 GPa)
G = 11350 ksi (78 GPa)

I_X = 24.4 in^4 (10.2x10^6 mm^4)
I_Y = 2.72 in^4 (1.13x10^6 mm^4)
I_{XY} = 5.74 in^4 (2.39x10^6 mm^4)
J = 5.19x10^{-3} in^4 (2160 mm^4)
C_W = 50.9 in^6 (13.6x10^9 mm^6)

Diaphragm properties
G' = 2500 lb/in (440 N/m)
Width = 54 in. (1370 mm)

Reference Location

Carter and Seaburg (pg. 4)
Ghazanfari and Murray (pg. 7)
Seek and Murray (pg. 12)
Zetlin and Winter (pg. 1)

Keywords

Purlin (pg.1)
Z-Purlin (pg. 1)
Purlin Horizontal Bracing (pg. 2)
Roof System (pg. 1)
Roof Diaphragm (pg. 1)
Lateral Restraint Force (pg. 1)
Metal Building (pg. 1)

Seek, M. W., and Murray, T.M. (2006). "Component Stiffness Method to Predict Lateral Restraint Forces in End Restrained Single Span Z-Section Supported Roof Systems With One Flange Attached To Sheathing." *Conference Proceedings, 18th International Specialty Conference on Cold-Formed Steel Structures.* Department of Civil Engineering, University of Missouri, Rolla. Rolla, Missouri.

Component Stiffness Method to Predict Lateral Restraint Forces in End Restrained Single Span Z-Section Supported Roof Systems with One Flange Attached to Sheathing

Michael W. Seek, PE[1] and Thomas M. Murray, PhD, PE[2]

Abstract

A method is proposed for the prediction of lateral restraint forces in Z-Section supported roof systems with restraints applied at the rafter location. The method incorporates the complex flexural and torsional behavior of the Z-Section and its interaction with the sheathing. The method has been modified using the Finite Element method to account for local deformations. The method shows good correlation with the finite element model and test results.

Introduction

The behavior of Z-sections in roof systems is very complex and subject to many subtleties. Z-sections are typically installed with the top flange attached to sheathing and the bottom flange located at the top of rafter elevation. On low slope roofs, Z-sections have the tendency to roll "uphill" towards the ridge while on roofs with steeper slopes, a Z-section will roll "downhill" towards the eave. Restraints are typically installed at or near the top flange of the Z-section to resist this tendency to rotate. Restraint anchorage is often applied at the supports location because of the ease in which the force can be transferred out of the system.

The prediction of the restraint forces is complex because the principal axes of a Z-section are rotated from the orthogonal planes of loading and restraint. As a result, they are subject to the nuances of unsymmetric bending in which an applied load in the plane of the web induces a lateral deflection. The diaphragm action in the sheathing resists the tendency of the Z-section to deflect laterally,

---

[1]Graduate Research Assistant, Virginia Tech, Blacksburg, VA, USA.
[2]Montague Betts Professor of Structural Steel Design, Virginia Tech, Blacksburg, VA, USA.

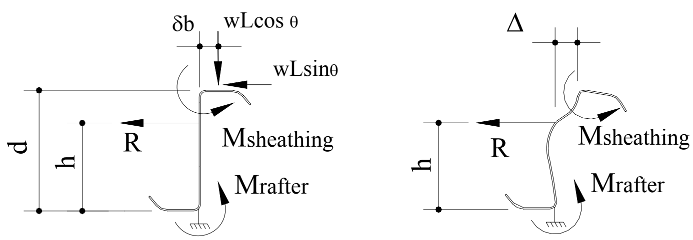

(a) Free Body Diagram (b) Rafter and Sheathing Stiffness

Figure 1 Forces Acting on Z-section

but because it is attached to the top flange of the Z-section, it causes rotation of the Z-section. The bending stiffness of the sheathing helps to resist the rotation of the Z-section but in the process affects the magnitude of the force in the external restraints. The analysis is further complicated by local deformations of the Z-section where large concentrated transverse loads and moments are applied to the relatively thin material. Despite the complexities in analysis, Z-section supported roof systems remain popular due to their efficiency and economy.

Methodology

The magnitude of the restraint force can be found from the free body diagram of the Z-section shown in Figure 1(a). The vertical component of gravity load acts at an eccentricity, δ, along the width of the flange, b, causing a clockwise rotation of the Z-section. This eccentricity is generally accepted to be 1/3 the width of the flange. The downslope component of the gravity load, $w \cdot L \cdot \sin\theta$, acting in the plane of the sheathing causes a counter-clockwise rotation of the Z-section. Deformation of the Z-section generates moments at the connection between the Z-section and the rafter support (M_{Rafter}) and the connection between the Z-section and sheathing ($M_{Sheathing}$). Summing moments about the base of the Z-section, the lateral restraint force becomes

$$R = \frac{wL(\delta b\cos\theta - d\sin\theta) - M_{Sheathing} - M_{Rafter}}{h} \qquad (1)$$

A positive restraint force signifies resistance to upslope translation while a negative restraint force signifies resistance to downslope translation.

While the free body diagram is quite simple, determining the magnitude of the moments at the sheathing and rafter is not. A stiffness approach is used to relate the restraint force to the rafter and sheathing moments. Each component of the system (restraint, rafter, sheathing) generates some force or moment relative to the displacement of the top flange at the restraint location. The stiffness of the restraint, $K_{restraint}$, is the force in the restraint per unit displacement of the top flange. The stiffness of the sheathing, K_{shtg}, and the stiffness of the rafter, K_{rafter}, are the moments in the sheathing or rafter per unit displacement of the top flange. The stiffness of both the sheathing connection and the rafter connection is dependent upon whether the Z-section is directly restrained (a "restrained" Z-section) or restraint is provided indirectly through the sheathing (a "system" Z-section). Thus, there are five components that contribute to the total lateral stiffness of the system: $K_{restraint}$, $K_{shtg,rest}$, $K_{shtg,sys}$, $K_{rafter,rest}$, $K_{rafter,sys}$.

The method assumes that the system of Z-sections has a single degree of freedom. That is, there is some rigid connection linking the displacement at the top of each Z-section in the system. For a through fastened system, this link is provided by the sheathing, while for a standing seam system that permits lateral slip between the sheathing and the Z-section, the rigid link must be provided by some external component such as strapping. As a single degree of freedom, the total stiffness of the system, K_{total}, is the sum of the stiffness of the individual components, or

$$K_{total} = \sum_{n_{rest}} 2K_{rest} + \frac{\sum_{n_{rest}} \left(2K_{rafter,restr} + K_{shtg,restr}\right) + \sum_{n_{sys}} \left(2K_{rafter,sys} + K_{shtg,sys}\right)}{h} \quad (2)$$

where n_{rest} is the number of restrained Z-sections and n_{sys} is the number of system Z-sections. The force generated at the restraint is determined from Equation (3) from the relative stiffness of the restraint to the total stiffnes of all of the components in the system.

$$R = wL \frac{(\delta b \cos\theta - d \sin\theta)}{h} \cdot \frac{\sum K_{rest}}{K_{total}} \quad (3)$$

To develop equations for the stiffness of each of the components, a series of finite element models was performed. The model used was a linear-elastic plate finite element model as described by Seek and Murray (2004a). A total of 282 models were analyzed with three data points taken from each model at roof pitches of 0:12, 3:12 and 6:12. The range of parameters shown in Table 1 was investigated in an attempt to represent the most common systems in use today.

Table 1 Parameters Investigated in Finite Element Analysis

Parameter	Values Tested
Purlin Depth, in (mm)	8 (203), 10 (254), 12 (305)
Purlin Thickness, in. (mm)	0.060 (1.52), 0.097 (2.46), 0.135 (3.43)
Purlin Span, ft, (m)	20 (6.10), 30 (9.14)
Rotational Stiffness of Sheathing Connection, lb-in/ft (N-m/m)	500 (2223), 1000 (4445), 5000 (22,225), 10,000 (44,450)
Diaphragm Stiffness, lb/in (N,mm)	250 (43.8), 1000 (175), 2500 (438), 7500 (1313), 27500 (4816)
Restraint Height	d, 3/4d, 1/2d
Number of Purlins	4, 8

Restraint Stiffness

The stiffness of the restraint is the combination of two sources of deformation at the restraint. The stiffness of the restraint device, K_{device}, is defined as the force at the restraint device relative to the displacement of the device at the height, h, at which the restraint is applied. The configuration stiffness, K_{config}, accounts for the deformation of the Z-section top flange relative to the restraint device. The combination of the two results in the net stiffness of the restraint, K_{rest}.

$$K_{rest} = \frac{\frac{h}{d} K_{device} \cdot K_{config}}{\frac{h}{d} K_{device} + K_{config}} \tag{4}$$

Two basic types of restraint configurations are considered – a discrete restraint and an antiroll device. A discrete restraint is a lateral restraint applied at some discrete location along the height of the Z-section and typically accompanied by flange bolts as shown in Figure 2(a). An antiroll device is considered a device in which the web of the Z-section is clamped to the device with bolts at multiple locations along the height of the Z-section. Bottom flange bolts may or may not be incorporated into an anti-roll device.

To determine the stiffness for a discrete restraint configuration, the web of the Z-section at the restraint was represented by a two dimensional beam model bent about the thickness of the web. To account for the effective width of the web and sheathing in the model, the representative equation was modified based on finite element model results. The resulting configuration stiffness for a discrete restraint per end of restrained Z-section is given in Equation (5).

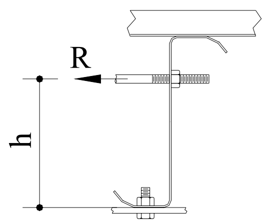

(a) Discrete Restraint

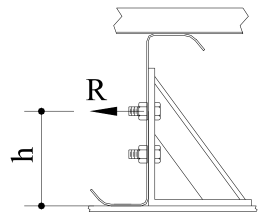

(b) Antiroll Device

Figure 2 Restraint Devices

$$. K_{config} = \frac{\frac{1}{15} d \cdot (3Et^3)}{h(d-h)^2} \left[\frac{\frac{1}{15} d \cdot 2Et^3 (3d-h) + \frac{L}{80} \cdot K_{MDeck} \cdot d(3d-2h)}{\frac{1}{15} d \cdot Et^3 (4d-h) + \frac{L}{80} \cdot K_{MDeck} \cdot d(d-h)} \right] \quad (5)$$

An antiroll device is assumed to provide restraint at the location of the top bolt connecting the Z-section web to the antiroll device as shown in Figure 2(b). The stiffness of the configuration for an antiroll device is based on a representative 2- dimensional beam model with a fixed base located at the elevation of the top bolt and a rotational spring at the top flange of the Z-section. This representation is accurate for the case where the antiroll device resists "downhill" displacement of the top flange. For "uphill" displacement of the top flange, the extension of the top of the antiroll clip results in increase in stiffness relative to the downslope case. Because antiroll devices were not included in the finite element analysis, the lower bound approximation considering the downslope case is used. The effective width of the Z-section is assumed to be the width of the antiroll device and the effective width of the sheathing rotational stiffness is taken to be the same as for a discrete restraint. The configuration stiffness for an antiroll device becomes

$$K_{config} = \frac{Eb_{ar} t^3}{(d-h)^3} \left(\frac{\frac{L}{80} k_{MDeck} (d-h) + \frac{1}{3} Eb_{ar} t^3}{\frac{L}{80} k_{MDeck} (d-h) + \frac{1}{12} Eb_{ar} t^3} \right) \quad (6)$$

Restrained Rafter Stiffness

As there were two restraint configuration stiffness equations to represent the differences between discrete braces and antiroll devices, there are two corresponding rafter stiffness values for each type of restraint. The rafter stiffness for a discrete brace uses the same representative beam model as the discrete restraint configuration with the moment generated at the base of the Z-section. Because of the nature of the displaced shape, an upslope displacement (positive) generates a negative moment at the rafter, consequently the rafter is assigned a negative stiffness, that is

$$K_{Rafter,rest} = \frac{-0.09 \cdot Et^3 \cdot h}{(d-h) \cdot d} \tag{7}$$

The rafter stiffness for an antiroll device is taken as the moment generated at the point at which the antiroll device is assumed to fix the web of the Z-section - the restraint height, h. Because there is no finite element information or test information available for antiroll devices, it is desirable to underestimate the rafter stiffness. The rotational stiffness of the connection between the Z-section and sheathing is ignored and the effective bending width of the Z-section is taken to be the width of the antiroll device. The rafter stiffness, therefore, for a restrained Z-section at an antiroll device is

$$K_{Rafter,rest} = \frac{\frac{1}{2} Eb_{ar} t^3}{(d-h)^2} \left(\frac{\frac{L}{80} K_{MDeck} (d-h) + \frac{1}{6} Eb_{ar} t^3}{\frac{L}{80} K_{MDeck} (d-h) + \frac{1}{3} Eb_{ar} t^3} \right) \tag{8}$$

System Rafter Stiffness

Two system Z-section configurations are considered for rafter stiffness. The first is the case for the bottom flange of the Z-section bolted to the top flange of the rafter support, referred to as a flange bolted connection. The stiffness is derived from a 2 dimensional beam model fixed at the base and at the top. The rafter stiffness, defined as the moment generated at the base of the Z-section relative to the top flange displacement, is given by

$$K_{Rafter,sys} = 0.45 \frac{Et^3}{2d} \tag{9}$$

The second type of system rafter configuration considered was that of a Z-section with its web bolted to a rafter clip. A rafter clip is considered a single plate extending from the rafter whether the plate is bolted or welded to the rafter. A rafter clip is similar in behavior to an antiroll device although it is not explicitly considered a restraint device in this formulation. The stiffness is defined as the moment at the base of the rafter clip relative to the top flange displacement. The deformation is the combination of the lateral displacement of the rafter clip at the location of the top bolts and the deformation of the Z-section above the rafter clip. The combined stiffness is given by Equation 10.

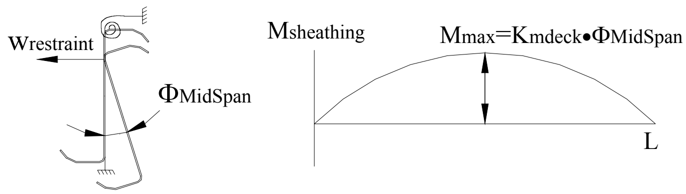

(a) Midspan Displaced Shape (b) Moment Distribution along Length

Figure 3 Sheathing Moment – Rigid End Restraints

$$K_{Rafter,sys} = \frac{E \cdot b_{pl} \cdot t_{pl}^{3} \cdot t^{3}}{2t^{3}\left(h^{2}(3d-h)\right) + 4t_{pl}^{3}(d-h)^{3}} \tag{10}$$

Sheathing Stiffness

The moment generated in the sheathing is a function of many factors – the flexural and torsional properties of the Z-section and the diaphragm and bending stiffness of the sheathing. The moment in the sheathing can be quantified using the concept of unrestrained and restoring displacements discussed by Seek and Murray (2005). Considering a Z-section rigidly restrained at each end and ignoring the the bending stiffness of the sheathing, by equating the mid-span lateral unrestrained displacement of the Z-section due to applied forces with the horizontal restoring displacement provided by the sheathing, the uniform restraint provided by the sheathing, $w_{Restraint}$, and the final midspan rotation, $\Phi_{MidSpan}$, can be calculated. by Equations (11) and (12), respectively.

$$w_{Restraint} = w\frac{\dfrac{5\left(\dfrac{I_{XY}}{I_X}\cos\theta\right)L^4}{384EI_{mY}} + \dfrac{(\delta b\cos\theta)d}{2}\dfrac{a^2\beta}{GJ} + \dfrac{L^2\sin\theta}{8G'Width}}{\dfrac{5L^4}{384EI_{mY}} + \dfrac{d^2}{4}\dfrac{a^2\beta}{GJ} + \dfrac{L^2}{8G'Width}} \tag{11}$$

$$\phi_{MidSpan} = \left(w(\delta b\cos\theta) - w_{Restraint}\frac{d}{2}\right)\frac{a^2\beta}{GJ} \tag{12}$$

In this formulation, the restraints applied at each end of the Z-section rigidly restrain the top flange of the purlin and thus the rotation at each end of the Z-section is zero. It is approximated to vary parabolically to the maximum at midspan. If the bending stiffness of the sheathing is considered, the moment in the sheathing is directly proportional to the rotation of the purlin. The moment in the sheathing therefore has a parabolic distribution.along the length of the Z-section as shown in Figure 3. The midspan rotation of a Z-section subjected to a parabolic moment distribution along the length is

$$\phi_{parabola} = M_{Max} \frac{\kappa}{GJ} \tag{13}$$

Mmax is the maximum moment at the peak of the parabola (at the Z-section midspan). Because the moment in the sheathing is a function of the rotation,

$$M_{Max} = -K_{MDeck} \cdot \phi_{MidSpan} \tag{14}$$

The net Mid Span rotation becomes

$$\phi_{MidSpan} = \left(w(\delta b \cos\theta) - w_{restraint} \cdot \frac{d}{2} \right)\tau \tag{15}$$

and the uniform restraint provided by the sheathing is

$$w_{Restraint} = w \frac{\dfrac{5\left(\dfrac{I_{XY}}{I_X}\cos\theta\right)L^4}{384EI_{mY}} + \dfrac{(\delta b \cos\theta)d}{2}\tau + \dfrac{L^2 \sin\theta}{8G'Width}}{\dfrac{5L^4}{384EI_{mY}} + \dfrac{d^2}{4}\tau + \dfrac{L^2}{8G'Width}} \tag{16}$$

The total moment generated in the connection between the Z-section and sheathing for a Z-section rigidly restrained at each end is

$$M_{Shtg} = -\tfrac{2}{3} L \cdot K_{MDeck} \cdot \phi_{MidSpan} \tag{17}$$

The sheathing moment in Equation (17) is generated as a result of the unsymmetric bending properties of the Z-section. Additional moments are generated if the rigid end restraints are replaced with restraints that permit lateral deflection of the top flange of the purlin at the restraint location. As the restraint permits the lateral translation of the top flange, the Z-section rotates relative to the sheathing, generating a uniform moment in the sheathing as shown in Figure 4(a). Due to the torsional moments along the length of the purlin, there is some rotation of the midspan of the Z-section relative to the end rotation. Similar to the case with rigid end restraints, the additional rotation generates a moment that varies parabolically along the length of the Z-section as shown in Figure 4(b). The resulting displaced shapes and sheathing moment distributions can be superposed as shown in the Figure 4(c).

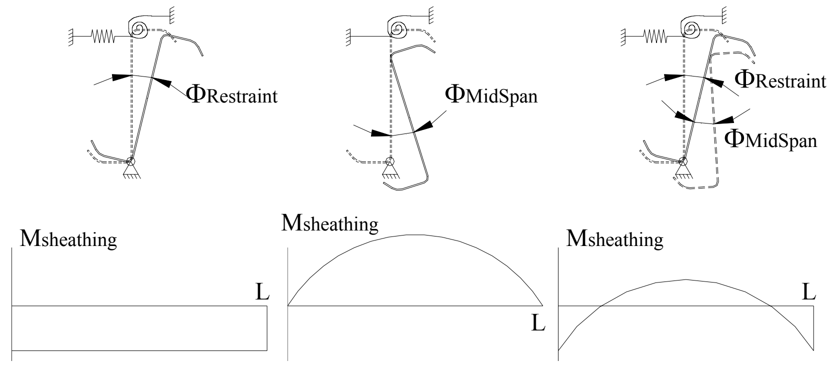

(a) Uniform Moment (b) Parabolic Moment (c) Combined Moment

Figure 4 Sheathing Moment - Z-section with Flexible End Restraints

The magnitude of the uniform moment in the sheathing is equal to

$$M_{uniform} = K_{MDeck}\phi_{restraint} = K_{mdeck} \cdot \frac{\Delta_{restraint}}{d} \quad (18)$$

Including the effects of the additional uniform moment to the midspan rotation given in Equation (18), the midspan rotation relative to the end rotation becomes

$$\phi_{MS} = \left(w(\delta b \cos\theta) - \frac{w_{restraint} d}{2} \right)\tau - \frac{\Delta}{d} K_{MDeck}\tau \quad (19)$$

Equation (16) is used to approximate $w_{restraint}$ for use in Equation (19). A parameter study was performed comparing the exact solution for $w_{restraint}$ considering the effects of the deformation at the restraint with the approximate solution of Equation (16). The difference between the two equations was negligible, warranting the use of the simpler equation. The net moment in the sheathing due to the parabolic distribution becomes

$$M_{Parabola} = \tfrac{2}{3} L \cdot K_{MDeck} \cdot \phi_{MS} \quad (20)$$

Combining the uniform moment and parabolic distribution yields the total sheathing moment

$$Mshtg = \tfrac{2}{3} L \cdot K_{MDeck} \cdot \left(w(\delta b \cos\theta) - \frac{w_{restraint} d}{2} \right)\tau + \Delta \frac{L \cdot K_{MDeck}}{d}\left(1 - \tfrac{2}{3} K_{MDeck}\tau\right) \quad (21)$$

The first half of the sum is constant with respect to a given Z-section system while the second varies with respect to the displacement of the top flange of the Z-section. The two components are separated, the former applied as constant moment to the restraint equation and the latter applied as a stiffness term. Considering the second term of Equation (21), the stiffness of the sheathing, defined as the total uniform moment developed in the sheathing per unit lateral displacement of the sheathing becomes

$$K_{shtg} = \frac{L \cdot K_{MDeck}}{d} \lambda \left(1 - \tfrac{2}{3} K_{MDeck} \tau\right) \tag{22}$$

The above formulation is derived using the typical bending assumption that plane sections remain plane. Because Z-sections are a relatively thin material, they undergo substantial local deformations as they undergo these rotations. To account for these local deformations, the multiplier λ, derived from the results of finite element models, is applied.

The sheathing stiffness for a restrained Z-section follows the same format, although the stiffness is increased slightly. There is a local deformation in the region of the restraint that results in a large local rotation between the Z-section web and deck. Consequently there is an increase in the moment in the sheathing near the restraint. The restrained Z-section sheathing stiffness becomes

$$K_{shtg,rest} = \left(\frac{1.43L}{d} + \frac{L_{Fast}}{d-h}\right) K_{MDeck} \lambda \left(1 - \tfrac{2}{3} K_{MDeck} \tau\right) \tag{23}$$

Restraint Force Equation

To include the "constant" sheathing moment, the restraint force in Equation (3) is modified to

$$R = \left(\Sigma wL \cdot \frac{\delta b \cos\theta - d \sin\theta}{h} + \frac{\tfrac{2}{3} L \cdot K_{MDeck} \lambda}{h} \left(\frac{d}{2} \Sigma w_{restraint} - \Sigma w \cos\theta \cdot \delta b\right) \tau\right) \frac{K_{rest}}{K_{total}} \tag{24}$$

The result of Equation (24) is the force in an individual restraint in a system of purlins. Any number of restraints can be incorporated for any number of purlins. It is assumed that the restraint force between multiple restraints in a bay is distributed according to the relative stiffness of each restraint. Combinations of different purlins with different end conditions can be used in the same bay with the component stiffness method.

A conservative approximation of restraint force for a single restraint in a system can be made by setting the ratio K_{rest}/K_{total} equal to 0.5. For multiple restraints in a homogenous system, the ratio K_{rest}/K_{total} should be set to $0.5/n_{rest}$. This approximation may be further simplified for low slope roofs where $\delta b \cdot \cos\theta > d \cdot \sin\theta$ by approximating $w_{restraint} \sim w \cdot Ixy/2Ix$. For a restraint system that effectively restrains the top flange of the Z-section, these approximations will result in a slightly conservative result on the order of 10%-30%. For a system with a fairly flexible restraint relative to the stiffness of the system, these approximations can lead to an overly conservative approximation of the restraint force greater than 100%.

Several other important quantities may be extracted from this method. The required force per unit length that must be transfered between the sheathing and the Z-section is $w_{restraint}$, given in Equation (16). Along the length of the purlin, this force is nominal. However, at the restraint location, a significant force must be transferred out of the sheathing, through the Z-section and into the restraint. The magnitude of this force is

$$FastenerForce = R\frac{h}{d} + 0.45Lw_{restraint} - \frac{wL}{2}\frac{\delta b\cos\theta}{d} \tag{25}$$

Note that this fastener force can be significant and must be transferred over a small distance – a tributary panel width that this force can be expected to be transferred is approximately 12 in. (300 mm) either side of the restraint location.

To check the effectiveness of a bracing system the deformation of the system can be calculated. Based on this method, in general as a Z-section is allowed to displace, the calculated restraint force decreases. The method does not account for any second order effects, therefore displacements should be minimized, particularly at the restraint location. The lateral deflection of the top flange of the Z-section at the restraint location can be approximated by

$$\Delta = \left(\Sigma wL \cdot \frac{\delta b\cos\theta - d\sin\theta}{h} + \frac{\frac{2}{3}L \cdot K_{MDeck}\lambda}{h}\left(\frac{d}{2}\sum w_{restraint} - \sum w\cos\theta \cdot \delta b\right)\tau \right) K_{total}^{-1} \tag{26}$$

With a flexible diaphragm, lateral deflection of the Z-section mid-span relative to the restraints is expected. The midspan lateral deflection of the diaphragm can be approximated as

$$\Delta = \sum\left(w_{restraint} - w\sin\theta\right)\frac{L^2}{8G'\sum Width \cdot} \tag{27}$$

The midspan rotation, Φ_{MS}, of the Z-section relative to the end rotation as shown in Figure 3(c) can be approximated by Equation (19).

Comparison of Prediction Method with Tests and Finite Element Models

In Figure 5, the restraint force predicted using the component stiffness method is plotted on the vertical axis relative to the restraint force from finite element model analysis plotted on the horizontal axis. The solid diagonal line represents an exact 1 to 1 correlation between the prediction method and finite element model while each dashed line represents a 20% deviation from exact correlation. The data points represent all of the finite element models from which the method was derived as discussed in the methodology section.

The equations are compared to full scale laboratory tests by Seek and Murray (2004b) in Figure 6 . The testing program consisted of full scale tests of Z-section roof systems with two, four and six Z-section lines with both through fastened and standing seam sheathing. The Z-sections were tested on pitches

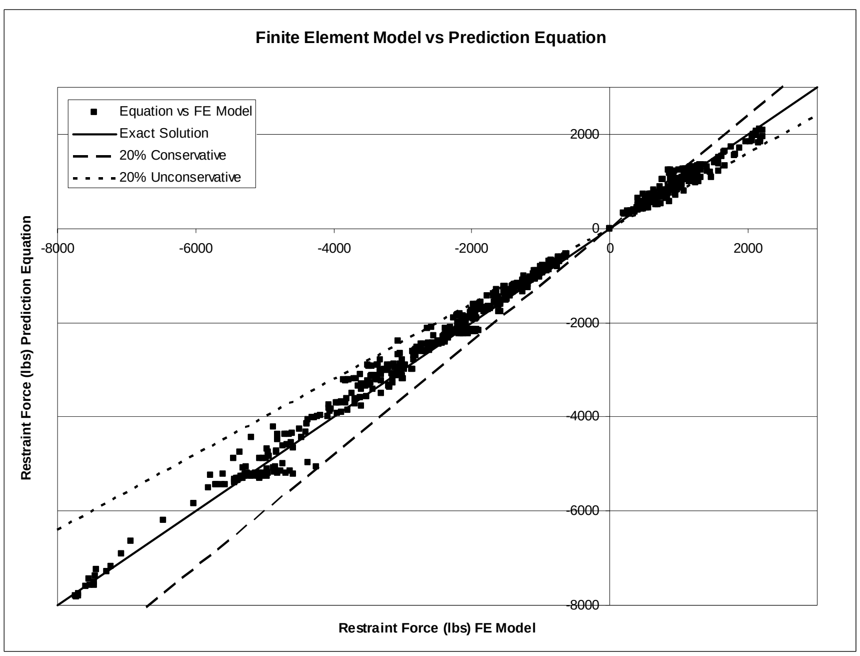

Figure 5 Comparison of Prediction Method with Finite Element Results

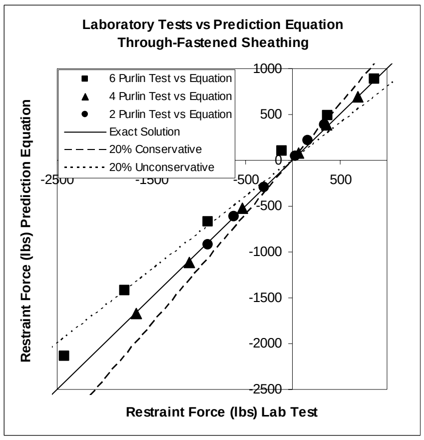

(a) Through Fastened Sheathing

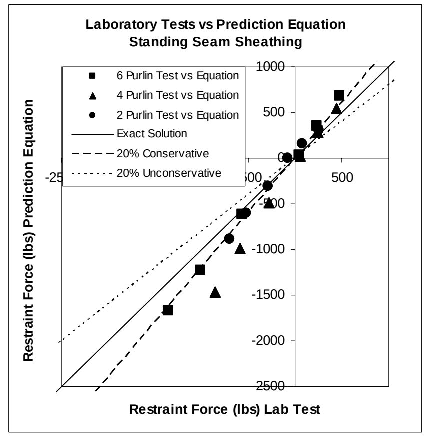

(b) Standing Seam Sheathing

Figure 6 Comparison of Prediction Equation with Laboratory Tests

ranging from 0:12 to 4:12. Restraint was applied by a ½ in. diameter rod attached to the web at 2.25 in. from the top of the Z-section.

The prediction method is compared to the results of the through fastened tests in Figure 6 (a). The results of the two and four Z-section line tests correlate well with the prediction method, falling almost exactly on the predicted line. For the six Z-section line tests, the force predicted by the equations is less than that of the test. In the test, a backing plate was placed between the anchorage and the Z-section to reduce local deformations. This backing plate effectively increases the stiffness of the restraint, which would lead to higher restraint forces than predicted. In the case where an unconventional system such as the backing plate is used, a simple test of the configuration could be used to determine the actual stiffness of the configuration.

Comparison of the prediction method with the results of the standing seam tests by Seek and Murray (2004b) are shown in Figure 6 (b). The tests show greater deviation from the prediction equations although the deviation is consistently conservative. Because a standing seam system with an articulating clip was used for the test, 1/2 in diameter rods connected each purlin at the restraint location provide a means to transfer the restraint force through the system,. The prediction method assumes this system to be rigid when in reality it has some flexibility. Consequently, the actual restraint stiffness of the test (or any real system) is less than rigid and the prediction method will always predict the restraint force conservatively, although in this case the deformation will be underestimated.

Conclusions

The component stiffness method for the determination of lateral brace forces in single span Z-purlin roof systems outlined here is a complex solution to the complex problem of Z-purlin behavior. The method approximates the behavior of Z-section roofs as a single degree of freedom system and attempts to quantify the contribution of all of the components of the system that resist the tendency of the Z-section to rotate and deflect laterally. While complex, the methodology has the ultimate flexibility to accommodate a wide array of system configurations. Because the method is based on stiffness principles, actual stiffness values of components not explicitly quantified herein may be determined from tests and substituted for the equations provided.

Acknowledgements

This study was funded in part by the American Iron and Steel Institute and the Metal Building Manufacturers Association, as well as the Virginia Tech Department of Civil and Environmental Engineering, Via Fellowship Program.

Appendix - References

Seek, M. W. and Murray, T. M. (2004a). "Computer Modeling of Sloped Z-Purlin Supported Roof Systems to Predict Lateral Restraint Force Requirements." *Conference Proceedings, 17th International Specialty Conference on Cold-Formed SteelStructures.* Department of Civil Engineering, University of Missouri-Rolla. Rolla, Missouri.

Seek, M. W. and Murray, T.M. (2004b). "Testing of the Lateral Restraint Force Requirements of Sloped Z-Purlin Supported Standing Seam and Through-Fastened Roof Systems with Two, Four and Six Purlin Lines." Research Report CE/VPI-ST-04/01. Department of Civil and Environmental Engineering, Virginia Polytechnic Institute and State University, Blacksburg, VA, 67 Pages.

Seek, M.W. and Murray, T.M. (2005) Mechanics of Lateral Brace Forces in Z-Purlin Roof Systems. *Conference Proceedings, Structural Stability Council Annual Stability Conference*. Structural Stability Research Council. University of Missouri-Rolla. Rolla, Missouri.

Appendix – Notation

$$I_{mY} = \frac{I_X I_Y - I_{XY}^2}{I_X} \qquad a = \sqrt{\frac{EC_W}{GJ}} \qquad \lambda = \frac{0.71\,{}^1\!/_4\,Et^3}{0.38K_{MDeck}\,d + 0.71\,{}^1\!/_4\,Et^3}$$

$$\tau = \frac{\dfrac{a^2\beta}{GJ}}{1 + \dfrac{K_{MDeck}}{GJ}\kappa} \qquad \beta = \frac{L^2}{8a^2} + \frac{1}{\cosh\left(\dfrac{L}{2a}\right)} - 1$$

$$\kappa = \frac{8a^4}{L^2}\left(1 - \cosh\left(\frac{L}{2a}\right) + \frac{\cosh\left(\dfrac{L}{a}\right) - 1}{\sinh\left(\dfrac{L}{a}\right)}\sinh\left(\frac{L}{2a}\right)\right) + \frac{5L^2}{48} - a^2$$

b	= width of Z-section top flange (in) (mm)
b_{ar}	= width of anti-roll clip (in) (mm)
b_{pl}	= width of single plate rafter clip (in) (mm)
d	= depth of Z-section (in) (mm)
E	= modulus of elasticity (29,500,000 psi) (203,400 MPa)
G	= shear modulus (11,200,00 psi) (77,200 MPa)
h	= height of applied restraint measured from base of Z-section parallel to web (in)
K_{MDeck}	= combined rotational stiffness of sheathing and the connection between the Z-section and sheathing (lb-in/ft) (N-m/m)
L	= span of Z-section (ft) (m)
L_{Fast}	= Spacing between fasteners connection Z-section to Sheathing
n_{sys}	= number of system Z-sections
n_{rest}	= number of restrained Z-sections
t	= thickness of Z-section (in)
t_{pl}	= thickness of single plate rafter clip (in) (mm)
w	= uniform loading on Z-section (lb/ft) (N/m)
Width	= Tributary width of diaphragm (perpendicular to Z-Section Span) per Z-section.(in) (mm)
δ	= load eccentricity on Z-section top flange (1/3)
θ	= angle between the vertical and the plane of the web of the Z-section (degrees)

Seek, M.W. and Murray, T.M. (2007) "Lateral Brace Forces in Single Span Z-Section Roof Systems with Interior Restraints using the Component Stiffness Method." *Conference Proceedings, Structural Stability Research Council Annual Stability Conference.* Structural Stability Research Council. University of Missouri-Rolla. Rolla, Missouri.

LATERAL BRACE FORCES IN SINGLE SPAN Z-SECTION ROOF SYSTEMS WITH INTERIOR RESTRAINTS USING THE COMPONENT STIFFNESS METHOD

Michael W Seek, PE[1] and Thomas M Murray, Ph.D, PE[2]

There are many advantages to roof system utilizing Z-sections topped with metal sheathing. The system is structurally efficient, easy to install, and utilizes recyclable material. Two of the greatest advantages of the Z-section is that its shape allows for nesting – which facilitates transportation and allows for lapping in multiple span systems. For the Z-sections to be lapped, the bottom flange of the Z-section is placed at the top flange of the rafter and sheathing is attached to the top flange of the Z-section. Consequently, loads applied at the sheathing elevation must be transferred over the depth of the Z-section to the rafter elevation. To limit lateral movement of the system, lateral restraints must be applied.

It is most common to provide lateral restraint along the frame lines, considered a supports lateral restraint configuration. Forces are simply transferred from the sheathing elevation to the rafter elevation through the use of anti-roll anchorage devices. For long span systems and systems with flexible diaphragms, large deformations can occur at the interior of the bay. To prevent these deformations and the associated second order effects, lateral restraints can be applied at the interior of the bay.

---

[1] VIA PhD Scholar , Virginia Tech, Blacksburg, VA, USA.
[2]Montague Betts Professor of Structural Steel Design, Virginia Tech, Blacksburg, VA, USA

Due to the interaction of the sheathing and Z-section, the mechanism generating the need for lateral restraint and the contributing resistance of the system make for a complex problem. The component stiffness method discussed herein provides a means of determining the magnitude of restraint forces by determining the contributing stiffness of each of the components of the system to the overall resistance to lateral movement. The method also provides a means of predicting the forces that must be transferred through the connection between the sheathing and Z-section. Finally, the component stiffness method provides a means of approximating the lateral deformation of the system which is necessary to assess the effectiveness of a restraint configuration.

COMPONENT STIFFNESS METHOD

The component stiffness method was introduced by Seek and Murray (2006) as a method to predict lateral restraint forces in roof systems supported by Z-sections restrained along the frame lines. The method approximates a bay of Z-sections as a single degree of freedom system and uses a stiffness formulation to determine the contribution of the different components in the system to the resistance of lateral movement. A free body diagram of the forces acting on the system requiring the need for restraint is shown in Figure 1 (a). Gravity loads are divided into a vertical component that acts in a plane parallel to the web of the purlin and a downslope component that acts in the plane of the sheathing. The vertical component of the gravity load, $w \cdot \cos\theta$, acts eccentrically on the top flange of the purlin creating an overturning moment. This force causes deformation of the Z-section that is resisted through the development of shear forces in the diaphragm and a moment, $M_{torsion}$, in the sheathing. Local bending of the flange generates an additional moment in the sheathing, M_{local}. The downslope component of the gravity load, $w \cdot \sin\theta$, acts in the plane of the sheathing, creating an overturning moment about the base of the purlin.

There are three "components" that provide resistance to the lateral/overturning forces as shown in Figure 1(b). The majority of

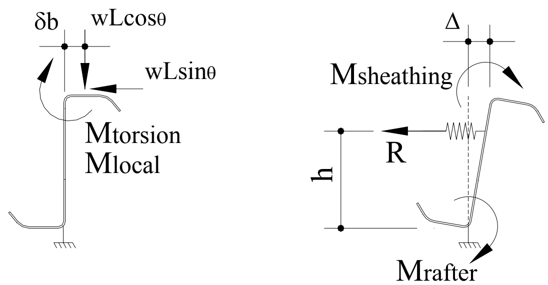

(a) Loads (b) Resistance

Figure 1. Free body diagram of external forces and resistance

resistance is provided by an external restraint, R. However, as the stiffness of this external restraint is reduced, moments are developed in the sheathing, $M_{Sheathing}$, and at the connection between the Z-section and rafter, M_{Rafter}, that provide additional resistance to the overturning. Because the resistance is inherent in the system, the moments M_{rafter} and $M_{sheathing}$ are considered system effects. Summing moments about the base of the purlin, the external restraint force, R, is

$$R = \frac{wL(\delta b \cos\theta - d \sin\theta) + M_{Torsion} + M_{Local} + M_{Sheathing} + M_{Rafter}}{h} \quad (1)$$

The external forces cause lateral movement of the top flange of the purlin relative to the base. Each of the purlins in the system is assumed to be rigidly linked together laterally by the sheathing or some mechanism that transfers force through the system to the restraints such as strapping. This assumption allows the system to be represented by a single degree of freedom and the forces in the components can be related to each other. The stiffness of the restraint is defined as the force developed in the restraint per unit of lateral deflection of the top flange of the purlin. The sheathing and rafter stiffness is defined as the moment generated in each component per unit lateral displacement of the top flange at the restraint location. The amount of the external forces distributed to each of the restraining components is determined from the ratio of the stiffness of each component to the total stiffness of the system. The force in the restraint therefore is

$$R = \frac{wL(\delta b \cos\theta - d \sin\theta) + M_{torsion} + M_{local}}{h} \cdot \frac{\sum K_{rest}}{K_{total}} \tag{2}$$

TORSIONAL MOMENT

The torsional moment developed due to the interaction between the sheathing and Z-section is a result of the peculiar flexural characteristics of the Z-section. The behavior of a Z-section with internal restraints is similar to one with restraints at supports with some subtle differences. To understand these differences it is first necessary to review the flexural behavior of a single purlin with supports restraints as presented by Seek and Murray (2006). The basic model considered is a Z-section with rotational restraints at the ends on a flat slope roof with a uniform load applied in the plane of the web. The uniformly applied load causes the Z-section to deflect vertically, Δ_V, and horizontally, Δ_H, at mid-span as shown in Figure 2 (a).

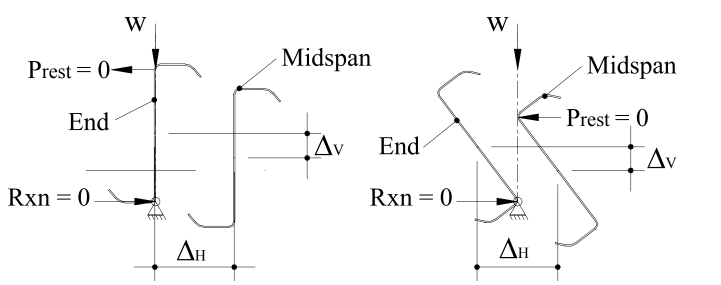

(a) Supports Restraints (b) Midpoint Restraint

Figure 2. Displaced shape of Purlin

The diaphragm attached to the top flange of the Z-section provides resistance to this lateral deformation. This resistance is approximated as a uniformly applied lateral force, w_{rest}, at the Z-section top flange. Because this force (or resistance) is applied eccentrically to the shear center of the Z-section, the force causes rotation of the section, Φ, as shown in Figure 3 (a). The rotational stiffness of the connection between the sheathing and the Z-section, k_{mclip}, resists the rotation of the purlin through the generation of a torsional moment along the length of the purlin. Because the moment is directly proportional to the rotation and the rotation varies from zero at the supports rotational restraints to maximum at mid-span, the moment in the sheathing is assumed to have a parabolic distribution. The moment reduces the rotation of the purlin by $\Phi_{Mtorsion}$, and the final midspan rotation is Φ_{net} as shown in Figure 3 (b).

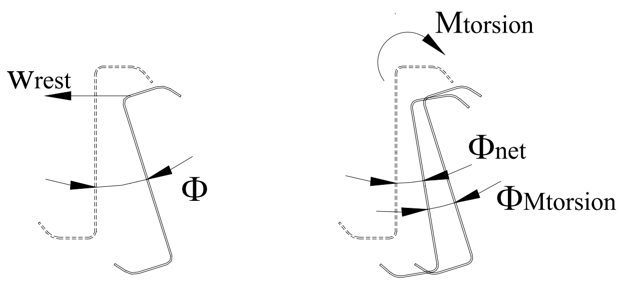

(a) due to diaphragm restraint (b) due to sheathing rotational restraint

Figure 3 Midspan rotation of a purlin with supports restraints

It has been hypothesized that the uniform gravity load in the sheathing is transferred into the purlin at some eccentricity, δ, along the top flange (Ghazanfari and Murray, 1983). This eccentrically applied load induces a torsion that results in rotation of the Z-section. Because the sheathing will always attempt to resist rotation, additional moments are generated in the sheathing. For a configuration with restraints only at the supports, the net torsional moment generated in the sheathing due to flexural effects is

$$M_{Torsion} = \tfrac{2}{3} K_{MClip} L \left(w_{rest} \cdot \frac{d}{2} - w\left(\delta b \cos\theta\right) \right) \tau \qquad (3)$$

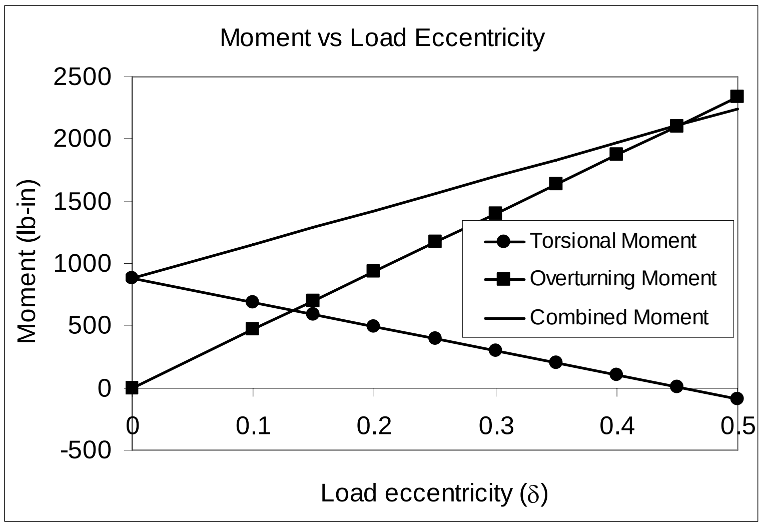

Figure 4. Overturning moment, Torsional Moment, and Combined Moment vs Load eccentricity on Z-section top flange.

The magnitude of the $M_{torsion}$ is maximum for $\delta = 0$ and decreases with increasing load eccentricity. Of course, as the eccentricity increases, the overturning moment ($wL \cdot \delta b \cdot \cos\theta$) increases and there is a net increase in the combined moment that must be restrained. The torsional moment, overturing moment and the combination of these two effects are plotted relative to the load eccentricity for a 10Z2.6x097 in Figure 4.

It is believed that the load eccentricity on the top flange is a function of the purlin and sheathing section properties. A Z-section with a low torsional stiffness relative to the sheathing rotational stiffness appears to have a larger eccentricity than a Z-section with a greater resistance to torsion. Most of the test results investigated showed good correlation for an assumed eccentricity of one third of the Z-section flange width, however for some cases the best correlation was for assumed eccentricities of one half the flange width. For a low slope roof (roof slope < 1:12), it is typically conservative to overestimate eccentricity. For steeper slope roofs, underestimating eccentricity is conservative. A more extensive investigation into the interaction between the purlin, connectors and sheathing is required to better understand this behavior.

Z-SECTION WITH INTERIOR LATERAL RESTRAINTS

The torsional behavior of a single purlin with interior restraints is similar to one with supports restraints. Considering a single purlin with internal restraints at the top flange of the purlin and ignoring the contribution of the sheathing, the Z-section has the tendency to deflect laterally. While the peak displacement of a supports configuration is at midspan, for an interior restraint configuration, the restraint at the top flange significantly reduces the deflection of the Z-section at mid-span. In order to maintain equilibrium this restraint force must be zero. To maintain compatibility, the vertical and lateral displacements, Δ_V and Δ_V, must exist between the ends and midspan. To accomplish this, the deflected shape of the Z-section is as shown in Figure 1 (b).

Like the supports restraint configuration, if the diaphragm stiffness of the sheathing is considered, the lateral deformation is reduced through the development of an internal uniformly distributed force in the diaphragm. This force is resolved entirely in the diaphragm and the restraint force remains zero. The uniform force in the sheathing, however induces a torsion on the purlin causing rotation of the mid-span relative to the ends, $\Phi_{Torsion}$, as shown in Figure 5. Because restraint is applied at the interior, an additional rotation occurs at each end as a result of diaphragm flexibility. The end rotation, Φ_{End}, is approximated as the diaphragm deflection at the end of the purlin relative to the restraint location divided by depth. As the diaphragm stiffness increases, the diaphragm displacement decreases. For a rigid diaphragm, the end rotation is zero and the midspan rotation matches that for a supports restraint configuration with a rigid diaphragm.

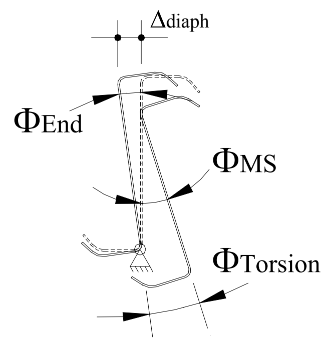

Figure 5. Torsional Rotation, End Rotation, and Net Rotation

To determine the effect of the purlin rotation on the moments in the sheathing, the two rotations of the purlin, $\Phi_{Torsion}$, and Φ_{End}, are considered separately. Like the supports restraint configuration, a portion of the rotation of the purlin, $\Phi_{Torsion}$ varies from zero at the end to maximum at midspan and therefore is approximated as parabolic. By separating out the torsional rotation, the end rotation can be considered as uniform (rigid body rotation). For a third points restraint configuration, the total moment in the sheathing due to these rotations is

$$M_{torsion} = \tfrac{2}{3} k_{mclip} \tau \cdot wL \left(\frac{\sigma}{2d} - \delta b \cos\theta \right) + \frac{wL^3 k_{mclip}}{6G' Width \cdot d} \left(\frac{\sigma}{3} + \frac{\sin\theta}{6} - \frac{\delta b \cos\theta}{2d} \right) \left(1 - \tfrac{2}{3} k_{mclip} \tau \right) \quad (4)$$

The first part of the summation is the same as Equation (3) for a supports restraint configuration. The second part of the summation accounts for the moment due to the end rotation. It is assumed to be uniform but as was shown previously, a uniform moment causes additional rotations, so the moment is modified by the term (1-2/3$k_{mclip}\tau$) to account for this rotation. For systems with a diaphragm stiffness, G', greater than 5000 lb/in, this effect is negligible. For roofs with pitches steeper than 1:12, it is conservative to eliminate this additional effect.

The approximations for the torsional moment given in Equation (4) assume that plane sections always remain plane. Because Z-sections can be made of rather thin material, the purlin cross section can deform without fully transferring the moments predicted in Equation (4). Consequently, a modification is made to the sheathing moment based upon finite element model results that attempts to account for this local deformation. The sheathing moment including the local deformation moment is

$$M_{local} = -wL \cdot \delta b \cos\theta \cdot \frac{K_{MClip}}{K_{MClip} + \frac{Et^3}{3d}} \tag{5}$$

The treatment of local deformations here is slightly different than that presented by Seek and Murray (2006) but results in a better approximation of behavior. Like the torsional moments, local deformations are believed to have some effect on the effective eccentricity. A thinner purlin has less resistance to this local deformation and effectively reduces the eccentricity, δ, at which the load is transferred to the flange of the purlin. A more rigorous investigation of the interaction between the sheathing and Z-section is required to better understand this behavior.

PROBLEM SOLUTION

There are three steps to determining the lateral restraint forces using the component stiffness method. The first step is to determine the uniform restraint force provided by the sheathing, w_{rest}. For a uniform system, this is a single calculation. For a system with different loadings, spacing, or section properties, the force must be calculated for each different Z-section in the system. Upon calculating the uniform restraint in the sheathing, the total lateral force that must be restrained is found using Equation (2). Stiffness values for each of the components of the system must be calculated. To determine the restraint force, the total force in the system is multiplied by the relative stiffness of the restraint to the total restraint of the system.

Fundamental to the problem is the solution of the uniform restraint force in the sheathing. The formulation presented applies to a third points restraint configuration, but the methodology could be applied to any restraint configuration symmetric about the midspan within the middle third of the Z-section span. By enforcing compatibility of the purlin and diaphragm utilizing the concept of unrestrained and restoring displacements as outlined by Seek and Murray (2005), the uniform restraint force in the sheathing is

$$w_{rest} = w \cdot \sigma \tag{6}$$

where

$$\sigma = \frac{\dfrac{11\left(\dfrac{I_{XY}}{I_X}\cos\theta\right)L^4}{972EI_{mY}} + \dfrac{(\delta b\cos\theta)d}{2}\tau - \dfrac{L^2\sin\theta}{18G'Width}}{\dfrac{11L^4}{972EI_{mY}} + \dfrac{d^2}{4}\tau + \dfrac{L^2}{9G'Width}} \tag{7}$$

Lateral deflections are taken at the third points along the span while the rotations are taken at the mid-span for simplicity of calculations. For an exact solution, lateral displacement and rotational compatibility should be satisfied at the same location. However, this approximation results in negligible error in the final results.

There are two components that are considered to contribute to the lateral stiffness of the system, the external restraint and the stiffness of the sheathing. The stiffness of the connection between the rafter and Z-section is considered to be negligible and therefore is not included in the formulation. The restraint is considered to be rigidly attached to the top flange of the purlin, i.e. there is no deformation in the purlin in transferring force out to the sheathing and into the restraint. Flexibility is assumed to be introduced through the deformation of the anchorage of the restraint. For example, if the third point is restrained by strapping anchored by an eave strut, the restraint stiffness is the bending stiffness of the eave strut at the third point location. Alternatively, the restraint stiffness may be determined by test. In lieu of calculating restraint stiffness, it may be assumed to be rigid, i.e. all the external force is distributed to the restraint. This will always lead to a conservative approximation of restraint force. This approximation will however lead to unconservative approximations of lateral deflection.

Determination of the sheathing stiffness for an interior restraint configuration is the same as was introduced by Seek and Murray (2006). As the external restraint permits lateral movement of the top flange of the Z-section, $\Delta_{restraint}$, it is assumed to rotate as a rigid body about the base of the purlin and the rotation is approximated as $\Delta_{restraint}/d$. This uniform rotation generates a uniform moment in the sheathing. The uniform moment causes additional rotation of the midspan relative to the ends that is assumed to have a parabolic distribution. Consequently, the moment is reduced for this effect of this additional rotation by the term $(1\text{-}2/3K_{mclip}\tau)$. Local deformations again come into play, so the stiffness is further modified based upon the results of finite element modeling, to yield

$$K_{shtg} = \frac{K_{mclip}L}{d}\left(1 - \tfrac{2}{3}K_{mclip}\tau\right)\left(\frac{\tfrac{1}{4}Et^3}{0.38K_{mclip}d + 0.71\tfrac{1}{4}Et^3}\right) \qquad (8)$$

In Seek and Murray (2006), purlins are categorized as to whether they are directly restrained or considered system purlins in which restraint is applied indirectly through the sheathing. The stiffness of a directly restrained purlin is slightly larger than that of an unrestrained purlin because local deformations of the purlin at the restraint location increase the moments per unit displacement. One of the assumptions in the formulation of the interior restraint case is that local deformation is at the restraint is ignored. Therefore, all of the purlins can be treated as system purlins. This approximation results in a conservative approximation of restraint force.

The total stiffness of system is the combination of the stiffness of each of the restraints and the stiffness of the sheathing for each of the purlins in the system,

$$K_{total} = \sum K_{rest} + \frac{\sum K_{shtg}}{d} \tag{9}$$

The lateral restraint force, P_L, is determined by multiplying the sum of the forces in the system by the ratio of the restraint stiffness to the total stiffness of the system.

$$P_L = \sum \left(wL \cdot \frac{\delta b \cos\theta - d \sin\theta}{h} + \frac{M_{torsion}}{h} + \frac{M_{local}}{h} \right) \frac{\sum K_{rest}}{K_{total}} \tag{10}$$

Equation (10) allows for variation of the restraint height although it is assumed that the height of the restraint is as close as possible to the top of the purlin. Lowering the restraint height in the calculations will typically lead to a conservative approximation of the restraint force. However, locating the restraint lower than two times the web-flange radius introduces additional flexibility into the system and reduces the effectiveness of the restraint. Unless this flexibility is accounted for in the stiffness of the restraint, Equation (10) will conservatively predict the restraint force but will underestimate the amount of deformation of the system.

In this formulation for third points restraints, it is assumed that that the connection between the rafter and purlins is rotationally pinned. For a Z-section flange-to-rafter bolted connection, this will typically result in a conservative restraint force. If the end connection significantly restrains the displacement of the top flange of the purlin (as in a web plate), the restraint force can be significantly different that calculated by Equation (10). In any case where the connection between the rafter and Z-section provides significant restraint, the restraint configuration should be considered a third points plus supports configuration rather than a purely third points configuration.

As important as the restraint force is the force in the connection between the purlin and sheathing at the restraint. This force is significant and must be transferred to the sheathing over a distance of approximately 12 in. (30 cm) to either side of the restraint. Conservatively, the fastener force can be assumed to equal the restraint force. A reduction in this force can typically be achieved using Equation (11).

$$FastenerForce = P_L \frac{h}{d} + \frac{wL}{20}\left(\frac{\delta b \cos\theta}{d} - 0.9\sigma\right) \tag{11}$$

To ensure effectiveness of the lateral restraints, the deformation of the system should be checked. There are two locations where the deformation is important: deformation at the restraint location and deformation at the frame line. The deflection at the restraint is

$$\Delta_{rest} = \frac{P_L}{K_{rest}} \tag{12}$$

Additional deformation of the system occurs along the frame lines. Using the shear forces developed in the diaphragm, the lateral displacement of the top flange of the purlin at the frame lines relative to the restraint location is

$$\Delta_{diaph} = -\frac{L^2}{9G'Bay}\sum w\left(\sigma + \tfrac{7}{2}\sin\theta \frac{\sum K_{rest}}{K_{total}}\right) + \frac{P_L \, \tfrac{h}{d} \, L}{3G'Bay} \tag{13}$$

In Equations (12) and (13), a positive deflection indicates upslope translation. The net displacement of the top flange of the purlin relative to its initial position is the sum of Δ_{rest} and Δ_{diaph}. The deflection of the restraint calculated at factored load levels should be limited to

$$\Delta_{rest} \le \phi \frac{d}{20} \tag{14}$$

The maximum lateral deflection of the top flange of the purlin along the purlin span relative to the restraint calculated at nominal load levels should be limited to the L/360.

CONCLUSIONS

Though originally developed for roof systems with lateral restraints at the support location, the component stiffness method can also be applied to single span Z-section roof systems with interior restraints. The method accounts for the effects that variations in the flexural and torsional properties of the Z-section and diaphragm and rotational stiffness properties of sheathing have on the lateral restraint forces. The method has the flexibility to incorporate systems with different purlins sizes or applied uniform loads. Just as important as the restraint forces, the method also predicts the lateral displacement of system, providing a means to determine the effectiveness of the lateral restraints.

Though the equations presented are applicable only to a third point restraint configuration, the equations require only slight modification for any interior bracing configuration symmetric about the mid-span within the middle third of the purlin span. Because the method is developed from mechanics principles familiar to engineers, it helps improve the understanding of the complex behavior of Z-section roof systems. The component stiffness method provides a rational means of predicting lateral restraint forces, ensuring that increasingly popular Z-section roof systems can be safely and efficiently designed.

REFERENCES

Ghazanfari, A. and Murray, T.M. (1983). "Prediction of the Lateral Restraint Forces of Single Span Z-Purlins with Experimental Verification." Fears Structural Engineering Laboratory Report No. FSEL/MBMA 83-04, University of Oklahoma, Norman, Oklahoma, 131 pages.

Seek, M.W. and Murray, T.M. (2005) Mechanics of Lateral Brace Forces in Z-Purlin Roof Systems. *Conference Proceedings, Structural Stability Council Annual Stability Conference.* Structural Stability Research Council. University of Missouri-Rolla. Rolla, Missouri.

Seek, M. W. and Murray, T. M. (2006). "Component Stiffness Method to Predict Lateral Restraint Forces in End Restrained Single Span Z-Section Supported Roof Systems with One Flange Attached to Sheathing." *Conference Proceedings, 18th International Specialty Conference on Cold-Formed Steel Structures.* Department of Civil Engineering, University of Missouri-Rolla. Rolla, Missouri.

APPENDIX – NOTATION

$$I_{mY} = \frac{I_X I_Y - I_{XY}^2}{I_X} \qquad a = \sqrt{\frac{EC_W}{GJ}}$$

$$\tau = \frac{\dfrac{a^2\beta}{GJ}}{1 + \dfrac{K_{mclip}}{GJ}\kappa} \qquad \beta = \frac{L^2}{8a^2} + \frac{1}{\cosh\left(\dfrac{L}{2a}\right)} - 1$$

$$\kappa = \frac{8a^4}{L^2}\left(\frac{\cosh\left(\dfrac{L}{2a}\right) - 1}{\cosh\left(\dfrac{L}{2a}\right)}\right) + \frac{5L^2}{48} - a^2$$

b	= width of Z-section top flange (in) (mm)
Bay	= total width of diaphragm perpendicular to span (ft) (m)
d	= depth of Z-section (in) (mm)
E	= modulus of elasticity (29,500,000 psi) (203,400 MPa)
G	= shear modulus (11,200,00 psi) (77,200 MPa)
h	= height of applied restraint measured from base of Z-section parallel to web (in)
K_{mclip}	= combined rotational stiffness of sheathing and connection between the Z-section and sheathing (lb-in/ft) (N-m/m)
L	= span of Z-section (ft) (m)
t	= thickness of Z-section (in)
w	= uniform loading on Z-section (lb/ft) (N/m)
Width	= Tributary width of diaphragm (perpendicular to Z-Section Span) per Z-section.(in) (mm)
δ	= load eccentricity on Z-section top flange (1/3)
θ	= angle between the vertical and the plane of the Z-section web (degrees)

Seek, M.W. and Murray, T.M. "Prediction of Lateral Restraint Forces in Single Span Z-section Roof Systems with One Flange attached to Sheathing using the Component Stiffness Method" Submitted to the Journal of Constructional Steel Research for publication July 2007.

Prediction of Lateral Restraint Forces in Single Span Z-section Roof Systems with One Flange attached to Sheathing using the Component Stiffness Method

Michael W. Seek, P.E.
Thomas M. Murray, Ph.D., P.E.

Abstract

The Component Stiffness Method is a method to predict lateral restraint forces in roof systems supported by Z-sections. The method approximates a bay of Z-sections as a single degree of freedom system and uses a stiffness formulation to determine the contribution of the different components in the system to the resistance of lateral movement. The forces generated by the roof system requiring restraint are derived from mechanics and supported through the results of finite element model analyses.

Introduction

In typical metal building roof systems, a Z-section is installed with the bottom flange attached to the top of the supporting rafter and the top flange is attached to sheathing as shown in Figure 1. This configuration allows for simple connections to the rafters and permits the Z-section to be installed as a continuous member. However, forces applied to the top flange of the Z-section must be transferred over the depth of the Z-section to the top of rafter elevation. Vertical loads, V, are transferred directly through the Z-section web. Overturning of the Z-section about its base must be resisted by the application of external restraints, R. Overturning forces result from the eccentricity of the applied loads relative to the base and internal forces developed from interaction between the Z-section and sheathing.

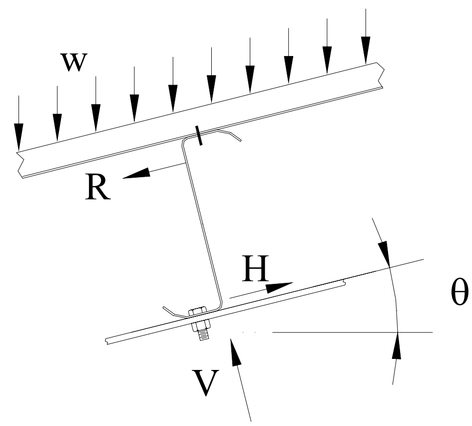

Figure 1. Forces on a sloped Z-section Roof System

The component stiffness method uses a stiffness approach to determine the external restraint forces. The externally applied restraint provides most of the resistance to overturning. However, the roof system has some inherent resistance to the overturning forces through the connection of the Z-section with the sheathing and the connection of the Z-section to the rafter. The roof system is therefore divided into three types of "components" – the external restraint, the connection between the purlin and rafter, and the connection between the sheathing and rafter. The roof system is treated as a single degree of freedom system and the contributions of each component are related by stiffness. The stiffness of each of the components is defined as the force or moment developed in the component per unit lateral displacement of the top flange at the restraint.

There are three main steps to determining the restraint forces in a Z-section supported roof system using the component stiffness method. First it is necessary to determine the forces generated in the roof system. The lateral forces generated are primarily a function of the geometry of the system, but the Z-section also interacts with the sheathing to contribute to the lateral forces that must be restrained. Using a displacement compatibility approach and assuming rigid restraints, the additional contribution of the sheathing/Z-section interaction to the lateral force in the system is determined. These sheathing/Z-section interaction forces are dependent upon the restraint configuration and therefore will vary slightly for each restraint configuration.

Once the forces generated by the system have been determined, the next step in the Component Stiffness Method is to determine the stiffness of the system and distribute forces through the system according to the stiffness of each of the omponents. Each purlin in the bay contributes a rafter stiffness and a sheathing stiffness to the overall stiffness of the system. The rafter stiffness is defined as the moment developed in the connection between the purlin and the rafter per unit displacement of the top flange of the Z-section at the rafter. The sheathing stiffness is defined as the total moment generated between the purlin and sheathing along the span of the purlin per unit lateral displacement of the top flange. The final component contributing to the stiffness of the system is the restraint. The restraint stiffness is the force resisted at the top of the purlin at the restraint per unit displacement of the top flange of the purlin at the restraint. The total stiffness of the bay of purlins then is the sum of the stiffness of each of the components: the sum of the sheathing and rafter stiffness for each purlin and the sum of each restraint applied in the bay. Once the total stiffness of the system has been determined, the force in each component of the system is determined by distributing the total force developed by the system of purlins according to the relative stiffness of the components.

The final step in the Component Stiffness Method is to evaluate the effectiveness of the bracing configuration by checking the forces in the sheathing and the deformation of the system. As the system of purlins generates restraint forces, the diaphragm is relied upon to help transfer and distribute forces throughout the system. These forces must be transferred out of the diaphragm and into the purlins. At the restraint location, these forces can be significant – even exceeding the restraint force. The component stiffness method provides a means of calculating the diaphragm shear forces transferred between the purlin and sheathing.

Deformation of the system must also be considered. Because the lateral bracing is provided to maintain stability of the roof system, it is important that the system be prevented from excessive deformations and the second order effects that accompany these deformations. Equations are provided that predict the lateral displacement of the roof system at the restraint location and the deformation of the diaphragm relative to the restraint location.

Forces Generated in Z-Section supported Roof Systems

The Component Stiffness Method is based upon the free body diagrams shown in Figures 2(a) and 2(b). Figure 2(a) displays the loads developed in the roof system requiring lateral restraints and Figure 2(b) shows the forces restraining the system. The gravity loads applied to the top flange of the Z-section as shown in Figure 2(a) are divided into a vertical component, $w \cdot L \cdot \cos\theta$, parallel to the plane of the web and a downslope component, $w \cdot L \cdot \sin\theta$ in the plane of the sheathing, where w is the uniformly applied gravity load along the span of the Z-section, L is the span of the Z-section and θ is the angle of the roof plane relative to the horizontal. The vertical component of the gravity load is approximated to act at some eccentricity, δb, along the top flange of the Z-section. As the gravity loads are applied to the Z-section, deformation of the Z-section is restrained through the development of diaphragm forces in the sheathing. Torsion of the Z-section and local rotations are resisted by the moments developed in the connection to the sheathing, $M_{torsion}$ and M_{local} respectively. The forces shown in Figure 2(a) have a net overturning effect on the Z-section its base at the rafter location. To determine these forces, the Z-section is considered rigidly restrained at the restraint location.

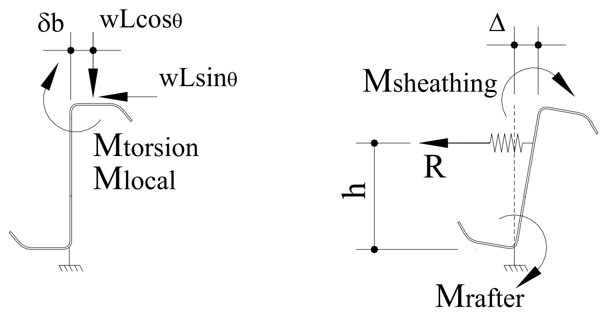

(a) Forces Generated (b) Resisting Forces

Figure 2 Free Body Diagram of Forces Acting on Z-section

Figure 2(b) shows the resistance of the system of Z-sections to these overturning forces. The majority of the resistance to the overturning forces is provided by the external restraint, R. However the restraints have a finite stiffness, and as the restraint permits displacement of the top flange, additional resistance is provided by the inherent lateral stiffness of the system. As the top of the Z-section moves laterally relative to the base, the Z-section rotates about the longitudinal axis relative to the sheathing and a resisting moment is developed in the sheathing, M_{shtg}. Similarly, the connection between the rafter and the Z-section resists the rotation of the Z-section through the development of a moment at the connection. Summing moments about the base of the Z-section, the restraint force is determined from

$$R = wL\left(\frac{\delta b \cos\theta}{h} - \frac{d}{h}\sin\theta\right) + \frac{M_{Torsion} + M_{Local}}{h} + \frac{M_{Sheathing} + M_{Rafter}}{h} \tag{1}$$

The forces resisted by each "component", the external restraint, the sheathing, and the connection of the Z-section to the rafter, are directly related to the displacement of the top flange at the restraint. The component stiffness method defines the stiffness of each of these components as the force or moment generated in the component per unit displacement of the top flange of the Z-section at the restraint. Therefore, the restraint stiffness, K_{rest}, is the force in the restraint at the top flange of the sheathing relative to the displacement of the top flange at the restraint. The sheathing stiffness, K_{shtg}, is the moment generated in the connection between the purlin and the sheathing per unit displacement of the Z-section top flange at the restraint. Similarly, the rafter stiffness is the moment generated at the rafter location per unit displacement of the top flange at the restraint location. By defining the stiffness of each of the components relative to the displacement of the top flange of the Z-section, the Z-setion is treated as a single degree of freedom system. The force resisted by the external restraint is the product of the total forces in the system and the relative stiffness of the restraint to the total stiffness of the system, or

$$R = \left(wL\left(\frac{\delta b \cos\theta}{h} - \frac{d}{h}\sin\theta \right) + \frac{M_{Torsion} + M_{Local}}{h} \right) \cdot \frac{K_{rest}}{K_{rest} + K_{shtg} + K_{rafter}} \tag{2}$$

Torsional Moment

The torsional moment developed due to the interaction between the sheathing and Z-section is a result of the peculiar flexural characteristics of the Z-section. To determine the torsional moment, the Z-section, subjected to a uniform gravity load, is rigidly restrained at the top flange at the restraint location, but is permitted to deflect laterally and vertically. The deformation of the Z-section is restrained by the sheathing through the development of shear forces through diaphragm action and moments due to the torsional restraint of the sheathing. Compatibility between the displaced shape of the Z-section and the sheathing is used to determine the restraining forces in the sheathing. Because the displaced shape of the Z-section is dependent upon the restraint location, an individual set of equations must be derived for each restraint configuration. Two of the more common configurations, a support restraint configuration and a third-points configuration are presented in this paper.

Torsional Moment - Supports Restraint Configuration.

To determine the interacting forces between the purlin and the sheathing for a supports configuration, compatibility of the displaced shape is determined at the mid-span of a single span Z-section. The Z-section is restrained laterally at the top and bottom flanges at the rafter support location and subjected to external gravity loads applied to the top flange. Allowing the Z-section to deform freely and neglecting second order effects, as the vertical component of the gravity load, $w \cdot L \cdot \cos\theta$, acts at an eccentricity, δb, on the top flange of the Z-section, as shown in Figure 2(a), the Z-section will deflect laterally ($\Delta_{x,cen}$) and twist clockwise about its longitudinal axis ($\Delta_{x,torsion}$) as shown in Figure 3. The sheathing attached to the top flange of the Z-section resists this deformation through the development of a uniform horizontal force along the length of the Z-section, w_{rest}, as shown in Figure 4. Application of this uniform force to the top flange of the Z-section results in a restoring lateral deflection ($\Delta_{x,restoring,center}$) and a counterclockwise twist of the Z-section ($\Delta_{x,restoring,torsion}$). The uniform restraint force in the sheathing, w_{rest}, and the downslope component of the gravity load, $w \cdot L \cdot \sin\theta$, result in additional deformation of the top flange of the Z-section at mid-span due to the diaphragm flexibility of the sheathing. Equating the unrestrained displacements to the restoring displacements, the uniform restraint force in the sheathing is determined by

$$w_{rest} = w \cdot \sigma \tag{3}$$

where

$$\sigma = \frac{\dfrac{5\left(\dfrac{I_{XY}}{I_X}\cos\theta\right)L^4}{384EI_{mY}} + \dfrac{(\delta b\cos\theta)d}{2}\tau + \dfrac{L^2\sin\theta}{8G'Width}}{\dfrac{5L^4}{384EI_{mY}} + \dfrac{d^2}{4}\tau + \dfrac{L^2}{8G'Width}} \tag{4}$$

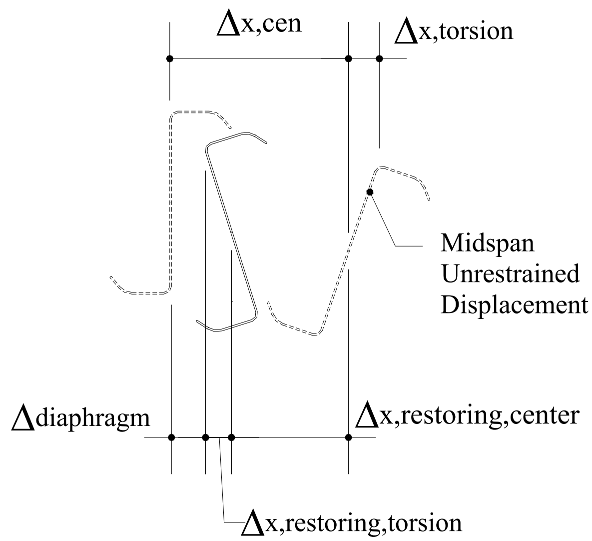

Figure 3. Midspan Displacement Compatibility

For definitions of the terms used in Equation (4) refer to the nomenclature in the Appendix. The term σ is used for convenience of calculation and is considered the proportion of the uniformly applied vertical force transferred to a horizontal force in the sheathing. This proportion can typically be approximated as $\sigma \approx I_{XY}/I_X$. As the combined torsional stiffness of the Z-section and sheathing increases, the second terms in the numerator and denominator will approach zero. Similarly, as the diaphragm stiffness increases, the third terms in the numerator and denominator will approach zero. Therefore, for a perfectly rigid diaphragm and torsionally rigid Z-section-sheathing connection, σ will reduce to I_{XY}/I_X. For low slope roofs, reducing the diaphragm stiffness will reduce the uniform restraint force in the sheathing which will result in $\sigma < I_{XY}/I_X$. For roofs with steeper slopes (typically greater than a 1:12 pitch) reducing the diaphragm stiffness will increase the uniform restraint force in the sheathing relative to the rigid case, or $\sigma > I_{XY}/I_X$. Unlike with the diaphragm stiffness, no simple trend was observed with respect to the torsional stiffness of the Z-section but in general, the torsional stiffness has a small effect on σ.

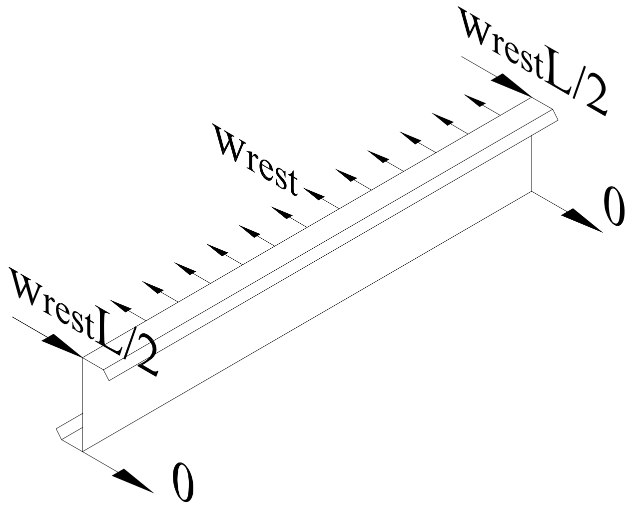

Figure 4. Uniform Restraint Force in Sheathing

Once the uniform restraint force in the sheathing has been determined, the midspan torsional rotation of the Z-section and corresponding moment generated in the sheathing is determined. For a Z-section with end restraints, the rotation of a Z-section about its longitudinal axis is restricted at its ends and increases to maximum at mid-span, Φ, as shown in Figure 5(a). The variation of the torsional rotation is approximated as parabolic along the length of the Z-section. The connection between the sheathing and the Z-section resists this torsion through the development of a moment along the length of the Z-section, $M_{torsion}$, as shown in Figure 5(b). The moment in the sheathing is proportional to the rotation of the Z-section about its longitudinal axis. The stiffness of the connection between the sheathing and Z-section, K_{mclip}, is defined as the moment developed in the connection per unit rotation of the Z-section per unit length along the span. The moment caused by the resistance of the sheathing results in an additional torsional rotation of the Z-section, $\Phi_{Mtorsion}$, as shown in Figure 5(b). The net torsional rotation of the Z-section at midspan, Φ_{net}, is the sum of the rotation caused by the eccentrically applied gravity load, the rotation caused by the uniform lateral resistance of the sheathing at the top flange, and the rotation due to the sheathing moment, or

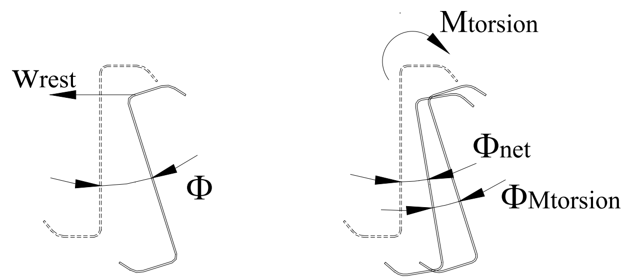

(a) Rotation without Rotational Resistance (b) Net Rotation with Rotational Resitance

Figure 5 Rotation of Z-section at Midspan

$$\phi_{net} = \left(w(\delta b \cos\theta) - w_{rest}\frac{d}{2} \right) \frac{a^2\beta}{GJ} - \phi_{net} \cdot K_{mclip} \left(\frac{\kappa}{GJ} \right) \tag{5}$$

Equation (5) is simplified to yield

$$\phi_{net} = \left(w(\delta b \cos\theta) - w_{rest}\frac{d}{2} \right) \tau \tag{6}$$

Where

$$\tau = \frac{\dfrac{a^2\beta}{GJ}}{1 + K_{mclip}\dfrac{\kappa}{GJ}} \tag{7}$$

The net torsional rotation of the Z-section provided by equation (6) at mid-span is the peak rotation in the parabolic distribution. Relating the moment in the sheathing to the rotation by $M=\Phi_{net} \cdot K_{mclip}$ and integrating along the length of the Z-section, the total moment in the connection between the sheathing and Z-section generated along the length of the Z-section for a supports restraint configuration is

$$M_{Torsion} = \tfrac{2}{3} K_{mclip} \cdot wL \left(\sigma\frac{d}{2} - (\delta b \cos\theta) \right) \tau \tag{8}$$

As the Z-section is shown in Figure 5, with the top flange facing to the right, the positive direction for the torsional rotation and the torsional moment is clockwise. Therefore, as the Z-section undergoes positive torsion, a negeative moment is developed.

The torsional moment, $M_{torsion}$; overturing moment, $w \cdot L \cdot \delta b \cdot \cos\theta$; and the combination of these two effects are plotted relative to the load eccentricity in Figure 6 for a particular Z-section and panel combination. The magnitude of the $M_{torsion}$ is maximum for $\delta = 0$ and decreases with increasing load eccentricity. For an approximate load eccentricity $\delta = 0.45$, the twist angle Φ and corresponding torsional moment equal zero. As the eccentricity increases, the overturning moment ($wL \cdot \delta b \cdot \cos\theta$) increases and there is a net increase in the combined moment that must be restrained.

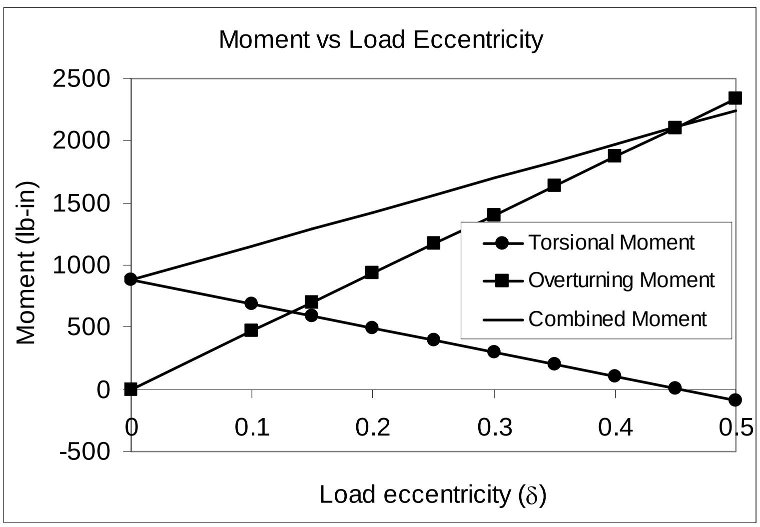

Figure 6. Overturning moment, Torsional Moment, and Combined Moment vs Load Eccentricity on Z-section Top Flange

It is believed that the load eccentricity on the top flange is a function of the Z-section and sheathing section properties. As a Z-section has the greater tendency to twist, the line of action of the vertical component of the gravity load becomes more eccentric to counter the tendency to twist. Ghazanfari and Murray (1983) proposed that the vertical component of the gravity load acts at an eccentricity of $\delta b = b/3$. Comparison of the component stiffness method to test results by Lee and Murray (2001) and Seek and Murray (2004) show good correlation for an eccentricity of one third of the flange width, however for some cases the best correlation was observed for an eccentricity as much as one-half the flange width. For a low slope roof (roof slope < 1:12), it is typically conservative to overestimate eccentricity. For steeper slope roofs, underestimating eccentricity is conservative. A more extensive investigation into the interaction between the Z-section, connectors and sheathing is required to better understand this behavior.

Torsional Moment – Interior Restraint Configuration.

The torsional behavior of a single Z-section with interior restraints is similar to one with supports restraints. Considering a single Z-section with internal restraints at the top flange and ignoring the contribution of the sheathing, when loaded in the plane of the web, the Z-section has the tendency to deflect laterally. While the peak displacement of a supports configuration is at mid-span, for an interior restraint configuration, the restraint at the top flange prevents the deflection of the Z-section at mid-span. To maintain equilibrium this restraint force must be zero. To maintain compatibility, the vertical and lateral displacements, Δ_V and Δ_H, must exist between the ends and mid-span. To accomplish this, the deflected shape of the Z-section is as shown in Figure 7.

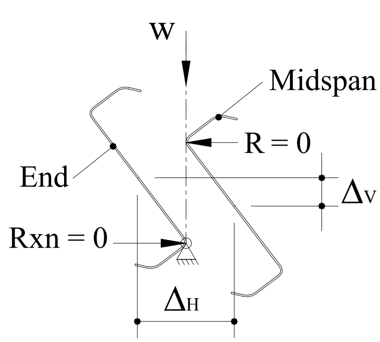

Figure 7 Displacement of Z-section Restrained at Mid-span

Like the supports restraint configuration, if the diaphragm stiffness of the sheathing is considered, the lateral deformation is reduced through the development of an internal uniformly distributed force in the diaphragm. This uniform force in the sheathing induces torsional rotation of the mid-span relative to the ends, $\Phi_{Torsion}$, as shown in Figure 8. Because restraint is applied at the interior, an additional longitudinal axis rotation occurs at each end as a result of diaphragm flexibility. The end rotation, Φ_{End}, is approximated as the diaphragm deflection at the end of the purlin relative to the restraint location divided by depth. The net torsional rotation of the Z-section, Φ_{End}, is the sum of $\Phi_{Torsion}$ and Φ_{End}. As the diaphragm stiffness increases, the diaphragm displacement at the end decreases. For a rigid diaphragm, the end rotation is zero and the midspan rotation matches that for a supports restraint configuration with a rigid diaphragm.

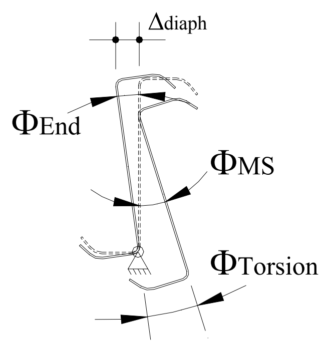

Figure 8. Interior Restraint Configuration: Torsional Rotation, End Rotation, and Net Rotation

To determine the magnitude of the moments in the sheathing due to the rotation of the Z-section about its longitudinal axis, the rotations of the Z-section, $\Phi_{Torsion}$, and Φ_{End}, are treated indepenedently. The first portion of the rotation, $\Phi_{Torsion}$ varies from zero at the end to maximum at midspan and therefore is approximated as parabolic, the same as for a supports restraint configuration. By separating out the torsional rotation, the end rotation, Φ_{End}, can be considered as uniform along the length of the Z-section. Using small angle approximation, this uniform rotation of the Z-section relative to the sheathing is $\Phi_{End} = \Delta_{diaph}/d$. The shear forces in the diaphragm for a third points restraint configuration are distributed along the span of the Z-section as shown in Figure 9. The vertical load effects are shown in Figure 9(a) and the load effects for the downslope component are shown in Figure 9(b). The deformation of the diaphragm is determined at the end of the Z-section relative to the third point by integrating the shear force from the end of the Z-section to the third point (shaded region in Figure 9) and superimposing the vertical load effects and downslope load effects. The approximate restraint force considering only the overturning force, R_0, is required to approximate the forces in the diaphragm. The deflection of the diaphragm at the end of the Z-section relative to the third point is

$$\Delta_{diaph} = \frac{wL^2}{3G' \cdot Width \cdot d}\left(\frac{\sigma}{3} + \frac{\sin\theta}{6} - \frac{\delta b \cos\theta}{2d}\right) \tag{9}$$

Relating the rotation of the Z-section about its longitudinal axis to the moment in the sheathing through the stiffness of the sheathing-to-Z-section connection, K_{mclip}, and accounting for the fact that a uniformly applied torque causes additional torsional rotations distributed parabolically as shown previously, the moment in the sheathing due to the end rotation, Φ_{End}, is

$$M_{End} = \frac{wL^3 k_{mclip}}{6G' \cdot Width \cdot d}\left(\frac{\sigma}{3} + \frac{\sin\theta}{6} - \frac{\delta b \cos\theta}{2d}\right)\left(1 - \tfrac{2}{3} k_{mclip}\tau\right) \tag{10}$$

Combining the end moment with the torsional moment developed previously for the supports restraint configuration, the total moment in the sheathing for a third point restraint configuration is

$$M_{torsion} = \tfrac{2}{3} k_{mclip}\tau \cdot wL\left(\frac{\sigma}{2d} - \delta b \cos\theta\right) + \frac{wL^3 k_{mclip}}{6G' \cdot Width \cdot d}\left(\frac{\sigma}{3} + \frac{\sin\theta}{6} - \frac{\delta b \cos\theta}{2d}\right)\left(1 - \tfrac{2}{3} k_{mclip}\tau\right) \tag{11}$$

For systems with a diaphragm stiffness, G', greater than 5000 lb/in, the additional end rotation moment, M_{end}, is typically negligible. For roofs with pitches steeper than 1:12, it is conservative to eliminate M_{end}.

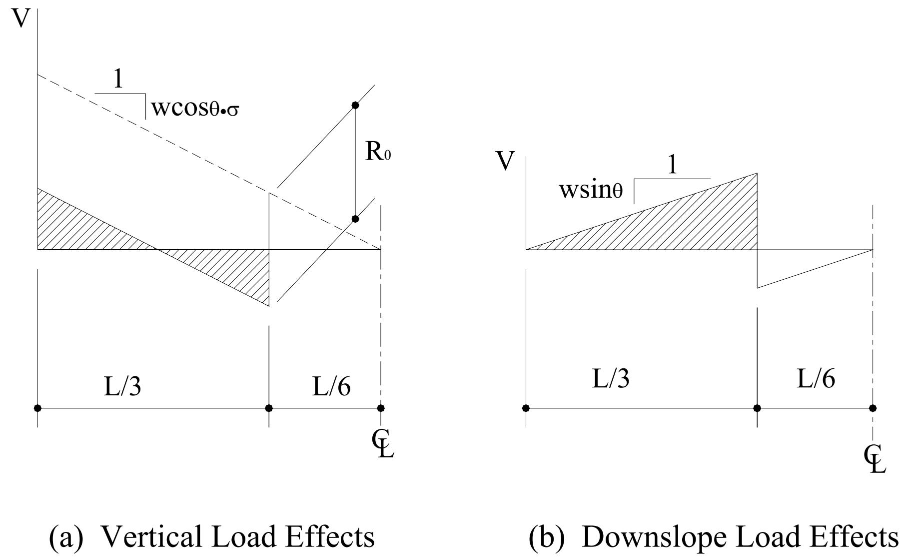

Figure 9 Diaphragm Forces for a Third Points Restraint Configuration

Local Bending Moment

The approximations for the torsional moment given in Equations 8 and 11 assume that plane sections always remain plane. Because Z-sections are manufactured from relatively thin material, the Z-section cross section can deform without fully transferring the moments predicted in Equations 8 and 11. An attempt to capture this additional deformation is made with the model shown in Figure 10. As the vertical component of the gravity load acts eccentrically on the top flange of the Z-section, the flange deflects causing a local rotation of the Z-section relative to the sheathing. Due to the rotational resistance of the connection between the Z-section and sheathing, a moment is developed in the sheathing. The magnitude of this moment, referred to as the local bending moment, is

$$M_{local} = -wL \cdot \delta b \cos\theta \cdot \frac{K_{MClip}}{K_{MClip} + \dfrac{Et^3}{3d}} \tag{12}$$

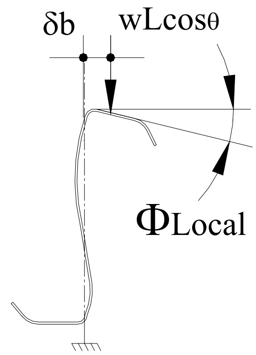

Figure 10 Local deformation of Z-section

Stiffness of Components

Restraint Stiffness

For the purposes of determining the restraint stiffness, restraints are divided into two categories: support restraint and interior restraint. A restraint is considered a “support” restraint for lateral restraint applied along the frame line and an interior restraint is for restraints applied along the interior of the span.

Restraint Stiffness – Support Restraint

The stiffness of each restraint is defined as the force developed at the top flange of the Z-section at the restraint per unit displacement of the top flange at the restraint location. As shown in Figure 11, the deformation at the restraint is the combination of the deformation of the restraint device, Δ_{device}, and the deformation of the web of the purlin relative to the restraint, Δ_{config}. The total stiffness at the restraint, K_{rest}, provided in Equation 13 is the combination of the stiffness of the device at the height at which the restraint is applied, K_{device}, and the stiffness of the web of the purlin as the force is transferred transverse to the web of the purlin from the top flange to the height of the restraint, K_{config}. The net stiffness of the restraint is defined as the restraint as the force at the top flange of the Z-section per unit displacement of the top flange.

$$K_{rest} = \frac{\left(\frac{h}{d}\right)^2 K_{device} \cdot K_{config}}{\frac{h}{d} K_{device} + K_{config}} \tag{13}$$

For a support restraint configuration, the stiffness of the device is generally very high relative to the configuration stiffness. The device stiffness will typically have a negligible effect on the restraint stiffness and can be considered rigid in many cases. For determination of the restraint force, this approximation will be conservative, although the predicted deformation of the system will be unconservative.

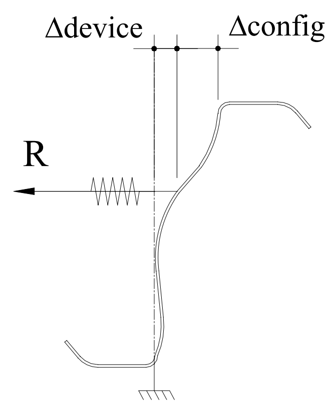

Figure 11 Combined Displacement of Device and Configuration

Support restraints are divided into two categories – discrete anchorage devices and antiroll anchorage devices. A discrete anchorage device provides lateral resistance at a discrete location along the height of the Z-section as shown in Figure 12(b) while an antiroll anchorage device clamps to the web of the Z-section at multiple locations along the depth as shown in Figure 12(a). The antiroll anchorage device prevents deformation of the Z-section web below the restraint location while a discrete restraint permits some deformation, resulting in a variation in stiffness. An equation to predict the stiffness of each type of configuration is provided due to this variation in stiffness.

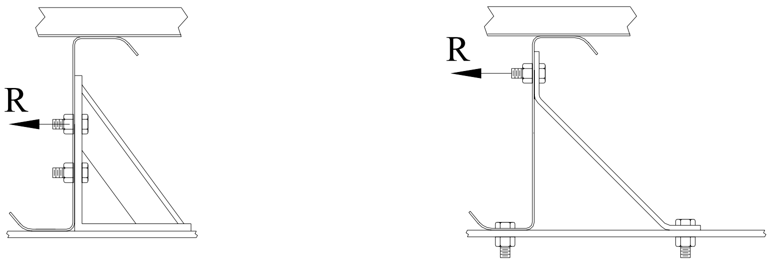

(a) Anti-roll Anchorage Device (b) Discrete Anchorage Device

Figure 12 Supports Restraint Configurations

The equation to predict the configuration stiffness of a discrete restraint configuration is based on a two dimensional beam model bent about the thickness of the web as shown in Figure 13. To account for the third dimension, the effective width of the web and sheathing, the representative equation was calibrated to the results of finite element models as described by Seek and Murray (2004). The resulting configuration stiffness for a discrete restraint is

$$K_{config} = \frac{\frac{1}{15} d \cdot (3Et^3)}{h(d-h)^2} \left[\frac{\frac{1}{15} d \cdot 2Et^3 (3d-h) + \frac{L}{80} \cdot K_{mclip} \cdot d(3d-2h)}{\frac{1}{15} d \cdot Et^3 (4d-h) + \frac{L}{80} \cdot K_{mclip} \cdot d(d-h)} \right] \tag{14}$$

where d is the depth of the section, h is the height of the restraint, L is the span length of the Z-section and k_{mclip} is the rotational stiffness of the connection between the purlin and sheathing.

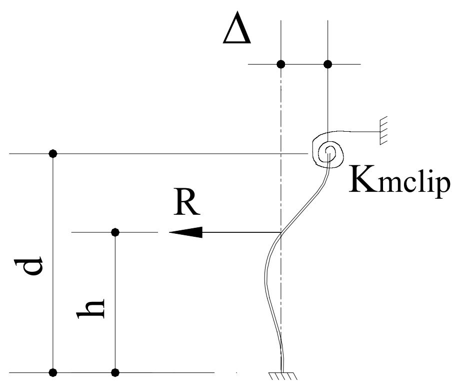

Figure 13 Stiffness Model – Discrete Restraint

For an antiroll anchorage device, the configuration stiffness is based upon the two-dimensional line element model shown in Figure 14. The model assumes that restraint is applied at the top row of bolts and the web of the Z-section is rotationally fixed at this point. The effective width of the web is assumed to be the width of the antiroll clip, b_{ar} and the top of the purlin is assumed to be fixed to the sheathing. The configuration stiffness equation given by Equation 15 is the familiar formula for a fixed-fixed cantilever beam multiplied by d/h to transfer the stiffness to the restraint height h.

$$K_{config} = \frac{Eb_{ar}t^3}{(d-h)^3}\left(\frac{d}{h}\right) \tag{15}$$

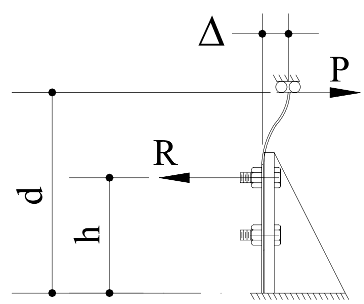

Figure 14 Stiffness Model – Antiroll Anchorage Device

A type of anti-roll anchorage device is a single web plate, sometimes referred to as a rafter clip. The device stiffness and the configuration stiffness of the web plate is calculated directly by modeling the web plate and Z-section web as a two dimensional cantilever beam model as shown in Figure 15. The beam, modeled as a prismatic section, has a width equal to width of the web plate. For a distance from the top of rafter elevation to the top row of bolts, the beam has a thickness equal to that of the web plate. Above the top row of bolts the beam model has the thickness equal to Z-section web thickness. The model incorporates both the device and configuration stiffness, and the resulting restraint stiffness for a web bolted rafter plate is

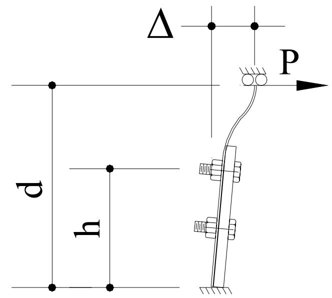

Figure 15 Stiffness Model – Rafter Plate

$$K_{Rest,WebPlate} = \frac{E \cdot b_{pl} \cdot t_{pl}{}^{3} \cdot t^{3}\left(t^{3}h + t_{pl}^{3}(d-h)\right)}{\left(t^{3}h^{2} - t_{pl}^{3}(d-h)^{2}\right)^{2} + 4t^{3}t_{pl}{}^{3}d^{2}h(d-h)} \tag{16}$$

The provided equations for the configuration stiffness for a discrete anchorage device will typically overestimate the stiffness of the restraint configuration, which will lead to a conservative approximation of restraint force but may underestimate the amount of deflection in the system. Conversely, for an antiroll anchorage device, the provided equation will typically underestimate the stiffness which will result in an overestimation of deformation at the restraint location. Most antiroll anchorage devices have substantial strength and the design of such systems will typically be deflection controlled. Because no testing or finite element modeling was performed with antiroll anchorage devices, it is conservative to underestimate the stiffness of the anti-roll anchorage device.

The restraint stiffness at the frame line may also be determined by a fairly simple test procedure with the apparatus shown in Figure 16. The apparatus consists of a segment of Z-section approximately 2 ft. long anchored in the manner representing the representing the typical anchorage device connection. For a typical through fastened rib style sheathing, a total of 3 fasteners at 12 in. intervals should be used to connect the purlin to the sheathing, with the center fastener located directly over the centerline of the restraint. For a standing seam profile deck, the seam of the deck with a single clip should be centered directly over the restraint. The stiffness of the sheathing connection is affected by the presence of insulation so if insulation is to be incorporated into the actual roof system it should be included in the test as well. Displacement should be recorded as close as possible to the top flange of the purlin, Δ_1, and if it is desirable to capture the relative slip between the Z-section and sheathing, the deflection of the sheathing, Δ_2. The sheathing is permitted to move laterally but prevented from moving vertically at a distance of span/2 from the Z-section where span is the Z-section spacing. Horizontal load, P, is applied through the sheathing parallel to the original plane of the sheathing. Applying the load through the sheathing provides verification of the strength of the sheathing-to-Z-section connection as well. Alternatively, the horizontal load, P_{Alt}, can be applied directly to the top flange of the Z-section if the connection between the purlin and sheathing possesses considerable slip. The restraint stiffness is defined as the load applied at the top flange, P, per unit displacement at the top flange, Δ_1. For a non-linear relationship between displacement and applied load, a criterion for determining the nominal stiffness similar to that of AISI Test TS-1-02 in the *Cold-Formed Steel Design Manual* (2002) should be used. This test procedure captures the net restraint stiffness, that is, the combined effect of the device stiffness and the configuration stiffness. The component stiffness method does not make accommodations for slip between the Z-section and sheathing so if excessive slip between the Z-section and sheathing is observed through this test procedure, some mechanism for transferring forces through the system of Z-sections should be considered.

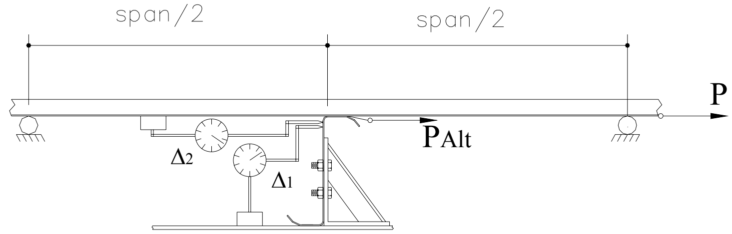

Figure 16 Test to Determine Stiffness of Support Restraint

Restraint Stiffness - Interior Restraints

For interior lateral restraints, the restraint is considered to be attached to the top flange of the Z-section in such a way that there is no deformation of the Z-section web as the restraint force is transferred out of the sheathing and into the restraint. Flexibility, therefore is introduced only through the deformation of the anchorage of the restraint. From Equation (13), the configuration stiffness is considered infinite and the restraint stiffness reduces to

$$K_{rest} = \left(\tfrac{h}{d}\right)^2 K_{device} \tag{17}$$

For example, consider third point restraints anchored by strapping attached to the eave strut. The device stiffness in this case is the weak axis bending stiffness of the eave strut. The bending stiffness is the deflection at the third point due to a concentrated load at the third point. From flexural mechanics, the restraint stiffness is

$$K_{rest} = \left(\tfrac{h}{d}\right)^2 K_{device} = \left(\tfrac{h}{d}\right)^2 \frac{162EI_Y}{5L^3} \tag{18}$$

where I_Y is the weak axis moment of inertia of the eave strut and L is the span of the eave strut. Alternatively, in lieu of calculating restraint stiffness, it may be assumed to be rigid, i.e. all the external force is distributed to the restraint. This will always lead to a conservative approximation of the restraint force, however this approximation will result in an unconservative approximation of lateral deflection at the restraint.

Stiffness of System

The system of purlins has an inherent resistance to lateral forces through the connection of the Z-section to the rafter and through the connection of the sheathing to the Z-section, referred to as the rafter stiffness, K_{rafter} and sheathing stiffness, K_{shtg}, respectively. For determining both lateral restraint forces and the deformation of the system, it is conservative to underestimate the rafter and sheathing stiffnesses. A low estimate of the rafter and sheathing stiffnesses will result in the prediction of larger restraint force than actual and will result in a larger calculation of system displacement. For simplicity, the rafter and sheathing stiffnesses can conservatively be eliminated. However, the contribution of the sheathing and the rafter connection to the resistance of lateral forces can be significant and economically advantageous to include.

Rafter Stiffness

The connection of the Z-section to the rafter provides resistance to lateral forces through the development of a moment at the base of the Z-section. The rafter stiffness is defined as the moment generated at the base of the Z-section per unit lateral displacement of the top flange of the Z-section. Two basic connection configurations are considered, a flange-bolted connection, shown in Figure 17(a) and a web bolted rafter plate connection, shown in Figure 17(b). In a flange-bolted configuration, the bottom flange of the Z-section is through-bolted to the top flange of the rafter with two bolts in line with the web of the Z-section. The clamping action of the bolts permits the development of a moment, M_{rafter}, of the base of the Z-section as the top flange of the Z–Section moves laterally. The stiffness of a flange bolted connection, derived from two dimensional beam element model and calibrated to the results of finite element models as described in Seek and Murray (2006), is

$$K_{Rafter} = 0.45\frac{Et^3}{2d} \tag{19}$$

Where E is the modulus of elasticity of the Z-section, t is the thickness of the Z-section and d is the depth of the Z-section.

The second rafter connection configuration considered is a web bolted rafter plate. In this connection configuration, a plate, typically welded to the rafter, is bolted to the web of the Z-section. Like the flange bolted connection, as the top flange of Z-section moves laterally, a moment is generated at the base of the Z-section to resist this movement. Because of the added stiffness of the rafter plate, the web-bolted rafter plate configuration has considerably more stiffness than the flange bolted configuration. The rafter stiffness for a web plate shown in Equation (20) is the same as Equation (16) for a supports restraint except the stiffness is multiplied by the depth of the Z-section, d, to convert it to moment at the base of the Z-section per unit displacement of the top of the Z-section.

$$K_{Rafter} = \frac{E \cdot b_{pl} \cdot {t_{pl}}^3 \cdot t^3 \left(t^3 h + t_{pl}^3 (d-h)\right) \cdot d}{\left(t^3 h^2 - t_{pl}^3 (d-h)^2\right)^2 + 4t^3 {t_{pl}}^3 d^2 h (d-h)} \tag{20}$$

It is important not to count the stiffness of a rafter plate twice when using the Component Stiffness Method. When considered a restraint, the stiffness of the rafter plate should only be considered in the restraint stiffness. When the rafter plate is considered a typical rafter connection and used in conjunction with stiffer anti-roll anchorage devices, the stiffness of the rafter plate should be considered part of the rafter stiffness.

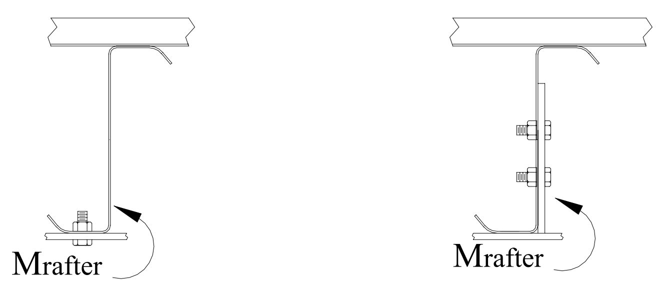

(a) Flange Bolted (b) Web Bolted Rafter Plate

Figure 17 Typical rafter to Purlin Connections

Sheathing Stiffness

The second inherent contribution of the system to the lateral resistance comes from the connection between the purlin and the sheathing. As the top flange of the Z-section moves laterally, the Z-section is approximated to rotate about its base as shown in Figure 18. As the Z-section rotates relative to the plane of the sheathing, a moment is developed in the connection between the sheathing and Z-section. The rotation of the Z-section about its base is approximated to be uniform and thus generates a uniform moment in the connection between the Z-section and sheathing along the length of the Z-section. As the uniform moment is applied to the Z-section, additional torsional rotations are generated in the Z-section. These torsional rotations are approximated to vary parabolically along the length of the Z-section and are accounted for by the ($1\text{-}2/3K_{mclip}\tau$) term in equation (21). The theoretical equation for the sheathing stiffness was further modified through comparison of the equation to the results of finite element models as described in Seek and Murray (2004; (2006). The resulting equation for the stiffness of the sheathing is

$$K_{shtg} = \frac{K_{mclip}L}{d}\left(\frac{\frac{1}{4}Et^3}{0.38K_{mclip}d + 0.71\frac{1}{4}Et^3}\right)\left(1 - \tfrac{2}{3}K_{mclip}\tau\right) \tag{21}$$

Where L is the Z-section span, d is the depth of the Z-section, t is the thickness of the Z-section, K_{mclip} is the rotational stiffness of the connection between the purlin and the sheathing and τ is the torsional term defined by Equation 7.

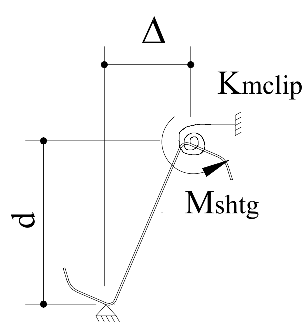

Figure 18 Sheathing Moment Stiffness

The rotational stiffness of the connection between the purlin and the sheathing is defined as the moment generated per unit rotation of the Z-section per unit length of the Z-section. The moment in the connection between the Z-section and the sheathing is developed as a result of prying action. For a through fastened system, the connection is made with a single screw placed near a rib of the sheathing and into the top flange of the Z-section. As the Z-section rotates, a compressive force is developed between the sheathing and the tip of the flange, and tension is developed in the fastener. The stiffness of the connection is a function of many factors: the purlin thickness, flange width and spacing, the deck thickness and moment of inertia, the fastener spacing, position of the fastener relative to the web of the purlin and relative to the sheathing rib and the presence of insulation.

For a standing seam clip, as the Z-section rotates, compression is developed in the shoulders of the clip and tension is developed in the tab as it pulls from the seam. Because it is connected directly to the seam it can posses considerable stiffness. For a standing seam system, the stiffness of the sheathing-to-Z-section connection is a function of the clip material and geometry, the "tightness" of clip tab in the panel seam, the Z-section thickness and the presence of insulation.

With so many factors involved, the stiffness of the connection between the Z-section and sheathing, K_{mclip}, cannot easily be determined analytically but can be readily determined by test. The test procedure is outlined in the *Cold-Formed Steel Design Manual* (2002): *AISI TS-1-02 Rotational Lateral Test Method for Beam-to-Panel Assemblies*. The basic test assembly is shown in Figure 19. A panel segment with a span representative of the Z-section spacing in a roof system is attached to a segment of Z-section and a load is applied to the free flange of the Z-section. As the lateral load, P, is applied to the free flange of the Z-section, the lateral displacement, Δ, of the free flange is measured. By relating the displacement to the applied load the rotational-lateral stiffness is determined. Some modifications to the results of the test procedure are required to determine the rotational stiffness of the sheathing-to-Z-section connection, K_{mclip}.

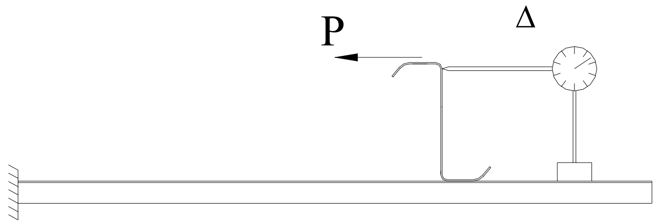

Figure 19 Test Set-up for Determining Stiffness of Sheathing Z-section Connection

The displacement of the free flange measured by test TS-1-02 is the combined displacement of the flexure in the web of the Z-section and the rotation of the sheathing-to-Z-section connection. Provided the apparatus is set up as prescribed in TS-1-02, additional deformation due to flexure of the sheathing is eliminated. To determine the sheathing-to-Z-section connection stiffness, K_{mclip}, the displacement due to the flexibility of the purlin web must be eliminated as described by Heinz (1994). The displacement of the web is approximated from theory by treating the Z-section web as fixed-free cantilever beam element, and the resulting stiffness of the connection between the sheathing and the deck is

$$k_{conn} = \frac{P_N d^2}{L_B}\left(\frac{1}{\Delta_N - \frac{4P_N d^3}{EL_B t^3}}\right) \tag{22}$$

where P_N is the nominal test load, Δ_N is the nominal test displacement, L_B is the Z-section length, d is the depth of the Z-section, and t is the thickness of the Z-section. Equation 22 thus provides the stiffness of the connection between the purlin and the sheathing in terms of moment per unit displacement of the free flange per unit length of the Z-section. The net rotational stiffness, K_{mclip}, must also include the rotational flexibility of the sheathing spanning between purlin lines. This flexibility, derived from theory, is added to the flexibility of the sheathing-to-Z-section connection and the net stiffness of the purlin-sheathing connection is

$$k_{mclip} = \frac{12E \cdot I_{Deck} \cdot k_{conn}}{spa \cdot k_{conn} + 12E \cdot I_{Deck}} \quad (23)$$

Where I_{Deck} is the moment of inertia of the sheathing and *span* is the distance between the centerline of each span of the sheathing as shown in Figure 20.

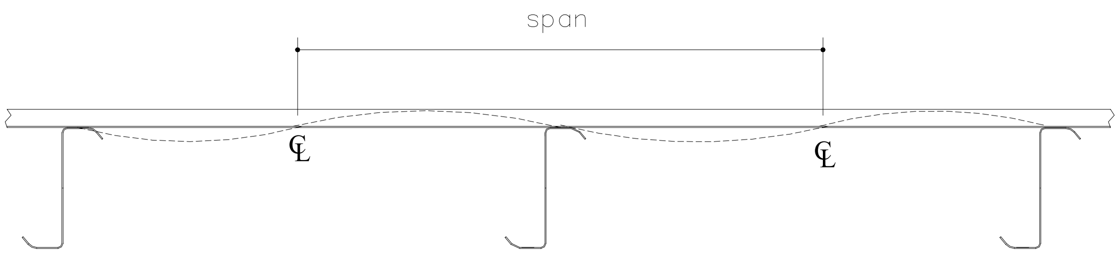

Figure 20 Flexibility of Sheathing included in Stiffness of Sheathing-toZ-section Connection

Application to Multiple Purlin Line Systems

In multiple purlin line systems, restraint is typically applied to only a few of the purlin lines in the system. In development of the equations, it is assumed that there is some mechanism that that transfers the restraint force from the system Z-sections, those Z-sections not directly restrained, to the external restraints. In through-fastened sheathing systems, the sheathing efficiently transfers this force. In standing seam systems where lateral movement between the sheathing and Z-section is permitted by articulating clips, some external mechanism such as strapping must be provided to help transfer the restraint force.

To relate each purlin line, the system of purlins is approximated as a single degree of freedom system. The mechanism that transfers the restraint force from the system purlins to the restraint is assumed to be rigid. The displacement of the top flange of each purlin at the restraint location is therefore the same. The force in each component of the system is related to the lateral deflection of the system at the restraint location through the stiffness of each component. The total stiffness of the system then is the sum of the restraint stiffness, rafter stiffness, and sheathing stiffness for each purlin.

$$K_{total} = \sum K_{rest} + \frac{\sum K_{shtg} + \sum K_{rafter}}{d} \tag{24}$$

Note that for an interior restraint configuration, the connection between the rafter and the Z-section is assumed to be pinned. Consequently, when considering an interior restraint configuration, the rafter stiffness should not be included in the total stiffness of the system. Typically, the stiffness of a flange bolted rafter connection is minimal and this approximation results in a conservative approximation of the restraint force and system deformation. When the connection to the rafter has considerable stiffness such as with a rafter web plate, the added stiffness of the web plate changes the distribution of forces in the sheathing and invalidates the equations provided for the interior third points restraint configuration. In the case of a stiff rafter connection in conjunction with an interior third point restraint, the restraint configuration is considered a third point plus support configuration and is beyond the scope of this paper.

The total lateral force generated by the system of Z-sections is the sum of the forces generated by each individual Z-section. To determine the total restraint force, the total lateral force generated by the system is multiplied by the ratio of the stiffness of the restraints to the total stiffness of the system, or

$$R_{Total} = \sum \left(wL \cdot \frac{\delta b \cos\theta - d \sin\theta}{h} + \frac{M_{torsion}}{h} + \frac{M_{local}}{h} \right) \frac{\sum K_{rest}}{K_{total}} \tag{25}$$

To determine the distribution of forces between multiple restraints, the force in each individual restraint determined by multiplying the total restraint force by the ratio of the stiffness of the individual restraint to the total restraint stiffness.

Transfer of Forces From Sheathing to Z-section

An aspect critical to the performance of the restraints that must be considered is the fastener force: the force transferred from the sheathing to the purlin at the restraint location. This force can be significant and must be transferred over a small width of panel approximately 12 in. (300 mm) either side of the restraint location. For a supports restraint configuration, the magnitude of the fastener force may actually exceed the restraint force and is calculated by.

$$\text{FastenerForce} = R\frac{h}{d} + 0.45Lw_{\text{restraint}} - \frac{wL}{2}\frac{\delta b\cos\theta}{d} \tag{26}$$

For a third points restraint configuration, the fastener force at each third point location may conservatively approximated as the restraint force. A reduction in this force can typically be achieved using Equation (27).

$$\text{FastenerForce} = R\frac{h}{d} + \frac{wL}{20}\left(\frac{\delta b\cos\theta}{d} - 0.9\sigma\right) \tag{27}$$

Deformation of System

Lateral deflection should be checked at the restraint location as excessive deformation undermines the intent of external restraints to prevent overturning of the Z-section. In the event that adequate stiffness is not provided to limit deflection, the stiffness of the restraints can be increased by adding restraints or increasing the stiffness of the existing restraints. Lateral deflection also should be checked at the extremes of the system to ensure that the diaphragm has sufficient stiffness to transfer the forces along the length of the purlin to the restraints. Based on this method, in general as a Z-section is allowed to displace, the calculated restraint force decreases. The method does not account for any second order effects, therefore displacements should be minimized, particularly at the restraint location. The lateral deflection of the top flange of the Z-section at the restraint location can be approximated by

$$\Delta_{rest} = \frac{R\left(\frac{h}{d}\right)}{K_{rest}} \tag{28}$$

With a flexible diaphragm, lateral deflection of the Z-section mid-span relative to the restraints is expected. For a supports restraint configuration, the lateral displacement of the diaphragm at the midspan of the Z-section relative to the restraint location is

$$\Delta_{diaph,spt} = \Sigma\left(w_{rest} - w\sin\theta\right)\frac{L^2}{8G'\sum Width\cdot} \tag{29}$$

For a third points restraint configuration, the deformation of the diaphragm at the frame line relative to the third points is

$$\Delta_{diaph,3rd} = -\frac{L^2}{9G'Bay}\sum w\left(\sigma + 7/2\sin\theta\frac{\sum K_{rest}}{K_{total}}\right) + \frac{R\,h/d\,L}{3G'Bay} \tag{30}$$

In Equations 28, 29 and 30, a positive deflection indicates upslope translation. For a supports restraint configuration, the total mid-span lateral displacement of the Z-section top flange is the sum of the restraint displacement and diaphragm displacement. Likewise, for a third points configuration, the netl lateral displacement of the top flange at the frame line is the sum of the restraint displacement and the diaphragm displacement.

Conclusions

The Component Stiffness Method provides a means of calculating restraint forces in single-span Z-section supported roof systems in which the top flange is attached to sheathing. The method has three major steps to determine the restraint forces in external restraints. In the first step, the overturning moment generated by the system of Z-sections is determined. Some of the moment is a result of the overturning effects of the external gravity loads applied eccentric to the base of the Z-section. The remainder of the overturning moment results from torsional and local bending moments generated in the connection between the Z-section and sheathing. The torsional moment is developed as the Z-section twists under applied load and is determined from displacement compatibility of the Z-section. The local bending moment captures the local deformations of the top flange of the Z-section relative to the sheathing.

In the second step of the Component Stiffness Method, the stiffness of the "components" of the roof system in resisting the overturning moment is determined. Most of the resistance is provided by the external restraint, but the system has some inherent resistance in the connection between the Z-section and sheathing and in the connection between the Z-section and the rafter. Equations for the stiffness of each of the components that are based on mechanics and modified using the results of finite element models are provided. By comparing the relative stiffness of each of the components of the system, the overturning forces are distributed to each of the components.

In the final step of the Component Stiffness Method, the effectiveness of the restraints is determined by considering the lateral deformation of the system. Equations for predicting the lateral deflection of the top flange of the Z-section at the restraint location, at the mid-span for a support restraint configuration, and at the frame line for a third point configuration are provided. Equations are also provided to calculate the required shear capacity of the connection between the Z-section and sheathing at the restraint location necessary to transfer forces out of the sheathing and into the restraint.

Appendix - Nomenclature

$$I_{mY} = \frac{I_X I_Y - I_{XY}^2}{I_X} \qquad a = \sqrt{\frac{EC_W}{GJ}} \qquad \lambda = \frac{1}{a} = \sqrt{\frac{GJ}{EC_W}}$$

$$\tau = \frac{\dfrac{a^2\beta}{GJ}}{1 + \dfrac{K_{mclip}}{GJ}\kappa} \qquad \beta = \frac{L^2}{8a^2} + \frac{1}{\cosh\left(\dfrac{L}{2a}\right)} - 1 \qquad \kappa = \frac{8a^4}{L^2}\left(\frac{\cosh\left(\dfrac{L}{2a}\right) - 1}{\cosh\left(\dfrac{L}{2a}\right)}\right) + \frac{5L^2}{48} - a^2$$

b = width of Z-section top flange (in) (mm)
b_{ar} = width of antiroll anchorage device or web bolted rafter plate
Bay = total width of diaphragm perpendicular to span (ft) (m)
d = depth of Z-section (in) (mm)
E = modulus of elasticity (29,500,000 psi) (203,400 MPa)
G = shear modulus (11,200,00 psi) (77,200 MPa)
h = height of applied restraint measured from base of Z-section parallel to web (in) (mm)
I_X = moment of inertia of full unreduced section about axis perpendicular to the plane of the web (in^4) (mm^4)
I_{XY} = product of inertia of full unreduced section about major and minor centroidal axes (in^4) (mm^4)
I_{Deck} = Gross moment of inertia of sheathing
K_{mclip} = combined rotational stiffness of sheathing and connection between the Z-section and sheathing (lb-in/ft) (N-m/m)
K_{rafter} = Moment developed in connection between Z-section and rafter per unit lateral displacement of top flange of Z-section at restraint
K_{rest} = Force restrained at top flange of Z-section per unit lateral displacement of top flange at restraint location
K_{shtg} = Moment developed in connection between Z-section and sheathing per unit lateral displacement of top flange of Z-section at restraint
L = span of Z-section (ft) (m)
M_{local} = Moment developed in sheathing due to local deformation of top flange
M_{rafter} = Moment developed in connection between rafter and Z-section due to lateral movement of top flange relative to base
M_{shtg} = Moment developed in sheathing due to lateral movement of top flange relative to base
$M_{torsion}$ = Moment developed in sheathing due to twist of Z-section relative to sheathing
n_P = number of restrained purlins per anchorage device
t = thickness of Z-section (in)
t_{pl} = thickness of web bolted rafter plate
w = uniform loading on Z-section (lb/ft) (N/m)
Width = tributary width of diaphragm (perpendicular to Z-Section Span) per Z-section.(in) (mm)
δ = load eccentricity on Z-section top flange (1/3)
θ = angle between the vertical and the plane of the Z-section web (degrees)

References

Cold-Formed Steel Design Manual, (2002). American Iron and Steel Institute, Washington, D.C.

Ghazanfari, A., and T. M. Murray. (1983). "Prediction of the Lateral Restraint Forces of Single Span Z-purlins with Experimental Verification." *Fears Structural Engineering Laboratory Laboratory Report No. FSEL/MBMA 83-04*, University of Oklahoma, Norman, Oklahoma.

Heinz, D. A. (1994). "Application of Generalized Beam Theory to the Design of Thin-Walled Purlins." *Thin Walled Structures*, 19, 311-335.

Lee, S., and T. M. Murray. (2001). "Experimental Determination of Required Lateral Restraint Forces For Z-Purlin Supported, Sloped Metal Roof Systems." *CE/VPI-ST 01/09*, Virginia Polytechnic Institute and State University, Blacksburg, VA.

Seek, M. W., and T. M. Murray. (2004). "Computer Modeling of Sloped Z-Purlin Supported Roof Systems to Predict Lateral Restraint Force Requirements." *Conference Proceedings, 17th International Specialty Conference on Cold-Formed Steel Structures*, Department of Civil Engineering, University of Missouri-Rolla. Rolla, Missouri.

Seek, M. W., and T. M. Murray. (2006). "Component Stiffness Method to Predict Lateral Restraint Forces in End Restrained Single Span Z-Section Supported Roof Systems with One Flange Attached to Sheathing." *Conference Proceedings, 18th International Specialty Conference on Cold-Formed Steel Structures*, Department of Civil Engineering, University of Missouri-Rolla. Rolla, Missouri.

APPENDIX II

RESULTS OF LABORATORY TESTS OF LATERAL RESTRAINT FORCES

II.1 Introduction

In an effort to better understand the lateral force bracing requirements of Z-purlin supported roof systems, a series of tests was performed on full scale roof specimens. All specimens utilized 10ZS2.6x0.097 purlins spanning 20 ft. The tests were performed on two, four and six purlin lines in a single span configuration and six purlin lines in a 3-span configuration. Each specimen was loaded to approximately 20 psf and the restraint forces were measured at incremental pitches between between 0:12 and 4:12. Supports, Third Points, Midpoints, Quarter Points and Third Points + Supports bracing configurations were investigated. The test results are compared to results from shell finite element models.

II.2 Testing Program

Forty tests were performed as a part of this research program. The tests are divided into eight series with five tests each. The series are divided according to number of purlins, sheathing type, and number of spans. Series 1 through 3 implemented two, four and six purlin lines respectively over a single 20 ft span with through fastened sheathing. Series 4, 5 and 6 similarly had two, four and six purlin lines respectively over a single 20 ft span but utilized standing seam sheathing with sliding clips. Series 7 was a multiple span system with six purlin lines over three 20 ft spans with through fastened sheathing. Series 8 used the same purlin layout as Series 7 only with standing seam sheathing. Within each series, five bracing configurations were investigated: Supports, third points, midpoints, quarter points, and third points + supports. For each individual test, the roof pitch was varied at slopes between 0:12 and 4:12 with data points taken at 0:12, ½:12, 1:12, 2:12, 3:12, and 4:12. A summary test matrix is shown in Table II.1

II.3 Test Assembly

II.3.1 Test Frame

A cross section of the test frame utilized in this project is shown in Figure II.1. The test frame was similar to the frame used by Lee and Murray (2001) with modifications. The “rafter” used to support the purlins was a W14x22 beam that was hinged on the eave side and supported by shoring at the ridge side. The hinge was created by a 1 ¼ inch diameter threaded rod in double shear between plates welded to the rafter and welded to an anchor beam which in turn was anchored to the floor. Roof slope was simulated by raising the ridge side of the specimen with 5 ton capacity bridge cranes.

Table II.1

Test Series	Number of Purlins	Sheathing Type	Number of Spans
Series 1	2	Through-Fastened	One
Series 2	4	Through-Fastened	One
Series 3	6	Through-Fastened	One
Series 4	2	Standing Seam	One
Series 5	4	Standing Seam	One
Series 6	6	Standing Seam	One
Series 7	6	Through-Fastened	Three
Series 8	6	Standing Seam	Three

A beam was bolted to the eave and ridge edges of the rafter that connected each rafter. This beam helped stabilize the rafters and provided anchorage for the purlin braces. A W8x48 beam was used on the eave and a W6x25 at the ridge (refer to Figures II.2 and II.3). The anchorage beams were attached to the rafters with two 1 in. diameter threaded rods through the web of the anchor beam and flanges of the rafter. Steel plate was used as spacers between the anchor beam and rafter to correctly set the elevation of the anchor beam. For the multiple span tests, the anchor beams were spliced with an eight ft long section of W8x48 at the eave and W8x24 at the ridge as shown in the plan view of the multiple span test frame in Figure II.3.

II.3.2 Purlins

The purlins used in all tests were 10Z2.60x0.097. The measured cross sectional dimensions and calculated properties for each purlin used are shown in Table II.3. The purlins spanned 20 ft and were spaced at 54 in. for all tests. The bottom flange of each purlin was attached to the top flange of the rafter with two ½ in. diameter A307 bolts as shown in Figure II.4. The bolts were on a 2 ½ in. gage and located at 1 ½ in. from the purlin web.

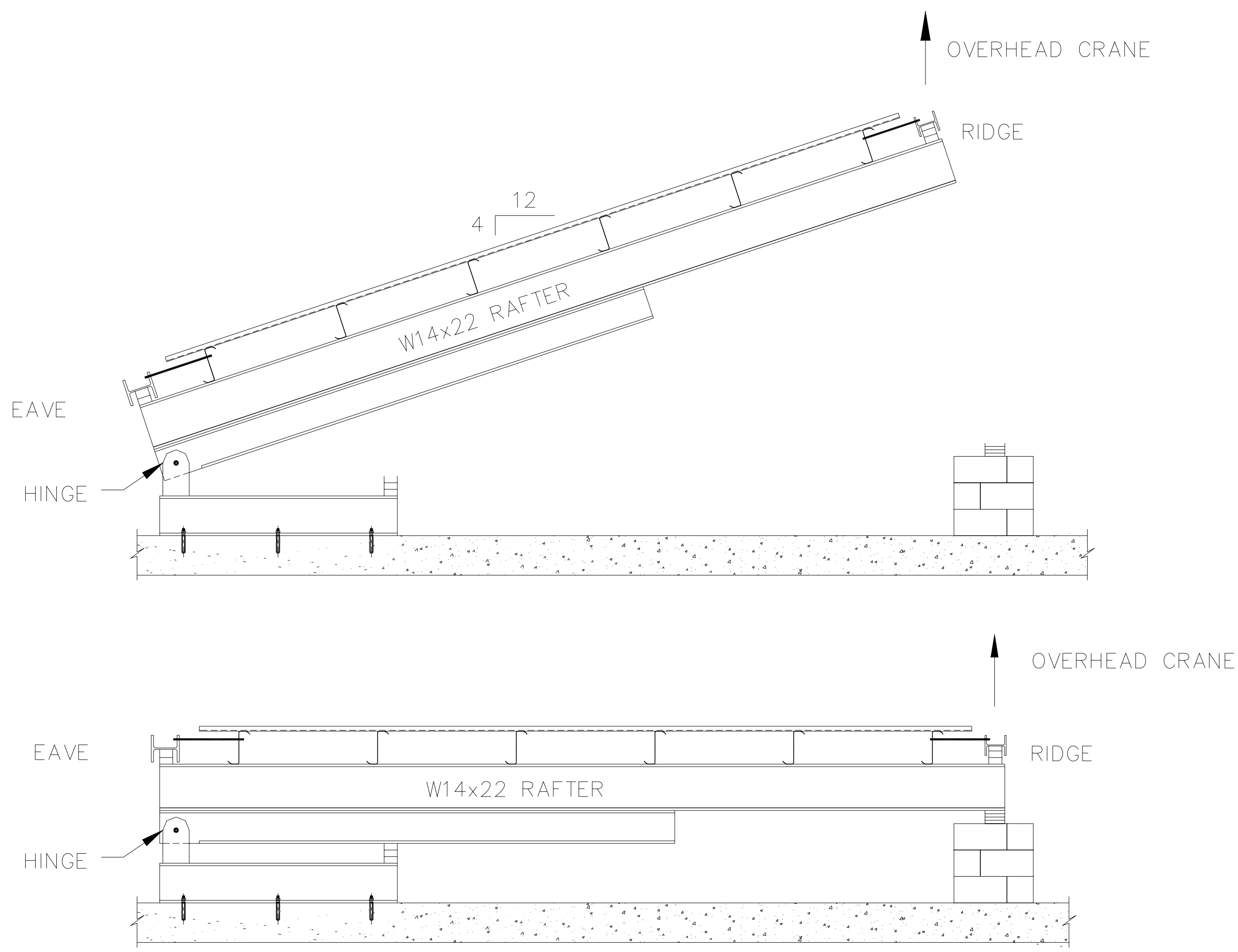

Figure II.1 Cross Section of Test Frame

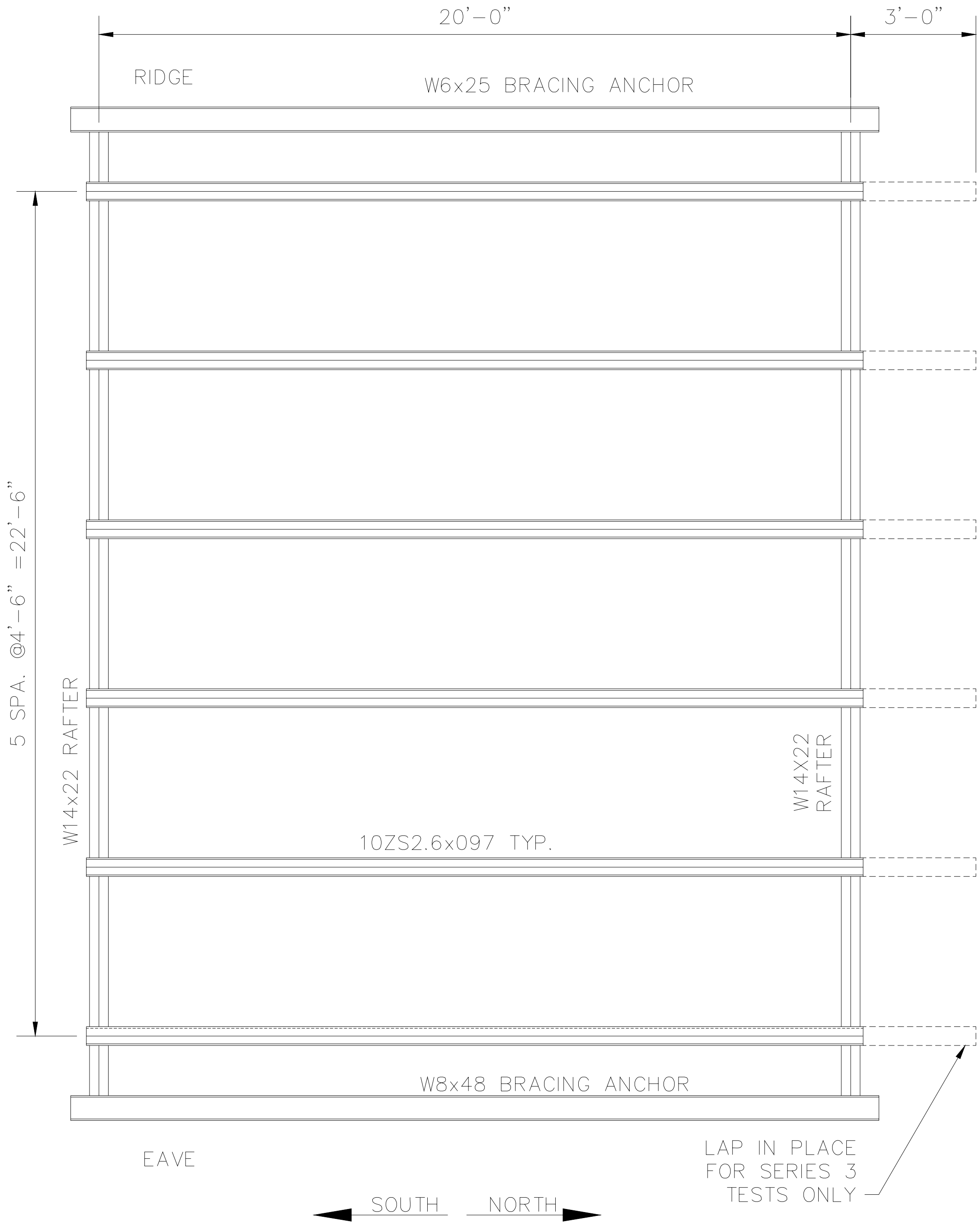

Figure II.2 Plan of Single Span Test Frame

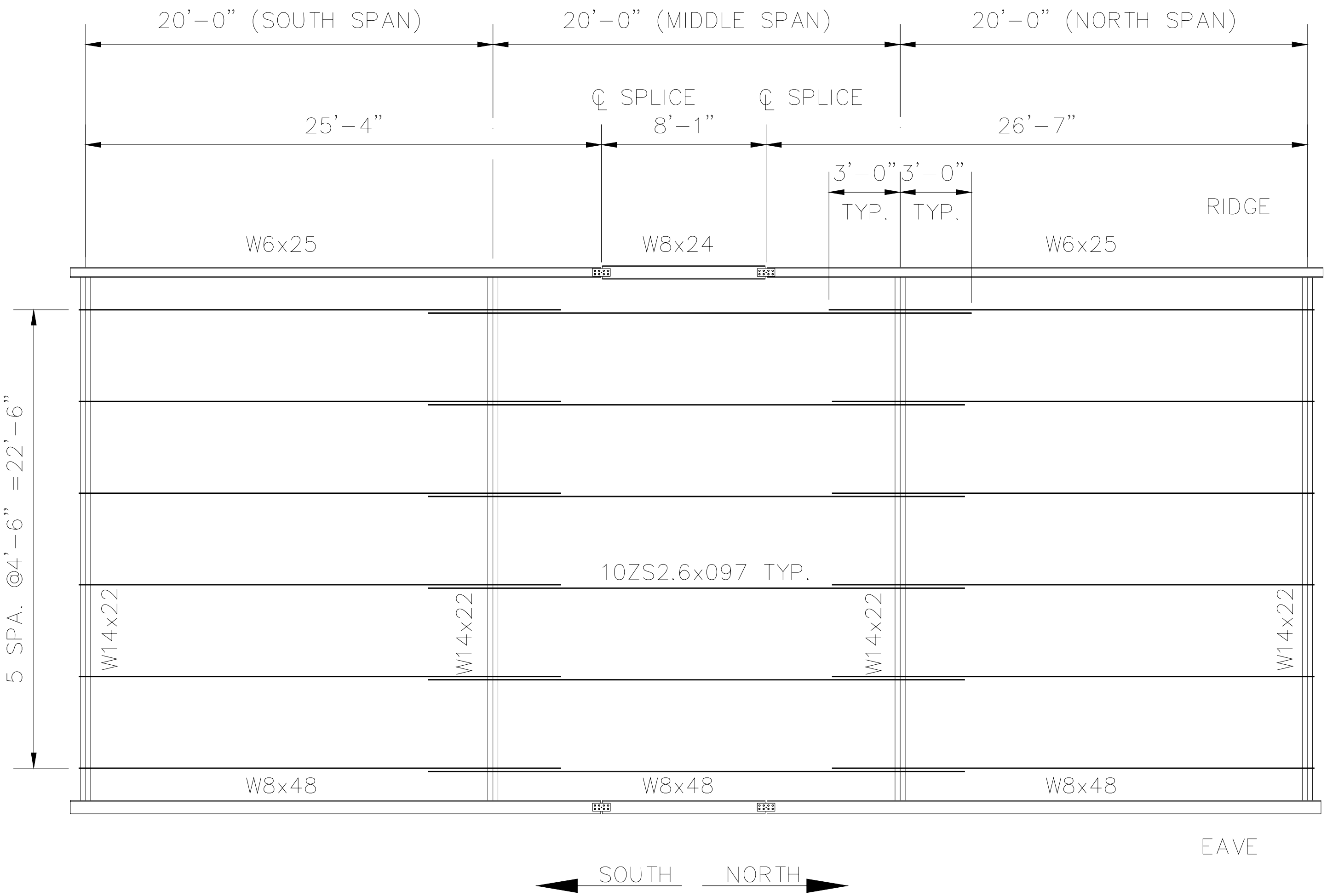

Figure II.3 Plan of Multiple Span Test Frame

For the multiple span tests (Series 7 and 8), the purlins were lapped over the two interior rafters. The lap length measured 3 ft to either side of the rafter with (two) ½ in. diameter A307 bolts at the end of each lap through the purlin web as shown in Figure II.5. For test Series 3, the lap portion of the purlin extended beyond the test specimen as shown in Figure II.6, while this portion was removed for Series 1,2, 4,5 and 6.

II.3.3 Through-fastened Sheathing

The sheathing used for the through-fastened tests was Nucor Type “R” 26 Ga. sheathing. The sheathing has a 36 in. coverage with 1 ¼ in. ribs at 12 in. intervals. The sheathing was fastened to each purlin with 12-14x1 ¼ in. self drilling screws with sealing washers at 12 in. intervals. For each test specimen, the sheathing extended the length of the specimen, that is, there were no end laps. Along the panel side laps, 1/4-14x3/4 in. self drilling screws with sealing washers were installed at 36 in. intervals. For the 20 ft single span tests, because the sheathing had a coverage width of 36 in., seven panels resulted in a coverage of 21 ft. Rather than remove the excess sheathing, the extra 12 in. of sheathing was left in place at the north end of the specimen, but no fasteners were installed beyond 20 ft.

II.3.4 Standing Seam Sheathing

The standing seam sheathing used for test Series 4, 5, 6 and 8 was a “CFR” type panel provided by Nucor Building Systems. Each panel had a coverage of 24 in. The specimen utilized a short sliding clip, Nucor type MPS 602 shown in Figure II.7, to provide connection between the purlin and sheathing. The clip was fastened to the purlin with (two) ¼-14x1 ¼ in. self drilling screws per clip. The screws were located in the first two holes from the left side of the clip as viewed in Figure II.7, which resulted in a 1 ¼ in. spacing. The top portion of the clip was sandwiched between the male and female portions of the seam. At the eave, the seam was hand crimped for 12 in. and mechanically seamed the remaining length, forming what is referred to as a “Power Lock Seam” by Nucor Building Systems. The sheathing was fastened directly to the purlin closest to the eave edge with 12-14x1 ¼ in. self drilling screws with sealing washer at 12 in. intervals to avoid a “floating” sheathing condition.

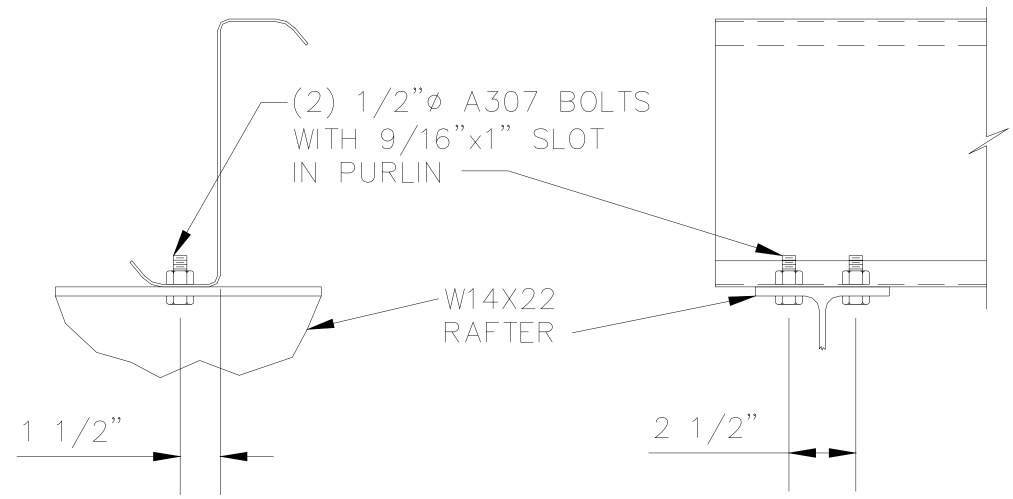

Figure II.4 Purlin to Rafter Connection

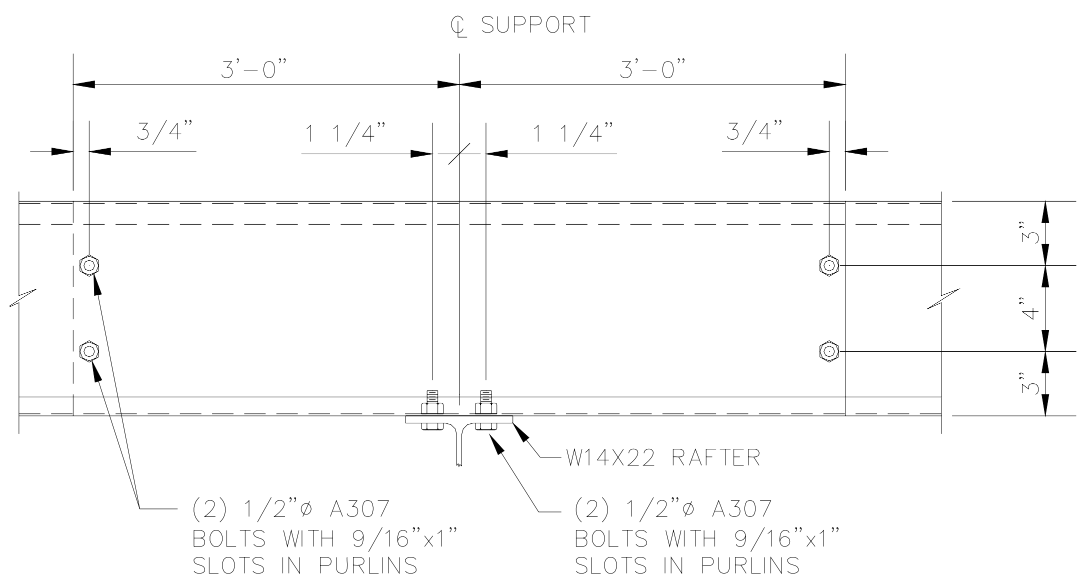

Figure II.5 Typical Purlin Lap

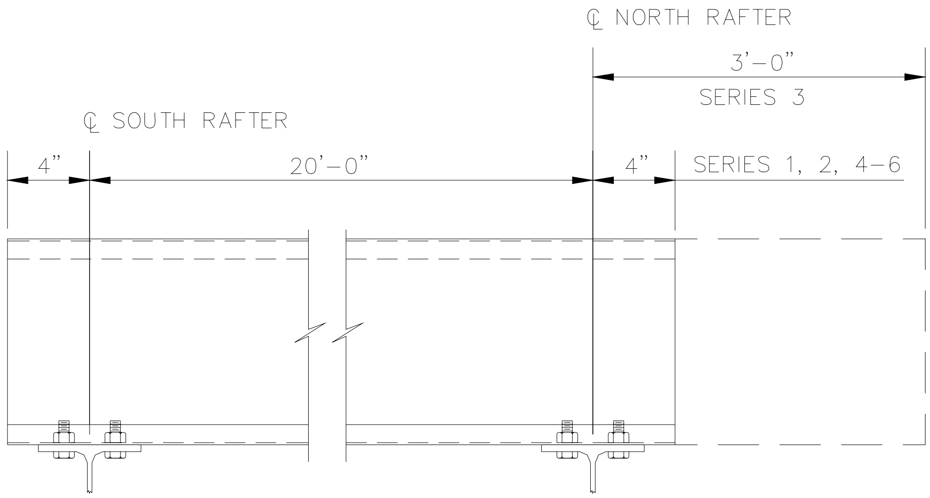

Figure II.6. Purlin Layout For Single Span Tests

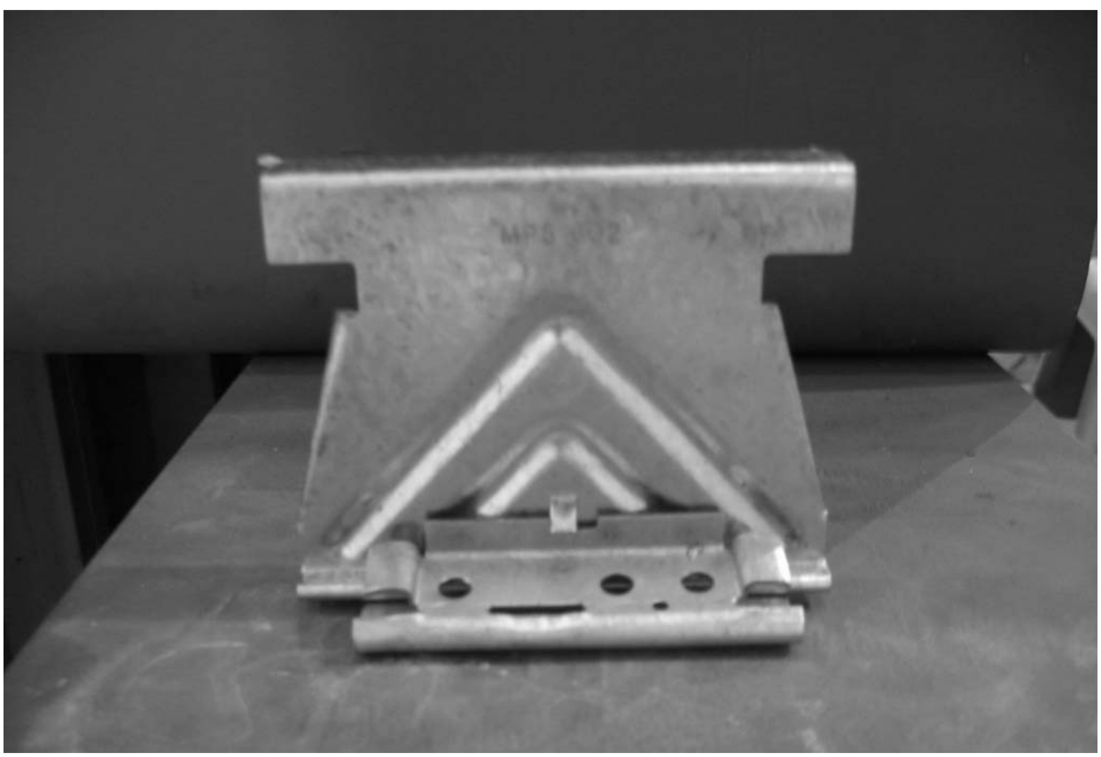

Figure II.7 Standing Seam Clip

II.3.5 Bracing Anchorage

Five bracing configurations were used: supports, third points, midpoints quarter points and third points plus supports. Restraint was applied via a ½ in. diameter threaded rod attached at 7-½ in. from the bottom of the purlin and secured by an A307 nut as shown in Figures II.8 and II.12. At the eave side, the restraint rods were attached to the flange of a W8x48 anchor beam at 3 in. from the centerline of web and at the ridge at 1-7/8 in. from the centerline of a W6x25 anchor beam. Due to the high brace forces and concern that purlins might sustain permanent local deformation at the anchor zones, for the six purlin through fastened tests (Series 3 and 7), a backing plate 3/16x6 ¾x4¼ as shown in Figure II.11 was used in the anchorage zones to help distribute the large forces.

For the standing seam test series, a 5 ft long ½ in. diameter rod was used to help transfer the bracing force through each purlin. The layout of the bracing rods is shown in Figure II.9 and the typical location along the depth of the purlin is shown in Figure II.12.

The braces were set up in each test series in five different configurations: supports restraint, third point restrain, midpoint Restraint, quarter point restraint, and third points plus support restraint. The layout of each multiple span restraint configuration along with the corresponding brace location nomenclature is shown in Figure II.10.

II.3.6 Instrumentation

The ½ in. diameter brace rods at the eave and ridge were instrumented each with four strain gages located radially at 90 degrees to remove any errors in bending. The net strain in the brace rod was calculated as the average of the four strains and the brace force was in turn directly calculated. Additionally, several S-shaped strain gage based load cells were used to measure the brace force in place of the instrumented rods. These included two 2000 lb capacity cells manufactured by Hottinger Baldwin, two 10,000 lb cells manufactured by Hottinger Baldwin and two 10,000 lb models manufactured by Sentran. Due to the symmetry of the test specimens, the S-shaped load cells provided a means of checking the results of the instrumented rods.

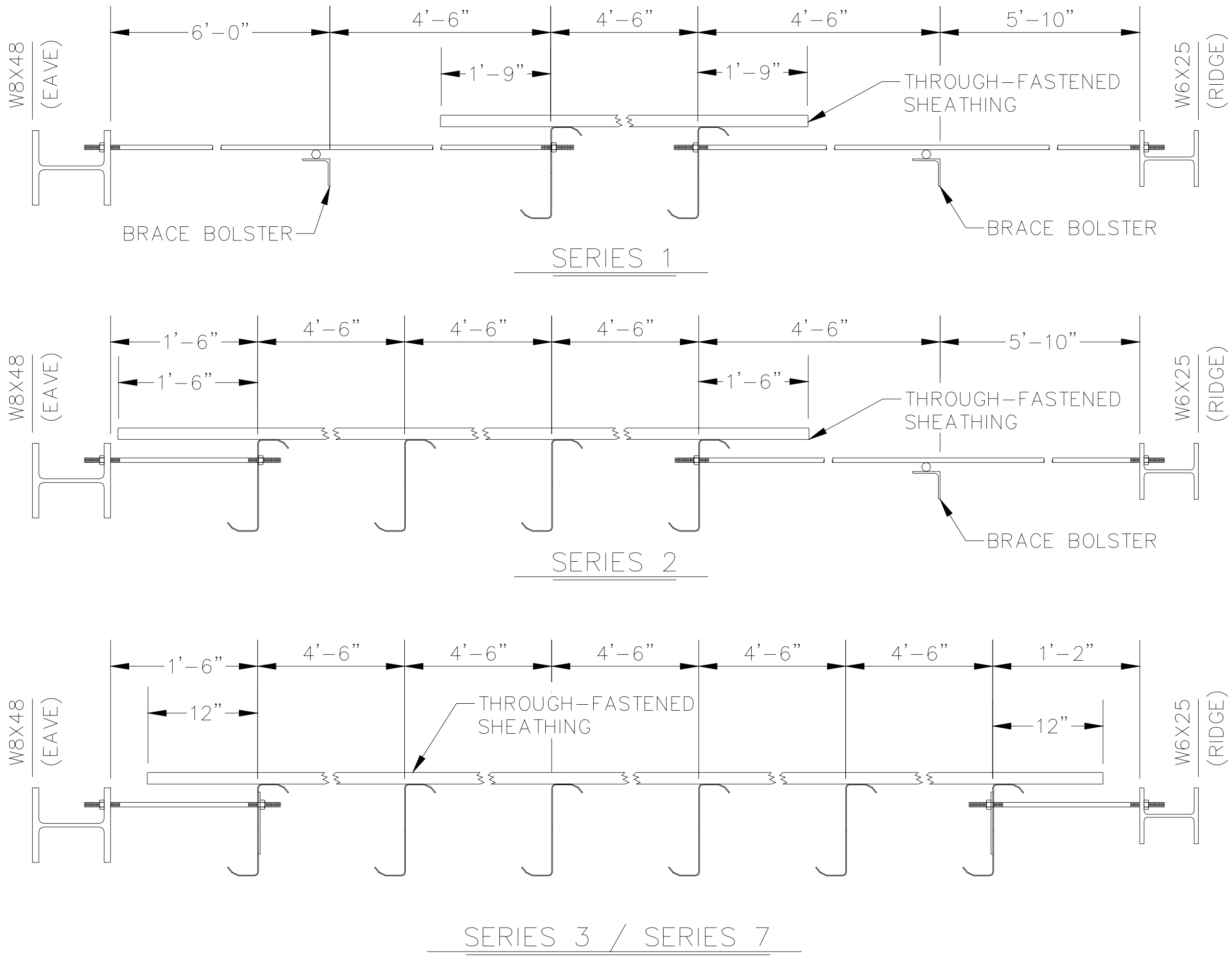

Figure II.8 Typical Cross Section – Through Fastened Tests

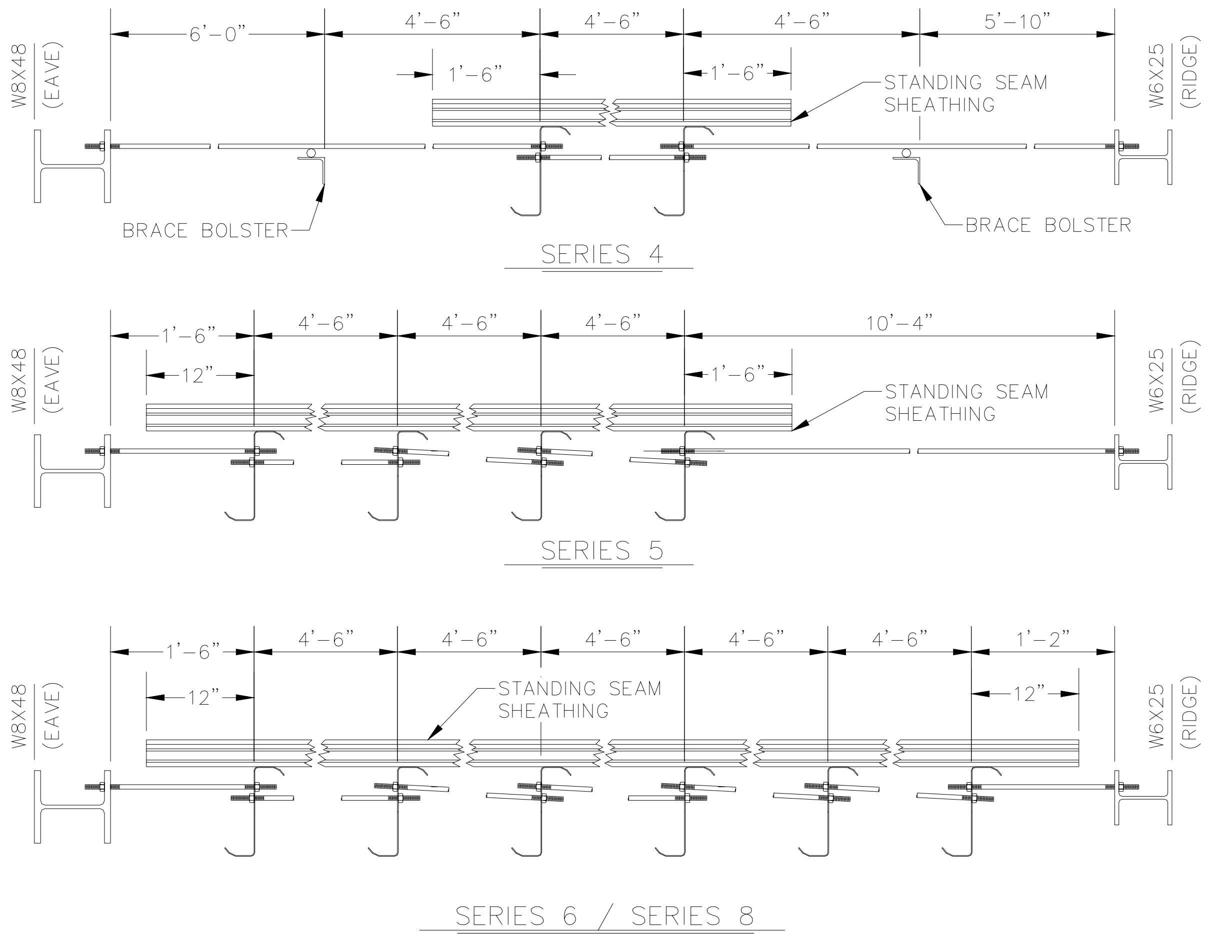

Figure II.9 Typical Cross Section – Standing Seam Tests

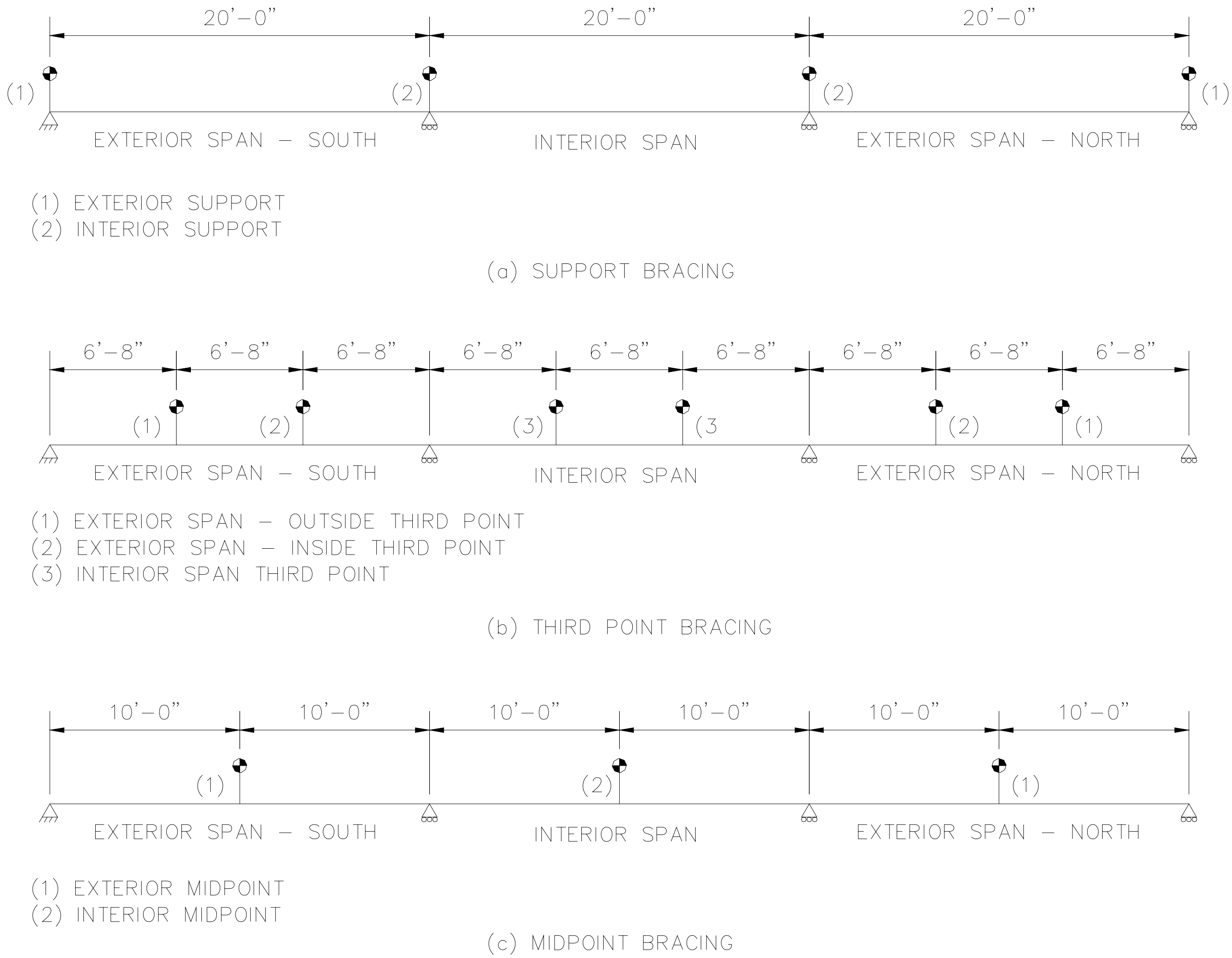

Figure II.10 Multiple Span Bracing Configurations

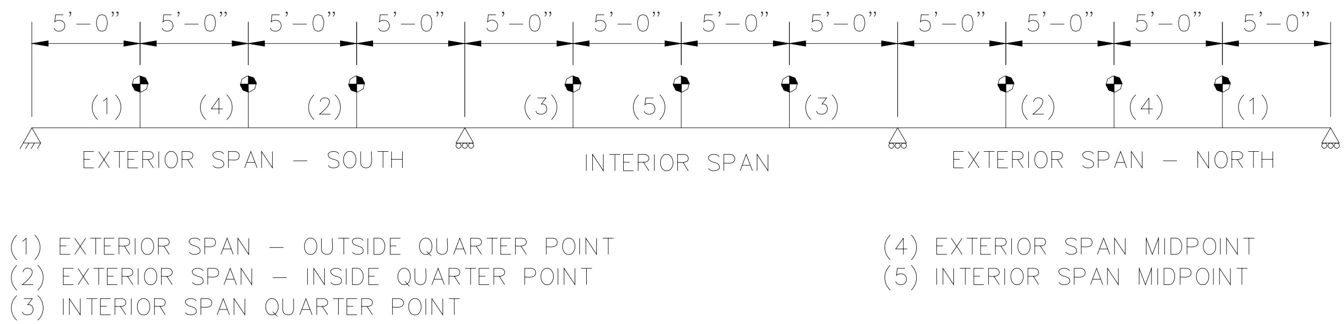

(a) QUARTER POINT BRACING

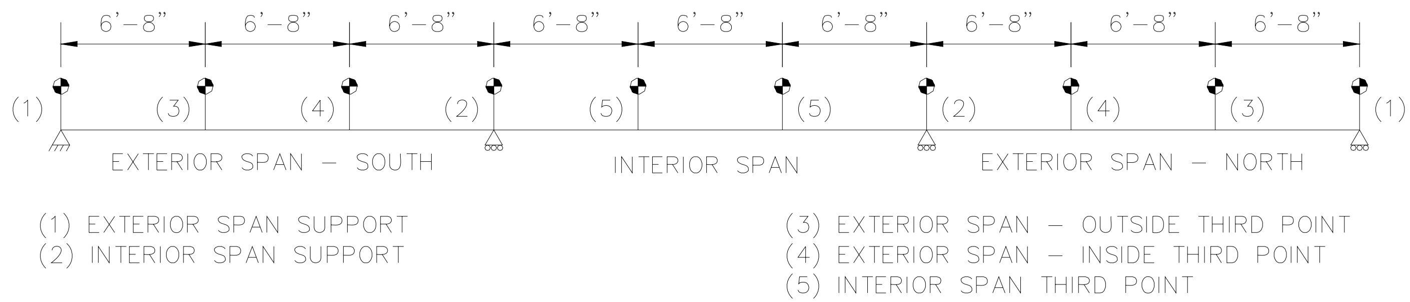

(b) THIRD POINT + SUPPORT BRACING

Figure II.10 (Continued) Multiple Span Bracing Configurations

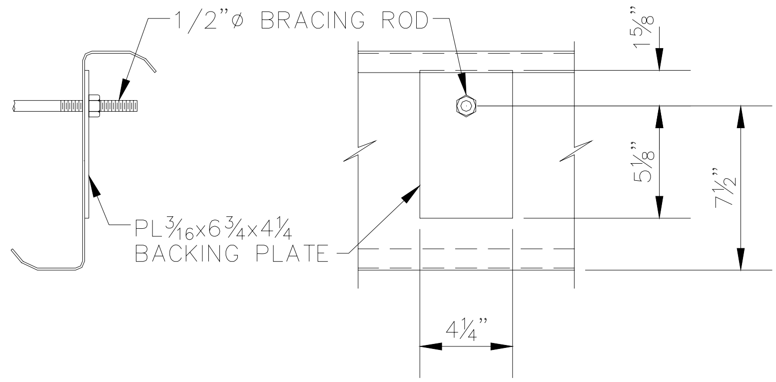

Figure II.11 Backing Plate Used for Series 3 and Series 7

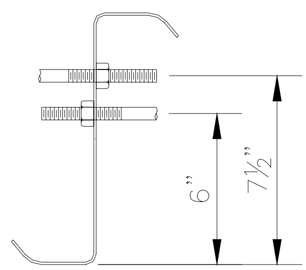

Figure II.12 Typical Brace Locations

The roof slope was measured by a four ft long digital level. The level measures slope to a precision of 0.1 degrees. The level was placed on the bottom flange of one the rafter beam near the ridge side and was monitored to set the test specimen at the desired slope. Once the specimen was in position, the level was moved to the other rafters to ensure that each rafter was within 0.1 degrees of the desired slope.

II.4 Loading

The test specimens were loaded with 1 in. diameter steel round stock. The rounds were cut to lengths of 8 ft 0 in., 17ft 6 in., and 24 ft 6 in. corresponding to the lengths of the sheathing for each test series and welded together in groups of eight. Lifting lugs were welded to each set of rounds to facilitate placing them between the ribs of the sheathing with overhead bridge cranes. The specimen was loaded symmetrically, starting at the rafter supports and moving inwards toward the middle of the span. By the end of the testing, more than half a million pounds had been applied to the various test specimens.

II.5 Test Procedure

At the beginning of each test, the braces were installed at both the eave and ridge according to the bracing configuration investigated. For the standing seam tests, the bracing rods between each purlin were tightened finger tight. The eave bracing was pretensioned by hand. The pretension forces ranged from 20 lb to 60 lb and were recorded for most of the tests. The ridge restraints were left slack at the beginning of the test.

The test specimen was loaded to approximately 20 psf and the restraint forces were recorded at the zero slope condition. The crane was attached to the ridge and the specimen was lifted to a slope of one degree to ensure that the crane was centered. If uneven, the specimen was lowered and the crane repositioned. When the crane was found to be satisfactorily centered, the test proceeded to a pitch of ½:12 (2.4 degrees). The restraint forces at each brace location were denoted, and the specimen was then raised incremently to pitches of 1:12, 2:12, 3:12, 4:12. At each incremental slope, the slope at each rafter was checked to insure that the specimen was raised evenly. When each eave restraint approached zero force, the roof angle was denoted and the corresponding ridge restraint was pretensioned to a force ranging from 20 to 60 lb. No adjustments were made to the eave restraints at this point. After the specimen reached a pitch of 4:12 (18.4 degrees), it was returned to a zero slope and the restraint forces at the eave were once again recorded. A tensile force in the eave restraint is considered a positive bracing force (resistance to upslope translation) while a tensile force at the ridge restraint is considered a negative force (resistance to downslope translation).

II.6 Test Series Summary

The results of each test are shown on data sheets at the end of this appendix sequentially from test Series 1 through Series 8. The numerical values of roof slope and corresponding bracing restraint force are tabulated in addition to the restraint forces as predicted by the shell finite element model. A second table lists the eave and ridge restraint pretensions as well as the roof slope at which the restraint force shifts from the eave to the ridge (the zero-force roof slope). A brief summary and notes on each test series is provided in the following sections.

II.6.1 Test Series 1

Test Series 1 was a two purlin system on a single span with through-fastened sheathing. The specimens were loaded with 3400 lb that was distributed uniformly. For a tributary width of 54 in. for each purlin, the equivalent uniform loading is 18.9 psf.

II.6.2 Test Series 2

Test Series 2 was a single span, four purlin system with through fastened sheathing. 7150 lbs was applied uniformly to the specimen, which for a 54 in. tributary width on each purlin yields and equivalent load of 19.9 psf. Tests of two bracing configurations, supports and midpoints, were performed both with and without the same backing plate used for test Series 3 and 7. The difference between the two tests was on the order of 10 percent and since permanent deformation of the purlins was unlikely given the magnitude of the brace forces, the remaining tests were performed without the backing plate. Figure II.13 shows the difference in purlin local deformation with and without the backing plate. For comparison purposes, the results of the supports and midpoints restraint cases with and without backing plates are provided.

(a) Without backing plate

(b) With Backing Plate

Figure II.13 Purlin Local Deformation

II.6.3 Test Series 3

Test Series 3 was the first test series performed and consequently the one in which many of the nuances of the testing procedure were discovered. The test series consisted of six single span purlins with through fastened sheathing. Initial tests showed large local deformation in the purlins at bracing locations due to the large restraint forces. To prevent permanent deformation of the purlins, a PL3/16x4 ¼x6¾ was placed between the web of the purlin and brace rod nut as shown in Figures II.11 and II.13(b) to help distribute the brace force. It is felt that this results in conservative brace forces results when compared to actual field conditions in which would not utilize such a reinforcing plate. Large pretensions on the order of 50-60lbs were applied to the restraint rods, however the actual pretension force was not recorded. The specimen was loaded with a total gravity load of 10,460 lb, which distributed uniformly over a tributary width of 54 in. for each purlin yields a uniform load of 19.4 psf.

II.6.4 Test Series 4

Test Series 4 was a single span test with two purlins decked with standing seam sheathing. The clips and sheathing used for test Series 4 was the same sheathing used previously in test Series 8, 6 and 5. Consequently, the sheathing had been through at least fifteen test cycles prior to its use in Series 4. Similar to test Series 1, the total load applied to the specimen was 3400 lb, which, uniformly distributed over a tributary width of 54 in. for each purlin equates to a uniform load of 18.9 psf.

II.6.5 Test Series 5

Test Series 5 utilized four single span purlins with standing seam sheathing. The Series 5 specimen utilized the same specimen as Series 6, with the two purlins closest to the ridge taken out and the standing seam sheathing cut to the proper length. Thus the clips and sheathing had been through at least ten test cycles prior to the Series 5 tests. A total of 7150 lb was applied uniformly to the test specimen. Considering a tributary width of 54 in on each purlin, the equivalent uniform load is equal to 19.9 psf. Large pretensions were applied to the ridge restraint rods to take out as much sag as possible because they spanned the entire10 ft 4 in. distance between the anchor beam and purlin closest to the ridge. This need for large pretensioning was remedied in subsequent tests (Series 4, 2 and 1) by providing a bolster for the brace at the mid-span of the rod.

II.6.6 Test Series 6

Test Series 6 was a six pulin system with standing seam sheathing spanning a single 20 ft span. The total load applied to the specimen was 10,460 lb. With a tributary width of 54 in. for each purlin, the equivalent uniform load is 19.4 psf. The clips, purlins and sheathing utilized in the south span of test Series 8 was reused for Test Series 6, thus the components had been through at least five prior test cycles.

II.6.7 Test Series 7

Test Series 7 was a three span system with six purlin lines covered by through fastened sheathing. The total load applied per span was 10,460 lb. Divided evenly over the 54 in. tributary width of each purlin equates to a uniform load of 19.4 psf. The specimen was expanded from test Series 6, thus the south span utilized the same fasteners and sheathing.

II.6.8 Test Series 8

Test Series 8 utilized the same six purlin line, three span system as Test Series 7, but was decked with standing seam sheathing. With a total load of 10,460 lb per span and a tributary width of 54 in. per purlin, the equivalent uniform load was 19.4 psf. The tests in Series 8 were stopped before reaching a 4:12 pitch because, due to the coating on the decking, the rods simulating the gravity load began to slip. Thus the specimens were brought to the point of incipient slippage (about 17.5 degrees), and the slope and corresponding brace restraint force were recorded.

II.7 Finite Element Comparison with Test Results

In the following sections, the results of the laboratory tests are compared to the shell element finite element model. A summary of the properties of the elements used in the finite element model is provided. Discussion of the models is divided according to the type of sheathing (through-fastened or standing seam) and the span condition (single or multiple span). A plot is provided for each restraint configuration comparing the results of the finite element model to the laboratory test results. The plots show the measured restraint force on the ordinate axis versus the roof slope on the abscissa. Each data point from the test result is shown as the average of the restraint forces at a particular location, symmetric about the center of the system.

II.7.1 Finite Element Model Compared to Single Span Through-fastened Tests

In comparing the finite element models to the single span through-fastened tests, that is Series 1-3, a panel diaphragm stiffness of 27500 lb/in was used. The gross moment of inertia of the panel was calculated to be 0.0385 in^4/ft, and thus an equivalent bending thickness of 0.33 in. was used to represent the panel in the finite element model. Best correlation was found when the rotational stiffness of the connection between the panel and sheathing was 1000 lb-in./rad. To simulate laboratory conditions, frame elements representing the anchor rods were anchored in the strong axis direction to a W8x48 spanning between the rafters.

In Figures II.14(a-g), the finite element results are compared to the test results for each restraint configuration with results for two, four and six purlin line tests shown on the same plot. Figure II.14(a) shows the excellent correlation between the finite element model and the test result for the supports restraint configuration. Figures II.14(b) and II.14(c) show the midpoints and third points restraint configurations, respectively. Correlation is good with both restraint configurations although at larger slopes there is slight deviation on the unconservative side. The next two figures show the quarter points restraint configuration with the quarter span restraint shown in Figure II.14(d) and the mid-span restraint shown in Figure II.14(e). Correlation at the quarter span location is good but only fair at the midspan location due to fairly large unconservative deviations at small slopes. It is believed that this is a result of the sensitivity of the test to the initial pretension of the restraint rods. Good correlation is realized with the third points + supports restraint configuration, shown in Figure II.14(f) (supports restraint) and Figure II.14(g) (third point restraint).

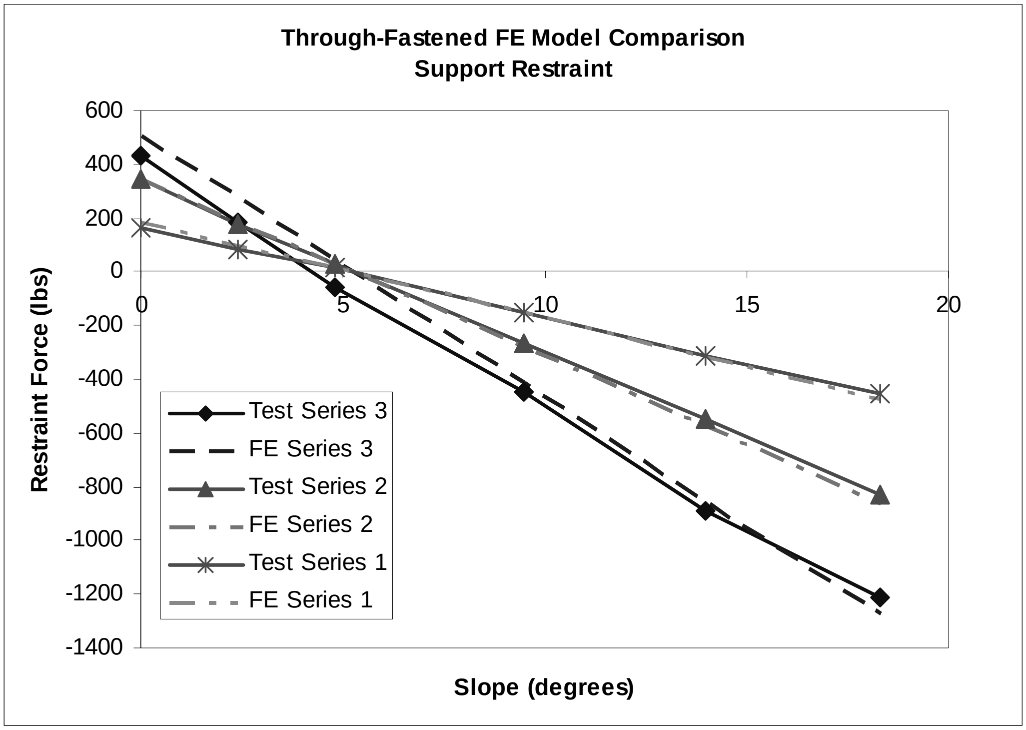

(a) Support Restraint

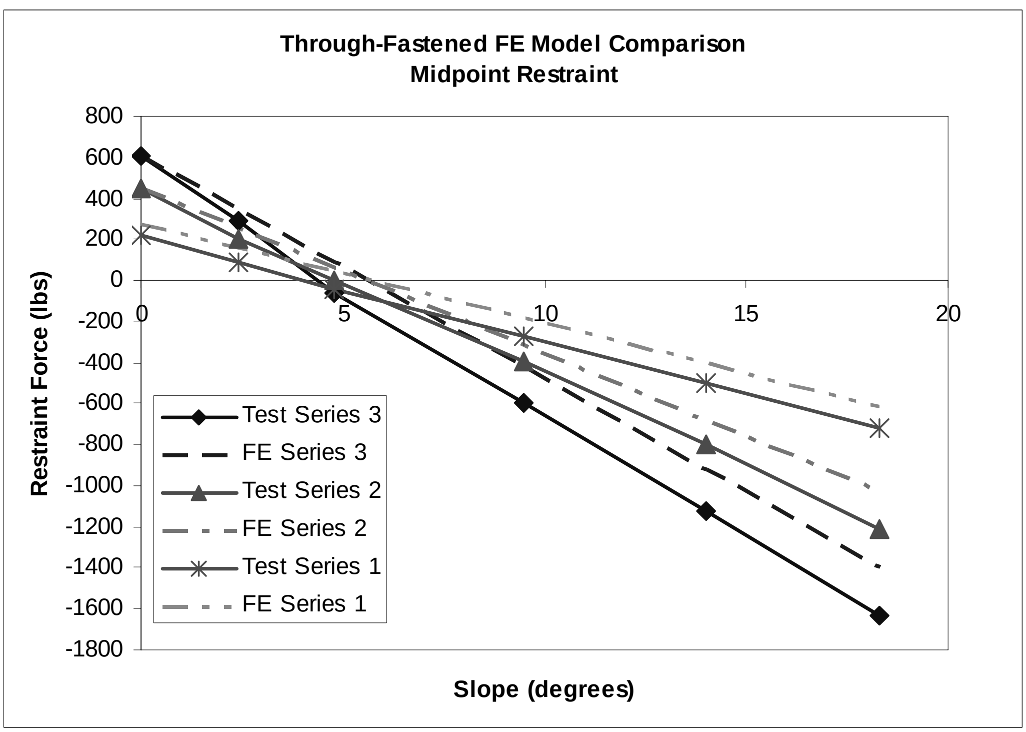

(b) Midpoint Restraint

***Figure II.14 Comparison of Finite Element Model with Through Fastened** Tests*

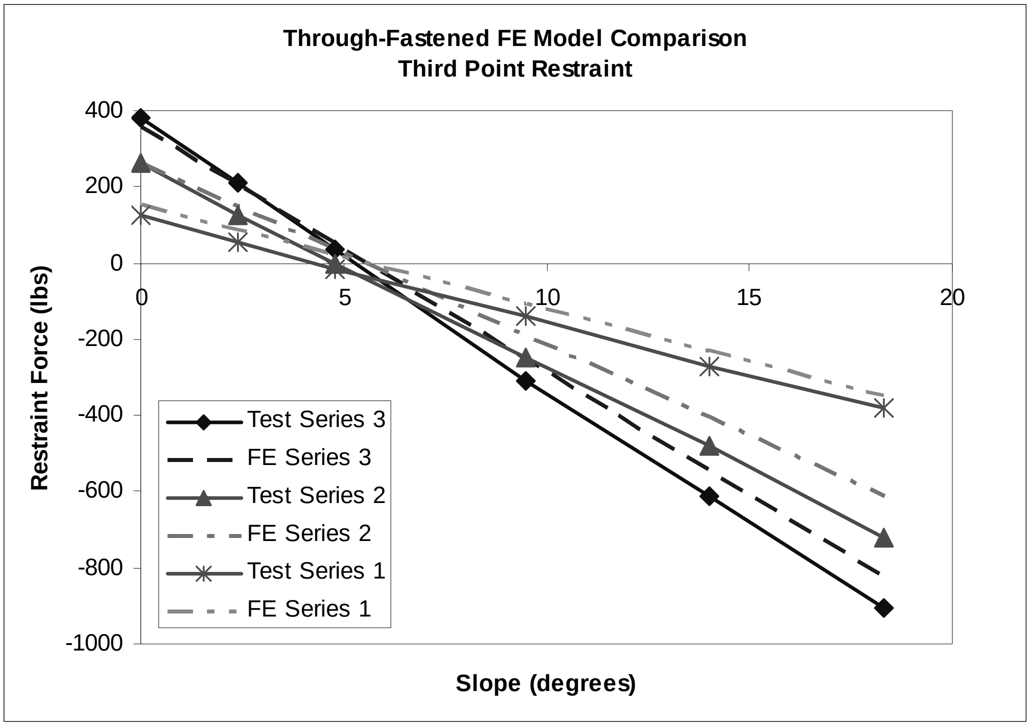

(c) Third Point Restraint

Figure II.14 Comparison of Finite Element Model with Through Fastened Tests, Continued.

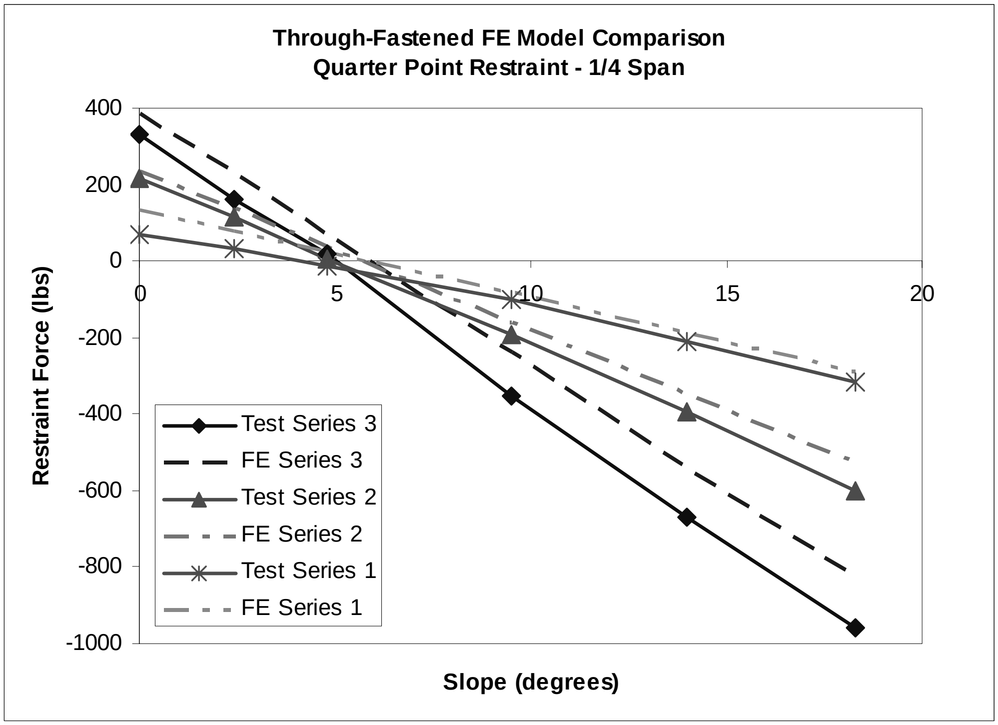

(d) Quarter Point Restraint – ¼ Span

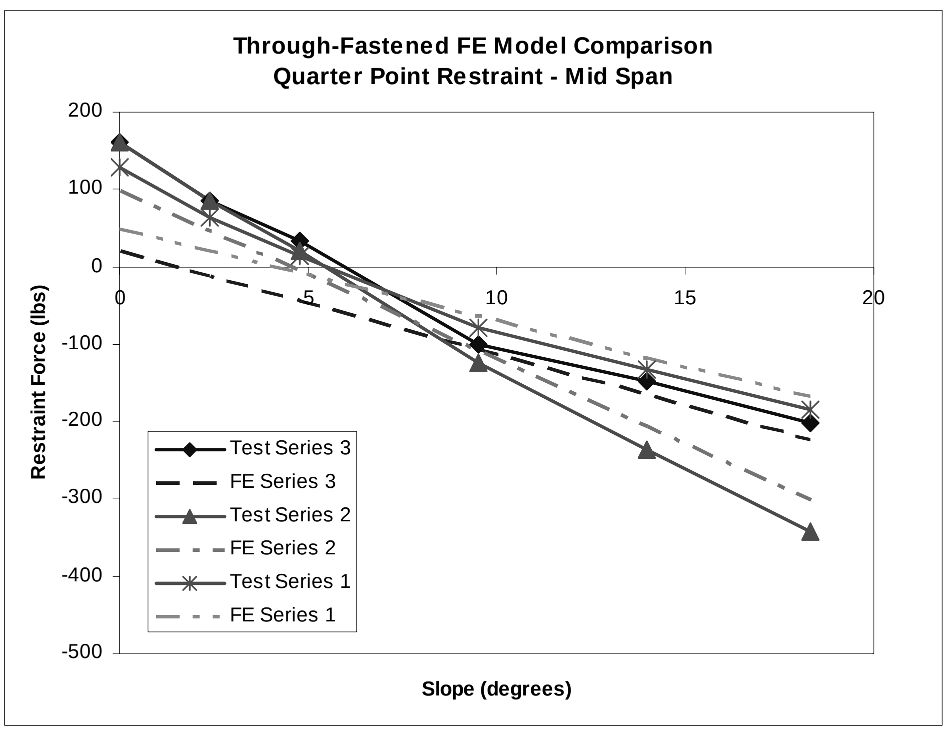

(e) Quarter Point Restraint – Midspan

Figure II.14 Comparison of Finite Element Model with Through Fastened Tests, Continued.

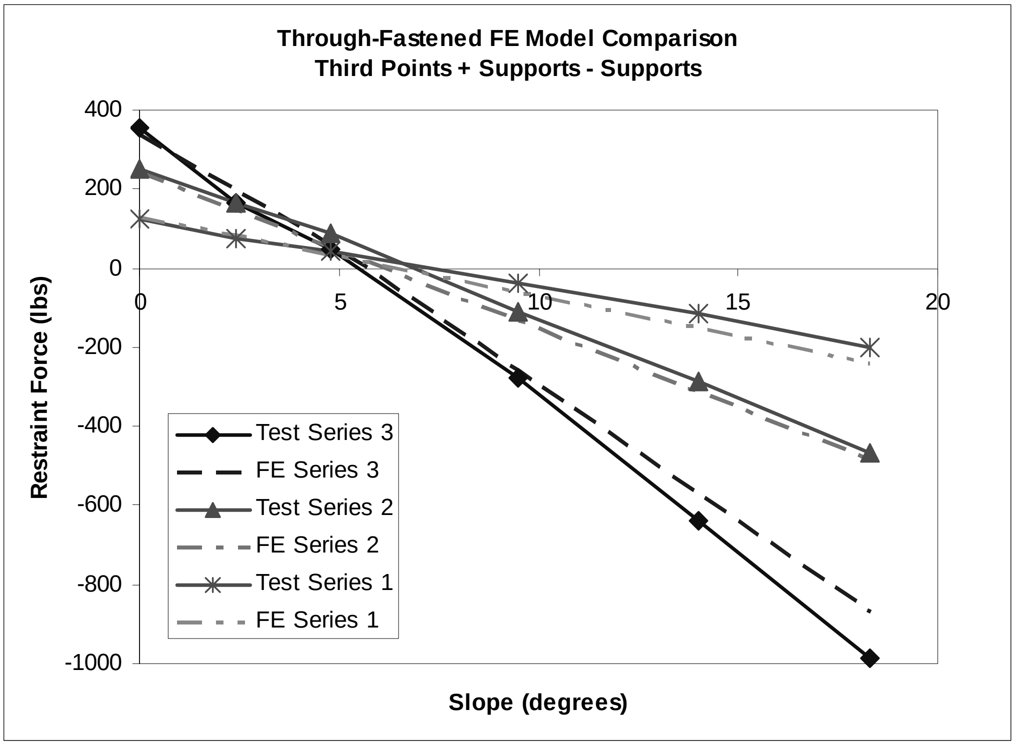

(f) Third Points + Supports Restraint - Supports

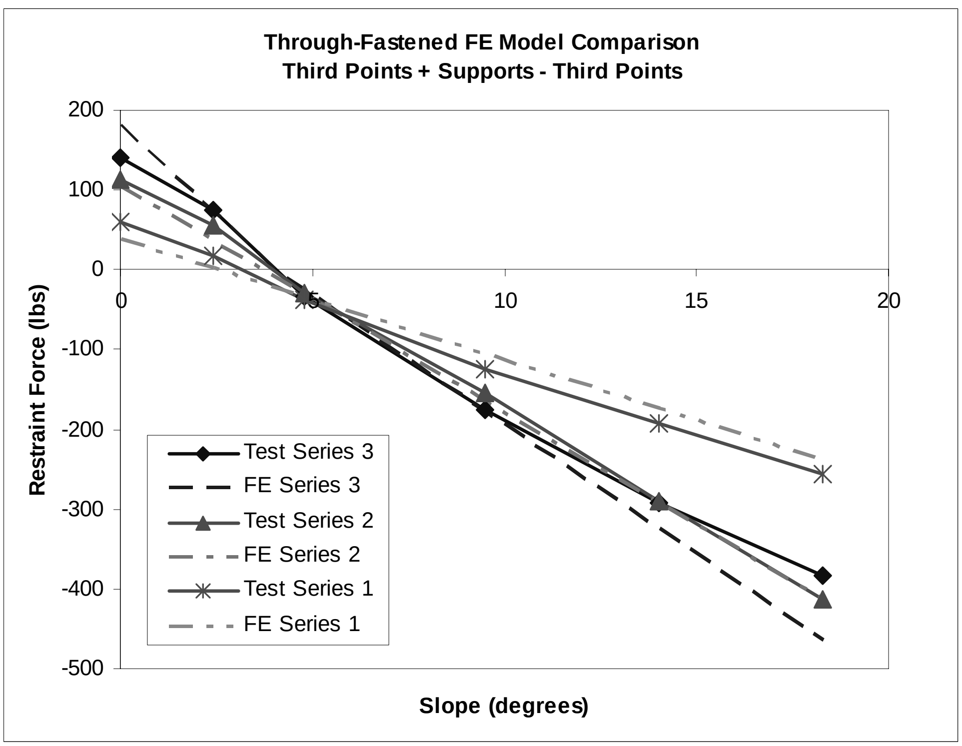

(g) Third Points + Supports Restraint, Third Points

Figure II.14 Comparison of Finite Element Model with Through Fastened Tests, Continued.

II.7.2 Comparison of Finite Element Model to Single Span Standing Seam Tests

For the single span standing seam tests, Series 4-6, to match the panel clip spacing at 2 ft 0 in., the sheathing was attached to the panel with link elements spaced at 2 ft 0 in intervals. The "link" elements were assigned a rotational stiffness of 4000 lb-in/rad.. Due to this increase in spacing, the net rotational stiffness of the purlin-sheathing connection is 2000 lb-in/rad-ft. The link elements were assigned a translational stiffness of 1000 lb/in (equivalent to 500 lb/in/ft) to account for the slip between the purlin and sheathing inherent in the clip. Assigning a panel diaphragm stiffness value of 10,000 lb/in to the sheathing, the combined diaphragm stiffness of the panel and sheathing-purlin link connection was calculated to be 900 lb/in. To prevent a floating system in the laboratory tests, the panel was fastened to the purlin with three screws in each panel pan at the eave of the system. In the finite element model, the link connection between the eave purlin and the sheathing was assigned a translational stiffness of $1x10^6$ lb/in to account for the stiffness of the added screws. The panel had a calculated gross moment of inertia of 0.422 in^4/ft and the corresponding bending thickness of the panel in the finite element model was found to be 0.75 in.

The stiffness of the connection of the through rods was conservatively assumed to be 5000 lb/in. Due to the flexibility of the through-rods and the rigid attachment of the sheathing to the purlin at the eave, the models gave different restraint forces depending upon whether restraint was applied at the eave or ridge. The finite element model result therefore is the combination of the eave restraint at low slopes (positive restraint force) and ridge restraint at steeper slopes (negative restraint force).

The finite element results are compared to the laboratory test results in Figures II.15(a-g). With a few exceptions, the finite element models show good correlation with the test results. The best correlation is observed for the supports restraint configuration, shown in Figure II.15(a). For the third points and midpoints configurations shown in Figures II.15(b) and II.15(c) respectively, good correlation is seen although some deviation is observed for Series 6 (six purlin lines). Similar to the through fastened cases, it is believed that the quarter points tests are sensitive to the pretension of the anchor rod. Despite this sensitivity, good correlation is observed in Figure II.15(d) (quarter span restraints) and Figure II.15(e) (mid-span restraint) for two and four purlin lines with fair correlation of the 6 purlin line test (Series 6) due to the large pretensions used in the Series 6 tests. Good correlation is observed for the third points +

supports configuration, which has proven difficult with previous finite element models and prediction methods.

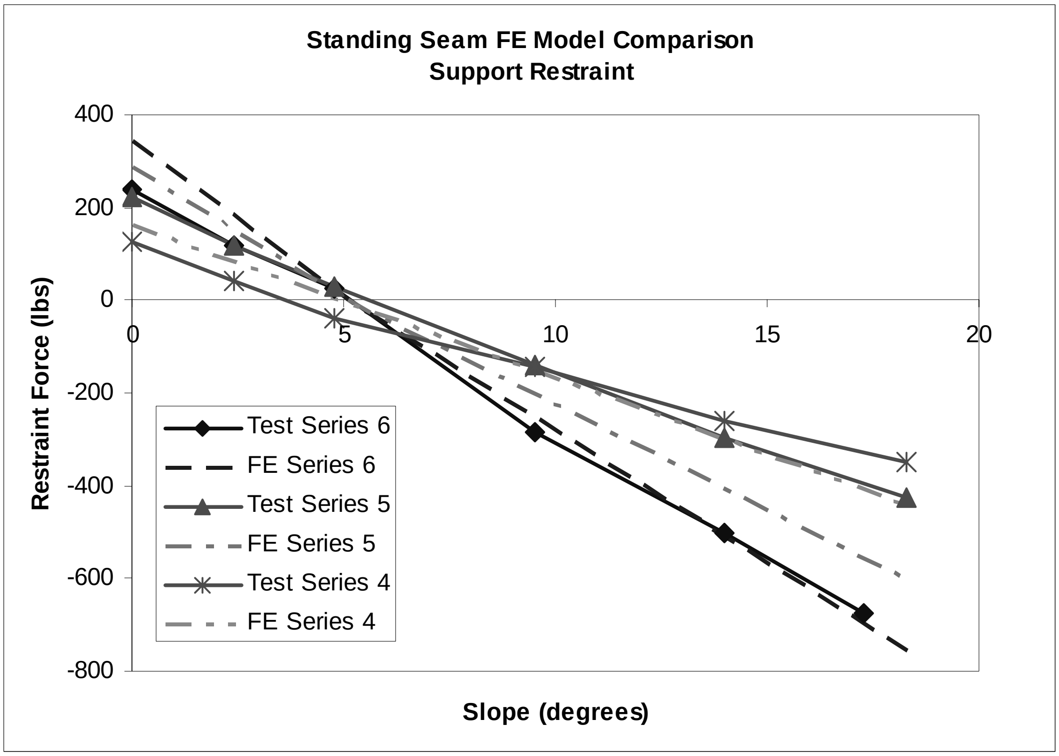

(a) Support Restraint

Figure II.15 Comparison of Finite Element Model with Standing Seam Tests

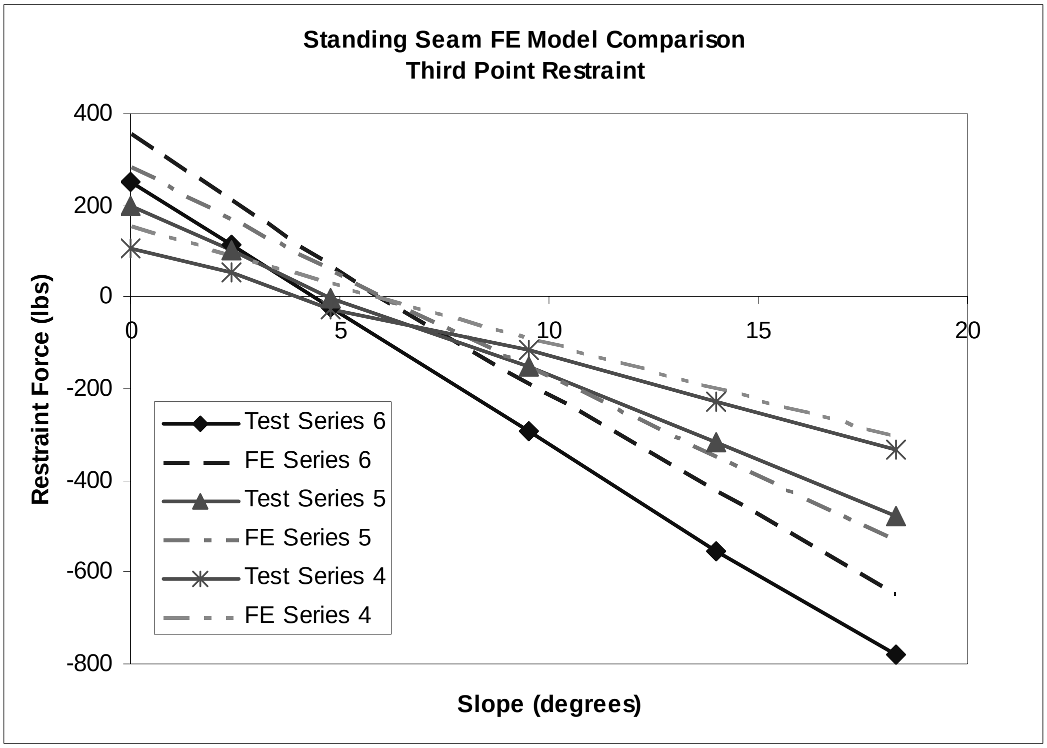

(b) Third Point Restraint

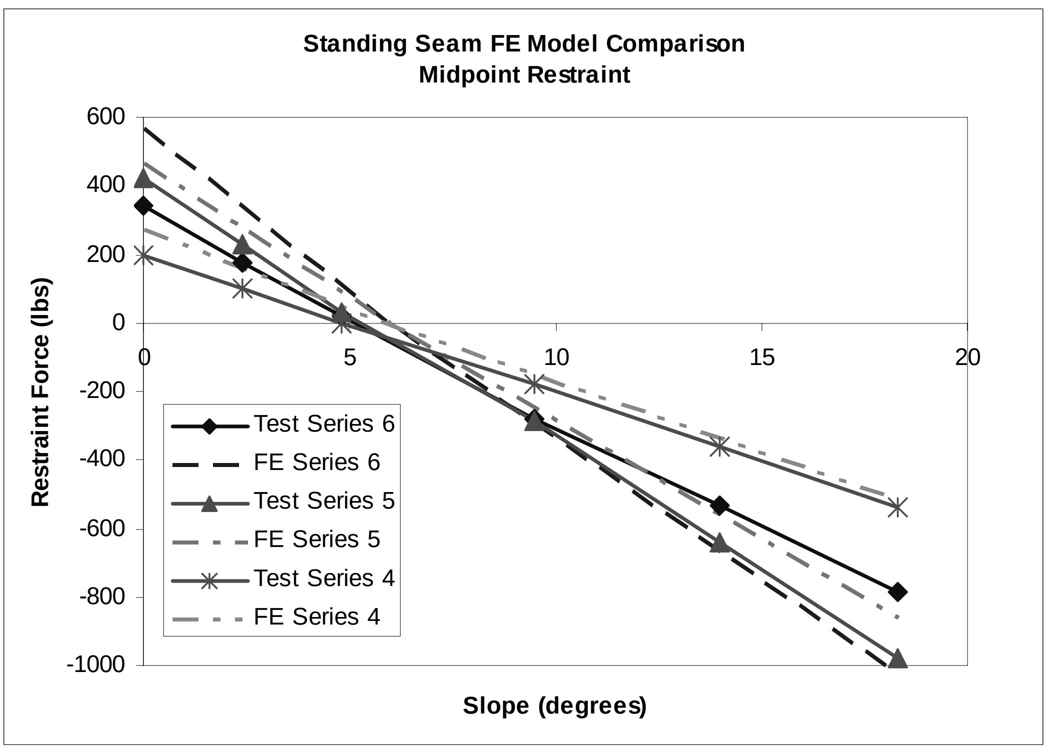

(c) Midpoint Restraint

Figure II.15 Comparison of Finite Element Model with Standing Seam Tests, Continued

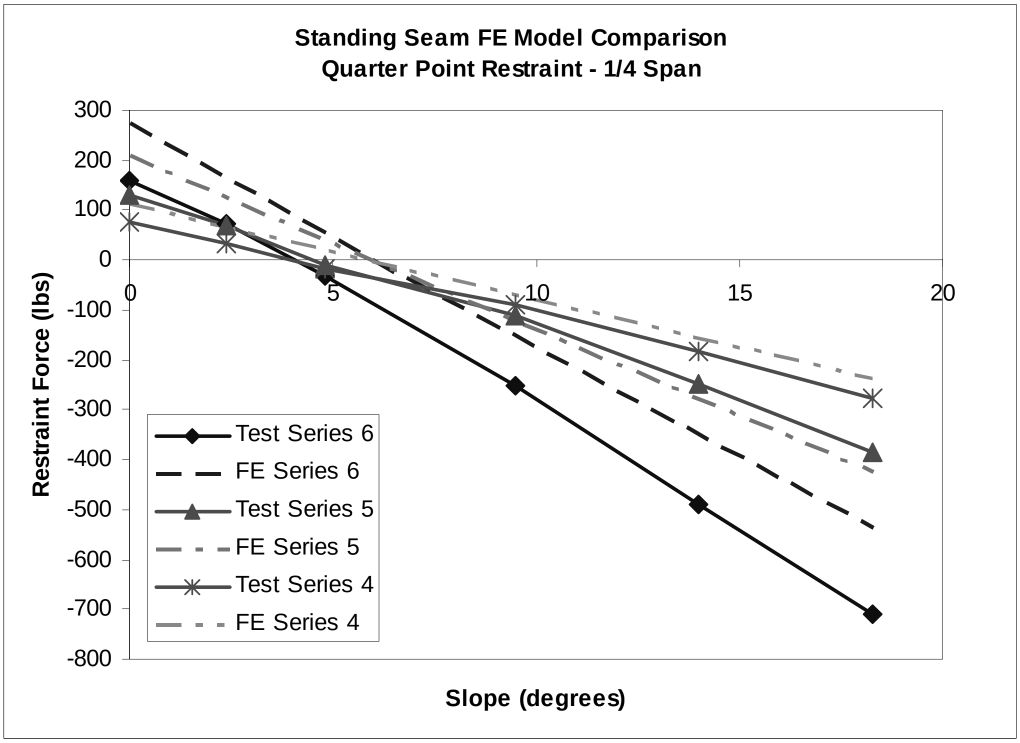

(d) Quarter Point Restraint – ¼ Span

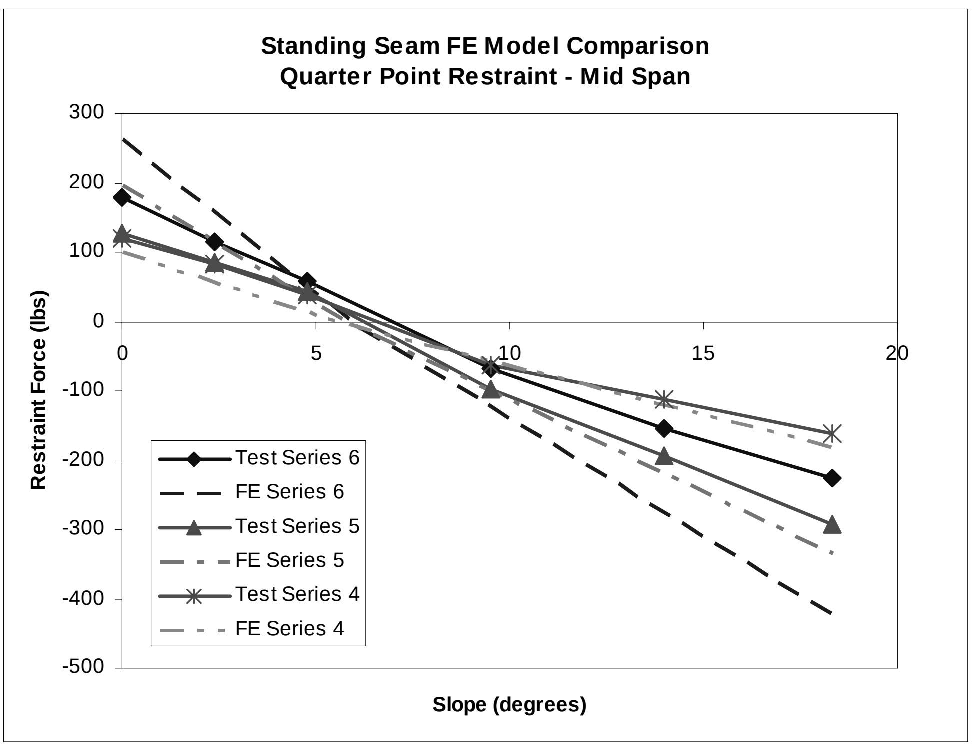

(e) Quarter Point Restraint – Midspan

Figure II.15 Comparison of Finite Element Model with Standing Seam Tests, Continued

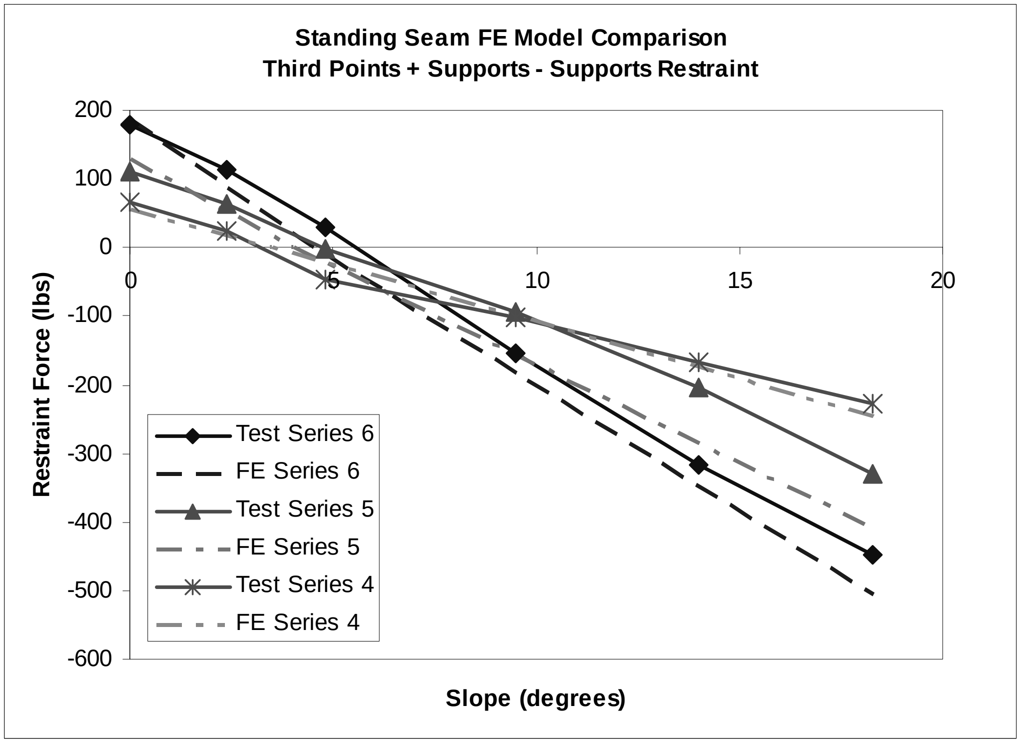

(f) Third Points + Supports Restraint - Supports

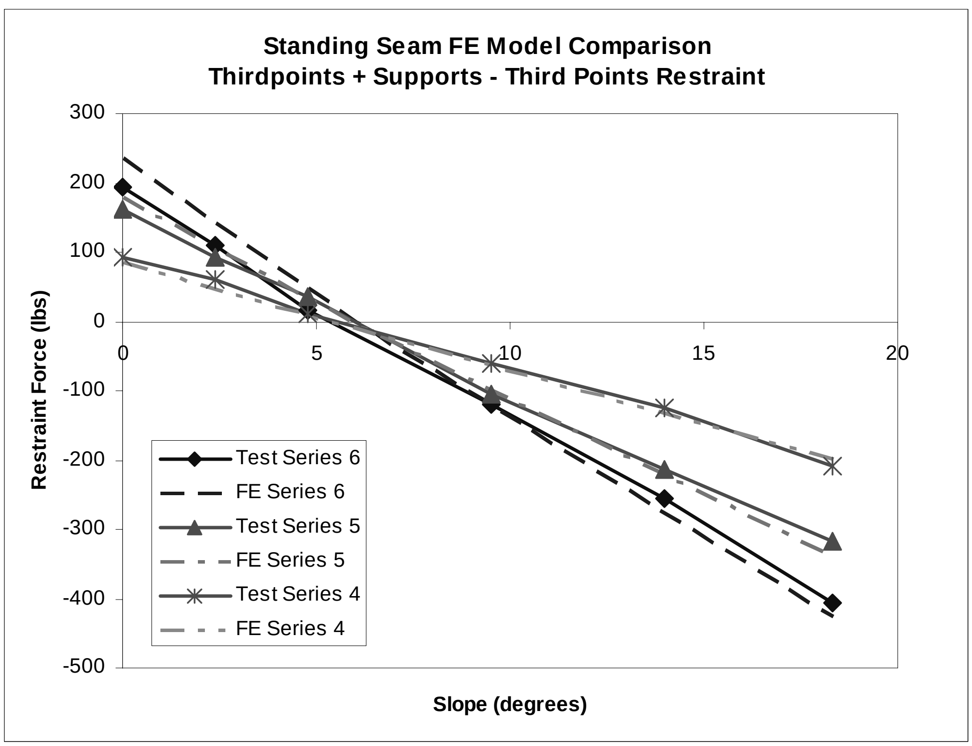

(g) Third Points + Supports Restraint, Third Points

Figure II.15 Comparison of Finite Element Model with Standing Seam Tests, Continued

II.7.3 Comparison of Finite Element Model to Multiple Span Through-fastened Tests

The finite element model used to evaluate the single span through-fastened models was expanded to the multi-span models. A panel diaphragm stiffness of 27500 lb/in and a link rotational stiffness of 1000lb-in/rad yielded the best correlation with the test results. The purlin is assigned “lapped” section properties extending 3 ft 0 in. to both sides of each interior rafter to match the layout of the laboratory tests.

The results of the comparison between the finite element model and the multiple span through-fastened tests are shown in Figures II.16(a-n.) and overall correlation is good. In Figure II.16(a), both the exterior and interior support restraints are shown on the same plot and excellent correlation is realized at both locations. The midpoints restraint configuration is compared in Figure II.16(b) showing good correlation with test results at both the interior and exterior midpoint restraint locations. The third point restraint configuration is divided into Figures II.16(c), II.16(d) and II.16(e) showing the exterior span outside third point, exterior span inside third point, and the interior span third point respectively. Good correlation is realized though slightly unconservative for the exterior span outside third point.

The quarter point restraint configuration is shown in Figures II.16(f) to II.16(i). The quarter span restraints show good correlation with the test results as each quarter span location is shown in individual plots, Figures II.16(f), II.16(g) and II.16(h). There is some deviation at larger roof pitches for the exterior span outside quarter point as shown in Figure II.16(f). At the midspan locations, with both the exterior and interior span restraints shown in Figure II.16(i), good correlation is realized at steeper roof slopes, with fair correlation at lower slopes. Due to the nonlinear nature of the test results at low slopes, it is believed that discrepancies between the finite element model and the test result from poor test data as the restraint forces are very sensitive to the restraint pretension for quarter point configurations.

The results of the comparison of the third points plus supports restraint configuration is shown in Figures II.16(j) to II.16(n). The supports restraints are shown on the same plot (Figure II.16(j)) and give excellent correlation with the test results. The third point restraints are shown on separate plots, each showing good correlation with the test results. The exterior span inside third point (Figure II.16(m)) and interior third point (Figure II.16(n)) both give conservative results while the exterior span outside third point (Figure II.16(k)) gives slightly unconservative results.

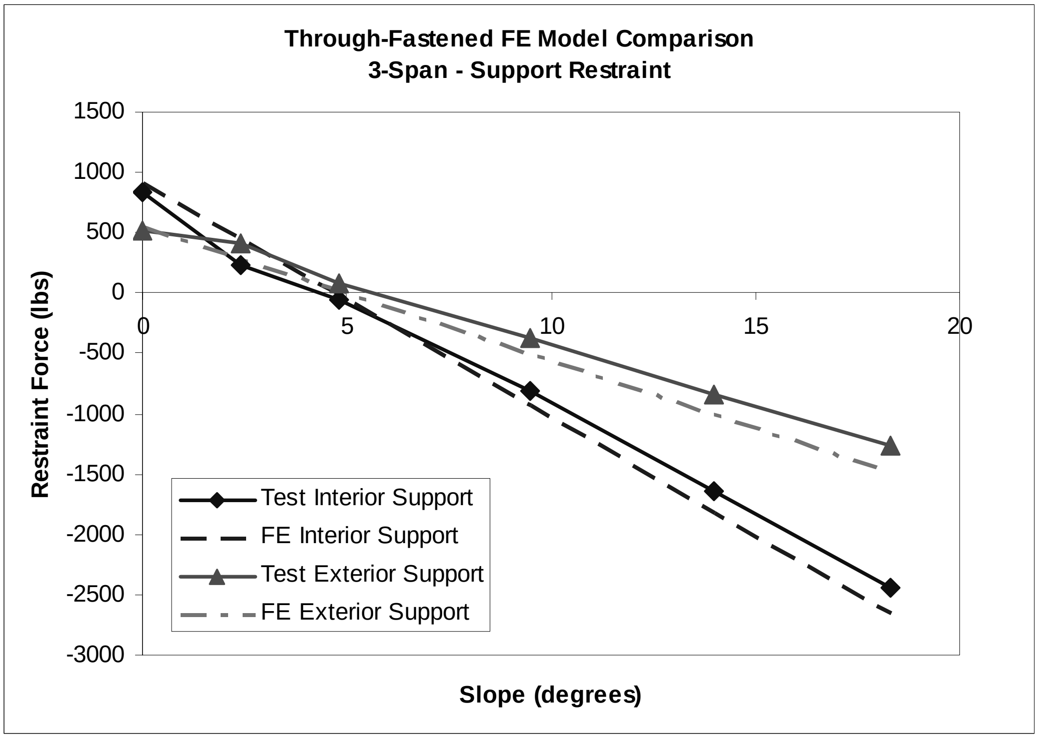

(a) Support Restraint

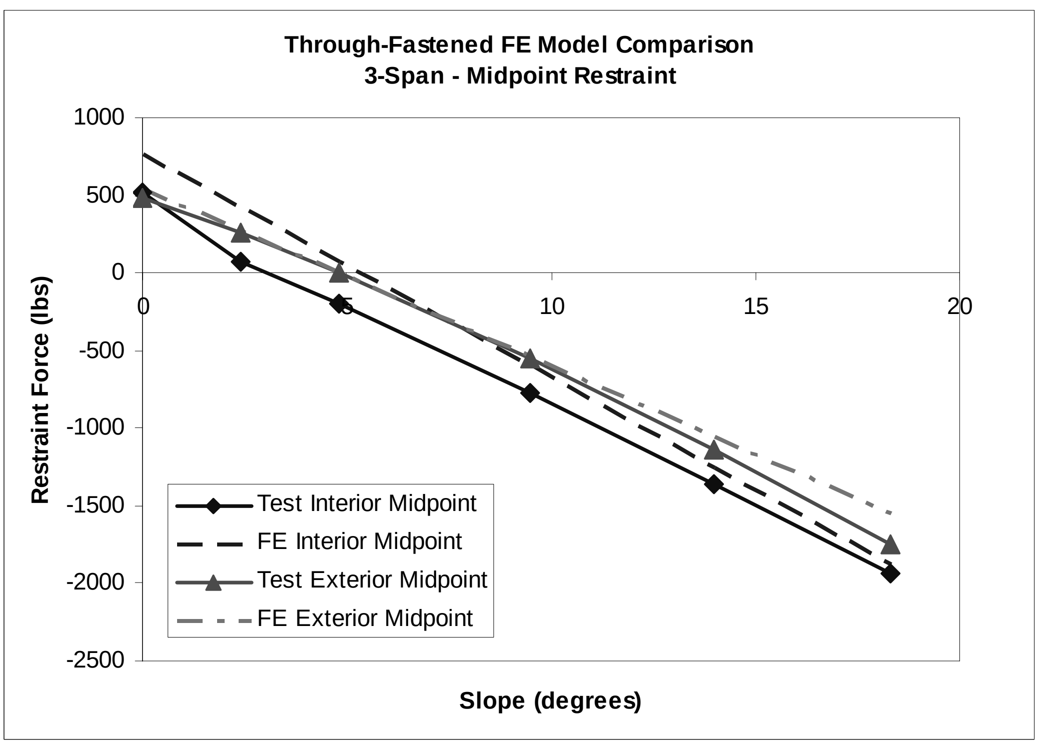

(b) Midpoint Restraint

Figure II.16 Comparison of Finite Element Model with Three-Span Through-Fastened Tests

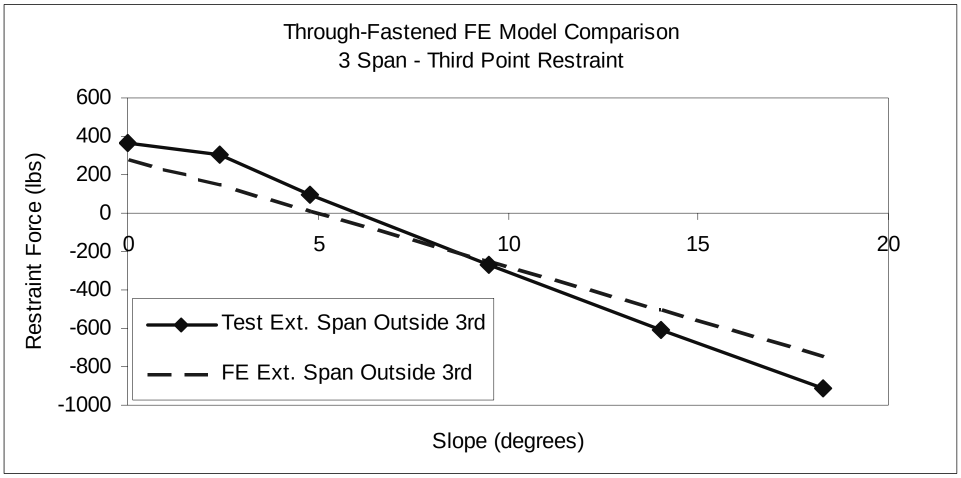

(c) Third Point Restraint – Exterior Span Outside Third Point

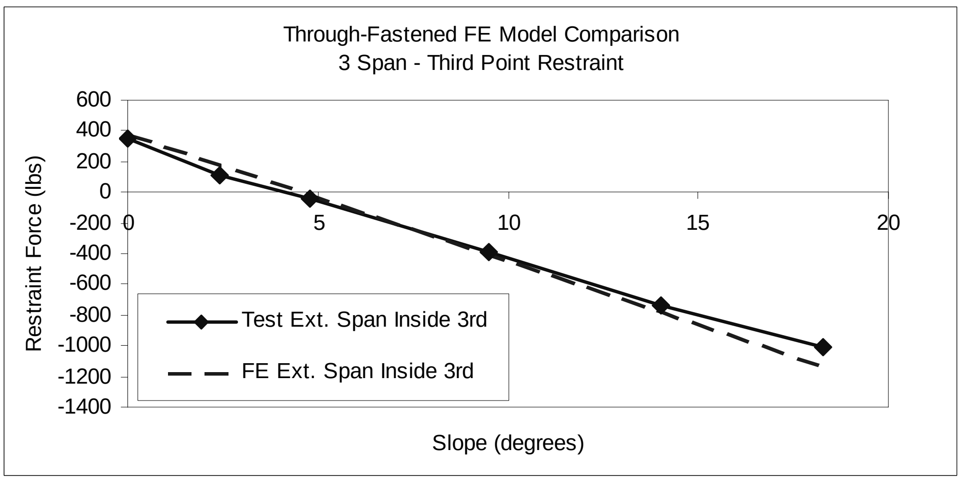

(d) Third Point Restraint – Exterior Span Inside Third Point

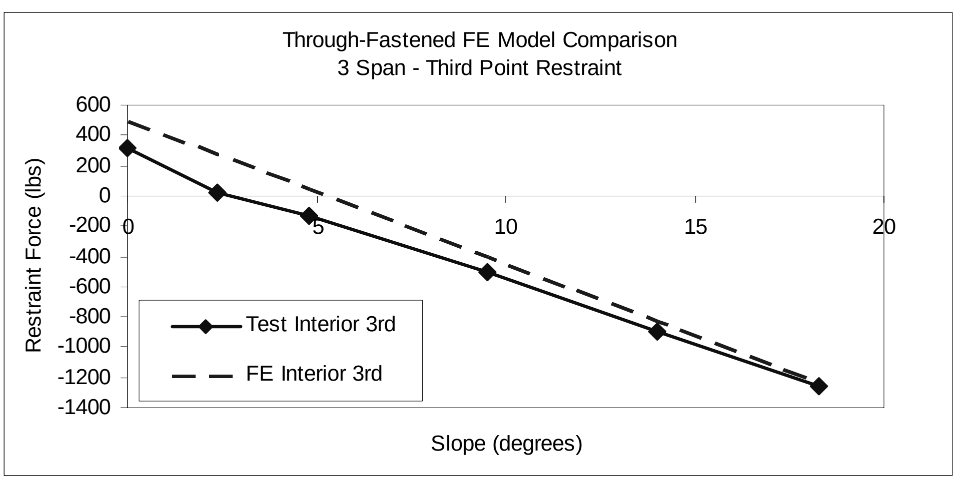

(e) Third Point Restraint – Interior Span Third Point

Figure II.16 Comparison of Finite Element with Three-Span Through-Fastened Tests, Cont.

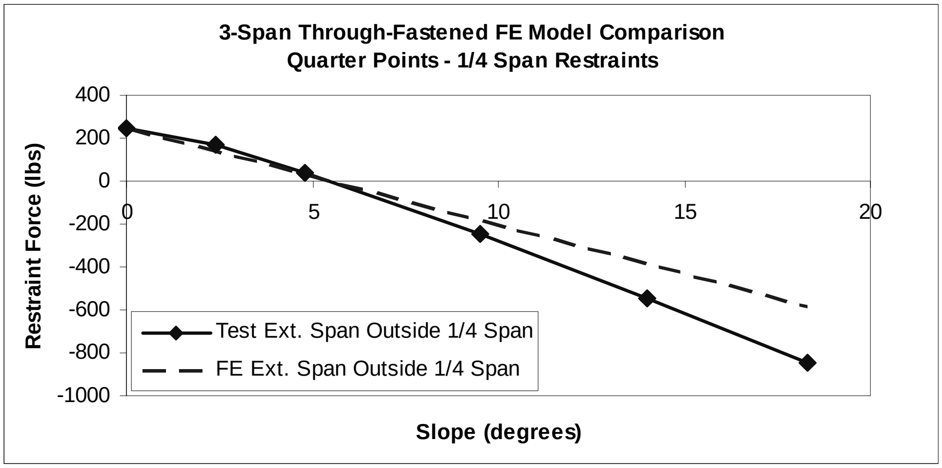

(f) Quarter Point Restraints – Exterior Span Outside ¼ Span

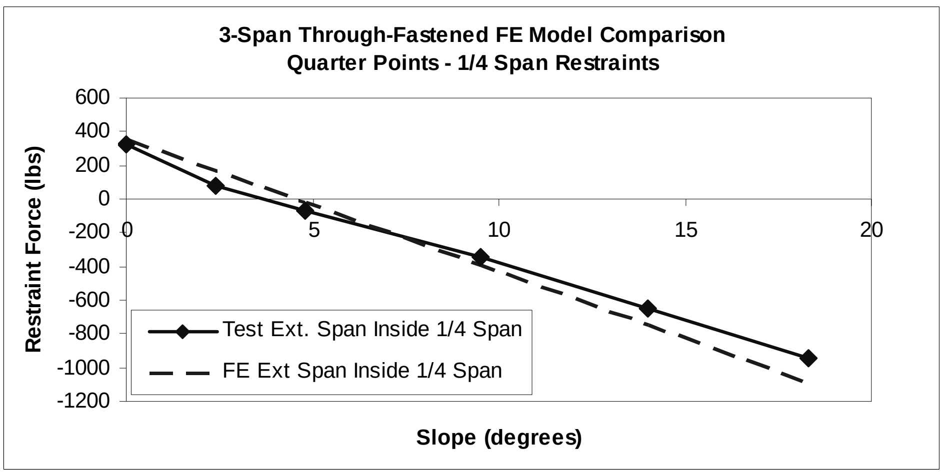

(g) Quarter Point Restraints – Exterior Span Inside ¼ Span

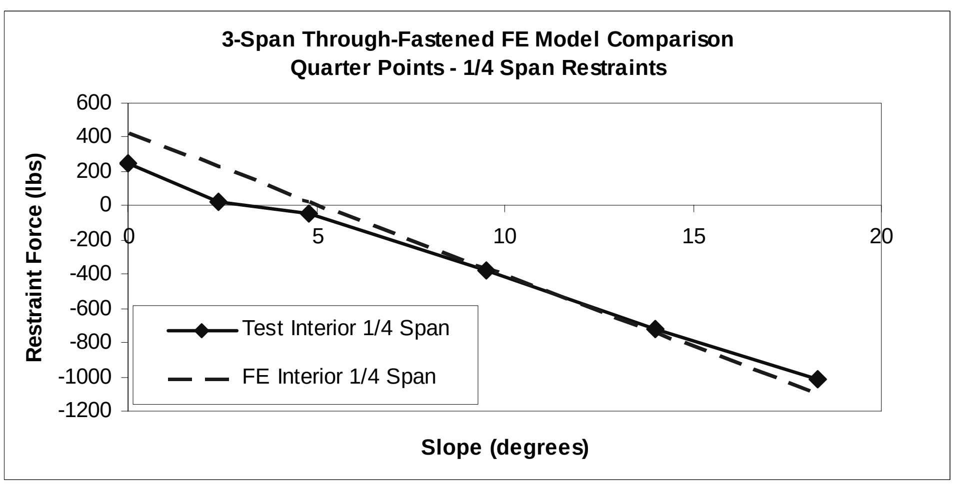

(h) Quarter Point Restraints – Interior Span ¼ Span

Figure II.16 Comparison of Finite Element with Three-Span Through-Fastened Tests, Cont.

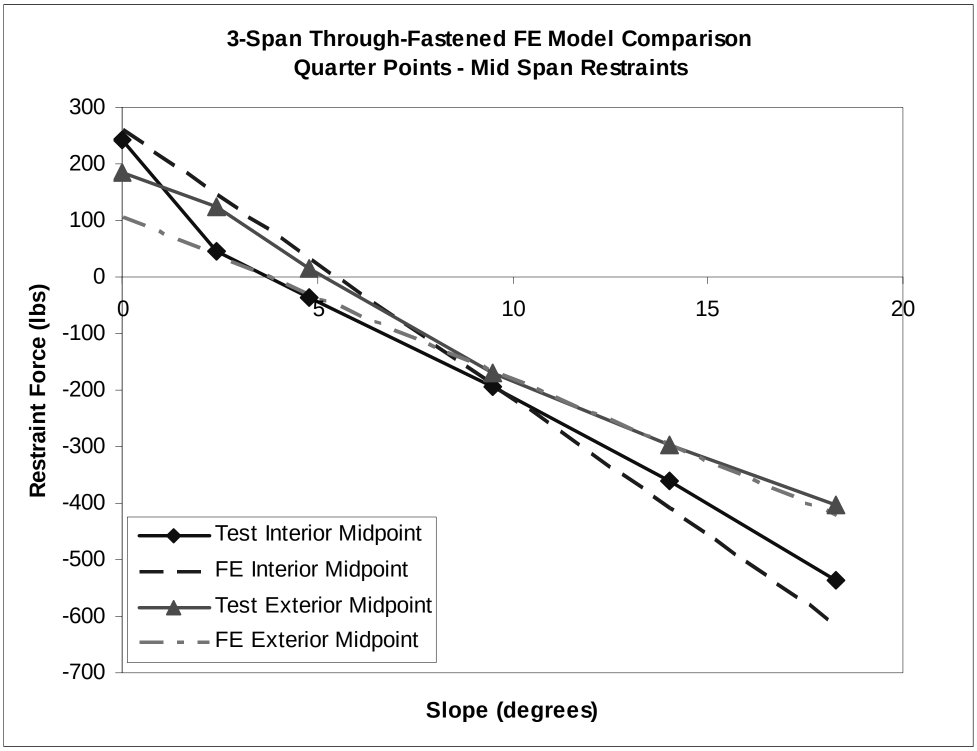

(i) Quarter Point Restraints – Midspan

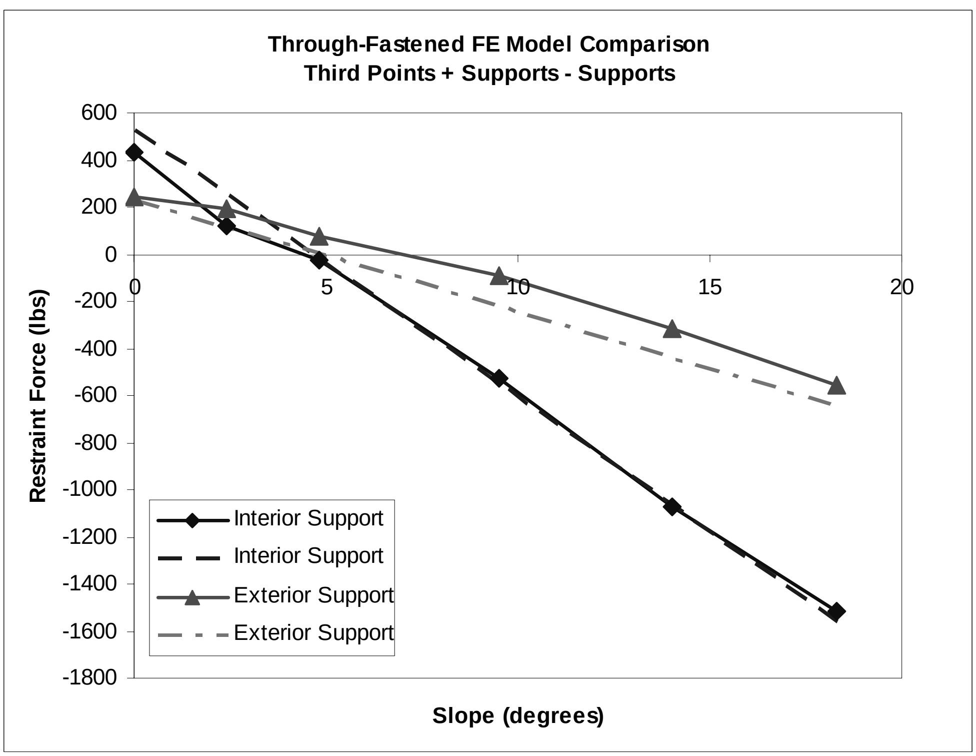

(j) Third Points + Supports Restraints - Supports

Figure II.16 Comparison of Finite Element Model Three-Span Through-Fastened Tests, Cont

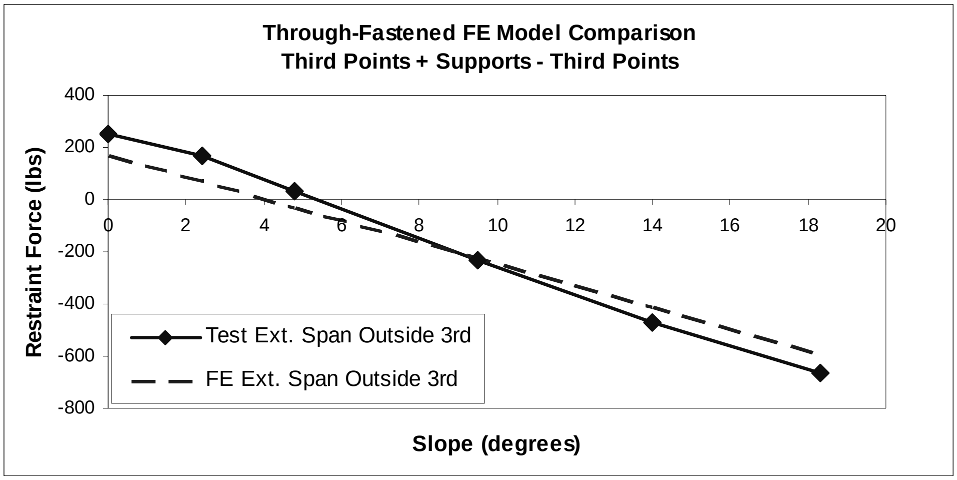

(k) Third Points + Supports – Exterior Span Outside Third Point

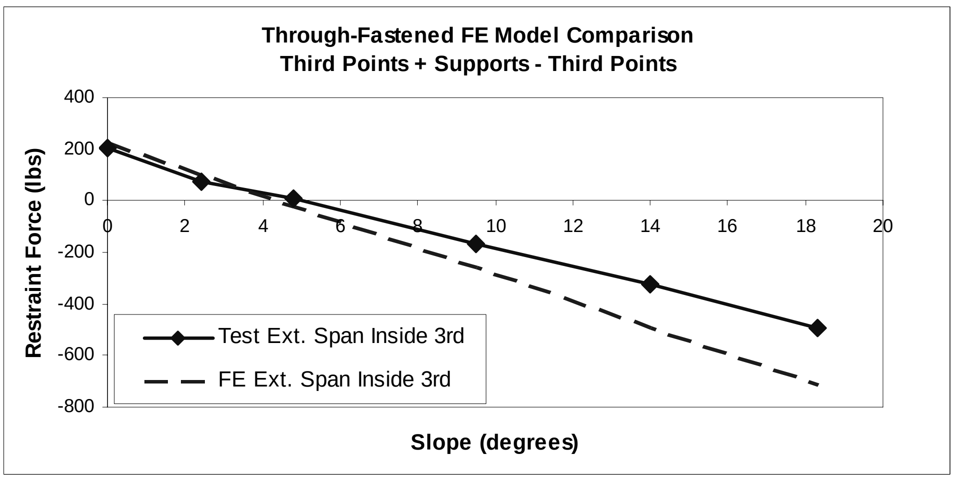

(m) Third Points + Supports – Exterior Span Inside Third Point

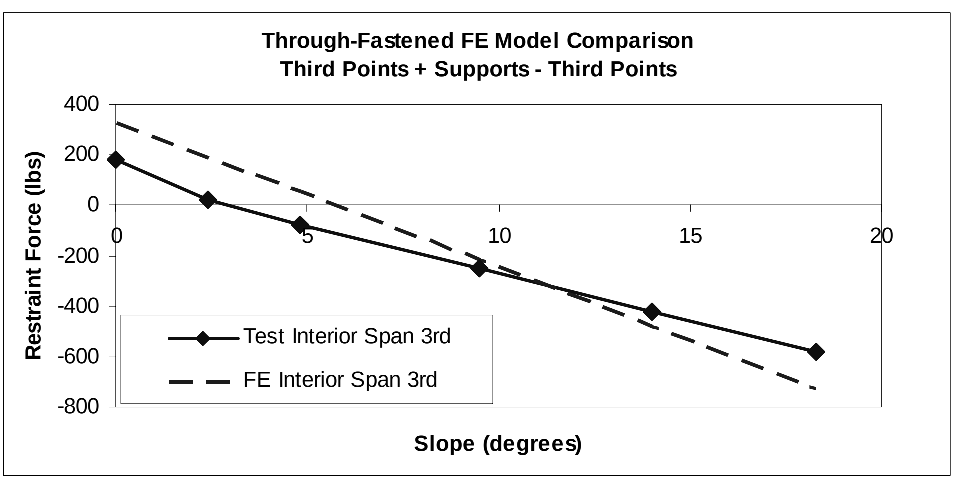

(n) Third Points + Supports – Interior Span Third Point

FigureII.16 Comparison of Finite Element with Three-Span Through-Fastened Tests, Cont.

II.7.4 Comparison of Finite Element Model to Multiple Span Standing Seam Tests

A finite element model with the same parameters as the single span standing seam model was used to evaluate the multiple span standing seam tests. A panel diaphragm stiffness of 10000 lb/in was combined with a link translational stiffness of 1000 lb/in to yield a net diaphragm stiffness of 900 lb/in. Links connecting the purlin to the sheathing are spaced at 2 ft 0 in. to match the laboratory tests. Best correlation was found with a rotational link stiffness of 4,000 lb-in/rad. Purlins are given "lapped" section properties 3 ft 0 in. to each side of the interior rafters. Restraint beams spanned between the rafters and were modeled as continuous across the interior supports.

Figures II.17(a) to II.17(n) show the comparison between the multiple span standing seam model and laboratory tests. Both the exterior and interior supports of the supports restraint configuration are shown in Figure II.17(a). Correlation with test results is good, though the finite element model slightly underestimates restraint force of the exterior support and at low slopes and the interior support at large slopes. The midpoints restraint configuration, shown in Figure II.17(b), correlates fairly well with the test results although the exterior midpoint is slightly unconservative at low slopes while the interior midpoint is slightly conservative at all slopes. The results of the third point restraint configuration are shown in Figures II.17(c) to II.17(e) with each restraint location shown on a separate plot. Good correlation is realized at all third point locations

The quarter points restraint configuration is compared to laboratory test results in Figures II.17(f) to II.17(i). Each quarter span restraint location is shown on a separate plot (Figures II.17(f) to II.17(h)) and each shows good correlation with the test results, with the exception of the interior span quarter point which deviates slightly at steeper slopes. Both the exterior and interior midspan restraints are shown in Figure II.17(i). Correlation is fair although unconservative for the exterior midspan restraint at small slopes.

Figures II.17(j) to II.17(n) display the comparison of the finite element model to test results for the third points plus supports restraint configuration. The supports restraints are both shown in Figure II.17(j). Correlation is fair although there is some offset between the trendlines. Each third point location is shown in an individual plot. Correlation is fair for the exterior span outside third point (Figure II.17(k)) and the interior span third point (Figure II.17(n)) and excellent for the exterior span inside third point (Figure II.17(m)).

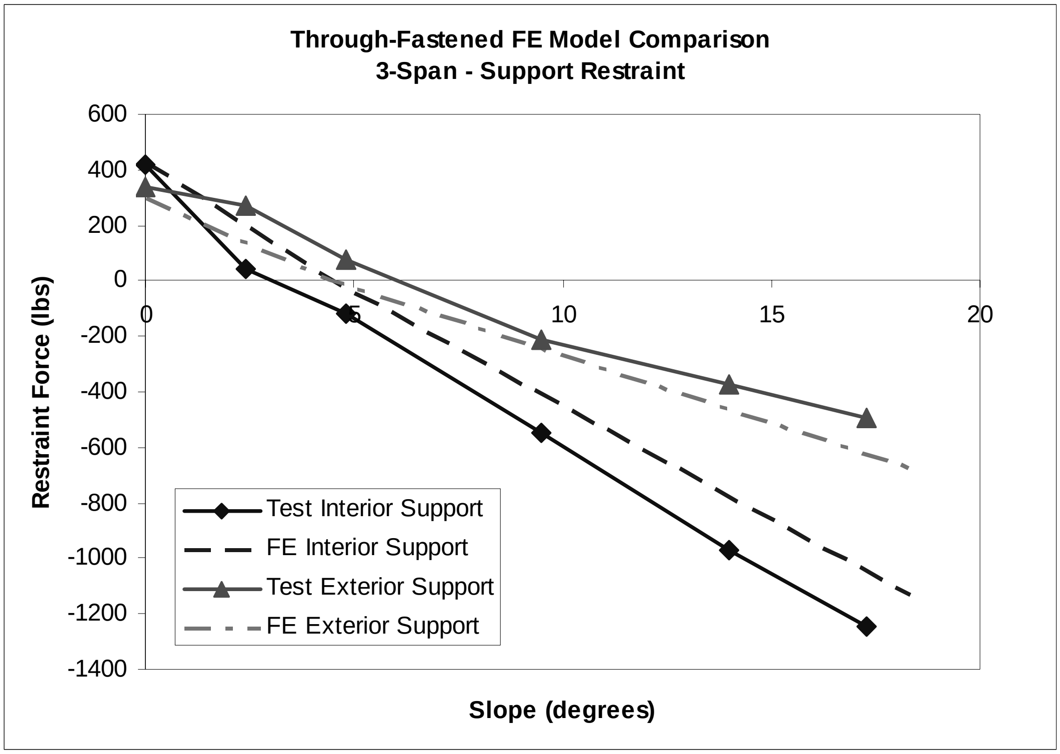

(a) Support Restraint

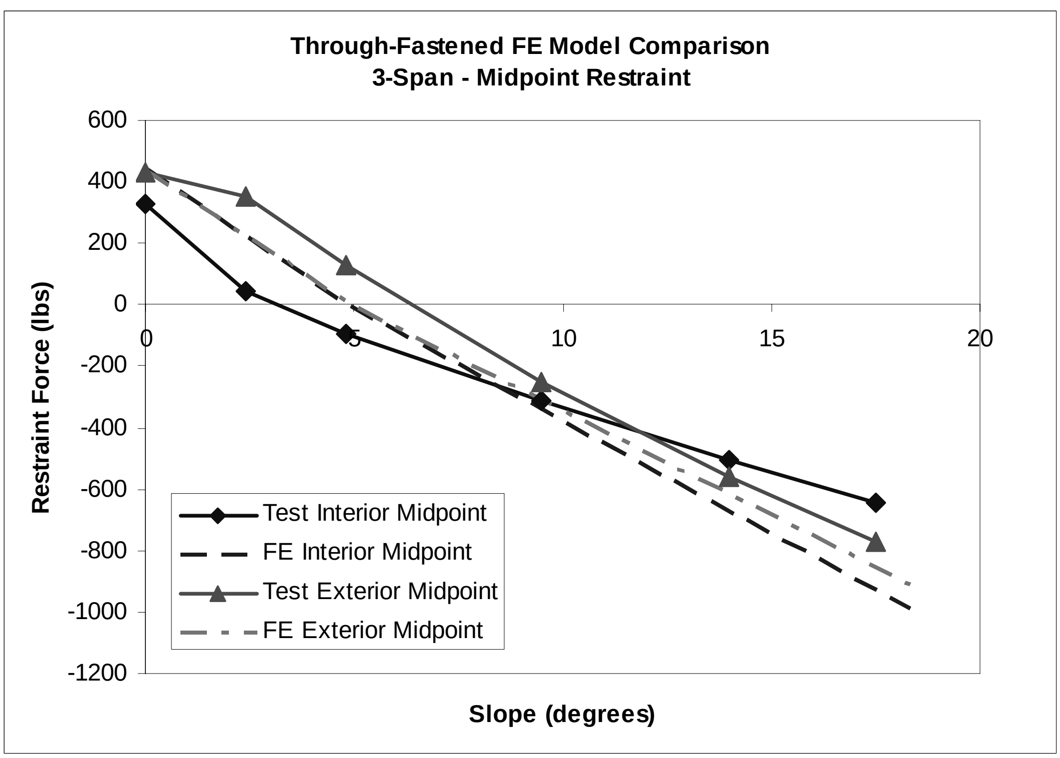

(b) Midpoint Restraint

Figure II.17 Comparison of Finite Element Model with Three-Span Standing Seam Tests

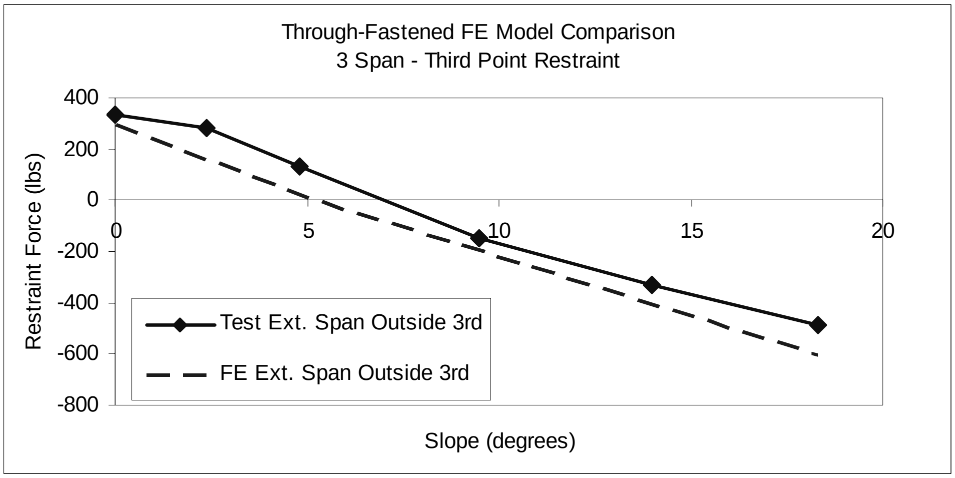

(c) Third Point Restraint – Exterior Span Outside Third Point

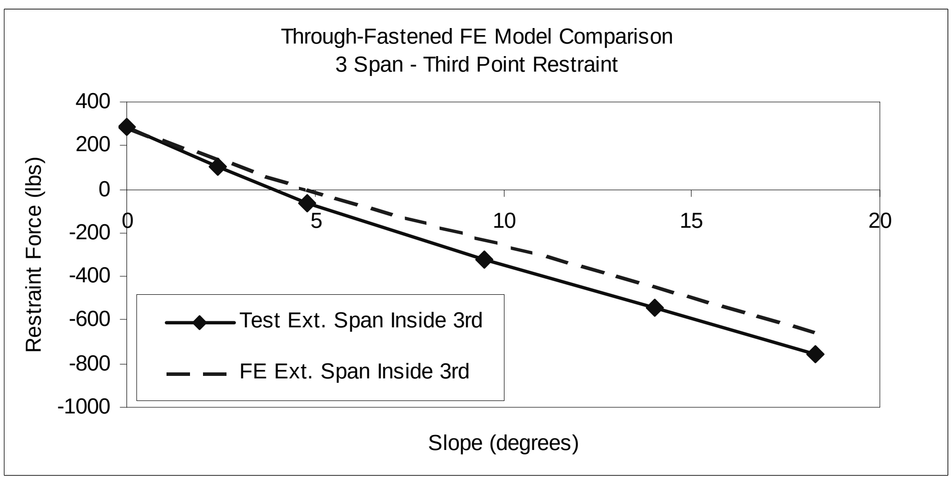

(d) Third Point Restraint – Exterior Span Inside Third Point

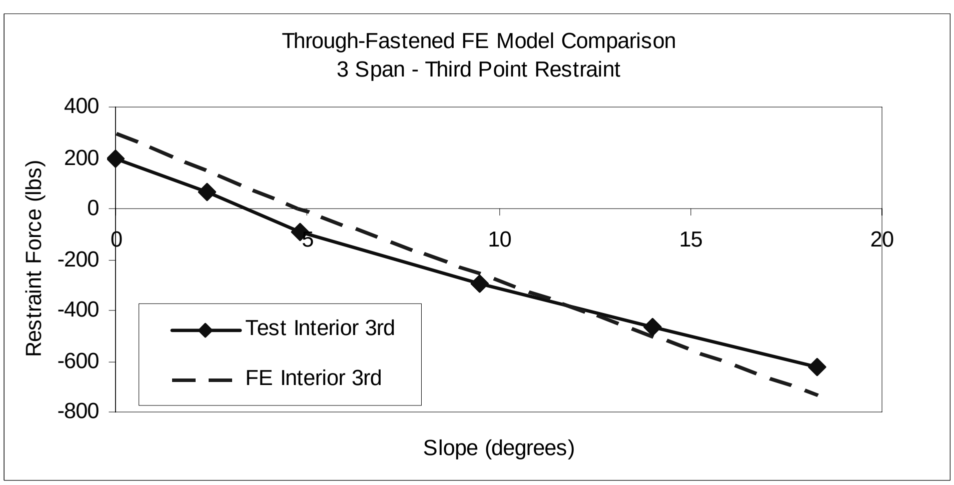

(e) Third Point Restraint – Interior Span Third Point

FigureII.17 Comparison of Finite Element Model with Three-Span Standing Seam Tests,Cont

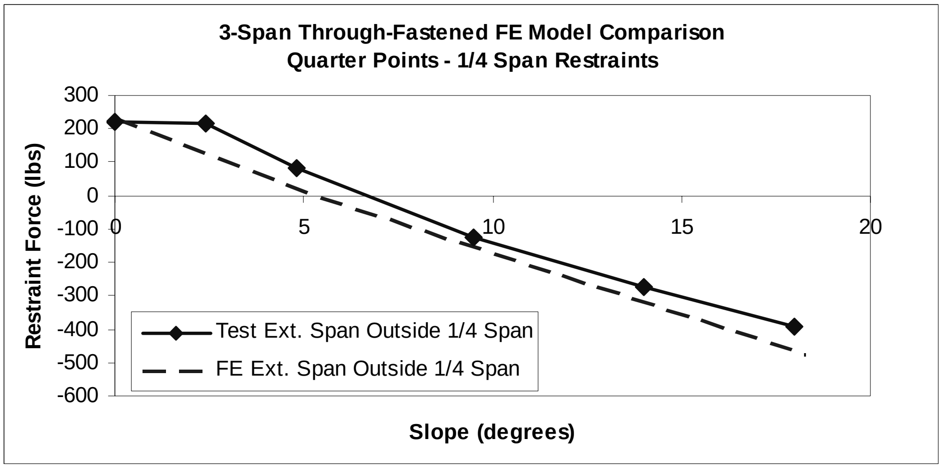

(f) Quarter Point Restraints – Exterior Span Outside ¼ Span

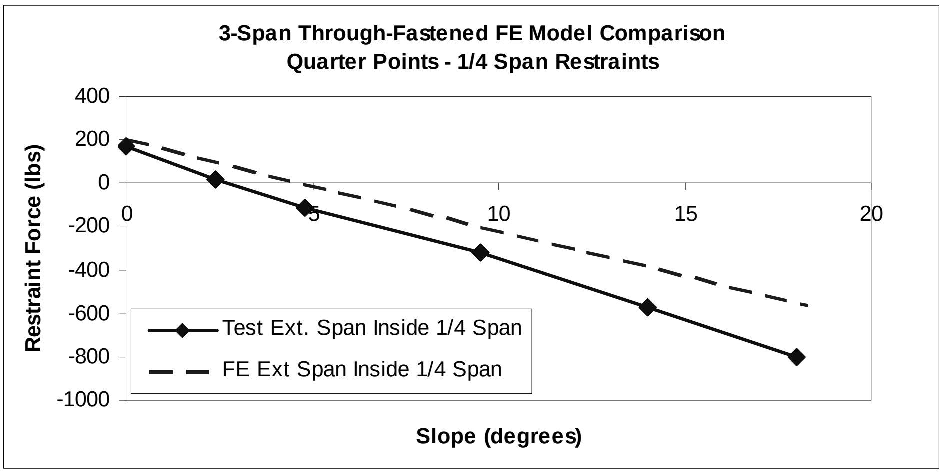

(g) Quarter Point Restraints – Exterior Span Inside ¼ Span

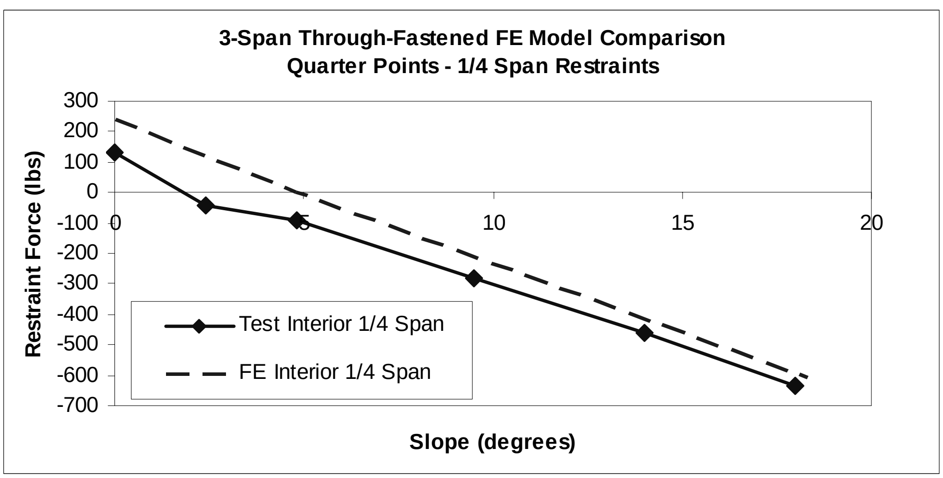

(h) Quarter Point Restraints – Interior Span ¼ Span

FigureII.17 Comparison of Finite Element Model with Three-Span Standing Seam Tests,Con.

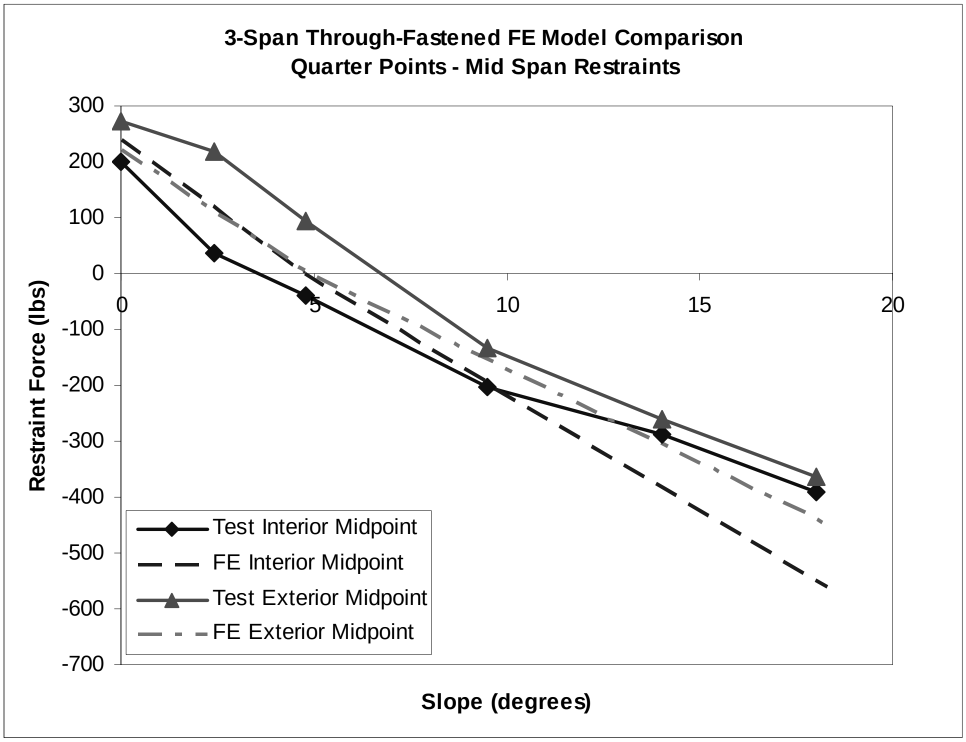

(i) Quarter Point Restraints – Midspan

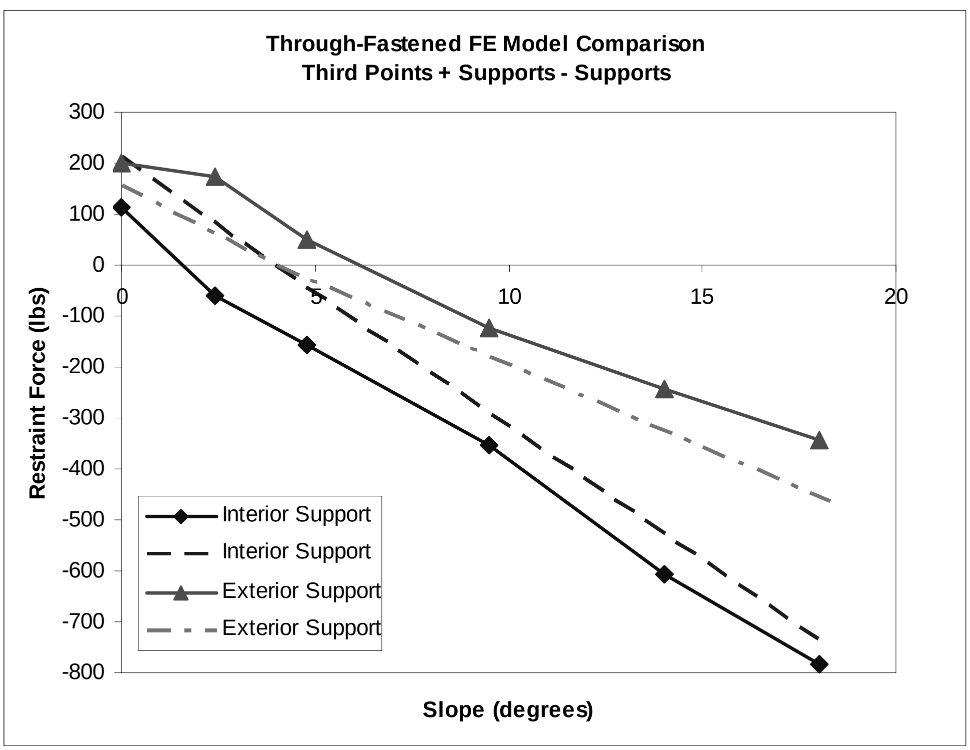

(j) Third Points + Supports Restraints - Supports

FigureII.17 Comparison of Finite Element Model with Three-Span Standing Seam Tests,Cont

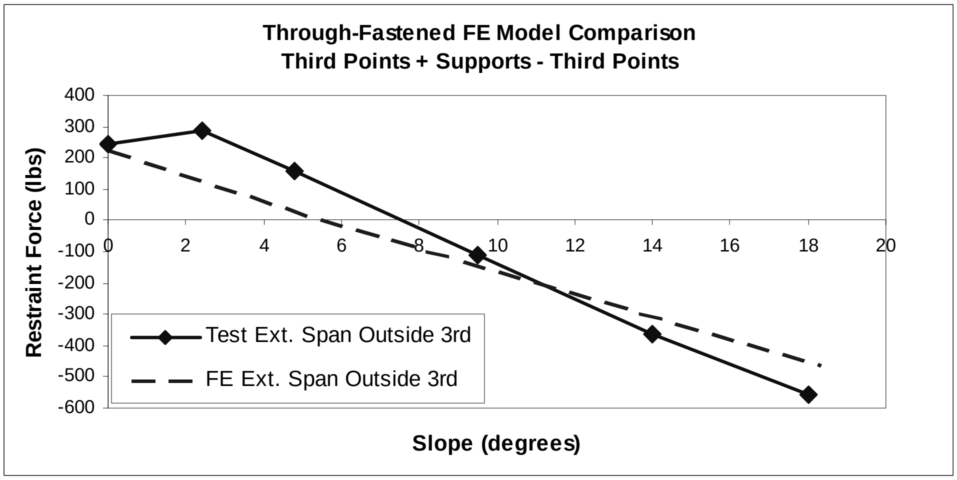

(k) Third Points + Supports – Exterior Span Outside Third Point

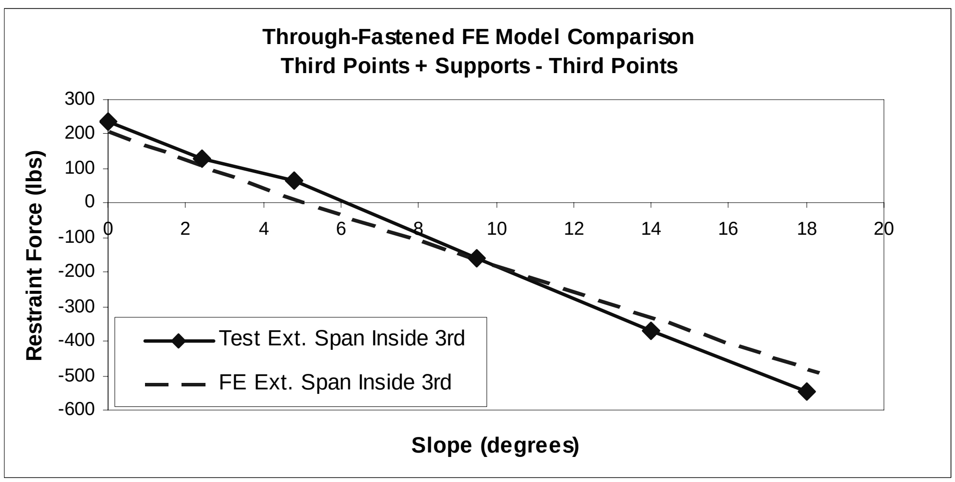

(m) Third Points + Supports – Exterior Span Inside Third Point

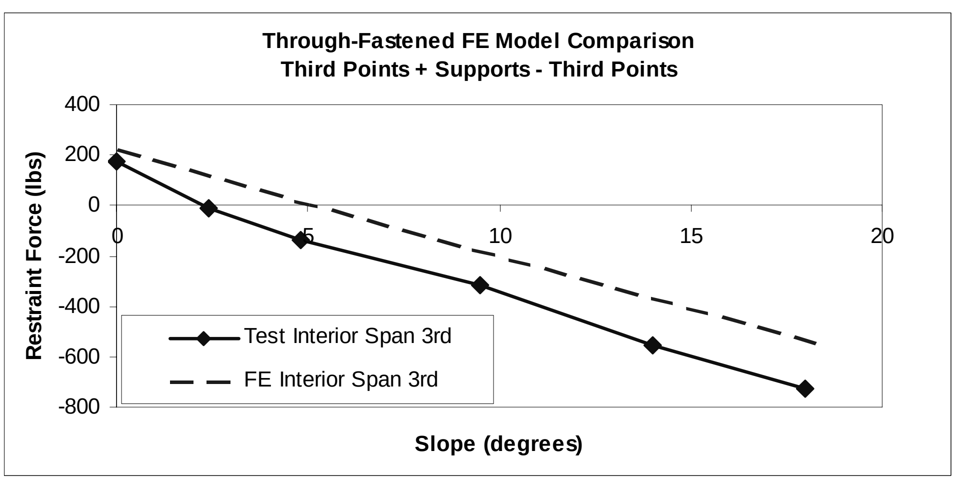

(n) Third Points + Supports – Interior Span Third Point

FigureII.17 Comparison of Finite Element Model with Three-Span Standing Seam Tests,Cont

II.7.5 Summary of Comparison between Test and Finite Element Models

Overall correlation between the finite element models and laboratory tests is good. Best correlation is realized for the single span, through fastened tests. Correlation is good for the single span standing seam cases, although some deviation from the test data is seen due to the inherent variability of standing seam systems. Correlation with the 3-span through fastened tests is good, although it is believed that some deviation from the tests is due to test errors resulting primarily from the sheer size of the test specimen relative to the forces being measured. Similar scale issues cause the deviation of the 3-span standing seam models from the tests results but are compounded by the flexibility of the standing seam system.

Throughout the different test series, the best correlation is realized for the supports restraint case and it has historically been the simplest case to predict. Midpoints and third points cases typically give good correlation although some deviation is due to variables introduced because (1) restraint anchorage is provided by a flexible beam and (2) unlike the support restraint case, the bottom flange is free to rotate and translate at the restraint location, adding flexibility. The quarter points and third points plus supports are the most complex cases and consequently provide the greatest challenges to predict. Previous attempts to model these restraint cases have proven difficult. In addition to the variables inherent in the third points and midpoints cases, the distribution of forces in quarter point and third point plus supports cases are extremely sensitive to diaphragm stiffness and the initial pretensions placed on the restraining rods in the laboratory tests.

As the size of the system evaluated grows and as the bracing configurations become more complex, that is, more braces per span are added, some deviation between the test results and the finite element models is observed. It is believed that much of this deviation is due primarily to the inherent variability of the tests. Taking these variations into account, the finite element models provide a satisfactory means of representing the laboratory tests. Furthermore, the models take into account many parameters that have not been previously considered – rotational restraint provided by the bending stiffness of the sheathing, height of restraint along purlin web, and translational stiffness of the connection between the purlin and sheathing.

Table II.2 Purlin Average Properties Used for Prediction of Restraint Forces

Test	Purlins	Average Properties							
		d	B	T	A_g	I_X	I_Y	I_{XY}	θ
		(in)	(in)	(in)	(in^2)	(in^4)	(in^4)	(in^4)	(deg)
Series 1 Series 4	Purlin 1-3 (Eave) to Purlin 1-4 (Ridge)	10.07	2.60	0.096	1.60	23.04	2.56	5.46	14.0
Series 2 Series 5	Purlin 1-1 (Eave) to Purlin 1-4 (Ridge)	10.07	2.60	0.096	1.60	23.11	2.57	5.48	14.0
Series 3 Series 6	Purlin 1-1 (Eave) to Purlin 1-6 (Ridge)	10.07	2.60	0.097	1.61	23.23	2.57	5.49	14.0
Series 7 Series 8	South Span Purlin 1-1 (Eave) to Purlin 1-4 (Ridge)	10.07	2.60	0.097	1.61	23.23	2.57	5.49	14.0
	Middle Span Purlin 2-1 (Eave) to Purlin 2-6 (Ridge)	10.07	2.60	0.097	1.61	23.23	2.62	5.56	14.2
	North Span Purlin 3-1 (Eave) to Purlin 3-6 (Ridge)	10.07	2.61	0.097	1.63	23.33	2.63	5.58	14.2

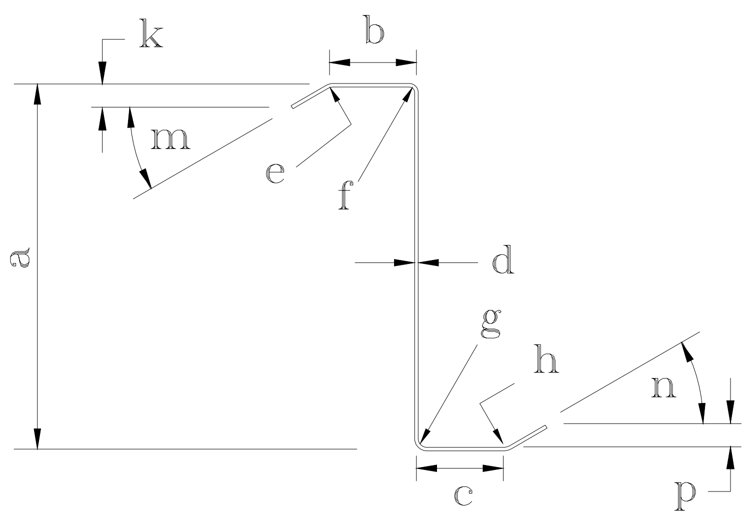

Figure II.18 Purlin Measured Properties

Table II.3 Measured and Calculated Properties of Test Purlins

Purlin Designation	Purlin Measured Properties												Derived Properties				
	A	b	C	d	E	f	g	h	k	m	n	P	A	I_X	I_Y	I_{XY}	Θ_P
	(in)	(in)	(in)	(in)	(in)	(in)	(in)	(in)	(in)	(deg)	(deg)	(in)	(in^2)	(in^4)	(in^4)	(in^4)	deg
Purlin 1-1	10.069	2.600	2.589	0.097	0.90	21/64	5/16	0.90	0.970	50.5	50.7	0.760	1.61	23.30	2.70	5.64	14.4
Purlin 1-2	10.075	2.600	2.500	0.097	0.95	21/64	21/64	0.90	0.844	50.7	50.0	0.745	1.60	23.07	2.70	5.35	13.7
Purlin 1-3	10.065	2.607	2.560	0.096	0.80	23/64	5/16	0.90	0.890	49.7	50.0	0.735	1.60	23.06	2.58	5.49	14.1
Purlin 1-4	10.070	2.589	2.509	0.096	0.89	21/64	5/16	0.90	0.890	48.9	50.2	0.750	1.60	23.01	2.54	5.43	14.0
Purlin 1-5	10.080	2.617	2.520	0.097	0.80	21/64	5/16	0.90	0.898	50.8	50.7	0.750	1.61	23.30	2.56	5.49	13.9
Purlin 1-6	10.075	2.610	2.530	0.099	0.80	21/64	5/16	0.90	0.869	51.0	49.8	0.720	1.64	23.14	2.55	5.51	13.8
Purlin 2-1	10.060	2.612	2.512	0.095	0.84	21/64	21/64	0.95	0.891	50.9	48.0	0.780	1.58	22.84	2.57	5.46	14.2
Purlin 2-2	10.070	2.583	2.513	0.097	0.95	3/8	5/16	0.95	0.812	50.6	47.5	0.813	1.61	23.18	2.55	5.47	14.0
Purlin 2-3	10.070	2.605	2.468	0.097	0.95	23/64	21/64	0.95	0.860	49.0	49.0	0.845	1.62	23.30	2.63	5.57	14.2
Purlin 2-4	10.045	2.571	2.480	0.097	0.84	21/64	5/16	0.95	0.882	50.0	48.0	0.818	1.61	23.17	2.60	5.52	14.1
Purlin 2-5	10.080	2.635	2.523	0.097	0.84	21/64	5/16	0.95	0.865	50.0	47.5	0.824	1.63	23.62	2.72	5.72	14.3
Purlin 2-6	10.040	2.607	2.550	0.097	0.84	21/64	5/16	0.84	0.905	50.5	48.5	0.760	1.62	23.28	2.65	5.60	14.2
Purlin 3-1	10.085	2.609	2.502	0.097	0.84	11/32	5/16	0.84	0.890	50.0	48.0	0.835	1.63	23.59	2.71	5.69	14.3
Purlin 3-2	10.075	2.600	2.541	0.097	0.84	21/64	5/16	0.84	0.895	50.0	50.0	0.912	1.64	23.71	2.80	5.81	14.5
Purlin 3-3	10.067	2.600	2.50	0.097	0.84	21/64	5/16	0.84	0.89	48.5	48.0	0.828	1.63	23.53	2.72	5.70	14.4
Purlin 3-4	10.079	2.600	2.528	0.097	0.84	21/64	5/16	0.84	0.903	50.0	50.0	0.805	1.62	23.48	2.66	5.62	14.2
Purlin 3-5	10.070	2.640	2.552	0.097	0.84	23/64	5/16	0.84	0.895	50.0	47.0	0.792	1.63	23.65	2.78	5.79	14.5
Purlin 3-6	10.060	2.580	2.515	0.097	0.83	11/32	19/64	0.84	0.898	51	49.0	0.792	1.62	23.26	2.59	5.52	14.1

Test Summary

Test Series 1
Bracing Configuration: Supports
Number of Purlins: 2
Deck Type: Through Fastened

Test Date: 8/29/03
Total Weight: 3400 lbs
Purlin Designation: 10Z0.097
Span Length: 20 ft

Test Series 1 - 10Z-0.097 - 2 - TF				
Support Restraints				
Slope (deg)	South Support	North Support	Support Average	Finite Element
0.0	177	157	167	186
2.4	82	80	81	100
4.8	10	17	14	14
9.5	-158	-145	-152	-155
14.0	-326	-293	-310	-319
18.4	-463	-440	-452	-475
0.0	171	160	166	

Restraint Pretension			
	Eave Pretension	Zero Angle	Ridge Pretension
South Support	24.5	5.1	22
North Support	21.7	5.1	20

Test Summary

Test Series 1
Bracing Configuration: 3rd Point
Number of Purlins: 2
Deck Type: Through Fastened

Test Date: 9/1/03
Total Weight: 3400 lbs
Purlin Designation: 10Z0.097
Span Length: 20 ft

Test Series 1 - 10Z-0.097 - 2 - TF				
3rd Point Restraints				
Slope (deg)	South 3rd Point	North 3rd Point	3rd Point Average	Finite Element
0.0	130	125	128	153
2.4	55	55	55	88
4.8	-45	13	-16	23
9.5	-178	-100	-139	-104
14.0	-332	-213	-273	-227
18.4	-467	-298	-383	-345
0.0	138	125	132	

Restraint Pretension			
	Eave Pretension	Zero Angle	Ridge Pretension
South 3rd Point	20	4	22
North 3rd Point	20	5.3	22

Test Summary

Test Series 1
Bracing Configuration: Mid Point
Number of Purlins: 2
Deck Type: Through Fastened

Test Date: 9/02/03
Total Weight: 3400 lbs
Purlin Designation: 10Z0.097
Span Length: 20 ft

Test Series 1 - 10Z-0.097 - 2 - TF		
Midpoint Restraints		
Slope (deg)	Midpoint	Finite Element
0.0	218	275
2.4	85	159
4.8	-43	44
9.5	-270	-184
14.0	-503	-404
18.4	-720	-614
0.0	205	

Restraint Pretension			
	Eave Pretension	Zero Angle	Ridge Pretension
Midpoint	23.3	4.2	23

Test Summary

Test Series 1
Bracing Configuration: Quarter Point
Number of Purlins: 2
Deck Type: Through Fastened

Test Date: 9/02/03
Total Weight: 3400 lbs
Purlin Designation: 10Z0.097
Span Length: 20 ft

Test Series 1 - 10Z-0.097 - 2 - TF				
Quarter Point Restraints - Exterior				
Slope (deg)	South Qtr Point	North Qtr Point	Qtr Point Average	Finite Element
0.0	80	58	69	135
2.4	50	18	34	80
4.8	13	-35	-11	25
9.5	-88	-113	-101	-83
14.0	-194	-230	-212	-188
18.4	-303	-325	-314	-287
0.0	118	38	78	

Restraint Pretension			
	Eave Pretension	Zero Angle	Ridge Pretension
South Qtr Point	16.6	5.1	21
North Qtr Point	16.7	3.4	20

Test Summary

Test Series 1
Bracing Configuration: Quarter Point
Number of Purlins: 2
Deck Type: Through Fastened

Test Date: 9/02/03
Total Weight: 3400 lbs
Purlin Designation: 10Z0.097
Span Length: 20 ft

Test Series 1 - 10Z-0.097 - 2 - TF		
Qtr Point Restraints - Interior		
Slope (deg)	Interior Qtr Point	Finite Element
0.0	128	49.0
2.4	63	20.0
4.8	15	-8.0
9.5	-78	-63.0
14.0	-132	-117.0
18.4	-185	-168.0
0.0	108	

Restraint Pretension			
	Eave Pretension	Zero Angle	Ridge Pretension
Interior Qtr Point	20	5.1	22

Test Summary

Test Series 1
Bracing Configuration: 3rd Point + Support
Number of Purlins: 2
Deck Type: Through Fastened

Test Date: 9/01/03
Total Weight: 3400 lbs
Purlin Designation: 10Z0.097
Span Length: 20 ft

Test Series 1 - 10Z-0.097 - 2 - TF				
3rd Point + Support Restraints				
Slope (deg)	South Support	North Support	Support Average	Finite Element
0.0	136	113	125	130
2.4	78	73	76	82
4.8	40	50	45	34
9.5	-41	-35	-38	-61
14.0	-126	-100	-113	-153
18.4	-228	-177	-203	-241
0.0	134	117	126	

Restraint Pretension			
	Eave Pretension	Zero Angle	Ridge Pretension
South Support	18.5	8	19
North Support	23	8	23

Test Summary

Test Series 1
Bracing Configuration: 3rd Point + Support
Number of Purlins: 2
Deck Type: Through Fastened

Test Date: 9/01/03
Total Weight: 3400 lbs
Purlin Designation: 10Z0.097
Span Length: 20 ft

Test Series 1 - 10Z-0.097 - 2 - TF				
3rd Point + Support Restraints				
Slope (deg)	South 3rd Point	North 3rd Point	3rd Point Average	Finite Element
0.0	60	60	60	38
2.4	23	14	19	2
4.8	-37	-37	-37	-34
9.5	-125	-124	-125	-105
14.0	-198	-188	-193	-174
18.4	-267	-243	-255	-239
0.0	48	72	60	

Restraint Pretension			
	Eave Pretension	Zero Angle	Ridge Pretension
South 3rd Point	20	3.3	22
North 3rd Point	24	3.5	23

Test Summary

Test Series 2
Bracing Configuration: Supports (without Backing Plate)
Number of Purlins: 4
Deck Type: Through Fastened

Test Date: 8/22/03
Total Weight: 7150 lbs
Purlin Designation: 10Z0.097
Span Length: 20 ft

Test Series 2 - 10Z-0.097 - 4 - TF				
Support Restraints Without Backing Plate				
Slope (deg)	South Support	North Support	Support Average	Finite Element
0.0	395	292	344	344
2.4	211	150	181	187
4.8	36	22	29	31
9.5	-277	-260	-269	-278
14.0	-555	-540	-548	-577
18.4	-880	-778	-829	-861
0.0	390	255	323	

Restraint Pretension			
	Eave Pretension	Zero Angle	Ridge Pretension
South Support	24	5.3	23
North Support	27	5.3	25

Test Summary

Test Series 2
Bracing Configuration: Supports (with Backing Plate)
Number of Purlins: 4
Deck Type: Through Fastened

Test Date: 8/25/03
Total Weight: 7150 lbs
Purlin Designation: 10Z0.097
Span Length: 20 ft

Test Series 2 - 10Z-0.097 - 4 - TF				
Support Restraints with Backing Plate				
Slope (deg)	South Support	North Support	Support Average	Finite Element
0.0	379	375	377	N/A
2.4	213	198	206	N/A
4.8	33	42	38	N/A
9.5	-309	-280	-295	N/A
14.0	-662	-605	-634	N/A
18.4	-990	-886	-938	N/A
0.0	380	348	364	

Test Summary

Test Series 2 | Test Date: 8/26/03
Bracing Configuration: 3rd Point | Total Weight: 7150 lbs
Number of Purlins: 4 | Purlin Designation: 10Z0.097
Deck Type: Through Fastened | Span Length: 20 ft

Test Series 2 - 10Z-0.097 - 4 - TF				
3rd Point Restraints				
Slope (deg)	South 3rd Point	North 3rd Point	3rd Point Average	Finite Element
0.0	275	253	264	264
2.4	110	140	125	150
4.8	0	0	0	36
9.5	-293	-202	-248	-189
14.0	-550	-413	-482	-406
18.4	-822	-616	-719	-613
0.0	262	255	259	

Restraint Pretension			
	Eave Pretension	Zero Angle	Ridge Pretension
South 3rd Point	20	4.8	23
North 3rd Point	23	4.8	20

Test Summary

Test Series 2
Bracing Configuration: Mid Point (without Backing Plate)
Number of Purlins: 4
Deck Type: Through Fastened

Test Date: 8/27/03
Total Weight: 7150 lbs
Purlin Designation: 10Z0.097
Span Length: 20 ft

Test Series 2 - 10Z-0.097 - 4 - TF		
Midpoint Restraints without Backing Plate		
Slope (deg)	Midpoint	Finite Element
0.0	445	446
2.4	207	254
4.8	0	63
9.5	-395	-316
14.0	-802	-682
18.4	-1215	-1031
0.0	420	

Restraint Pretension			
	Eave Pretension	Zero Angle	Ridge Pretension
Midpoint	27	4.8	23

Test Summary

Test Series 2
Bracing Configuration: Mid Point (with Backing Plate)
Number of Purlins: 4
Deck Type: Through Fastened

Test Date: 8/27/03
Total Weight: 7150 lbs
Purlin Designation: 10Z0.097
Span Length: 20 ft

Test Series 2 - 10Z-0.097 - 4 - TF		
Midpoint Restraints with Backing Plate		
Slope (deg)	Midpoint	Finite Element
0.0	441	N/A
2.4	220	N/A
4.8	0	N/A
9.5	-433	N/A
14.0	-888	N/A
18.4	-1308	N/A
0.0	429	

Test Summary

Test Series 2
Bracing Configuration: Quarter Point
Number of Purlins: 4
Deck Type: Through Fastened

Test Date: 8/27/03
Total Weight: 7150 lbs
Purlin Designation: 10Z0.097
Span Length: 20 ft

Test Series 2 - 10Z-0.097 - 4 - TF				
Quarter Point Restraints - Exterior				
Slope (deg)	South Qtr Point	North Qtr Point	Qtr Point Average	Finite Element
0.0	224	208	216	236
2.4	97	130	114	137
4.8	-26	35	5	38
9.5	-231	-150	-191	-158
14.0	-451	-333	-392	-347
18.4	-680	-517	-599	-527
0.0	215	202	209	

Restraint Pretension			
	Eave Pretension	Zero Angle	Ridge Pretension
South Qtr Point	18.5	4.5	17
North Qtr Point	20	5.5	20

Test Summary

Test Series 2
Bracing Configuration: Quarter Point
Number of Purlins: 4
Deck Type: Through Fastened

Test Date: 8/27/03
Total Weight: 7150 lbs
Purlin Designation: 10Z0.097
Span Length: 20 ft

Test Series 2 - 10Z-0.097 - 4 - TF		
Qtr Point Restraints - Interior		
Slope (deg)	Interior Qtr Point	Finite Element
0.0	162	99
2.4	85	47
4.8	20	-5
9.5	-125	-108
14.0	-237	-207
18.4	-342	-302
0.0	160	

Restraint Pretension			
	Eave Pretension	Zero Angle	Ridge Pretension
Interior Qtr Point	22	5.3	22

Test Summary

Test Series 2
Bracing Configuration: 3rd Point + Support
Number of Purlins: 4
Deck Type: Through Fastened

Test Date: 8/25/03
Total Weight: 7150 lbs
Purlin Designation: 10Z0.097
Span Length: 20 ft

Test Series 2 - 10Z-0.097 - 4 - TF				
3rd Point + Support Restraints				
Slope (deg)	South Support	North Support	Support Average	Finite Element
0.0	314	192	253	241
2.4	217	117	167	146
4.8	123	52	88	52
9.5	-83	-135	-109	-135
14.0	-265	-308	-287	-315
18.4	-452	-478	-465	-487
0.0	320	193	257	

Restraint Pretension			
	Eave Pretension	Zero Angle	Ridge Pretension
South Support	23.5	7.5	23
North Support	23	6.1	18

Test Summary

Test Series 2
Bracing Configuration: 3rd Point + Support
Number of Purlins: 4
Deck Type: Through Fastened

Test Date: 8/25/03
Total Weight: 7150 lbs
Purlin Designation: 10Z0.097
Span Length: 20 ft

Test Series 2 - 10Z-0.097 - 4 - TF				
3rd Point + Support Restraints				
Slope (deg)	South 3rd Point	North 3rd Point	3rd Point Average	Finite Element
0.0	127	100	114	105
2.4	65	45	55	37
4.8	-18	-42	-30	-30
9.5	-123	-187	-155	-164
14.0	-255	-327	-291	-292
18.4	-372	-452	-412	-414
0.0	116	82	99	

Restraint Pretension			
	Eave Pretension	Zero Angle	Ridge Pretension
South 3rd Point	25	4.6	20
North 3rd Point	20	3.9	20

Test Summary

Test Series 3 | Test Date: 8/30/02
Bracing Configuration: Supports | Total Weight: 10460 lbs
Number of Purlins: 6 | Purlin Designation: 10Z0.097
Deck Type: Through Fastened | Span Length: 20 ft

Test Series 3 - 10Z-0.097 - 6 - TF				
Support Restraints				
Slope (deg)	South Support	North Support	Support Average	Finite Element
0.0	429	440	435	509
2.4	215	152	184	277
4.8	-59	-60	-60	46
9.5	-498	-400	-449	-412
14.0	-971	-811	-891	-855
18.4	-1387	-1035	-1211	-1275
0.0	478	353	416	

Test Summary

Test Series 3 | Test Date: 9/04/02
Bracing Configuration: 3rd Point | Total Weight: 10460 lbs
Number of Purlins: 6 | Purlin Designation: 10Z0.097
Deck Type: Through Fastened | Span Length: 20 ft

Test Series 3 - 10Z-0.097 - 6 - TF				
3rd Point Restraints				
Slope (deg)	South 3rd Point	North 3rd Point	3rd Point Average	Finite Element
0.0	343	422	383	359
2.4	202	216	209	205
4.8	23	52	38	51
9.5	-303	-313	-308	-253
14.0	-640	-580	-610	-547
18.4	-1080	-733	-907	-826
0.0	258	440	349	

Test Summary

Test Series 3
Bracing Configuration: Mid Point
Number of Purlins: 6
Deck Type: Through Fastened

Test Date: 9/13/02
Total Weight: 10460 lbs
Purlin Designation: 10Z0.097
Span Length: 20 ft

Test Series 3 - 10Z-0.097 - 6 - TF		
Midpoint Restraints		
Slope (deg)	Midpoint	Finite Element
0.0	604	610.0
2.4	289	350.0
4.8	-61.3	90.0
9.5	-595	-424.0
14.0	-1121	-922.0
18.4	-1632	-1395.0
0.0	528	

Test Summary

Test Series 3
Bracing Configuration: Quarter Point
Number of Purlins: 6
Deck Type: Through Fastened

Test Date: 9/16/02
Total Weight: 10460 lbs
Purlin Designation: 10Z0.097
Span Length: 20 ft

Test Series 3 - 10Z-0.097 - 6 - TF				
Quarter Point Restraints - Exterior				
Slope (deg)	South Qtr Point	North Qtr Point	Qtr Point Average	Finite Element
0.0	306	357	332	386
2.4	96	230	163	228
4.8	-123	163	20	71
9.5	-464	-239	-352	-239
14.0	-837	-502	-670	-539
18.4	-1207	-707	-957	-825
0.0	297	506	402	

Test Summary

Test Series 3
Bracing Configuration: Quarter Point
Number of Purlins: 6
Deck Type: Through Fastened

Test Date: 9/16/02
Total Weight: 10460 lbs
Purlin Designation: 10Z0.097
Span Length: 20 ft

Test Series 3 - 10Z-0.097 - 6 - TF		
Qtr Point Restraints - Interior		
Slope (deg)	Interior Qtr Point	Finite Element
0.0	161	20
2.4	85	-12
4.8	33	-44
9.5	-100	-106
14.0	-148	-166
18.4	-202	-223
0.0	177	

Test Summary

Test Series 3
Bracing Configuration: 3rd Point + Support
Number of Purlins: 6
Deck Type: Through Fastened

Test Date: 9/24/02
Total Weight: 10460 lbs
Purlin Designation: 10Z0.097
Span Length: 20 ft

Test Series 3 - 10Z-0.097 - 6 - TF				
3rd Point + Support Restraints				
Slope (deg)	South Support	North Support	Support Average	Finite Element
0.0	356	355	356	338
2.4	193	136	165	197
4.8	43	51	47	55
9.5	-324	-230	-277	-260
14.0	-715	-558	-637	-570
18.4	-1102	-872	-987	-867
0.0	419	336	378	

Restraint Pretension			
	Eave Pretension	Zero Angle	Ridge Pretension
South Support	40	3.7	60.3
North Support	47.2	7.5	50.6

Test Summary

Test Series 3
Bracing Configuration: 3rd Point + Support
Number of Purlins: 6
Deck Type: Through Fastened

Test Date: 9/24/02
Total Weight: 10460 lbs
Purlin Designation: 10Z0.097
Span Length: 20 ft

Test Series 3 - 10Z-0.097 - 6 - TF				
3rd Point + Support Restraints				
Slope (deg)	South 3rd Point	North 3rd Point	3rd Point Average	Finite Element
0.0	99	184	142	181
2.4	49	100	75	73
4.8	-75	10	-33	-25
9.5	-211	-141	-176	-178
14.0	-346	-238	-292	-324
18.4	-456	-309	-383	-464
0.0	118	147	133	

Restraint Pretension			
	Eave Pretension	Zero Angle	Ridge Pretension
South 3rd Point	49	3.7	25.8
North 3rd Point	44.7	7	50

Test Summary

Test Series 4
Bracing Configuration: Supports
Number of Purlins: 2
Deck Type: Standing Seam

Test Date: 8/18/03
Total Weight: 3400 lbs
Purlin Designation: 10Z0.097
Span Length: 20 ft

Test Series 4 - 10Z-0.097 - 2 - SS				
Support Restraints				
Slope (deg)	South Support	North Support	Support Average	Finite Element
0.0	137	118	128	164
2.4	38	45	42	85
4.8	-42	-33	-38	5
9.5	-153	-132	-143	-150
14.0	-268	-252	-260	-299
18.4	-385	-311	-348	-441
0.0	140	108	124	

Restraint Pretension			
	Eave Pretension	Zero Angle	Ridge Pretension
South Support	30	3.7	19
North Support	30	4	23

Test Summary

Test Series 4
Bracing Configuration: 3rd Point
Number of Purlins: 2
Deck Type: Standing Seam

Test Date: 8/18/03
Total Weight: 3400 lbs
Purlin Designation: 10Z0.097
Span Length: 20 ft

Test Series 4 - 10Z-0.097 - 2 - SS				
3rd Point Restraints				
Slope (deg)	South 3rd Point	North 3rd Point	3rd Point Average	Finite Element
0.0	122	92	107	154
2.4	42	67	55	91
4.8	-23	-28	-26	28
9.5	-97	-132	-115	-89
14.0	-223	-230	-227	-198
18.4	-338	-328	-333	-303
0.0	128	115	122	

Restraint Pretension			
	Eave Pretension	Zero Angle	Ridge Pretension
South 3rd Point	28	4.4	19.5
North 3rd Point	27	4.4	27

Test Summary

Test Series 4
Bracing Configuration: Mid Point
Number of Purlins: 2
Deck Type: Standing Seam

Test Date: 8/19/03
Total Weight: 3400 lbs
Purlin Designation: 10Z0.097
Span Length: 20 ft

Test Series 4 - 10Z-0.097 - 2 - SS		
Midpoint Restraints		
Slope (deg)	Midpoint	Finite Element
0.0	200	271
2.4	103	160
4.8	0	49
9.5	-177	-151
14.0	-360	-337
18.4	-537	-516
0.0	210	

Restraint Pretension			
	Eave Pretension	Zero Angle	Ridge Pretension
Midpoint	35	4.8	25

Test Summary

Test Series 4
Bracing Configuration: Quarter Point
Number of Purlins: 2
Deck Type: Standing Seam

Test Date: 8/19/03
Total Weight: 3400 lbs
Purlin Designation: 10Z0.097
Span Length: 20 ft

Test Series 4 - 10Z-0.097 - 2 - SS				
Quarter Point Restraints - Exterior				
Slope (deg)	South Qtr Point	North Qtr Point	Qtr Point Average	Finite Element
0.0	77	78	78	112
2.4	24	45	35	66
4.8	-32	0	-16	20
9.5	-103	-73	-88	-70
14.0	-210	-160	-185	-156
18.4	-320	-235	-278	-238
0.0	80	63	72	

Restraint Pretension			
	Eave Pretension	Zero Angle	Ridge Pretension
South Qtr Point	27.4	3.3	16.2
North Qtr Point	28.3	4.8	23

Test Summary

Test Series 4
Bracing Configuration: Quarter Point
Number of Purlins: 2
Deck Type: Standing Seam

Test Date: 8/19/03
Total Weight: 3400 lbs
Purlin Designation: 10Z0.097
Span Length: 20 ft

Test Series 4 - 10Z-0.097 - 2 - SS		
Qtr Point Restraints - Interior		
Slope (deg)	Interior Qtr Point	Finite Element
0.0	120	99
2.4	83	62
4.8	38	25
9.5	-63	-56
14.0	-112	-121
18.4	-162	-182
0.0	122	

Restraint Pretension			
	Eave Pretension	Zero Angle	Ridge Pretension
Interior Qtr Point	28.3	5.3	28

Test Summary

Test Series 4
Bracing Configuration: 3rd Point + Support
Number of Purlins: 2
Deck Type: Standing Seam

Test Date: 8/18/03
Total Weight: 3400 lbs
Purlin Designation: 10Z0.097
Span Length: 20 ft

Test Series 4 - 10Z-0.097 - 2 - SS				
3rd Point + Support Restraints				
Slope (deg)	South Support	North Support	Support Average	Finite Element
0.0	77	55	66	56
2.4	18.2	28	23	17
4.8	-52	-40	-46	-21
9.5	-123	-82	-103	-100
14.0	-192	-142	-167	-175
18.4	-257	-197	-227	-246
0.0	63	55	59	

Restraint Pretension			
	Eave Pretension	Zero Angle	Ridge Pretension
South Support	22	3	21
North Support	28	3.5	27

Test Summary

Test Series 4
Bracing Configuration: 3rd Point + Support
Number of Purlins: 2
Deck Type: Standing Seam

Test Date: 8/18/03
Total Weight: 3400 lbs
Purlin Designation: 10Z0.097
Span Length: 20 ft

Test Series 4 - 10Z-0.097 - 2 - SS				
3rd Point + Support Restraints				
Slope (deg)	South 3rd Point	North 3rd Point	3rd Point Average	Finite Element
0.0	83	101	92	85
2.4	62	60	61	48
4.8	10	14	12	11
9.5	-55	-68	-62	-63
14.0	-115	-134	-125	-133
18.4	-207	-210	-209	-199
0.0	58	130	94	

Restraint Pretension			
	Eave Pretension	Zero Angle	Ridge Pretension
South 3rd Point	32	6.1	22
North 3rd Point	21	5.3	29

Test Summary

Test Series 5
Bracing Configuration: Supports
Number of Purlins: 4
Deck Type: Standing Seam

Test Date: 8/12/03
Total Weight: 7150 lbs
Purlin Designation: 10Z0.097
Span Length: 20 ft

Test Series 5 - 10Z-0.097 - 4 - SS				
Support Restraints				
Slope (deg)	South Support	North Support	Support Average	Finite Element
0.0	199	248	224	286
2.4	123	117	120	150
4.8	47	13	30	13
9.5	-155	-128	-142	-202
14.0	-338	-256	-297	-406
18.4	-491	-360	-426	-601
0.0	212	235	224	

Restraint Pretension			
	Eave Pretension	Zero Angle	Ridge Pretension
South Support	24.5	5.8	45
North Support	23.3	4.8	41

Test Summary

Test Series 5
Bracing Configuration: 3rd Point
Number of Purlins: 4
Deck Type: Standing Seam

Test Date: 8/12/03
Total Weight: 7150 lbs
Purlin Designation: 10Z0.097
Span Length: 20 ft

Test Series 5 - 10Z-0.097 - 4 - SS				
3rd Point Restraints				
Slope (deg)	South 3rd Point	North 3rd Point	3rd Point Average	Finite Element
0.0	179	217	198	285
2.4	109	93	101	170
4.8	50	-52	-1	55
9.5	-140	-165	-153	-153
14.0	-345	-291	-318	-347
18.4	-547	-408	-478	-533
0.0	172	197	185	

Restraint Pretension			
	Eave Pretension	Zero Angle	Ridge Pretension
South 3rd Point	20	5.9	51
North 3rd Point	22	4.5	49

Test Summary

Test Series 5
Bracing Configuration: Mid Point
Number of Purlins: 4
Deck Type: Standing Seam

Test Date: 8/13/03
Total Weight: 7150 lbs
Purlin Designation: 10Z0.097
Span Length: 20 ft

Test Series 5 - 10Z-0.097 - 4 - SS		
Midpoint Restraints		
Slope (deg)	Midpoint	Finite Element
0.0	420	468
2.4	230	279
4.8	32	91
9.5	-285	-247
14.0	-642	-560
18.4	-980	-860
0.0	397	

Restraint Pretension			
	Eave Pretension	Zero Angle	Ridge Pretension
Midpoint	20	5	43

Test Summary

Test Series 5
Bracing Configuration: Quarter Point
Number of Purlins: 4
Deck Type: Standing Seam

Test Date: 8/13/03
Total Weight: 7150 lbs
Purlin Designation: 10Z0.097
Span Length: 20 ft

Test Series 5 - 10Z-0.097 - 4 - SS				
Quarter Point Restraints - Exterior				
Slope (deg)	South Qtr Point	North Qtr Point	Qtr Point Average	Finite Element
0.0	115	145	130	211
2.4	70	65	68	125
4.8	23	-43	-10	39
9.5	-95	-126	-111	-123
14.0	-264	-230	-247	-277
18.4	-441	-331	-386	-424
0.0	103	132	118	

Restraint Pretension			
	Eave Pretension	Zero Angle	Ridge Pretension
South Qtr Point	16	5.1	42
North Qtr Point	18	4.2	36

Test Summary

Test Series 5
Bracing Configuration: Quarter Point
Number of Purlins: 4
Deck Type: Standing Seam

Test Date: 8/13/03
Total Weight: 7150 lbs
Purlin Designation: 10Z0.097
Span Length: 20 ft

Test Series 5 - 10Z-0.097 - 4 - SS		
Qtr Point Restraints - Interior		
Slope (deg)	Interior Qtr Point	Finite Element
0.0	128	197
2.4	84	127
4.8	42	58
9.5	-97	-99
14.0	-195	-219
18.4	-293	-334
0.0	140	

Restraint Pretension			
	Eave Pretension	Zero Angle	Ridge Pretension
Interior Qtr Point	17	6.3	50

Test Summary

Test Series 5
Bracing Configuration: 3rd Point + Support
Number of Purlins: 4
Deck Type: Standing Seam

Test Date: 8/12/03
Total Weight: 7150 lbs
Purlin Designation: 10Z0.097
Span Length: 20 ft

Test Series 5 - 10Z-0.097 - 4 - SS				
3rd Point + Support Restraints				
Slope (deg)	South Support	North Support	Support Average	Finite element
0.0	114	110	112	129
2.4	82	43	63	52
4.8	38	-40	-1	-25
9.5	-106	-83	-95	-157
14.0	-219	-188	-204	-286
18.4	-326	-335	-331	-409
0.0	142	92	117	

Restraint Pretension			
	Eave Pretension	Zero Angle	Ridge Pretension
South Support	19.2	5.6	48
North Support	23.3	5.6	36

Test Summary

Test Series 5
Bracing Configuration: 3rd Point + Support
Number of Purlins: 4
Deck Type: Standing Seam

Test Date: 8/12/03
Total Weight: 7150 lbs
Purlin Designation: 10Z0.097
Span Length: 20 ft

Test Series 5 - 10Z-0.097 - 4 - SS				
3rd Point + Support Restraints				
Slope (deg)	South 3rd Point	North 3rd Point	3rd Point Average	Finite Element
0.0	103	220	162	179
2.4	65	121	93	111
4.8	24	50	37	43
9.5	-125	-85	-105	-98
14.0	-277	-149	-213	-221
18.4	-428	-209	-319	-339
0.0	100	175	138	

Restraint Pretension			
	Eave Pretension	Zero Angle	Ridge Pretension
South 3rd Point	18	5.6	48
North 3rd Point	31.2	5.6	53

Test Summary

Test Series 6
Bracing Configuration: Supports
Number of Purlins: 6
Deck Type: Standing Seam

Test Date: 7/11/03
Total Weight: 10460 lbs
Purlin Designation: 10Z0.097
Span Length: 20 ft

Test Series 6 - 10Z-0.097 - 6 - SS				
Support Restraints				
Slope (deg)	South Support	North Support	Support Average	Finite Element
0.0	258	223	241	343
2.4	117	120	119	181
4.8	21	28	25	19
9.5	-265	-305	-285	-252
14.0	-455	-552	-504	-510
18.4	-606	-747	-677	-698
0.0	183	227	205	

Restraint Pretension			
	Eave Pretension	Zero Angle	Ridge Pretension
South Support	28	5	21
North Support	30	5	15

Test Summary

Test Series 6
Bracing Configuration: 3rd Point
Number of Purlins: 6
Deck Type: Standing Seam

Test Date: 7/15/03
Total Weight: 10460 lbs
Purlin Designation: 10Z0.097
Span Length: 20 ft

Test Series 6 - 10Z-0.097 - 6 - SS				
3rd Point Restraints				
Slope (deg)	South 3rd Point	North 3rd Point	3rd Point Average	Finite Element
0.0	173	327	250	357
2.4	100	126	113	211
4.8	0	-43	-22	66
9.5	-282	-305	-294	-189
14.0	-567	-538	-553	-424
18.4	-812	-745	-779	-649
0.0	202	250	226	

Restraint Pretension			
	Eave Pretension	Zero Angle	Ridge Pretension
South 3rd Point	21	4.8	22.8
North 3rd Point	21.7	4.5	25

Test Summary

Test Series 6
Bracing Configuration: Mid Point
Number of Purlins: 6
Deck Type: Standing Seam

Test Date: 7/15/03
Total Weight: 10460 lbs
Purlin Designation: 10Z0.097
Span Length: 20 ft

Test Series 6 - 10Z-0.097 - 6 - SS		
Midpoint Restraints		
Slope (deg)	Midpoint	Finite Element
0.0	356	568
2.4	199	339
4.8	49	111
9.5	-259	-294
14.0	-526	-668
18.4	-788	-1026
0.0	255	

Restraint Pretension			
	Eave Pretension	Zero Angle	Ridge Pretension
Midpoint	21	5.6	22

Test Summary

Test Series 6
Bracing Configuration: Quarter Point
Number of Purlins: 6
Deck Type: Standing Seam

Test Date: 7/21/03
Total Weight: 10460 lbs
Purlin Designation: 10Z0.097
Span Length: 20 ft

Test Series 6 - 10Z-0.097 - 6 - SS				
Quarter Point Restraints - Exterior				
Slope (deg)	South Qtr Point	North Qtr Point	Qtr Point Average	Finite Element
0.0	159	163	161	276
2.4	78	71	75	165
4.8	0	-67	-34	53
9.5	-226	-277	-252	-155
14.0	-485	-497	-491	-351
18.4	-703	-717	-710	-538
0.0	143	138	141	

Restraint Pretension			
	Eave Pretension	Zero Angle	Ridge Pretension
South Qtr Point	18.2	4.8	16
North Qtr Point	20	3.8	22

Test Summary

Test Series 6
Bracing Configuration: Quarter Point
Number of Purlins: 6
Deck Type: Standing Seam

Test Date: 7/21/03
Total Weight: 10460 lbs
Purlin Designation: 10Z0.097
Span Length: 20 ft

Test Series 6 - 10Z-0.097 - 6 - SS		
Qtr Point Restraints - Interior		
Slope (deg)	Interior Qtr Point	Finite Element
0.0	179	263
2.4	115	173
4.8	58	83
9.5	-68	-122
14.0	-154	-276
18.4	-226	-424
0.0	179	

Restraint Pretension			
	Eave Pretension	Zero Angle	Ridge Pretension
Interior Qtr Point	19	6.5	20

Test Summary

Test Series 6
Bracing Configuration: 3rd Point + Support
Number of Purlins: 6
Deck Type: Standing Seam

Test Date: 7/22/03
Total Weight: 10460 lbs
Purlin Designation: 10Z0.097
Span Length: 20 ft

Test Series 6 - 10Z-0.097 - 6 - SS				
3rd Point + Support Restraints				
Slope (deg)	South Support	North Support	Support Average	Finite Element
0.0	120	238	179	187
2.4	47	178	113	88
4.8	-53	110	29	-12
9.5	-250	-58	-154	-183
14.0	-423	-213	-318	-347
18.4	-543	-352	-448	-505
0.0	131	260	196	

Restraint Pretension			
	Eave Pretension	Zero Angle	Ridge Pretension
South Support	19.2	3.9	21
North Support	25	8.4	24.4

Test Summary

Test Series 6
Bracing Configuration: 3rd Point + Support
Number of Purlins: 6
Deck Type: Standing Seam

Test Date: 7/22/03
Total Weight: 10460 lbs
Purlin Designation: 10Z0.097
Span Length: 20 ft

Test Series 6 - 10Z-0.097 - 6 - SS				
3rd Point + Support Restraints				
Slope (deg)	South 3rd Point	North 3rd Point	3rd Point Average	Finite Element
0.0	126	262	194	235
2.4	61	157	109	148
4.8	-19	53	17	62
9.5	-114	-127	-121	-121
14.0	-233	-278	-256	-277
18.4	-372	-440	-406	-426
0.0	127	257	192	

Restraint Pretension			
	Eave Pretension	Zero Angle	Ridge Pretension
South 3rd Point	23	4.5	14
North 3rd Point	26	6.1	16.7

Test Summary

Test Series 7
Bracing Configuration: Supports
Number of Purlins: 6
Deck Type: Through Fastened

Test Date: 11/08/02
Weight: 10460 lbs per span
Purlin Designation: 10Z0.097
Span Length: 3 @ 20 ft

Test Series 7 - 10Z-0.097 - 6 - TF - MS				
Multi-Span Support Restraints - Exterior Supports				
Slope (deg)	Exterior South Support	Exterior North Support	Exterior Support Average	Finite Element
0.0	581	451	516	549
2.4	413	404	408	283
4.8	37	116	77	17
9.5	-552	-195	-374	-507
14.0	-1137	-535	-836	-1014
18.4	-1691	-848	-1270	-1495
0.0	431	447	439	

Restraint Pretension			
	Eave Pretension	Zero Angle	Ridge Pretension
Ext. South Support	37	4.8	39
Ext. North Support	35	7.6	47

Test Summary

Test Series 7
Bracing Configuration: Supports
Number of Purlins: 6
Deck Type: Through Fastened

Test Date: 11/08/02
Weight: 10460 lbs per span
Purlin Designation: 10Z0.097
Span Length: 3 @ 20 ft

Test Series 7 - 10Z-0.097 - 6 - TF - MS				
Multi-Span Support Restraints - Interior				
Slope (deg)	Interior South Support	Interior North Support	Interior Support Average	Finite Element
0.0	628	1029	829	912
2.4	101	351	226	448
4.8	-50	-50	-50	-15
9.5	-749	-858	-804	-930
14.0	-1482	-1798	-1640	-1815
18.4	-2296	-2586	-2441	-2655
0.0	520	971	746	

Restraint Pretension			
	Eave Pretension	Zero Angle	Ridge Pretension
Int. South Support	30	4.8	31
Int. North Support	45	4.8	42

Test Summary

Test Series 7
Bracing Configuration: 3rd Points
Number of Purlins: 6
Deck Type: Through Fastened

Test Date: 11/21/02
Weight: 10460 lbs per span
Purlin Designation: 10Z0.097
Span Length: 3 @ 20 ft

Test Series 7 - 10Z-0.097 - 6 - TF - MS				
Multi-Span 3rd Point Restraints - Exterior Span Outside 3rd Points				
Slope (deg)	Outside South 3rd Point	Outside North 3rd Point	Ext. Outside 3rd Point Average	Finite Element
0.0	435	295	365	280
2.4	319	286	303	147
4.8	127	60	94	13
9.5	-248	-291	-270	-250
14.0	-583	-635	-609	-505
18.4	-874	-952	-913	-746
0.0	445	354	400	

Restraint Pretension			
	Eave Pretension	Zero Angle	Ridge Pretension
Ext. Outside South 3rd Point		6.9	63.4
Ext. Outside North 3rd Point		5.9	33.7

Test Summary

Test Series 7
Bracing Configuration: 3rd Points
Number of Purlins: 6
Deck Type: Through Fastened

Test Date: 11/21/02
Weight: 10460 lbs per span
Purlin Designation: 10Z0.097
Span Length: 3 @ 20 ft

Test Series 7 - 10Z-0.097 - 6 - TF - MS				
Multi-Span 3rd Point Restraints - Exterior Span Inside 3rd Points				
Slope (deg)	Ext. Span Inside South 3rd Point	Ext. Span Inside North 3rd Point	Ext. Inside 3rd Point Average	Finite Element
0.0	441	251	346	371
2.4	175	39	107	175
4.8	24	-96	-36	-22
9.5	-383	-406	-395	-409
14.0	-768	-715	-742	-783
18.4	-1126	-886	-1006	-1139
0.0	413	333	373	

Restraint Pretension			
	Eave Pretension	Zero Angle	Ridge Pretension
Ext. Inside South 3rd Point		5.4	48.9
Ext. Inside North 3rd Point		4	42.2

Test Summary

Test Series 7
Bracing Configuration: 3rd Points
Number of Purlins: 6
Deck Type: Through Fastened

Test Date: 11/21/02
Weight: 10460 lbs per span
Purlin Designation: 10Z0.097
Span Length: 3 @ 20 ft

Test Series 7 - 10Z-0.097 - 6 - TF - MS				
Multi-Span 3rd Point Restraints - Interior 3rd Points				
Slope (deg)	Interior South 3rd Point	Interior North 3rd Point	Interior 3rd Point Average	Finite Element
0.0	222	405	314	493
2.4	43	8	26	268
4.8	-136	-136	-136	44
9.5	-525	-488	-507	-400
14.0	-970	-829	-900	-830
18.4	-1371	-1135	-1253	-1237
0.0	225	387	306	

Restraint Pretension			
	Eave Pretension	Zero Angle	Ridge Pretension
Int. South 3rd Point		3.1	44.7
Int. North 3rd Point		3.1	44.4

Test Summary

Test Series 7
Bracing Configuration: Midpoints
Number of Purlins: 6
Deck Type: Through Fastened

Test Date: 11/12/02
Weight: 10460 lbs per span
Purlin Designation: 10Z0.097
Span Length: 3 @ 20 ft

Test Series 7 - 10Z-0.097 - 6 - TF - MS				
Multi-Span Midpoint Restraints - Exterior				
Slope (deg)	Exterior South Midpoint	Exterior North Midpoint	Exterior Midpoint Average	Finite Element
0.0	429	546	488	537
2.4	227	299	263	266
4.8	0	0	0	-4
9.5	-581	-518	-550	-539
14.0	-1219	-1056	-1138	-1055
18.4	-1851	-1635	-1743	-1545
0.0	374	506	440	

Restraint Pretension			
	Eave Pretension	Zero Angle	Ridge Pretension
Ext. South Midpoint	54.5	4.8	39.1
Ext. North Midpoint	41.3	4.8	41.4

Test Summary

Test Series 7
Bracing Configuration: Midpoints
Number of Purlins: 6
Deck Type: Through Fastened

Test Date: 11/12/02
Weight: 10460 lbs per span
Purlin Designation: 10Z0.097
Span Length: 3 @ 20 ft

Test Series 7 - 10Z-0.097 - 6 - TF - MS		
Multi-Span Midpoint Restraints - Interior		
Slope (deg)	Interior Midpoint	Finite Element
0.0	514	762
2.4	72	420
4.8	-202	77
9.5	-768	-598
14.0	-1355	-1252
18.4	-1936	-1874
0.0	581	

Restraint Pretension			
	Eave Pretension	Zero Angle	Ridge Pretension
Interior Midpoint	45.9	3.3	51

Test Summary

Test Series 7
Bracing Configuration: Quarter Points
Number of Purlins: 6
Deck Type: Through Fastened

Test Date: 12/11/02
Weight: 10460 lbs per span
Purlin Designation: 10Z0.097
Span Length: 3 @ 20 ft

Test Series 7 - 10Z-0.097 - 6 - TF - MS				
Multi-Span Quarter Point Restraints - Exterior Span Outside 1/4 Span				
Slope (deg)	Outside South 1/4 Span	Outside North 1/4 Span	Ext. Span Outside 1/4 Span Average	Finite Element
0.0	225	171	198	250
2.4	240	127	184	141
4.8	100	50	75	33
9.5	-204	-278	-241	-181
14.0	-502	-595	-549	-388
18.4	-824	-904	-864	-584
0.0	264	150	207	

Restraint Pretension			
	Eave Pretension	Zero Angle	Ridge Pretension
Ext. Outside South 1/4 Span	47.3	7	72
Ext. Outside North 1/4 Span	27	6	61

Test Summary

Test Series 7
Bracing Configuration: Quarter Points
Number of Purlins: 6
Deck Type: Through Fastened

Test Date: 12/11/02
Weight: 10460 lbs per span
Purlin Designation: 10Z0.097
Span Length: 3 @ 20 ft

Test Series 7 - 10Z-0.097 - 6 - TF - MS				
Multi-Span Quarter Point Restraints - Exterior Span Inside 1/4 Span				
Slope (deg)	Ext. Span Inside South 1/4 Span	Ext. Span Inside North 1/4 Span	Ext. Span Inside 1/4 Span Average	Finite Element
0.0	277	379	328	354
2.4	98	57	78	166
4.8	-49	-91	-70	-21
9.5	-383	-307	-345	-391
14.0	-727	-578	-653	-748
18.4	-1043	-842	-943	-1087
0.0	264	456	360	

Restraint Pretension			
	Eave Pretension	Zero Angle	Ridge Pretension
Ext. Inside South 1/4 Span	42.6	4.8	56
Ext. Inside North 1/4 Span	53.1	3.8	69

Test Summary

Test Series 7
Bracing Configuration: Quarter Points
Number of Purlins: 6
Deck Type: Through Fastened

Test Date: 12/11/02
Weight: 10460 lbs per span
Purlin Designation: 10Z0.097
Span Length: 3 @ 20 ft

Test Series 7 - 10Z-0.097 - 6 - TF - MS				
Multi-Span Quarter Point Restraints - Interior Span 1/4 Span				
Slope (deg)	Interior Span South 1/4 Span	Interior Span North 1/4 Span	Interior Span 1/4 Span Average	Finite Element
0.0	215	282	249	425
2.4	32	17	25	226
4.8	-41	-60	-51	27
9.5	-380	-383	-382	-365
14.0	-729	-705	-717	-745
18.4	-1048	-988	-1018	-1106
0.0	283	273	278	

Restraint Pretension			
	Eave Pretension	Zero Angle	Ridge Pretension
Interior Span South 1/4 Spa	50.6	2.7	38
Interior Span North 1/4 Spa	42	2.7	49

Test Summary

Test Series 7
Bracing Configuration: Quarter Points
Number of Purlins: 6
Deck Type: Through Fastened

Test Date: 12/11/02
Weight: 10460 lbs per span
Purlin Designation: 10Z0.097
Span Length: 3 @ 20 ft

Test Series 7 - 10Z-0.097 - 6 - TF - MS				
Multi-Span Quarter Point Restraints - Exterior Span 1/2 Span				
Slope (deg)	Exterior Span South 1/2 Span	Exterior Span North 1/2 Span	Exterior Span 1/2 Span Average	Finite Element
0.0	230	140	185	107
2.4	188	63	126	38
4.8	90	-60	15	-31
9.5	-130	-207	-169	-166
14.0	-254	-342	-298	-297
18.4	-351	-455	-403	-421
0.0	249	142	196	

Restraint Pretension			
	Eave Pretension	Zero Angle	Ridge Pretension
Exterior South 1/2 Span	48.8	6.5	57
Exterior North 1/2 Span	30.4	4.3	50

Test Summary

Test Series 7
Bracing Configuration: Quarter Points
Number of Purlins: 6
Deck Type: Through Fastened

Test Date: 12/11/02
Weight: 10460 lbs per span
Purlin Designation: 10Z0.097
Span Length: 3 @ 20 ft

Test Series 7 - 10Z-0.097 - 6 - TF - MS		
Multi-Span Quarter Point Restraints - Interior		
Slope (deg)	Interior Span 1/2 Span	Finite Element
0.0	243	260
2.4	46	146
4.8	-36	33
9.5	-193	-192
14.0	-362	-409
18.4	-536	-616
0.0	277	

Restraint Pretension			
	Eave Pretension	Zero Angle	Ridge Pretension
Interior Span 1/2 Span	67.5	3.3	37

Test Summary

Test Series 7
Bracing Configuration: 3rd Points + Supports
Number of Purlins: 6
Deck Type: Through Fastened

Test Date: 12/18/02
Weight: 10460 lbs per span
Purlin Designation: 10Z0.097
Span Length: 3 @ 20 ft

Test Series 7 - 10Z-0.097 - 6 - TF - MS				
Multi-Span 3rd Point + Support Restraints - Exterior Supports				
Slope (deg)	Exterior South Support	Exterior North Support	Exterior Support Average	Finite Element
0.0	343	144	244	227
2.4	250	135	193	114
4.8	65	83	74	1
9.5	-187	0	-94	-223
14.0	-505	-135	-320	-439
18.4	-868	-243	-556	-644
0.0	343	124	234	

Restraint Pretension			
	Eave Pretension	Zero Angle	Ridge Pretension
Ext. South Support	38	7.5	47
Ext. North Support	29	9.5	23

Test Summary

Test Series 7
Bracing Configuration: 3rd Points + Supports
Number of Purlins: 6
Deck Type: Through Fastened

Test Date: 12/18/02
Weight: 10460 lbs per span
Purlin Designation: 10Z0.097
Span Length: 3 @ 20 ft

Test Series 7 - 10Z-0.097 - 6 - TF - MS				
Multi-Span 3rd Point + Support Restraints - Interior Supports				
Slope (deg)	Interior South Support	Interior North Support	Interior Support Average	Finite Element
0.0	370	500	435	527
2.4	120	123	122	255
4.8	0	-47	-24	-16
9.5	-489	-572	-531	-551
14.0	-1011	-1138	-1075	-1068
18.4	-1336	-1694	-1515	-1559
0.0	337	501	419	

Restraint Pretension			
	Eave Pretension	Zero Angle	Ridge Pretension
Int. South Support	28	4.8	43
Int. North Support	28	4.2	34

Test Summary

Test Series 7
Bracing Configuration: 3rd Points + Supports
Number of Purlins: 6
Deck Type: Through Fastened

Test Date: 12/18/02
Weight: 10460 lbs per span
Purlin Designation: 10Z0.097
Span Length: 3 @ 20 ft

Test Series 7 - 10Z-0.097 - 6 - TF - MS				
Multi-Span 3rd Point + Support Restraints - Exterior Span Outside 3rd Points				
Slope (deg)	Outside South 3rd Point	Outside North 3rd Point	Ext. Outside 3rd Point Average	Finite Element
0.0	210	287	249	168
2.4	130	200	165	68
4.8	38	30	34	-31
9.5	-207	-261	-234	-227
14.0	-407	-531	-469	-416
18.4	-554	-772	-663	-595
0.0	222	284	253	

Restraint Pretension			
	Eave Pretension	Zero Angle	Ridge Pretension
Ext. Outside South 3rd Poin	45	5.4	25
Ext. Outside North 3rd Poin	49	5.4	49

Test Summary

Test Series 7
Bracing Configuration: 3rd Points + Supports
Number of Purlins: 6
Deck Type: Through Fastened

Test Date: 12/18/02
Weight: 10460 lbs per span
Purlin Designation: 10Z0.097
Span Length: 3 @ 20 ft

Test Series 7 - 10Z-0.097 - 6 - TF - MS				
Multi-Span 3rd Point + Support Restraints - Exterior Span Inside 3rd Points				
Slope (deg)	Ext. Span Inside South 3rd Point	Ext. Span Inside North 3rd Point	Ext. Inside 3rd Point Average	Finite Element
0.0	221	191	206	223
2.4	93	55	74	101
4.8	19	0	10	-21
9.5	-163	-173	-168	-261
14.0	-351	-294	-323	-493
18.4	-485	-503	-494	-713
0.0	210	190	200	

Restraint Pretension			
	Eave Pretension	Zero Angle	Ridge Pretension
Ext. Inside South 3rd Point	45	5.4	37
Ext. Inside North 3rd Point	33	4.8	38

Test Summary

Test Series 7
Bracing Configuration: 3rd Points + Supports
Number of Purlins: 6
Deck Type: Through Fastened

Test Date: 12/18/02
Weight: 10460 lbs per span
Purlin Designation: 10Z0.097
Span Length: 3 @ 20 ft

Test Series 7 - 10Z-0.097 - 6 - TF - MS				
Multi-Span 3rd Point + Support Restraints - Interior 3rd Points				
Slope (deg)	Interior South 3rd Point	Interior North 3rd Point	Interior 3rd Point Average	Finite Element
0.0	160	201	181	328
2.4	19	26	23	190
4.8	-97	-61	-79	53
9.5	-233	-263	-248	-218
14.0	-369	-475	-422	-480
18.4	-469	-696	-583	-730
0.0	189	220	205	

Restraint Pretension			
	Eave Pretension	Zero Angle	Ridge Pretension
Interior South 3rd Point	51	2.8	25
Interior North 3rd Point	33	2.8	32

Test Summary

Test Series 8
Bracing Configuration: Supports
Number of Purlins: 6
Deck Type: Standing Seam

Test Date: 3/5/03
Weight: 10460 lbs per span
Purlin Designation: 10Z0.097
Span Length: 3 @ 20 ft

Test Series 8 - 10Z-0.097 - 6 - SS - MS				
Multi-Span Support Restraints - Exterior Supports				
Slope (deg)	Exterior South Support	Exterior North Support	Exterior Support Average	Finite Element
0.0	428	249	339	298
2.4	347	197	272	136
4.8	78	71	75	-18
9.5	-260	-160	-210	-246
14.0	-441	-300	-371	-464
17.3	-619	-372	-496	-624
0.0	193	170	182	

Restraint Pretension			
	Eave Pretension	Zero Angle	Ridge Pretension
Ext. South Support	43	6	30
Ext. North Support	27	6	36

Test Summary

Test Series 8
Bracing Configuration: Supports
Number of Purlins: 6
Deck Type: Standing Seam

Test Date: 3/5/03
Weight: 10460 lbs per span
Purlin Designation: 10Z0.097
Span Length: 3 @ 20 ft

Test Series 8 - 10Z-0.097 - 6 - SS - MS				
Multi-Span Support Restraints - Interior				
Slope (deg)	Interior South Support	Interior North Support	Interior Support Average	Finite Element
0.0	347	493	420	423
2.4	40	48	44	195
4.8	-99	-142	-121	-29
9.5	-414	-680	-547	-414
14.0	-735	-1203	-969	-782
17.3	-896	-1596	-1246	-1052
0.0	221	358	290	

Restraint Pretension			
	Eave Pretension	Zero Angle	Ridge Pretension
Int. South Support	50	3.4	28
Int. North Support	42	3.4	39

Test Summary

Test Series 8
Bracing Configuration: 3rd Points
Number of Purlins: 6
Deck Type: Standing Seam

Test Date: 2/28/03
Weight: 10460 lbs per span
Purlin Designation: 10Z0.097
Span Length: 3 @ 20 ft

Test Series 8 - 10Z-0.097 - 6 - SS - MS				
Multi-Span 3rd Point Restraints - Exterior Span Outside 3rd Points				
Slope (deg)	Outside South 3rd Point	Outside North 3rd Point	Ext. Outside 3rd Point Average	Finite Element
0.0	414	260	337	298
2.4	329	232	281	159
4.8	141	120	131	19
9.5	-210	-88	-149	-201
14.0	-435	-228	-332	-408
18.0	-619	-351	-485	-606
0.0	244	192	218	

Restraint Pretension			
	Eave Pretension	Zero Angle	Ridge Pretension
Ext. Outside South 3rd Poin	29	6.6	32
Ext. Outside North 3rd Point	24	7.5	30

Test Summary

Test Series 8
Bracing Configuration: 3rd Points
Number of Purlins: 6
Deck Type: Standing Seam

Test Date: 2/28/03
Weight: 10460 lbs per span
Purlin Designation: 10Z0.097
Span Length: 3 @ 20 ft

Test Series 8 - 10Z-0.097 - 6 - SS - MS				
Multi-Span 3rd Point Restraints - Exterior Span Inside 3rd Points				
Slope (deg)	Ext. Span Inside South 3rd Point	Ext. Span Inside North 3rd Point	Ext. Inside 3rd Point Average	Finite Element
0.0	282	289	286	280
2.4	70	139	105	139
4.8	-102	-31	-67	-2
9.5	-347	-294	-321	-231
14.0	-568	-518	-543	-451
18.0	-797	-716	-757	-661
0.0	223	372	298	

Restraint Pretension			
	Eave Pretension	Zero Angle	Ridge Pretension
Ext. Inside South 3rd Point	40	3.5	35
Ext. Inside North 3rd Point	28	4	31

Test Summary

Test Series 8
Bracing Configuration: 3rd Points
Number of Purlins: 6
Deck Type: Standing Seam

Test Date: 2/28/03
Weight: 10460 lbs per span
Purlin Designation: 10Z0.097
Span Length: 3 @ 20 ft

Test Series 8 - 10Z-0.097 - 6 - SS - MS				
Multi-Span 3rd Point Restraints - Interior 3rd Points				
Slope (deg)	Interior South 3rd Point	Interior North 3rd Point	Interior 3rd Point Average	Finite Element
0.0	185	203	194	294
2.4	57	71	64	145
4.8	-113	-72	-93	-3
9.5	-228	-360	-294	-258
14.0	-350	-583	-467	-501
18.0	-454	-789	-622	-734
0.0	238	215	227	

Restraint Pretension			
	Eave Pretension	Zero Angle	Ridge Pretension
Int. South 3rd Point	25		22
Int. North 3rd Point	22		30

Test Summary

Test Series 8
Bracing Configuration: Midpoints
Number of Purlins: 6
Deck Type: Standing Seam

Test Date: 2/20/03
Weight: 10460 lbs per span
Purlin Designation: 10Z0.097
Span Length: 3 @ 20 ft

Test Series 8 - 10Z-0.097 - 6 - SS - MS				
Multi-Span Midpoint Restraints - Exterior				
Slope (deg)	Exterior South Midpoint	Exterior North Midpoint	Exterior Midpoint Average	Finite Element
0.0	503	356	430	438
2.4	588	113	351	224
4.8	307	-47	130	9
9.5	-206	-294	-250	-313
14.0	-634	-488	-561	-618
17.5	-907	-637	-772	-856
0.0	640	220	430	

Restraint Pretension			
	Eave Pretension	Zero Angle	Ridge Pretension
Ext. South Midpoint	37	7.5	35
Ext. North Midpoint	33	4.2	28

Test Summary

Test Series 8
Bracing Configuration: Midpoints
Number of Purlins: 6
Deck Type: Standing Seam

Test Date: 2/20/03
Weight: 10460 lbs per span
Purlin Designation: 10Z0.097
Span Length: 3 @ 20 ft

Test Series 8 - 10Z-0.097 - 6 - SS - MS		
Multi-Span Midpoint Restraints - Interior		
Slope (deg)	Interior Midpoint	Finite Element
0.0	330	443
2.4	45	221
4.8	-93	0
9.5	-311	-343
14.0	-505	-672
17.5	-647	-928
0.0	345	

Restraint Pretension			
	Eave Pretension	Zero Angle	Ridge Pretension
Interior Midpoint	28	3	27

Test Summary

Test Series 8
Bracing Configuration: Quarter Points
Number of Purlins: 6
Deck Type: Standing Seam

Test Date: 2/26/03
Weight: 10460 lbs per span
Purlin Designation: 10Z0.097
Span Length: 3 @ 20 ft

Test Series 8 - 10Z-0.097 - 6 - SS - MS				
Multi-Span Quarter Point Restraints - Exterior Span Outside 1/4 Span				
Slope (deg)	Outside South 1/4 Span	Outside North 1/4 Span	Ext. Span Outside 1/4 Span Average	Finite Element
0.0	268	172	220	229
2.4	325	106	216	125
4.8	161	0	81	21
9.5	-102	-153	-128	-155
14.0	-285	-262	-274	-320
18.0	-418	-371	-395	-466
0.0	132	43	88	

Restraint Pretension			
	Eave Pretension	Zero Angle	Ridge Pretension
Ext. Outside South 1/4 Span	47.3	7	72
Ext. Outside North 1/4 Span	27	6	61

Test Summary

Test Series 8
Bracing Configuration: Quarter Points
Number of Purlins: 6
Deck Type: Standing Seam

Test Date: 2/26/03
Weight: 10460 lbs per span
Purlin Designation: 10Z0.097
Span Length: 3 @ 20 ft

Test Series 8 - 10Z-0.097 - 6 - SS - MS				
Multi-Span Quarter Point Restraints - Exterior Span Inside 1/4 Span				
Slope (deg)	Ext. Span Inside South 1/4 Span	Ext. Span Inside North 1/4 Span	Ext. Span Inside 1/4 Span Average	Finite Element
0.0	160	188	174	204
2.4	17	16	17	97
4.8	-88	-132	-110	-9
9.5	-298	-342	-320	-203
14.0	-533	-614	-574	-388
18.0	-780	-819	-800	-552
0.0	102	263	183	

Restraint Pretension			
	Eave Pretension	Zero Angle	Ridge Pretension
Ext. Inside South 1/4 Span	42.6	4.8	56
Ext. Inside North 1/4 Span	53.1	3.8	69

Test Summary

Test Series 8
Bracing Configuration: Quarter Points
Number of Purlins: 6
Deck Type: Standing Seam

Test Date: 2/26/03
Weight: 10460 lbs per span
Purlin Designation: 10Z0.097
Span Length: 3 @ 20 ft

Test Series 8 - 10Z-0.097 - 6 - SS - MS				
Multi-Span Quarter Point Restraints - Interior Span 1/4 Span				
Slope (deg)	Interior Span South 1/4 Span	Interior Span North 1/4 Span	Interior Span 1/4 Span Average	Finite Element
0.0	123	142	133	238
2.4	-44	-45	-45	118
4.8	-68	-113	-91	-2
9.5	-187	-376	-282	-213
14.0	-313	-614	-464	-415
18.0	-418	-848	-633	-594
0.0	61	145	103	

Restraint Pretension			
	Eave Pretension	Zero Angle	Ridge Pretension
Interior Span South 1/4 Spa	50.6	2.7	38
Interior Span North 1/4 Spa	42	2.7	49

Test Summary

Test Series 8
Bracing Configuration: Quarter Points
Number of Purlins: 6
Deck Type: Standing Seam

Test Date: 2/26/03
Weight: 10460 lbs per span
Purlin Designation: 10Z0.097
Span Length: 3 @ 20 ft

Test Series 8 - 10Z-0.097 - 6 - SS - MS				
Multi-Span Quarter Point Restraints - Exterior Span 1/2 Span				
Slope (deg)	Exterior Span South 1/2 Span	Exterior Span North 1/2 Span	Exterior Span 1/2 Span Average	Finite Element
0.0	309	235	272	220
2.4	315	124	220	112
4.8	188	0	94	4
9.5	-67	-197	-132	-154
14.0	-247	-273	-260	-305
18.0	-350	-378	-364	-439
0.0	391	297	344	

Restraint Pretension			
	Eave Pretension	Zero Angle	Ridge Pretension
Exterior South 1/2 Span	48.8	6.5	57
Exterior North 1/2 Span	30.4	4.3	50

Test Summary

Test Series 8
Bracing Configuration: Quarter Points
Number of Purlins: 6
Deck Type: Standing Seam

Test Date: 2/26/03
Weight: 10460 lbs per span
Purlin Designation: 10Z0.097
Span Length: 3 @ 20 ft

Test Series 8 - 10Z-0.097 - 6 - SS - MS		
Multi-Span Quarter Point Restraints - Interior		
Slope (deg)	Interior Span 1/2 Span	Finite Element
0.0	200	238
2.4	35	118
4.8	-38	-1
9.5	-202	-196
14.0	-289	-383
18.0	-390	-549
0.0	250	

Restraint Pretension			
	Eave Pretension	Zero Angle	Ridge Pretension
Interior Span 1/2 Span	67.5	3.3	37

Test Summary

Test Series 8 | Test Date: 3/03/03
Bracing Configuration: 3rd Points + Supports | Weight: 10460 lbs per span
Number of Purlins: 6 | Purlin Designation: 10Z0.097
Deck Type: Standing Seam | Span Length: 3 @ 20 ft

Test Series 8 - 10Z-0.097 - 6 - SS - MS				
Multi-Span 3rd Point + Support Restraints - Exterior Supports				
Slope (deg)	Exterior South Support	Exterior North Support	Exterior Support Average	Finite Element
0.0	255	144	200	156
2.4	217	129	173	63
4.8	45	55	50	-31
9.5	-162	-85	-124	-178
14.0	-306	-178	-242	-323
18.0	-423	-261	-342	-453
0.0	33	72	53	

Restraint Pretension			
	Eave Pretension	Zero Angle	Ridge Pretension
Ext. South Support	59	6.3	33
Ext. North Support	38	6.3	32

Test Summary

Test Series 8 | Test Date: 3/03/03
Bracing Configuration: 3rd Points + Supports | Weight: 10460 lbs per span
Number of Purlins: 6 | Purlin Designation: 10Z0.097
Deck Type: Standing Seam | Span Length: 3 @ 20 ft

Test Series 8 - 10Z-0.097 - 6 - SS - MS				
Multi-Span 3rd Point + Support Restraints - Interior Supports				
Slope (deg)	Interior South Support	Interior North Support	Interior Support Average	Finite Element
0.0	46	183	115	215
2.4	-57	-66	-62	85
4.8	-168	-147	-158	-44
9.5	-283	-423	-353	-289
14.0	-471	-742	-607	-524
18.0	-625	-939	-782	-733
0.0	16	173	95	

Restraint Pretension			
	Eave Pretension	Zero Angle	Ridge Pretension
Int. South Support	40	1.6	20
Int. North Support	58	1.6	30

Test Summary

Test Series 8
Bracing Configuration: 3rd Points + Supports
Number of Purlins: 6
Deck Type: Standing Seam

Test Date: 3/03/03
Weight: 10460 lbs per span
Purlin Designation: 10Z0.097
Span Length: 3 @ 20 ft

Test Series 8 - 10Z-0.097 - 6 - SS - MS				
Multi-Span 3rd Point + Support Restraints - Exterior Span Outside 3rd Points				
Slope (deg)	Outside South 3rd Point	Outside North 3rd Point	Ext. Outside 3rd Point Average	Finite Element
0.0	249	244	247	221
2.4	233	340	287	124
4.8	134	181	158	27
9.5	-111	-106	-109	-146
14.0	-360	-364	-362	-309
18.0	-527	-588	-558	-454
0.0	240	399	320	

Restraint Pretension			
	Eave Pretension	Zero Angle	Ridge Pretension
Ext. Outside South 3rd Poin	42	7.6	28
Ext. Outside North 3rd Poin	42	7.6	36

Test Summary

Test Series 8
Bracing Configuration: 3rd Points + Supports
Number of Purlins: 6
Deck Type: Standing Seam

Test Date: 3/03/03
Weight: 10460 lbs per span
Purlin Designation: 10Z0.097
Span Length: 3 @ 20 ft

Test Series 8 - 10Z-0.097 - 6 - SS - MS				
Multi-Span 3rd Point + Support Restraints - Exterior Span Inside 3rd Points				
Slope (deg)	Ext. Span Inside South 3rd Point	Ext. Span Inside North 3rd Point	Ext. Inside 3rd Point Average	Finite Element
0.0	283	188	236	208
2.4	155	98	127	108
4.8	75	55	65	8
9.5	-160	-164	-162	-166
14.0	-378	-359	-369	-332
18.0	-600	-495	-548	-479
0.0	267	172	220	

Restraint Pretension			
	Eave Pretension	Zero Angle	Ridge Pretension
Ext. Inside South 3rd Point	68	6.3	43
Ext. Inside North 3rd Point	70	6.3	38

Test Summary

Test Series 8
Bracing Configuration: 3rd Points + Supports
Number of Purlins: 6
Deck Type: Standing Seam

Test Date: 3/03/03
Weight: 10460 lbs per span
Purlin Designation: 10Z0.097
Span Length: 3 @ 20 ft

Test Series 8 - 10Z-0.097 - 6 - SS - MS				
Multi-Span 3rd Point + Support Restraints - Interior 3rd Points				
Slope (deg)	Interior South 3rd Point	Interior North 3rd Point	Interior 3rd Point Average	Finite Element
0.0	212	141	177	223
2.4	-17	-6	-12	117
4.8	-113	-160	-137	10
9.5	-250	-387	-319	-185
14.0	-417	-697	-557	-371
18.4	-555	-899	-727	-537
0.0	256	220	238	

Restraint Pretension			
	Eave Pretension	Zero Angle	Ridge Pretension
Interior South 3rd Point	49	1.6	29
Interior North 3rd Point	46	1.6	29

APPENDIX III

EQUATION SUMMARY AND EXAMPLE PROBLEMS

Supports Restraint Configuration – Single Span

Restraint Force Per anchorage device

$$R = \sum P_L \cdot \frac{K_{rest}}{K_{total}} \tag{1}$$

Where

$$K_{total} = \sum K_{rest} + \frac{\sum\left(K_{shtg} + K_{rafter}\right)}{d} \tag{2}$$

with

K_{rest} = stiffness of externally applied restraint (lb/in)

K_{rafter} = rotational stiffness of the Z-section to rafter connection (lb-in/in)

K_{shtg} = rotational stiffness provided by the sheathing (lb-in/in)

Total overturning force generated per purlin

$$P_L = wL \cdot \left(\frac{\delta b \cos\theta}{h} - \frac{d}{h}\sin\theta\right) + \frac{M_{torsion} + M_{local}}{h} \tag{3}$$

where

$$M_{torsion} + M_{local} = wL \cdot \tfrac{2}{3} K_{mclip}\left(\sigma\frac{d}{2} - \delta b \cos\theta\right)\tau \tag{4}$$

$$M_{local} = -wL \cdot \delta b \cos\theta \cdot \frac{K_{mclip}}{K_{mclip} + \dfrac{E \cdot t^3}{3d}} \tag{5}$$

$$\sigma = \frac{\dfrac{5\left(\dfrac{I_{XY}}{I_X}\cos\theta\right)L^4}{384EI_{mY}} + \dfrac{(\delta b \cos\theta)d}{2}\tau + \dfrac{L^2 \sin\theta}{8G'Width}}{\dfrac{5L^4}{384EI_{mY}} + \dfrac{d^2}{4}\tau + \dfrac{L^2}{8G'Width}} \tag{6}$$

Restraint Stiffness

$$K_{rest} = \frac{\left(\frac{h}{d}\right)^2 K_{device} \cdot K_{config}}{\frac{h}{d}K_{device} + K_{config}} \tag{7}$$

with

K_{device} = stiffness of restraining device at restraint height (lb/in)

K_{config} = stiffness of restraint configuration (lb/in)

Discrete Brace

$$K_{config} = \frac{\frac{1}{15}d(3Et^3)}{h(d-h)^2}\left[\frac{\frac{1}{15}d \cdot 2Et^3(3d-h) + \frac{L}{80}K_{mclip} \cdot d(3d-2h)}{\frac{1}{15}d \cdot Et^3(4d-h) + \frac{L}{80}K_{mclip} \cdot d(d-h)}\right] \tag{8}$$

Antiroll Clip

$$K_{config} = \frac{3Eb_{ar}t^3}{(d-h)^3}\left(\frac{2d-h}{h}\right) \tag{9}$$

Web Bolted Plate

$$K_{Rafter} = \frac{E \cdot b_{pl} \cdot t_{pl}{}^3 \cdot t^3\left(t^3h + t_{pl}^3(d-h)\right)}{\left(t^3h^2 - t_{pl}^3(d-h)^2\right)^2 + 4t^3t_{pl}{}^3d^2h(d-h)} \tag{10}$$

Rafter Stiffness

Web Bolted to Rafter Clip

$$K_{Rafter} = \frac{E \cdot b_{pl} \cdot t_{pl}{}^3 \cdot t^3\left(t^3h + t_{pl}^3(d-h)\right) \cdot d}{\left(t^3h^2 - t_{pl}^3(d-h)^2\right)^2 + 4t^3t_{pl}{}^3d^2h(d-h)} \tag{11}$$

Flange Bolted

$$K_{Rafter} = 0.45\frac{Et^3}{2d} \tag{12}$$

Sheathing Stiffness

$$K_{shtg,sys} = \frac{K_{mclip}L}{d}\left(\frac{\frac{1}{4}Et^3}{0.38K_{mclip}d + 0.71\frac{1}{4}Et^3}\right)\left(1 - \tfrac{2}{3}K_{mclip}\tau\right) \tag{13}$$

Deformation of System

Deflection at restraint (Frame Line)

$$\Delta_{rest} = \frac{R}{K_{rest}} \tag{14}$$

Deflection of diaphragm relative to restraint

$$\Delta_{diaph} = \sum w(\sigma - \sin\theta)\frac{L^2}{8G'Bay} \tag{15}$$

Total mid-span deflection

$$\Delta_{MS} = \Delta_{rest} + \Delta_{diaph} \tag{16}$$

Fastener force at restraint

$$\text{FastenerForce} = R\frac{h}{d} + \frac{wL}{2}\left(0.9\sigma - \frac{\delta b\cos\theta}{d}\right) - \frac{M_{torsion}}{2d} \tag{17}$$

Third Points Restraint Configuration – Single Span

Restraint Force Per anchorage device

$$R = \sum P_L \cdot \frac{K_{rest}}{K_{total}} \tag{18}$$

Where

$$K_{total} = \sum K_{rest} + \frac{\sum K_{shtg}}{d} \tag{19}$$

with

K_{rest} = stiffness of externally applied restraint (lb/in)

K_{shtg} = rotational stiffness provided by the sheathing (lb-in/in)

Total overturning force generated per purlin

$$P_L = wL \cdot \left(\frac{\delta b \cos\theta}{h} - \frac{d}{h}\sin\theta \right) + \frac{M_{torsion} + M_{local}}{h} \tag{20}$$

where

$$M_{torsion} = wL\left[\tfrac{2}{3} k_{mclip} \tau \left(\sigma \frac{d}{2} - \delta b \cos\theta \right) + \frac{L^2 k_{mclip}}{6G' \cdot Width \cdot d} \left(\frac{\sigma}{3} + \frac{\sin\theta}{6} - \frac{\delta b \cos\theta}{2d} \right) \left(1 - \tfrac{2}{3} k_{mclip} \tau \right) \right] \tag{21}$$

$$M_{local} = -wL \cdot \delta b \cos\theta \cdot \frac{K_{mclip}}{K_{mclip} + \dfrac{E \cdot t^3}{3d}} \tag{22}$$

$$\sigma = \frac{\dfrac{11\left(\dfrac{I_{XY}}{I_X}\cos\theta\right)L^4}{972EI_{mY}} + \dfrac{(\delta b \cos\theta)d}{2}\tau - \dfrac{L^2 \sin\theta}{18G' Width}}{\dfrac{11L^4}{972EI_{mY}} + \dfrac{d^2}{4}\tau + \dfrac{L^2}{9G' Width}} \tag{23}$$

Restraint Stiffness

$$K_{rest} = \left(\tfrac{h}{d}\right)^2 K_{devuce} \tag{24}$$

with

K_{device} = stiffness of restraining device at restraint height (lb/in)

Sheathing Stiffness

$$K_{shtg,sys} = \frac{K_{mclip} L}{d} \left(\frac{\tfrac{1}{4} Et^3}{0.38 K_{mclip} d + 0.71 \tfrac{1}{4} Et^3} \right) \left(1 - \tfrac{2}{3} K_{mclip} \tau \right) \tag{25}$$

Deformation of System
Deflection at restraint

$$\Delta_{rest} = \frac{R}{K_{rest}} \tag{26}$$

Deflection of diaphragm at ends (frame line) relative to restraint

$$\Delta_{diaph} = -\frac{L^2}{9G'Bay}\left(\sum w\sigma + \tfrac{7}{4}\sum w\sin\theta\frac{\sum K_{rest}}{K_{total}}\right) + \frac{P_L \tfrac{h}{d} L}{3G'Bay} \tag{27}$$

Total deflection at frame line

$$\Delta_{MS} = \Delta_{rest} + \Delta_{diaph} \tag{28}$$

Fastener force at restraint

$$\text{FastenerForce} = R\frac{h}{d} + \frac{wL}{20}\left(\frac{\delta b\cos\theta}{d} - 0.9\sigma\right) \tag{29}$$

Nomenclature

$$I_{mY} = \frac{I_X I_Y - I_{XY}^2}{I_X} \tag{30}$$

$$\tau = \frac{\frac{a^2}{GJ}\beta}{1 + \frac{K_{MDeck}}{GJ}\kappa} \tag{31}$$

$$\beta = \frac{L^2}{8a^2} + \frac{1}{\cosh\left(\frac{L}{2a}\right)} - 1 \tag{32}$$

$$\kappa = \frac{8a^4}{L^2}\left(\frac{\cosh\left(\frac{L}{2a}\right) - 1}{\cosh\left(\frac{L}{2a}\right)}\right) + \frac{5L^2}{48} - a^2 \tag{33}$$

$$a = \sqrt{\frac{EC_W}{GJ}} \tag{34}$$

b = width of Z-section top flange (in) (mm)
b_{ar} = width of antiroll anchorage device or web bolted rafter plate
Bay = total width of diaphragm perpendicular to span (ft) (m)
d = depth of Z-section (in) (mm)
E = modulus of elasticity (29,500,000 psi) (203,400 MPa)
G = shear modulus (11,200,00 psi) (77,200 MPa)
h = height of applied restraint measured from base of Z-section parallel to web (in) (mm)
I_X = moment of inertia of full unreduced section about axis perpendicular to the plane of the web (in^4) (mm^4)
I_{XY} = product of inertia of full unreduced section about major and minor centroidal axes (in^4) (mm^4)
I_{Deck} = Gross moment of inertia of sheathing
K_{mclip} = combined rotational stiffness of sheathing and connection between the Z-section and sheathing (lb-in/ft) (N-m/m)
K_{rafter} = Moment developed in connection between Z-section and rafter per unit lateral displacement of top flange of Z-section at restraint
K_{rest} = Force restrained at top flange of Z-section per unit lateral displacement of top flange at restraint location
K_{shtg} = Moment developed in connection between Z-section and sheathing per unit lateral displacement of top flange of Z-section at restraint
L = span of Z-section (ft) (m)
M_{local} = Moment developed in sheathing due to local deformation of top flange
M_{rafter} = Moment developed in connection between rafter and Z-section due to lateral movement of top flange relative to base
M_{shtg} = Moment developed in sheathing due to lateral movement of top flange relative to base
$M_{torsion}$ = Moment developed in sheathing due to twist of Z-section relative to sheathing

n_P = number of restrained purlins per anchorage device
t = thickness of Z-section (in)
t_{pl} = thickness of web bolted rafter plate
w = uniform loading on Z-section (lb/ft) (N/m)
Width = tributary width of diaphragm (perpendicular to Z-Section Span) per Z-section.(in) (mm)
δ = load eccentricity on Z-section top flange (1/3)
θ = angle between the vertical and the plane of the Z-section web (degrees)

Example 1. Supports Restraint Configuration (Antiroll Anchorage Device)

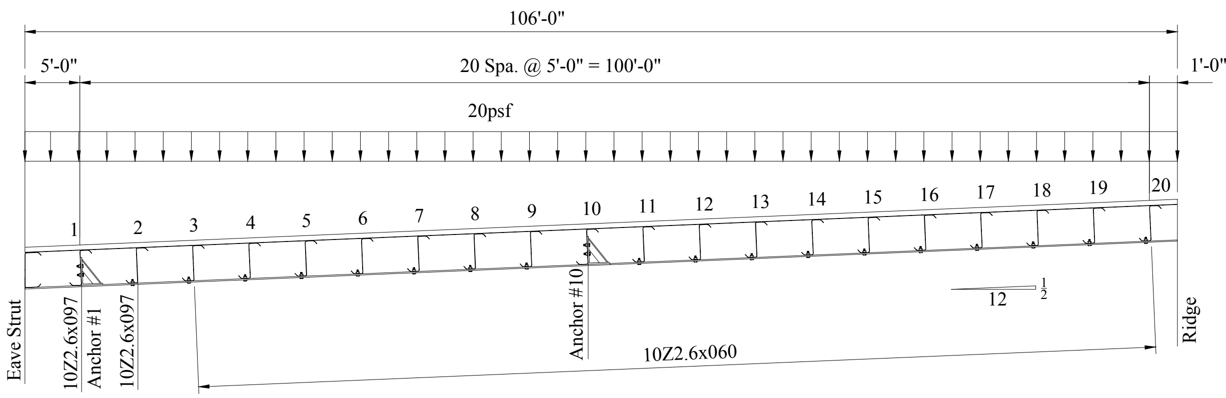

Figure III.1 Roof Layout Example 1

Determine the lateral restraint forces for a single span bay with Z-sections spanning 20 ft and an eave to ridge distance of 101 ft subjected to a nominal 20 psf uniform loading. The roof pitch is ½ in. on 12 in. There is an eave strut at the eave and Z-sections are spaced at 5 ft for a total of 20 Z-section lines. The distance from the last Z-section (#20) to the ridge is 1 ft. At the eave, Z-sections #1 and #2 are 10Z2.6x097 and the remaining Z-sections are 10Z2.6x060. Antiroll anchorage devices labeled Anchor 1 and Anchor 10 are applied at Z-section #1 and Z-section #10, respectively. The tested stiffness of Anchor 1 is 4000 lb/in and the stiffness of Anchor 10 is 3000 lb/in. These stiffness values were measured at the top of the sheathing. The sheathing is a standing seam system with a diaphragm stiffness of 1000 lb/in. Lateral slip between the purlin and the sheathing is prevented by the clip connection between the sheathing and purlin. The connection between the sheathing and the Z-section has a rotational stiffness of 1000 lb-in./rad./ft. The Z-sections are attached to the rafters with a flange bolted connection.

System Properties

L	= 20 ft
Bay	= 101 ft
Width	= 101 ft/20 purlins = 60.6 in
Uniform load	= 20 psf
Roof Slope, θ	= 2.4 degrees (1/2:12)
G'	=1000 lb/in
K_{MClip}	= 1000 lb-in/rad/ft
E	= 29,500,000 psi
G	= 11,200,000 psi

Purlin Section Properties

Z-section 1 – 2

d	= 10.07 in.
b	= 2.56 in.
t	= 0.097 in.
δ	= 1/3
I_X	= 24.31 in^4
I_Y	= 2.69 in^4

$$I_{MY} = \frac{I_X I_Y - I_{XY}^2}{I_X} = \frac{\left(24.31\text{in}^4\right)\left(2.69\text{in}^4\right) - \left(5.70\text{in}^4\right)^2}{24.31\text{in}^4} = 1.35\text{in}^4$$

$$a = \sqrt{\frac{EC_W}{GJ}} = \sqrt{\frac{E \cdot 50.48\text{in}^6}{G \cdot 0.005191\text{in}^4}} = 159.9\text{in}$$

I_{XY} = 5.70 in^4
J = 0.005191 in^4
C_W = 50.48 in^6

$$\beta = \frac{L^2}{8a^2} + \frac{1}{\cosh\left(\frac{L}{2a}\right)} - 1 = \frac{(240in)^2}{8\cdot(159.9in)^2} + \frac{1}{\cosh\left(\frac{240in}{2\cdot 159.9in}\right)} - 1 = 0.054rad$$

$$\kappa = \frac{8a^4}{L^2}\left(\frac{\cosh\left(\frac{L}{2a}\right)-1}{\cosh\left(\frac{L}{2a}\right)}\right) + \frac{5L^2}{48} - a^2$$

$$\kappa = \frac{8(159.9in)^4}{(240in)^2}\left(\frac{\cosh\left(\frac{240in}{2\cdot 159.9in}\right)-1}{\cosh\left(\frac{240in}{2\cdot 159.9in}\right)}\right) + \frac{5(240in)^2}{48} - (159.9in)^2 = 1119rad\cdot in^2$$

$$\tau = \frac{\frac{a^2\beta}{GJ}}{1+\frac{K_{MDeck}}{GJ}\kappa} = \frac{\frac{(159.9in)^2\cdot 0.054rad}{G\cdot 0.005191in^4}}{1+\frac{1000\,{}^{lb\cdot in}/_{rad\cdot ft}}{G\cdot 0.005191in^4}\cdot 1119rad\cdot in^2} = 0.0091\cdot\frac{rad}{lb}$$

Z-section 3 – 20
d = 10.07 in.
b = 2.56 in.
t = 0.060 in.
δ = 1/3
I_X = 15.29 in^4
I_Y = 1.72 in^4
I_{XY} = 3.61 in^4
J = 0.00124 in^4
C_W = 32.41 in^6

$$I_{MY} = \frac{I_X I_Y - I_{XY}^2}{I_X} = \frac{(15.29in^4)(1.72in^4) - (3.61in^4)^2}{15.29in^4} = 0.868in^4$$

$$a = \sqrt{\frac{EC_W}{GJ}} = \sqrt{\frac{E\cdot 32.41in^6}{G\cdot 0.00124in^4}} = 262.4in$$

$$\beta = \frac{L^2}{8a^2} + \frac{1}{\cosh\left(\frac{L}{2a}\right)} - 1 = \frac{(240in)^2}{8\cdot(262.4in)^2} + \frac{1}{\cosh\left(\frac{240in}{2\cdot 262.4in}\right)} - 1 = 0.0084rad$$

$$\kappa = \frac{8a^4}{L^2}\left(\frac{\cosh\left(\frac{L}{2a}\right)-1}{\cosh\left(\frac{L}{2a}\right)}\right) + \frac{5L^2}{48} - a^2$$

$$\kappa = \frac{8(262.4in)^4}{(240in)^2}\left(\frac{\cosh\left(\frac{240in}{2\cdot 262.4in}\right)-1}{\cosh\left(\frac{240in}{2\cdot 262.4in}\right)}\right) + \frac{5(240in)^2}{48} - (262.4in)^2 = 470.5rad\cdot in^2$$

$$\tau = \frac{\frac{a^2\beta}{GJ}}{1+\frac{K_{MDeck}}{GJ}\kappa} = \frac{\frac{(262.4in)^2 \cdot 0.0084rad}{G \cdot 0.00124in^4}}{1+\frac{1000\,{}^{lb\cdot in}\!/\!{}_{rad\cdot ft}}{G \cdot 0.00124in^4}\cdot 470.5rad \cdot in^2} = 0.011 \cdot \frac{rad}{lb}$$

$$\beta_{3rd} = \frac{L}{GJ}\left(\frac{1}{3}-\frac{a}{L}\frac{\sinh\left(\frac{L}{3a}\right)}{\cosh\left(\frac{L}{2a}\right)}\right) = \frac{(240in)}{G \cdot 0.00124in^4}\left(\frac{1}{3}-\frac{159.9in}{240in}\frac{\sinh\left(\frac{240in}{3\cdot 159.9in}\right)}{\cosh\left(\frac{240in}{2\cdot 159.9in}\right)}\right) = 0.000473\,{}^{1}\!/\!{}_{lb\cdot in}$$

Procedure

1. Calculate uniform restraint provided by sheathing, w_{rest}, expressed as a proportion of the applied uniform load.

$$w_{rest} = w \cdot \sigma$$

where

$$\sigma = \frac{\frac{5\left(\frac{I_{XY}}{I_X}\cos\theta\right)L^4}{384EI_{mY}} + \frac{(\delta b\cos\theta)d}{2}\tau + \frac{L^2\sin\theta}{8G'Width}}{\frac{5L^4}{384EI_{mY}} + \frac{d^2}{4}\tau + \frac{L^2}{8G'Width}}$$

Purlins 1-2

$$\sigma = \frac{\frac{5\left(\frac{5.70in^4}{24.31in^4}\cos(2.4°)\right)(240in)^4}{384\cdot E\cdot 1.354in^4} + \frac{\left(\frac{2.56in}{3}\cos(2.4°)\right)10.07in}{2\cdot rad}0.0091\frac{rad}{lb} + \frac{(240in)^2\sin(2.4°)}{8\cdot\left(1000\,{}^{lb}\!/\!{}_{in}\right)(60.6in)}}{\frac{5(240in)^4}{384\cdot E\cdot 1.354in^4} + \frac{(10.07in)^2}{4\cdot rad}0.0091\frac{rad}{lb} + \frac{(240in)^2}{8\cdot\left(1000\,{}^{lb}\!/\!{}_{in}\right)(60.6in)}}$$

$$\sigma = 0.208$$

Purlins 3-20

$$\sigma = \frac{\frac{5\left(\frac{3.61in^4}{15.29in^4}\cos(2.4°)\right)(240in)^4}{384\cdot E\cdot 0.868in^4} + \frac{\left(\frac{2.56in}{3}\cos(2.4°)\right)10.07in}{2\cdot rad}0.011\frac{rad}{lb} + \frac{(240in)^2\sin(2.4°)}{8\cdot\left(1000\,{}^{lb}\!/\!{}_{in}\right)(60.6in)}}{\frac{5(240in)^4}{384\cdot E\cdot 0.868in^4} + \frac{(10.07in)^2}{4\cdot rad}0.011\frac{rad}{lb} + \frac{(240in)^2}{8\cdot\left(1000\,{}^{lb}\!/\!{}_{in}\right)(60.6in)}}$$

$$\sigma = 0.216$$

2. Calculate $M_{torsion}$, the moment generated in the connection to the sheathing due to the bending effects of the Z-section and M_{local}, the local bending moment

$$M_{torsion} = wL \cdot \tfrac{2}{3}K_{mclip}\left(\sigma\frac{d}{2} - \delta b\cos\theta\right)\tau$$

$$M_{local} = -wL \cdot \delta b\cos\theta \cdot \frac{K_{mclip}}{K_{mclip} + \frac{E\cdot t^3}{3d}}$$

Z-section 1-2

$$w = 20\text{psf} \cdot 5\text{ft} = 100\text{plf}$$

$$M_{torsion} = 100\text{plf}\left(\frac{240\text{in}}{12\,{}^{\text{in}}\!/\!_{\text{ft}}}\right)\cdot\left(\left(\tfrac{2}{3}\right)\frac{1000\,{}^{\text{lb}\cdot\text{in}}\!/\!_{\text{rad}\cdot\text{ft}}}{12\,{}^{\text{in}}\!/\!_{\text{ft}}}\left(0.208\cdot\frac{10.07\text{in}}{2}-\frac{2.56\text{in}}{3}\cos(2.4°)\right)0.0091\,{}^{\text{rad}}\!/\!_{\text{lb}}\right)$$

$$M_{torsion} = 197\text{lb}\cdot\text{in}$$

$$M_{local} = -100\text{plf}\left(\frac{240\text{in}}{12\,{}^{\text{in}}\!/\!_{\text{ft}}}\right)\cdot\left(\frac{2.56\text{in}}{3}\cos(2.4°)\cdot\frac{1000\,{}^{\text{lb}\cdot\text{in}}\!/\!_{\text{rad}\cdot\text{ft}}}{1000\,{}^{\text{lb}\cdot\text{in}}\!/\!_{\text{rad}\cdot\text{ft}}+\dfrac{E\cdot(0.097\text{in})^3}{3\cdot 10.07\text{in}}}\right)$$

$$M_{local} = -147\text{lb}\cdot\text{in}$$

Z-section 3-19

$$w = 20\text{psf} \cdot 5\text{ft} = 100\text{plf}$$

$$M_{torsion} = 100\text{plf}\left(\frac{240\text{in}}{12\,{}^{\text{in}}\!/\!_{\text{ft}}}\right)\cdot\left(\left(\tfrac{2}{3}\right)\frac{1000\,{}^{\text{lb}\cdot\text{in}}\!/\!_{\text{rad}\cdot\text{ft}}}{12\,{}^{\text{in}}\!/\!_{\text{ft}}}\left(0.216\cdot\frac{10.07\text{in}}{2}-\frac{2.56\text{in}}{3}\cos(2.4°)\right)0.011\,{}^{\text{rad}}\!/\!_{\text{lb}}\right)$$

$$M_{torsion} = 287\text{lb}\cdot\text{in}$$

$$M_{local} = -100\text{plf}\left(\frac{240\text{in}}{12\,{}^{\text{in}}\!/\!_{\text{ft}}}\right)\cdot\left(\frac{2.56\text{in}}{3}\cos(2.4°)\cdot\frac{1000\,{}^{\text{lb}\cdot\text{in}}\!/\!_{\text{rad}\cdot\text{ft}}}{1000\,{}^{\text{lb}\cdot\text{in}}\!/\!_{\text{rad}\cdot\text{ft}}+\dfrac{E\cdot(0.060\text{in})^3}{3\cdot 10.07\text{in}}}\right)$$

$$M_{local} = -483\text{lb}\cdot\text{in}$$

Z-section 20

$$w = 20\text{psf}\cdot\left(\frac{5\text{ft}+2\text{ft}}{2}\right) = 70\text{plf}$$

$$M_{torsion} = 287\text{lb}\cdot\text{in}\cdot\frac{70\text{plf}}{100\text{plf}} = 201\text{lb}\cdot\text{in}$$

$$M_{local} = -483\text{lb}\cdot\text{in}\cdot\frac{70\text{plf}}{100\text{plf}} = -338\text{lb}\cdot\text{in}$$

3. Calculate the total force per Z-section generated requiring restraint

$$P_L = wL\cdot\left(\frac{\delta b\cos\theta}{h} - C8\frac{d}{h}\sin\theta\right) + \frac{M_{torsion}+M_{local}}{h}$$

Z-section 1-2

$$P_{1-2} = 100\,{}^{\text{lbf}}\!/\!_{\text{ft}}\left(\frac{240\text{in}}{12\,{}^{\text{in}}\!/\!_{\text{ft}}}\right)\cdot\left(\frac{\frac{2.56\text{in}}{3}\cos(2.4°)}{10.07\text{in}} - \frac{10.07\text{in}}{10.07\text{in}}\sin(2.4°)\right) + \frac{197\text{lb}\cdot\text{in}-147\text{lb}\cdot\text{in}}{10.07\text{in}} = 90\text{lb}$$

Z-section 3-19

$$P_{3-19} = 100\,{}^{lbf}\!/_{ft}\left(\frac{240in}{12\,{}^{in}\!/_{ft}}\right)\cdot\left(\frac{\frac{2.56in}{3}\cos(2.4°)}{10.07in} - \frac{10.07in}{10.07in}\sin(2.4°)\right) + \frac{287lb\cdot in - 483lb\cdot in}{10.07in} = 66lb$$

Z-section 20

$$P_{20} = 66lb\cdot\frac{70plf}{100plf} = 46lb$$

Total Force in System

$$\sum P_L = 2\cdot 90lb + 17\cdot 66lb + 46lb = 1348\cdot lb$$

4. Calculate the stiffness of the sheathing.

$$K_{shtg} = \frac{K_{mclip}L}{d}\left(\frac{\frac{1}{4}Et^3}{0.38K_{mclip}d + 0.71\frac{1}{4}Et^3}\right)\left(1 - \tfrac{2}{3}K_{mclip}\tau\right)$$

Z-section 1-2

$$K_{shtg} = \frac{1000\,{}^{lb\cdot in}\!/_{rad\cdot ft}\,20ft}{10.07in}\left(\frac{\frac{1}{4}E(0.097in)^3}{0.38\cdot 1000\,{}^{lb\cdot in}\!/_{rad\cdot ft}\cdot 10.07in + 0.71\cdot\frac{1}{4}E(0.097in)^3}\right)\left(1 - \tfrac{2}{3}1000\,{}^{lb\cdot in}\!/_{rad\cdot ft}\cdot 0.0091\frac{rad}{lb}\right)$$

$$K_{shtg} = 1300\,{}^{lb\cdot in}\!/_{in}$$

Z-section 3-20

$$K_{shtg} = \frac{1000\,{}^{lb\cdot in}\!/_{rad\cdot ft}\,20ft}{10.07in}\left(\frac{\frac{1}{4}E(0.060in)^3}{0.38\cdot 1000\,{}^{lb\cdot in}\!/_{rad\cdot ft}\cdot 10.07in + 0.71\cdot\frac{1}{4}E(0.060in)^3}\right)\left(1 - \tfrac{2}{3}1000\,{}^{lb\cdot in}\!/_{rad\cdot ft}\cdot 0.011\frac{rad}{lb}\right)$$

$$K_{shtg} = 862\,{}^{lb\cdot in}\!/_{in}$$

5. Calculate stiffness of connection between rafter and Z-section (flange bolted connection)

$$K_{Rafter} = 0.45\frac{Et^3}{2d}$$

Z-section 2

$$K_{Rafter} = 0.45\frac{E(0.097in)^3}{2\cdot 10.07in} = 602\,{}^{lb\cdot in}\!/_{in}$$

Z-section 3-9, 11-20

$$K_{Rafter} = 0.45\frac{E(0.060in)^3}{2\cdot 10.07in} = 142\,{}^{lb\cdot in}\!/_{in}$$

6. Calculate the total stiffness of the system and the force in each Anchorage Device

$$K_{total} = \sum K_{rest} + \frac{\sum(K_{shtg} + K_{rafter})}{d}$$

$$K_{total} = 2 \cdot \left(4000\,{}^{lb}\!/_{in} + 3000\,{}^{lb}\!/_{in}\right) + \frac{2 \cdot 1300\,{}^{lb\cdot in}\!/_{in} + 18 \cdot 862\,{}^{lb-in}\!/_{in}}{10.07 \cdot in} + 2 \cdot \frac{602\,{}^{lb\cdot in}\!/_{in} + 17 \cdot 142\,{}^{lb\cdot in}\!/_{in}}{10.07 \cdot in}$$

$$K_{total} = 16400\,{}^{lb}\!/_{in}$$

Anchor #1

$$R_1 = \sum_{np} P_L \cdot \frac{K_{rest}}{K_{total}}$$

$$R_1 = 1348lb \cdot \frac{4000\,{}^{lb}\!/_{in}}{16400\,{}^{lb}\!/_{in}} = 329lb$$

Anchor #10

$$R_2 = 1348lb \cdot \frac{3000\,{}^{lb}\!/_{in}}{16400\,{}^{lb}\!/_{in}} = 247lb$$

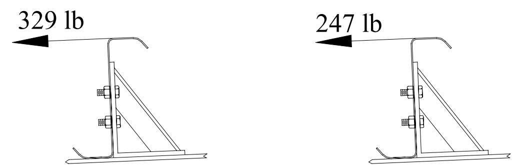

Anchor #1 Anchor #10

Figure III.2 Restraint Forces

7. Calculate the deformation of the system at a) Restraint, b) deflection of diaphragm relative to restraint and b) total deflection at Mid-span

a) Deflection at restraint (Frame Line)

$$\Delta_{rest} = \frac{R}{K_{rest}} = \frac{329lb}{4000\,{}^{lb}\!/_{in}} = 0.08in$$

b) Deflection of diaphragm relative to restraint

$$\Delta_{diaph} = \sum w(\sigma - \sin\theta)\frac{L^2}{8G'Bay}$$

$$\Delta_{diaph} = \frac{\left[\left(\left(2 \cdot 0.208 + 17 \cdot 0.216\right)100plf + 0.216 \cdot 70plf\right) - 20psf\left(101ft\right)\sin\left(2.4°\right)\right]\left(20ft\right)^2}{8 \cdot 1000\,{}^{lb}\!/_{in} \cdot 101ft} = 0.17in$$

c) Total mid-span deflection

$$\Delta_{MS} = \Delta_{rest} + \Delta_{diaph} = 0.08in + 0.21in = 0.29in$$

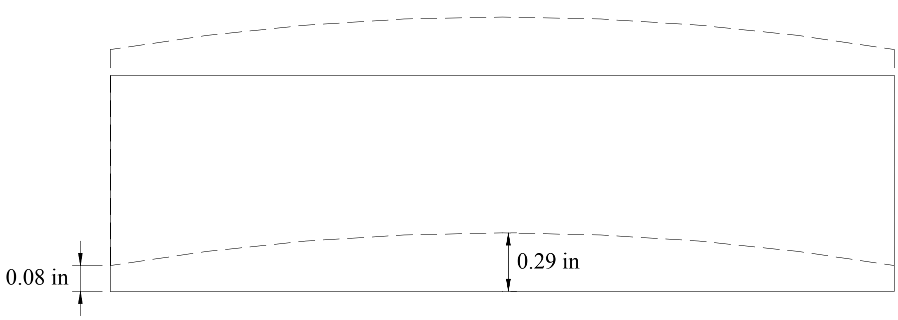

Figure III.3 System Displacement

8) Calculate fastener force at restraint

At Restraint

$$\text{FastenerForce} = R\frac{h}{d} + \frac{wL}{2}\left(0.9\sigma - \frac{\delta b\cos\theta}{d}\right) - \frac{M_{torsion} + M_{local}}{2d}$$

Fastener Force at Z-section 1 (Anchor #1)

$$\text{FastenerForce} = 329\text{lb}\frac{10.07\text{in}}{10.07\text{in}} + \frac{100\text{plf}\cdot 20\text{ft}}{2}\cdot\left(0.9\cdot 0.208 - \frac{\frac{2.56\text{in}}{3}\cos(2.4°)}{10.07\text{in}}\right) - \frac{197\text{lb}\cdot\text{in} - 147\text{lb}\cdot\text{in}}{2\cdot 10.07\text{in}}$$

$$\text{FastenerForce} = 430\text{lb}$$

Fastener Force at Z-section 10 (Anchor #10)

$$\text{FastenerForce} = 247\text{lb}\frac{10.07\text{in}}{10.07\text{in}} + \frac{100\text{plf}\cdot 20\text{ft}}{2}\cdot\left(0.9\cdot 0.216 - \frac{\frac{2.56\text{in}}{3}\cos(2.4°)}{10.07\text{in}}\right) - \frac{(287\text{lb}\cdot\text{in} - 483\text{lb}\cdot\text{in})}{2\cdot 10.07\text{in}}$$

$$\text{FastenerForce} = 367\text{lb}$$

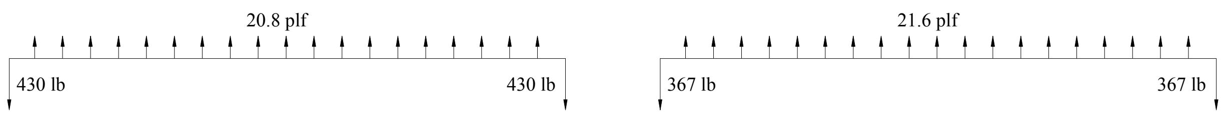

(a) Z-section 1 *(b) Z-section 10*

Figure III.4 Forces in connection between sheathing and Z-section along length of Z-section

Example 2. Supports Restraint Configuration (Z-section web plate connection)

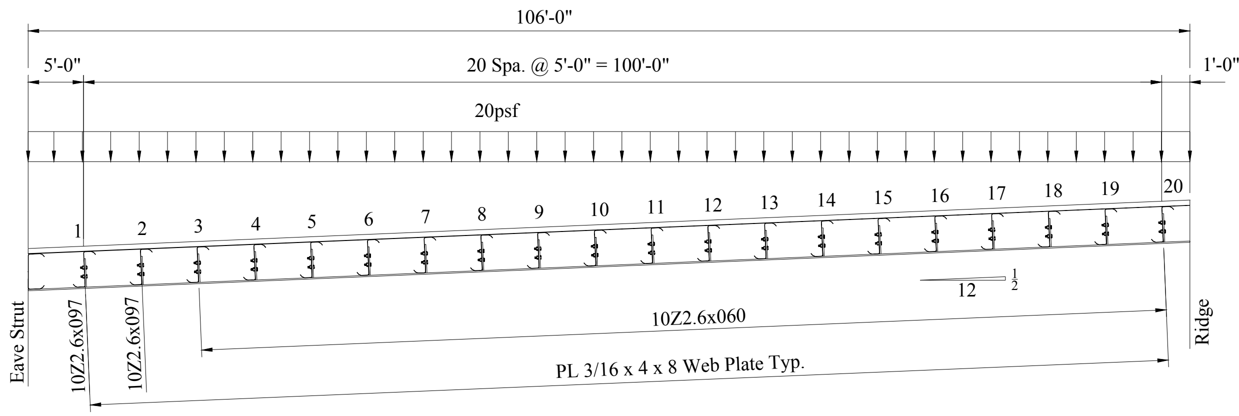

Figure III.5 Z-section Layout Example 2.

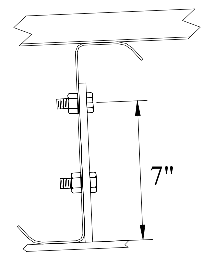

Using the same bay configuration as Example 1, calculate the restraint force if the antiroll anchorage devices are removed and the Z-section to rafter connection changed to a web plate connection for all Z-sections. The web plate is a PL 3/16x4x8 with the top bolts of located at 7 in. above the rafter as shown in Figure 6.

Figure 6. Web plate detail

Web Plate Properties
t_{pl} = 3/16 in.
b_{pl} = 4 in.
h = 7 in.

Proceedure

1. The force generated per purlin is calculated per parts 1-3 of Example 1.

Z-section 1-2 $P_{1\text{-}2}$ = 90 lb
Z-section 3-19 $P_{3\text{-}19}$ = 66lb
Z-section 20 P_{20} = 46lb

2. The sheathing stiffness is calculated per part 4 of Example 1

Z-section 1-2 K_{Shtg} = 1300 lb·in/in
Z-section 3-20 K_{Shtg} = 862 lb·in/in

3. Calculate the stiffness of the rafter connection

In this case, the rafter connection is considered to be an anchorage device, so Equation (10) is used

$$K_{Rest,WebPlate} = \frac{E \cdot b_{pl} \cdot t_{pl}^{\;3} \cdot t^3\left(t^3 h + t_{pl}^3 (d-h)\right)}{\left(t^3 h^2 - t_{pl}^3 (d-h)^2\right)^2 + 4t^3 t_{pl}^{\;3} d^2 h (d-h)}$$

Z-section 1-2

$$K_{Rest,WebPlate} = \frac{E \cdot 4in \cdot (0.1875in)^3 (0.097in)^3 \left((0.097in)^3 \cdot 7in + (0.1875in)^3 (10.07in - 7in)\right)}{\left((0.097in)^3 (7in)^2 - (0.1875in)^3 (10.07in - 7in)^2\right)^2 + 4(0.1875in)^3 (0.097in)^3 (10.07in)^2 7in(10.07in - 7in)}$$

$$K_{Rafter} = 358\,{}^{lb}\!/_{in}$$

Z-section 3-20

$$K_{Rest,WebPlate} = \frac{E \cdot 4in \cdot (0.1875in)^3 (0.06in)^3 \left((0.06in)^3 \cdot 7in + (0.1875in)^3 (10.07in - 7in)\right)}{\left((0.06in)^3 (7in)^2 - (0.1875in)^3 (10.07in - 7in)^2\right)^2 + 4(0.1875in)^3 (0.06in)^3 (10.07in)^2 7in(10.07in - 7in)}$$

$$K_{Rafter} = 242\,{}^{lb}\!/_{in}$$

4. Calculate the total stiffness of the system and the force in each web plate

$$K_{total} = \sum K_{rest} + \frac{\sum(K_{shtg} + K_{rafter})}{d}$$

$$K_{total} = 2 \cdot \left(2 \cdot 358\,{}^{lb}\!/_{in} + 18 \cdot 242\,{}^{lb}\!/_{in}\right) + \frac{2 \cdot 1300\,{}^{lb\text{-}in}\!/_{in} + 18 \cdot 862\,{}^{lb-in}\!/_{in}}{10.07 \cdot in}$$

$$K_{total} = 12000\,{}^{lb}\!/_{in}$$

Force resisted by the Web Plate

$$R = \sum P_L \cdot \frac{K_{rest}}{K_{total}}$$

Z-section 1-2

$$R = 1348lb \cdot \frac{358\,{}^{lb}\!/_{in}}{12000\,{}^{lb}\!/_{in}} = 40lb$$

The moment at the base of the web plate is

$$M_{Rafter} = 40lb \cdot 10.07in = 403lb \cdot in$$

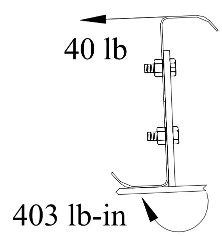

Figure III.7 Web Plate Forces Z-Section 1-2

Z-section 3-20

$$R = 1348lb \cdot \frac{242\,{}^{lb}\!/_{in}}{12000\,{}^{lb}\!/_{in}} = 27lb$$

The moment at the base of the web plate is

$$M_{Rafter} = 27lb \cdot 10.07in = 270lb \cdot in$$

7. Calculate the deformation of the system at a) Restraint, b) deflection of diaphragm relative to restraint and b) total deflection at Mid-span

a) Deflection at restraint

$$\Delta_{rest} = \frac{R}{K_{rest}} = \frac{40lb}{3610\,{}^{lb\cdot in}/_{in} \Big/ 10.07in} = 0.11in$$

b) Deflection of diaphragm relative to restraint

$\Delta_{diaph} = 0.210in$ (same as Example 1)

c) Total mid-span deflection

$$\Delta_{MS} = \Delta_{rest} + \Delta_{diaph} = 0.11in + 0.21in = 0.32in$$

8) Calculate fastener forces

At Restraint

$$FastenerForce = R\frac{h}{d} + \frac{wL}{2}\left(0.9\sigma - \frac{\delta b\cos\theta}{d}\right) - \frac{M_{torsion} + M_{local}}{2d}$$

Fastener Force at Z-section 1-2

$$FastenerForce = 40lb\frac{10.07in}{10.07in} + \frac{100plf \cdot 20ft}{2} \cdot \left(0.9 \cdot 0.208 - \frac{\frac{2.56in}{3}\cos(2.4°)}{10.07in}\right) - \frac{197lb \cdot in - 147lb \cdot in}{2 \cdot 10.07in}$$

$$FastenerForce = 140lb$$

Example 3 Third Point Restraint Configuration

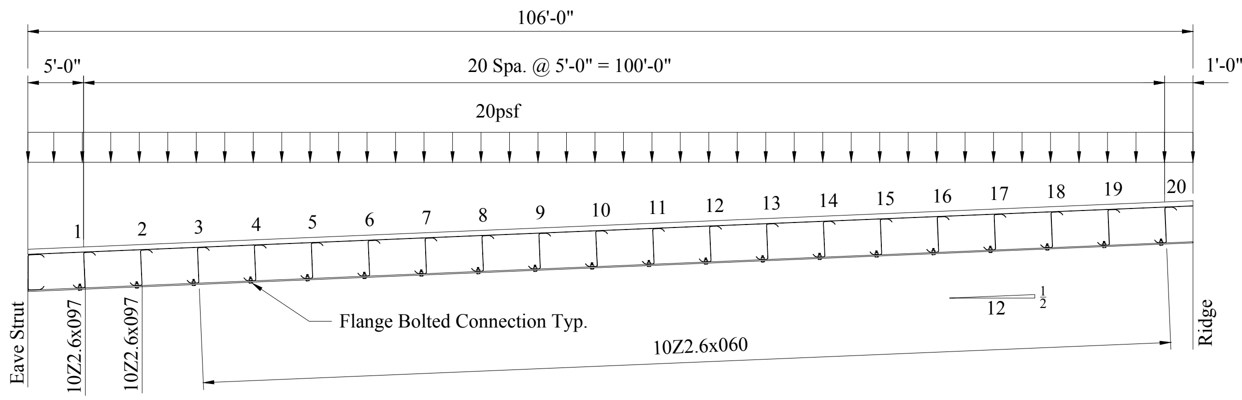

Figure III.8 Z-Section Layout Example 3

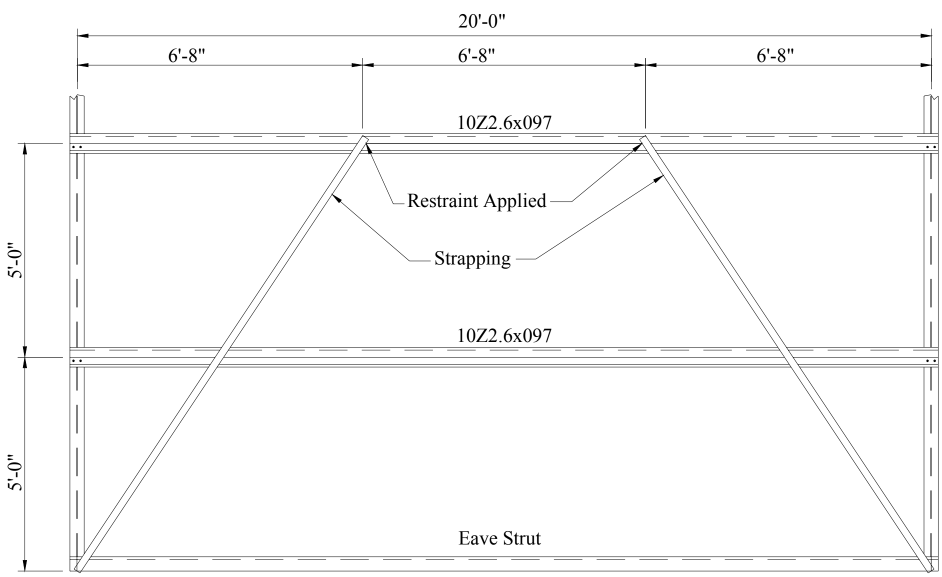

Figure III.9 3rd Point Restraint Layout Example 3

Using the same Z-section configuration as Example 1, antiroll anchorage devices at Z-section 1 and 10 are replaced by a third point restraint as shown in Figure 9. All Z-sections have a flange bolted connection to the rafter. Restraint is applied by 2 in. wide 12 gage strapping which is anchored to top of the eave strut at the frame lines and attached to the top flange of Z-section 2 at the third points. The connection to the top of the eave strut has a tested stiffness of 5000 lb/in.

1. Calculate uniform restraint provided by sheathing expressed as a proportion of the applied uniform load.

$$w_{rest} = w \cdot \sigma$$

Where

$$\sigma = \frac{\dfrac{11\left(\dfrac{I_{XY}}{I_X}\cos\theta\right)L^4}{972EI_{mY}} + \dfrac{(\delta b\cos\theta)d}{2}\tau - \dfrac{L^2\sin\theta}{18G'\mathrm{Width}}}{\dfrac{11L^4}{972EI_{mY}} + \dfrac{d^2}{4}\tau + \dfrac{L^2}{9G'\mathrm{Width}}}$$

Z-sections 1-2

$$\sigma = \frac{\dfrac{11\left(\dfrac{5.70\mathrm{in}^4}{24.31\mathrm{in}^4}\cos(2.4°)\right)(240\mathrm{in})^4}{972\cdot E\cdot 1.354\mathrm{in}^4} + \dfrac{\left(\frac{2.56\mathrm{in}}{3}\cos(2.4°)\right)10.07\mathrm{in}}{2\cdot \mathrm{rad}}0.0091\dfrac{\mathrm{rad}}{\mathrm{lb}} - \dfrac{(240\mathrm{in})^2\sin(2.4°)}{18\cdot(1000\,{}^{\mathrm{lb}}\!/\!_{\mathrm{in}})(60.6\mathrm{in})}}{\dfrac{11(240\mathrm{in})^4}{972\cdot E\cdot 1.354\mathrm{in}^4} + \dfrac{(10.07\mathrm{in})^2}{4\cdot \mathrm{rad}}0.0091\dfrac{\mathrm{rad}}{\mathrm{lb}} + \dfrac{(240\mathrm{in})^2}{9\cdot(1000\,{}^{\mathrm{lb}}\!/\!_{\mathrm{in}})(60.6\mathrm{in})}}$$

$\sigma = 0.201$

Z-sections 3-20

$$\sigma = \frac{\dfrac{11\left(\dfrac{3.61\mathrm{in}^4}{15.29\mathrm{in}^4}\cos(2.4°)\right)(240\mathrm{in})^4}{972\cdot E\cdot 0.868\mathrm{in}^4} + \dfrac{\left(\frac{2.56\mathrm{in}}{3}\cos(2.4°)\right)10.07\mathrm{in}}{2\cdot \mathrm{rad}}0.011\dfrac{\mathrm{rad}}{\mathrm{lb}} - \dfrac{(240\mathrm{in})^2\sin(2.4°)}{18\cdot(1000\,{}^{\mathrm{lb}}\!/\!_{\mathrm{in}})(60.6\mathrm{in})}}{\dfrac{11(240\mathrm{in})^4}{972\cdot E\cdot 0.868\mathrm{in}^4} + \dfrac{(10.07\mathrm{in})^2}{4\cdot \mathrm{rad}}0.011\dfrac{\mathrm{rad}}{\mathrm{lb}} + \dfrac{(240\mathrm{in})^2}{9\cdot(1000\,{}^{\mathrm{lb}}\!/\!_{\mathrm{in}})(60.6\mathrm{in})}}$$

$\sigma = 0.211$

2. Calculate $M_{torsion}$, the moment generated in the connection to the sheathing due to torsional effects of the Z-section.

$$M_{torsion} = wL\left[\tfrac{2}{3}k_{mclip}\left(\sigma\frac{d}{2} - \delta b\cos\theta\right)\tau + \frac{L^2k_{mclip}}{6G'\cdot\mathrm{Width}\cdot d}\left(\frac{\sigma}{3} + \frac{\sin\theta}{6} - \frac{\delta b\cos\theta}{2d}\right)\left(1 - \tfrac{2}{3}k_{mclip}\tau\right)\right]$$

$$M_{local} = -wL\cdot\delta b\cos\theta\cdot\frac{K_{mclip}}{K_{mclip} + \dfrac{E\cdot t^3}{3d}}$$

Z-sections 1-2

$w = 20\mathrm{psf}\cdot 5\mathrm{ft} = 100\mathrm{plf}$

$$M_{torsion} = 100\mathrm{plf}\left(\frac{240\mathrm{in}}{12\,{}^{\mathrm{in}}\!/\!_{\mathrm{ft}}}\right)\cdot\left(\begin{aligned}&\left(\tfrac{2}{3}\right)\frac{1000\,{}^{\mathrm{lb\cdot in}}\!/\!_{\mathrm{rad\cdot ft}}}{12\,{}^{\mathrm{in}}\!/\!_{\mathrm{ft}}}\left(0.201\cdot\frac{10.07\mathrm{in}}{2} - \frac{2.56\mathrm{in}}{3}\cos(2.4°)\right)0.0091\,{}^{\mathrm{rad}}\!/\!_{\mathrm{lb}} + \\ &+\frac{(240\mathrm{in})^2 1000\,{}^{\mathrm{lb\cdot in}}\!/\!_{\mathrm{rad\cdot ft}}\cdot{}^{\mathrm{1ft}}\!/\!_{\mathrm{12in}}}{6\cdot 1000\,{}^{\mathrm{lb}}\!/\!_{\mathrm{in}}\,'\cdot 60.6\mathrm{in}\cdot 10.07\,{}^{\mathrm{in}}\!/\!_{\mathrm{rad}}}\left(\frac{0.201}{3} + \frac{\sin(2.4°)}{6} - \frac{{}^{2.56\mathrm{in}}\!/\!_{3}\cos(2.4°)}{2\cdot 10.07\mathrm{in}}\right)\left(1 - \tfrac{2}{3}1000\,{}^{\mathrm{lb\cdot in}}\!/\!_{\mathrm{rad\cdot ft}}\cdot 0.0091\,{}^{\mathrm{rad}}\!/\!_{\mathrm{lb}}\cdot{}^{\mathrm{1ft}}\!/\!_{\mathrm{12in}}\right)\end{aligned}\right)$$

$M_{torsion} = 204\mathrm{lb}\cdot\mathrm{in}$

$$M_{local} = 100\mathrm{plf}\left(\frac{240\mathrm{in}}{12\,{}^{\mathrm{in}}\!/\!_{\mathrm{ft}}}\right)\cdot\frac{2.56\mathrm{in}}{3}\cos(2.4°)\cdot\frac{1000\,{}^{\mathrm{lb\cdot in}}\!/\!_{\mathrm{rad\cdot ft}}}{1000\,{}^{\mathrm{lb\cdot in}}\!/\!_{\mathrm{rad\cdot ft}} + \dfrac{E\cdot(0.097\mathrm{in})^3}{3\cdot 10.07\mathrm{in}}} = -146\mathrm{lb}\cdot\mathrm{in}$$

Z-sections 3-19

$$w = 20\text{psf} \cdot 5\text{ft} = 100\text{plf}$$

$$M_{torsion} = 100\text{plf}\left(\frac{240\text{in}}{12\ \text{in}/\text{ft}}\right) \cdot \left(\begin{array}{l} \left(\tfrac{2}{3}\right)\dfrac{1000\ \text{lb}\cdot\text{in}/\text{rad}\cdot\text{ft}}{12\ \text{in}/\text{ft}}\left(0.211 \cdot \dfrac{10.07\text{in}}{2} - \dfrac{2.56\text{in}}{3}\cos(2.4°)\right)0.011\ \text{rad}/\text{lb} + \\ + \dfrac{(240\text{in})^2 1000\ \text{lb}\cdot\text{in}/\text{rad}\cdot\text{ft} \cdot 1\text{ft}/12\text{in}}{6 \cdot 1000\ \text{lb}/\text{in}\ ' \cdot 60.6\text{in} \cdot 10.07\ \text{in}/\text{rad}}\left(\dfrac{0.211}{3} + \dfrac{\sin(2.4°)}{6} - \dfrac{2.56\text{in}/3\cos(2.4°)}{2 \cdot 10.07\text{in}}\right)\left(1 - \tfrac{2}{3}1000\ \text{lb}\cdot\text{in}/\text{rad}\cdot\text{ft} \cdot 0.011\ \text{rad}/\text{lb} \cdot 1\text{ft}/12\text{in}\right) \end{array}\right)$$

$$M_{torsion} = 292\text{lb} \cdot \text{in}$$

$$M_{local} = 100\text{plf}\left(\frac{240\text{in}}{12\ \text{in}/\text{ft}}\right) \cdot \frac{2.56\text{in}}{3}\cos(2.4°) \cdot \frac{1000\ \text{lb}\cdot\text{in}/\text{rad}\cdot\text{ft}}{1000\ \text{lb}\cdot\text{in}/\text{rad}\cdot\text{ft} + \dfrac{E \cdot (0.060\text{in})^3}{3 \cdot 10.07\text{in}}} = -483\text{lb} \cdot \text{in}$$

3. Calculate the total force per Z-section generated requiring restraint

$$P_L = wL \cdot \left(\frac{\delta b \cos\theta}{h} - \frac{d}{h}\sin\theta\right) + \frac{M_{torsional} + M_{local}}{h}$$

Z-sections 1-2

$$P_{1-2} = 100\ \text{lbf}/\text{ft}\left(\frac{240\text{in}}{12\ \text{in}/\text{ft}}\right) \cdot \left(\frac{\dfrac{2.56\text{in}}{3}\cos(2.4°)}{10.07\text{in}} - \frac{10.07\text{in}}{10.07\text{in}}\sin(2.4°)\right) + \frac{204\text{lb} \cdot \text{in}}{10.07\text{in}} - \frac{146\text{lb} \cdot \text{in}}{10.07\text{in}} = 92\text{lb}$$

Z-sections 3-19

$$P_{3-20} = 100\ \text{lbf}/\text{ft}\left(\frac{240\text{in}}{12\ \text{in}/\text{ft}}\right) \cdot \left(\frac{\dfrac{2.56\text{in}}{3}\cos(2.4°)}{10.07\text{in}} - \frac{10.07\text{in}}{10.07\text{in}}\sin(2.4°)\right) + \frac{292\text{lb} \cdot \text{in}}{10.07\text{in}} - \frac{483\text{lb} \cdot \text{in}}{10.07\text{in}} = 67\text{lb}$$

Z-section 20

$$P_{20} = 67\text{lb} \cdot \frac{70\text{plf}}{100\text{plf}} = 47\text{lb}$$

Total Force in System

$$\sum P_L = 2 \cdot 92\text{lb} + 17 \cdot 67\text{lb} + 47\text{lb} = 1554 \cdot \text{lb}$$

4. The sheathing stiffness is calculated per part 4 of Example 1

Z-section 1-2 K_{Shtg} = 1300 lb·in/in
Z-section 3-20 K_{Shtg} = 862 lb·in/in

5. Calculate the total stiffness of the system and the force in the third point brace

$$K_{total} = \sum K_{rest} + \frac{\sum(K_{shtg} + K_{rafter})}{d}$$

$$K_{total} = 2 \cdot (5000\,{}^{lb}\!/\!_{in}) + \frac{2 \cdot 1300\,{}^{lb\cdot in}\!/\!_{in} + 18 \cdot 862\,{}^{lb-in}\!/\!_{in}}{10.07 \cdot in}$$

$$K_{total} = 11800\,{}^{lb}\!/\!_{in}$$

Third Point Brace Force

$$R = \sum_{np} P_L \cdot \frac{K_{rest}}{K_{total}}$$

$$R = 1554lb \cdot \frac{5000\,{}^{lb}\!/\!_{in}}{11800\,{}^{lb}\!/\!_{in}} = 658lb$$

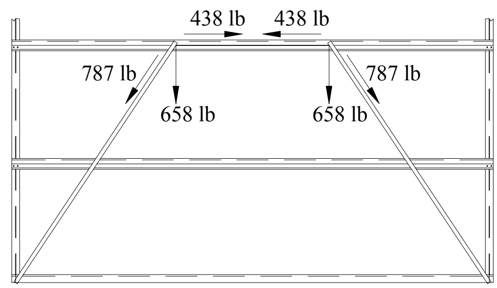

Figure III.10 3rd Point Brace Forces

6. Calculate a) the lateral deflection of the system at restraint, b) deflection of diaphragm relative to restraint and c) total deflection at rafter

a) Deflection at restraint

$$\Delta_{rest} = \frac{R}{K_{rest}} = \frac{658lb}{5000\,{}^{lb\cdot in}\!/\!_{in}} = 0.13in$$

b) Deflection of diaphragm relative to restraint

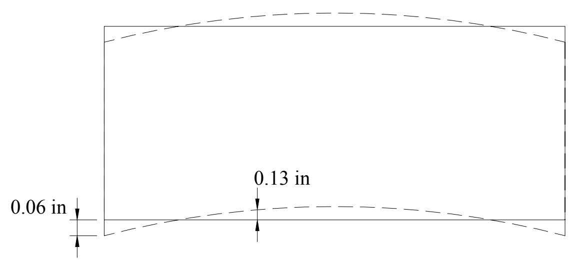

Figure III.11 System Deformation

$$\Delta_{diaph} = -\frac{L^2}{9G'Bay}\left(\sum w\sigma + \tfrac{7}{4}\sum w \sin\theta \frac{\sum K_{rest}}{K_{total}}\right) + \frac{P_L\,{}^{h}\!/\!_{d}\,L}{3G'Bay}$$

$$\Delta_{diaph} = -\frac{(20ft)^2}{9 \cdot 1000\,{}^{lb}\!/\!_{in} \cdot 101ft}\left[\left((2 \cdot 0.201 + 17 \cdot 0.211)100plf + 0.211 \cdot 70plf\right) + \tfrac{7}{4}20psf \cdot 100ft \cdot \sin(2.4°)\frac{2 \cdot 5000\,{}^{lb}\!/\!_{in}}{11800\,{}^{lb}\!/\!_{in}}\right] +$$

$$+\frac{658lb \cdot \frac{10.07in}{10.07in}(20ft)}{3 \cdot 1000\,{}^{lb}\!/\!_{in} \cdot 101ft}$$

$$\Delta_{diaph} = -0.19in$$

c) Total deflection at rafter

$$\Delta_{MS} = \Delta_{rest} + \Delta_{diaph} = 0.13in - 0.19in = -0.06in$$

8) Calculate fastener forces at restraint

$$FastenerForce = R\frac{h}{d} + \frac{wL}{20}\left(\frac{\delta b \cos\theta}{d} - 0.9\sigma\right)$$

$$FastenerForce = 658lb\frac{10.07in}{10.07in} + \frac{100plf \cdot 20ft}{20} \cdot \left(\frac{\frac{2.56in}{3}\cos(2.4°)}{10.07in} - 0.9 \cdot 0.201\right) = 648lb$$